Transactions

of the

ASME

An Introduction to Arc-Cast Molybdenum and Its Alloys . . . . . *J. L. Ham* 723

Experience With Austenitic Steels in High-Temperature Service in the Petroleum Industry . . . . . *M. E. Holmberg* 733

An Investigation of the Role of Aluminum in the Graphitization of Plain Carbon Steel . . . . . *A. M. Hall and E. E. Fletcher* 743

Nickel-Chromium-Molybdenum Steel Valve Casting After 50,000 Hours of Service at 900 F . . . . . *T. N. Armstrong and R. J. Greene* 751

The General Tensional Relaxation Properties of a Bolting Steel . . . *D. N. Frey* 755

Basic Factors in Hot-Machining of Metals . . *E. J. Krabacher and M. E. Merchant* 761

Cutting Temperatures and Metal-Cutting Phenomena . . *B. T. Chao and K. J. Trigger* 777

Design Features of the Nordberg Radial Engine . . *D. I. Bohn and Emil Grieshaber* 795

Heat Transfer to a Fluid Flowing Turbulently in a Smooth Pipe With Walls at Constant Temperature . . . . . *R. A. Seban and T. T. Shimazaki* 803

Basic Study for a Generating Station . . . . . *G. R. Milne* 811

Fireside Deposits on Steam Generators Minimized Through Humidification of Combustion Air . . . . . *Paul Murphy, Jr., J. D. Piper, and C. R. Schmeusky* 821

Developments in Spreader-Firing Wet Wood . . . . . *A. S. Weigel* 845

AUGUST, 1951

VOL. 73, No. 6

Transactions

of The American Society of Mechanical Engineers

Published on the tenth of every month, except March, June, September, and December

---

OFFICERS OF THE SOCIETY:

J. Calvin Brown, *President*

Joseph L. Koff, *Treasurer* — C. E. Davies, *Secretary*
Edgar J. Kates, *Ass't Treasurer*

COMMITTEE ON PUBLICATIONS:

John Haydock, *Chairman*

C. B. Campbell — Paul T. Norton, Jr.
George R. Rich — Otto de Lorenzi

D. R. Thomas, Morris Greif } *Junior Advisory Members*

George A. Stetson, *Editor* — K. W. Clenendinning, *Managing Editor*

REGIONAL ADVISORY BOARD OF THE PUBLICATIONS COMMITTEE:

Kerr Atkinson—I
J. de S. Coutinho—II
W. E. Reaser—III
F. C. Smith—IV
Hemdley Blackmon—V
Chester R. Earle—VI
R. G. Robbins—VII
M. A. Durland—VIII

Published monthly by The American Society of Mechanical Engineers. Publication office at 20th and Northampton Streets, Easton, Pa. The editorial department is located at the headquarters of the Society, 29 West Thirty-Ninth Street, New York 18, N. Y. Cable address, "Dynamic" New York. Price $1.50 a copy, $12.00 a year for Transactions and the *Journal of Applied Mechanics* to members and affiliates, $1.00 a copy, $6.00 a year. Changes of address must be received at Society headquarters four weeks before they are to be effective on the mailing list. Please send old as well as new address. . . . By-Law: The Society shall not be responsible for statements or opinions advanced in papers or . . . printed in its publications (B13, Par. 4). . . . Entered as second-class matter March 2, 1928, at the Post Office at Easton, Pa., under the Act of August 24, 1912. . . .

Copyrighted, 1951, by The American Society of Mechanical Engineers. Reprints from this publication may be made on condition that full credit be given the Transactions of the ASME and the author, and that date of publication be stated.

An Introduction to Arc-Cast Molybdenum and Its Alloys

By J. L. HAM,[1] DETROIT, MICH.

The advantages and limitations of the arc-casting method for producing metallic molybdenum and its alloys are discussed. The general properties of unalloyed cast molybdenum are described and curves are presented to show the room temperature tensile properties, hardness, and notched-bar values after annealing at various temperatures, the effect of testing temperature on hardness, and the transition temperatures for various types of impact tests.

The need for addition of alloying elements is discussed. Preliminary selection of appropriate alloying elements was based on their vapor pressures and known or expected solid solubility limits. Curves are presented showing the solid solubility limits of silicon, aluminum, iron, cobalt, and nickel in molybdenum at various temperatures as determined by the measurement of lattice parameters of arc-cast samples, and the effects of beryllium, aluminum, silicon, titanium, vanadium, chromium, iron, cobalt, nickel, zirconium, columbium, tantalum, and tungsten on the hardness of molybdenum at various temperatures.

Molybdenum containing a small amount of beryllium can be hardened by quenching and softened by slow cooling.

Regardless of which alloying element is used, there appears to be a limit to the increase in hardness that can be tolerated without causing difficulty in hot-working by the techniques applied so far.

The effects of several of the alloying elements on the rate of work-hardening and on the temperatures of softening and recrystallization were studied using a series of alloys which were extruded.

Introduction

MOLYBDENUM, because of its high melting point, becomes a logical choice for a basic metal in alloys for structural high-temperature applications. The recently developed arc-cast process now makes this metal available in large sections. The arc-cast (1)[2] process converts molybdenum powder to cast ingots. In consecutive stages, molybdenum powder is pressed into a vertical column which is sintered to increase its strength as it proceeds downward into a water-cooled mold where the metal is melted in an alternating-current arc established between the end of the formed powder electrode and the metal bath that comprises the top of the ingot.

Since applications for the pure metal are restricted by its limited strength at high temperatures, the development of molybdenum-base alloys with properties superior to those of pure molybdenum has recently been the subject of a considerable amount of experimental work. Selection of elements most suitable for addition to molybdenum requires the careful appraisal of existing information, and the judicious application of fundamental principles and theories likely to assist in the classification of the elements with respect to their effects on the properties of molybdenum.

Although the following information is primarily of a practical nature, it is hoped that it may also be of value to those working along more theoretical lines toward the development of refractory alloys.

The information developed herein is intended to lay the groundwork for further research on molybdenum-base alloys and to assist the engineer to recognize immediate applications for which the molybdenum or molybdenum-base alloys now available may be suited, and to appraise the situation with respect to the possible availability of superior alloys for future applications.

Some of the applications presently being investigated are as follows:

Piercing plugs for seamless-steel tubing.
Gas-turbine blades.
Electrodes for heating molten glass.
Die-casting dies for brass and other nonferrous metals.
Certain components of turbojets, ram jets, rockets, and nuclear reactors.
Parts exposed to corrosive chemicals.

Advantages and Limitations of Arc-Casting Method

In so far as is known at present, the size of ingot which can be produced by the arc-cast method is limited only by the capacity of available electrical and vacuum equipment. Ingots up to 6 in. diam and weighing 150 lb are now being produced, and equipment for the production of 1000-lb ingots, 9 in. diam, is under construction.

Production of large ingots requires high melting rates and therefore large arc currents and high-capacity vacuum pumps, since final deoxidation is usually accomplished by the use of carbon, and the pressure of carbon monoxide must be kept below certain limits to avoid hot shortness due to the presence of MoO_2 at the grain boundaries of the metal. In order to meet the low oxygen requirement, it is generally necessary to use molybdenum powder as low in oxygen content as is commercially available.

Certain alloying elements can be added in any desired proportion, but the range of alloy compositions which can be produced by melting in vacuum is quite limited for some elements, owing to excessive volatilization which lends to an ingot with a rough, wrinkled, encrusted surface. The behavior of various elements in this respect will be discussed in a later section. Many of the elements which volatilize excessively in vacuum can be added in large amounts with little or no loss if an inert atmosphere is employed. Since there is no very satisfactory way of removing carbon monoxide when melting is accomplished in an inert gas at atmospheric pressure, it is essential to use purer starting materials and add either special deoxidizers or relatively large amounts of carbon. Increased carbon additions are believed to raise the limit of the partial pressure of carbon monoxide under which adequate deoxidation of the molybdenum is attainable, but the ex-

---

[1] Climax Molybdenum Company of Michigan.

[2] Numbers in parentheses refer to the Bibliography at the end of the paper.

Contributed by the Joint ASTM-ASME Committee on Effect of Temperature on the Properties of Metals and presented at the Annual Meeting, New York, N. Y., November 26–December 1, 1950, of The American Society of Mechanical Engineers.

Note: Statements and opinions advanced in papers are to be understood as individual expressions of their authors and not those of the Society. Manuscript received at ASME Headquarters on September 11, 1950. Paper No. 50—A-70

cess carbon remains in the alloy. When special deoxidizers such as aluminum and magnesium are used, residual carbon can be held to a minimum and, although some of these deoxidizing elements remain in the casting, no deleterious effects so far have been detected.

To facilitate the preparation of materials for the study of molybdenum-base alloys, small ingots approximately 2 in. diam × 8 in. long were made in a special machine by remelting rolled bars of low oxygen content in an argon atmosphere, utilizing small additions of carbon and other deoxidizing agents to assure adequate deoxidation. By this method elements too volatile to be added during melting in vacuum could be added in appreciable quantities with adequate recovery and control of their concentrations. To be consistent throughout the investigation, alloys of elements which were not so highly volatile were also prepared in this manner.

The advent of the arc-cast process has greatly simplified the production of high-purity molybdenum and its alloys in sizes which permit extensive testing. Until quite recently the existing information on molybdenum-base alloys was founded almost entirely on studies of samples produced by powder metallurgy. The use of melted and cast samples eliminates the experimental difficulties connected with sintering at very high temperatures, and the uncertainties of homogeneity, density, and state of equilibrium inherent in the powder-metallurgy technique. The availability of cast samples, therefore, justifies a critical review of the nature of the alloy systems previously studied and invites the study of many new systems.

General Properties of Unalloyed Cast Molybdenum

Molybdenum ingots, pure except for carbon, are made up of very coarse columnar grains; nevertheless, they are quite malleable above 2200 F. After a certain amount of working and recrystallization, the metal is also malleable at lower temperatures and can be formed into useful shapes by conventional methods.

Heating for forging or rolling may be performed in an ordinary gas-fired furnace. If the mixture is adjusted to produce a slightly reducing atmosphere, the oxidation loss is insignificant. When the ingot is forged, however, some oxidation occurs while the molybdenum is exposed to the air. Oxidation losses during hot-working range from 1 to 2 per cent, when the metal is rolled in a conventional rolling mill, and heating is accomplished in a reducing atmosphere, to 6 to 10 per cent during extensive forging, when heating is accomplished in an oxidizing atmosphere. As properly deoxidized molybdenum is free from porosity, oxidation occurs only at the surface. The oxides developed can be removed readily by pickling in a bath composed of 90 per cent potassium hydroxide and 10 per cent sodium nitrite ($NaNO_2$), maintained at 600 to 700 F.

Pure molybdenum reacts to annealing in an orthodox manner. Reheating the cast ingot has no appreciable effect on grain size, carbide distribution, or hardness. Plastically deformed grains can be recrystallized at temperatures dependent upon the amount of work, the actual working temperature, and the time at the annealing temperature. The lowest temperature at which recrystallization will start is approximately 1650 F; only severely worked metal such as cold-rolled sheet begins to recrystallize at so low a temperature. Less severely worked metal, such as bar stock, rolled from billets heated to 2000 to 2100 F, begins to recrystallize at about 1900 F, and recrystallization may be completed after 1 hr at 2100 F. Bars reduced 15 per cent in cross-sectional area by forging in the range 2300 to 2600 F will undergo extensive recrystallization on annealing at 2600 to 2800 F.

Pure molybdenum is relatively soft as-cast, 170 to 190 VPN, but hardens rapidly on working and may attain 300 VPN after severe cold work. Complete recrystallization reduces the hardness to that of the metal as-cast, or slightly below.

Some representative curves have been selected to show the ductility, strength, and hardness of pure molybdenum. These properties, of course, depend to a large extent on the amount and type of work which has been applied. However, after working sufficiently to confer uniformity and a fine grain size, these properties depend primarily on the annealing temperature. Figs. 1 and 2 show the variation with annealing temperature of the hardness and tensile properties of samples of $^1/_2$-in. round bar stock from a single heat of arc-cast molybdenum. Recrystallization greatly increases the elongation, but also reduces the strength considerably.

In most types of service, deformation of a part is undesirable and since the unrecrystallized molybdenum has been found more resistant to impact, i.e., it has a lower temperature for the transition from a ductile to a brittle fracture, full recrystallization is not recommended, except where service above the recrystallization temperature is anticipated, or where it is necessary to prepare the metal for further working. Recrystallization appears to be particularly objectionable for the more complicated stress systems. In the bend test on sheet, fully recrystallized molybdenum proves to be quite inferior, maximum capacity for bending occurring upon annealing in the range 1600 to 1800 F.

As indicated by the curves, annealing at high temperature reduces ductility. Annealing at still higher temperatures, e.g., 3200 to 3300 F, generally leads to a completely brittle fracture. The temperature for embrittlement varies considerably from heat to heat and with annealing time. The cause of this embrittlement is not well understood but such embrittlement is characteristic of all molybdenum so far tested, whether cast or formed by powder metallurgy.

The tensile properties of molybdenum are sensitive to the gage section diameter of the specimen and the elastic strain rate used in the test. The elongation and reduction of area are affected by the gage section diameter, and the yield strength is sensitive to the elastic strain rate. These effects are demonstrated in Tables 1 and 2.

The yield strength of an unrecrystallized 2 per cent tungsten-molybdenum alloy was found to be less sensitive to strain rate.

In the standard notched-bar Charpy test, molybdenum is brittle at room temperature. On the other hand, as in the case of iron and other metals, particularly those of body-centered cubic structure, the transition from the brittle to the ductile fracture occurs abruptly as the testing temperature is raised, the stress sys-

TABLE 1 EFFECT OF STRAIN RATE ON YIELD STRENGTH ANNEALED AND RECRYSTALLIZED, UNALLOYED MOLYBDENUM—ROLLED $^1/_2$-IN. PLATE

Elastic strain rate, per cent per hr	Yield strength, psi
0.12	24100
0.70	34500
1.8	40400
9.7	43200
12.8	48200
19.8	49500

TABLE 2 EFFECT OF GAGE SECTION DIAMETER ON ELONGATION AND REDUCTION OF AREA, 2 PER CENT TUNGSTEN-MOLYBDENUM ALLOY—$^1/_2$-IN-DIAM HOT-ROLLED BAR

	Gage diameter = 0.500 in.				Gage diameter = 0.250 in.			
Condition	Tensile strength, psi	Yield strength, psi	El., per cent	RA, per cent	Tensile strength, psi	Yield strength, psi	El., per cent	RA, per cent
As-rolled	83200	72200	4.0	3.8	76400	69500	13.0	11.7
1 hr at 1800 F	77300	70000	3.5	3.0	77600	69900	23.5	18.2
1 hr at 2300 F	66400	49600	30.5	23.6	66700	49900	46.0	34.9

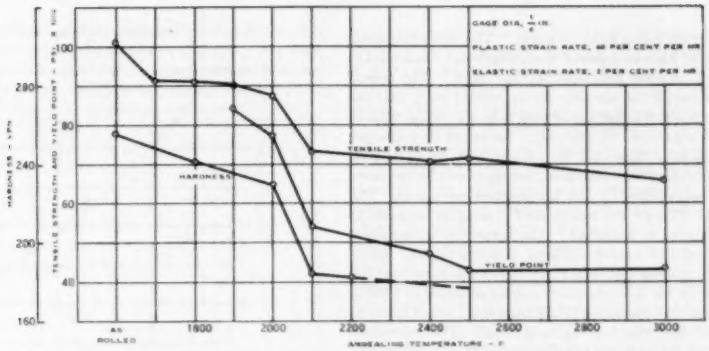

FIG. 1 TENSILE STRENGTH, YIELD POINT, AND HARDNESS OF 1/2-IN. ROLLED ROUNDS OF ARC-CAST MOLYBDENUM ANNEALED AT VARIOUS TEMPERATURES

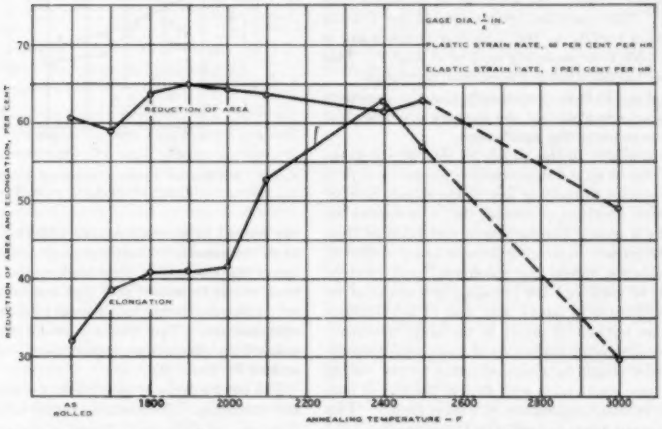

FIG. 2 ELONGATION AND REDUCTION OF AREA FOR 1/2-IN. ROLLED ROUNDS OF ARC-CAST MOLYBDENUM ANNEALED AT VARIOUS TEMPERATURES

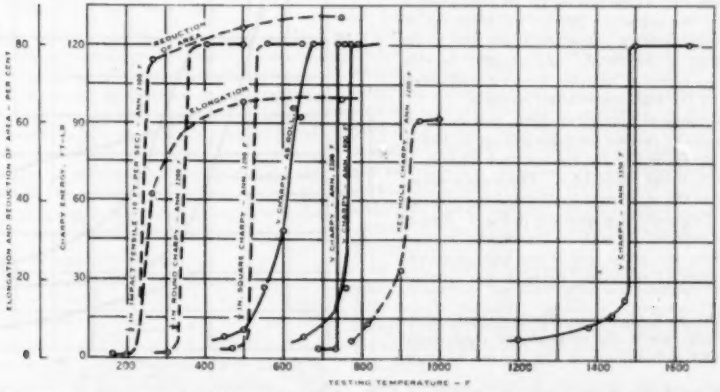

FIG. 3 EFFECT OF ANNEALING TEMPERATURE AND TYPE OF TEST ON THE BRITTLE-TO-DUCTILE TRANSITION TEMPERATURE OF ARC-CAST MOLYBDENUM; ROLLED BARS

tem and strain rate being held constant. The transition-temperature ranges for various types of impact tests are illustrated in Fig. 3 for rolled arc-cast molybdenum bar stock. The tensile impact test represents the simplest stress system used, and the values of elongation and reduction of area reflect a comparatively low transition temperature in this test. As would be expected, the energy absorption values for the Charpy test, using various specimen shapes, reflect high transition temperatures for the more complicated stress systems, i.e., for the notched specimens. The standard V-notch Charpy test was applied to samples annealed at various temperatures as indicated. The transition-temperature ranges for worked but unrecrystallized V-notch Charpy specimens, as rolled or annealed at 1800 F, are somewhat lower and less sharp than those for the recrystallized samples annealed at 2200 to 2300 F, indicating that the unrecrystallized metal is more likely to withstand impact than the recrystallized metal. The transition-temperature range for as-rolled samples probably depends on the finishing temperature. In some tests on 2 per cent tungsten-molybdenum alloys the transition-temperature range for samples as-rolled was found to be higher than the range for samples stress-relieved at 1800 F. The transition temperature in the V-notch Charpy test increases rapidly as the annealing temperature is raised and reaches 1500 F on annealing for 2 hr at 3350 F. This reflects the tendency to embrittlement mentioned previously.

The points placed at 120 ft-lb mean simply that the specimens stopped the pendulum completely at the temperature indicated; this energy value has no particular significance.

The few results available to the author at this time indicate that, above 1600 F, the creep and stress-rupture properties of pure molybdenum are superior to those of any of the cobalt, iron, or chromium-base alloys, provided, of course, that a protective atmosphere or coating is used. Comparison of molybdenum from various sources with respect to creep or stress-rupture properties may be quite misleading unless the specimens have received equivalent amounts of work and are in comparable states of recrystallization. Differences in purity may lead to recrystallization of some samples but not of others in the same treatment. Furthermore, before comparing samples by any elevated-temperature test, the samples should be annealed either at the testing temperature for a time comparable with that of the test or considerably above the testing temperature for a short period. This is particularly important when testing near the recrystallization-temperature range, of about 1600 to 2000 F, for pure molybdenum. It is recognized that the purity of molybdenum will vary as the process for its production is varied and that the impurities present will affect significantly the recrystallization temperature and the stress-rupture properties of the metal. Any impurity in solid solution may be expected to raise the recrystallization temperature and the high-temperature strength.

Some precise values of Young's modulus, bulk modulus, and Poisson's ratio at various temperatures up to 1600 F were obtained by Frederick[3] for arc-cast molybdenum in the form of $\frac{1}{2}$-in. round rolled bars. These are a valuable supplement to the other data on elevated-temperature properties and are presented graphically in Fig. 4. Special techniques are required for such measurements, since at high temperatures the creep rate is too high to permit accurate measurement of elastic strain in the ordinary tensile test.

Of the various tests applied to molybdenum and molybdenum-base alloys, one of the simplest and most useful has been the Vickers hot-hardness test, for hot hardness

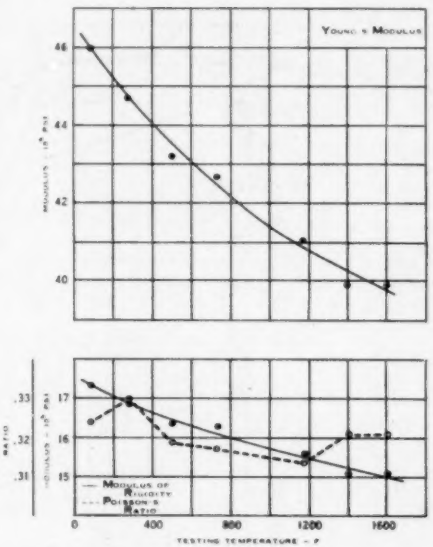

FIG. 4 EFFECT OF TEMPERATURE ON ELASTIC PROPERTIES OF ARC-CAST MOLYBDENUM AS HOT-ROLLED

has proved to be a convenient criterion for selecting materials likely to possess strength at high temperature and worthy of more time-consuming tests such as the stress-rupture test. At least, it can be shown that high hot hardness is a necessary—if not sufficient—property for good load-carrying capacity at high temperatures. The Vickers hot-hardness apparatus was developed for classifying chromium-base alloys and has been described by Bens (2).

The hot hardness of molybdenum is quite sensitive to working and annealing. Hot-hardness curves for pure molybdenum in its

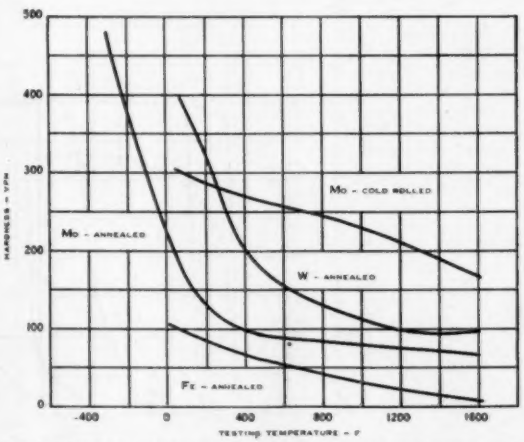

FIG. 5 MAXIMUM AND MINIMUM HOT HARDNESS OF PURE MOLYBDENUM, AND MINIMUM HOT HARDNESS OF TUNGSTEN AND IRON

[3] Dr. Julian R. Frederick, Brown University, Providence, R.I.

softest condition (worked and fully annealed) and in its hardest condition (severely cold-rolled) are presented in Fig. 5. For comparison, curves for fully annealed pure iron, and pure tungsten are included. Like other metals, molybdenum in its softest condition

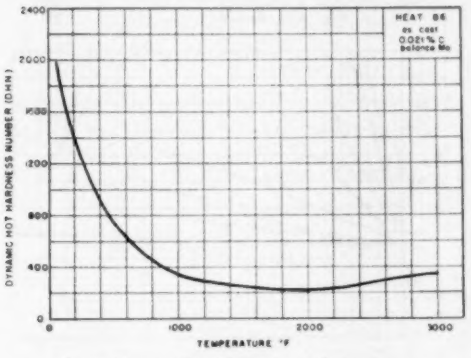

FIG. 6 DYNAMIC HOT HARDNESS OF MOLYBDENUM

exhibits a rapid rise in hardness when cooled below a characteristic temperature. For molybdenum, this temperature is about 400 F. The temperature at which the rapid change in slope occurs is reduced by cold-working, as shown by the upper curve.

Relative hardness up to 3000 F has also been determined for pure molybdenum and a number of its alloys by means of a specially built apparatus which drops a rod tipped with a tungsten-carbide ball onto a disk-shaped specimen resting horizontally in an argon-filled furnace. The rod is caught on the first bounce by a solenoid activated electronically. The hardness scale is arbitrary, each value being equal to the energy of the rod divided by the volume of the impression (kg per mm sq), but these values can be correlated with Vickers numbers quite nicely by applying both tests to a variety of specimens. This apparatus will be more completely described in a later publication. The weight of the rod is 385 grams and the height of fall 10 in. Fig. 6 shows the dynamic hardness of pure molybdenum up to 3000 F. By comparison with this curve, the effects of various alloys on hardness up to 3000 F may be evaluated.

THE NEED FOR ALLOY ADDITIONS

Although pure molybdenum is applicable for many purposes simply because it is a solid at temperatures where most metals and alloys are liquid, there are many potential applications requiring considerably more resistance to deformation at high temperatures than is possessed by pure molybdenum. Therefore a primary purpose of adding alloys is to improve hot strength. Since we have selected hot hardness as our preliminary index of strength, we will consider the possible effects of alloying elements on this property.

The addition of an alloying element may contribute to hot hardness by one or more of the following mechanisms:

1 Solid solution-hardening at equilibrium.
2 Solid solution-hardening enhanced by supersaturation.
3 Augmentation of work-hardening.
4 Precipitation-hardening.

The effect of temperature on the hardness as well as the permanence of the hardness at any given temperature will depend on the mechanism responsible for the increase in hardness. The first mechanism may be assumed to lead to a stable condition in which no change in hardness will occur at constant temperature. The others are inherently transient, and the hardness gained will decrease gradually at constant temperature if the temperature is high enough; however, these have the distinct advantage of permitting control of the hardness of a given alloy. Hardness also may be increased by adding sufficient alloy to introduce a large amount of a new phase or to change the structure entirely. However, experience so far in forging alloys indicates that many of the elements under consideration will increase the hot hardness beyond the limits of forgeability with available equipment and known techniques at concentrations far below the limit of solid solubility at the forging temperature. Since it is not likely that the presence of new phases will improve forgeability, there is no practical necessity for investigating two-phase alloys until forging techniques are further advanced, except in so far as is necessary to establish the solubility limits. At present, from a practical standpoint, our choice among the various binary systems depends largely on which encompass alloys that can be worked at the highest hot-hardness level.

Alloy additions reduce the grain size of the cast metal and, although it might be expected that fine-grained ingots would be less susceptible to cracking on forging, no elements have been found so far which will refine the grain to a useful extent without increasing the hardness beyond the forgeability limit.

PRELIMINARY SELECTION OF ALLOYING ELEMENTS ON BASIS OF SOLUBILITY AND VAPOR PRESSURE

The elements which are worthy of consideration in connection with molybdenum-base alloys have been reduced to a reasonable number by the following general considerations. Careful examination of published information together with a certain amount of previous experience indicated that only the transition elements were soluble in solid molybdenum to any appreciable extent. It was assumed that the addition of elements which simply formed hard, brittle, insoluble compounds would not be likely to broaden the usefulness of molybdenum. Of the transition elements, many are too rare or expensive to be considered. Those which were sufficiently common to be of interest are titanium, vanadium, chromium, manganese, iron, cobalt, nickel, zirconium, columbium, tantalum, tungsten.

Cerium, thorium, and uranium are also of some interest but will not be considered herein.

Though little solubility was expected, three nontransition elements were also considered since it was thought that they might prove to be effective deoxidizing agents, if not valuable as alloys, i.e., beryllium, aluminum, silicon.

The information available in the literature concerning the molybdenum-rich alloys of the elements under consideration can be summed up as follows: Fairly good evidence that tungsten, columbium, tantalum, and chromium form complete series of solid solutions with molybdenum is available from powder-metallurgy work (3, 4, 5, 6). Some data concerning the lattice parameter, oxidation resistance, and solidus temperatures of such alloys are also available (7). The molybdenum-chromium system exhibits a minimum in both solidus and liquidus at approximately 3200 F and 77 per cent chromium. Molybdenum-rich alloys of iron and cobalt were also studied by Sykes (8, 9), and those of nickel by Ellinger (10).

Little information has been published concerning the molybdenum-rich alloys of the other transition elements under consideration, namely, titanium, vanadium, manganese, and zirconium. Likewise, little is available from the literature as to the effect of the nontransition metals being considered (beryllium, aluminum, and silicon).

The solubility limits of aluminum, silicon, iron, cobalt, and nickel have been determined recently in the laboratory of the

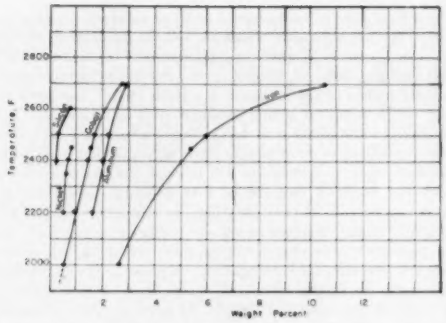

FIG. 7 SOLUBILITY LIMIT OF VARIOUS ELEMENTS IN MOLYBDENUM

author's company by measuring the lattice parameters of a large number of cast samples containing these elements in various amounts after appropriate heat-treatment. These limits are shown in Fig. 7 as a function of temperature. Although the values for iron, cobalt, and nickel at the higher temperatures differ only slightly from those reported by other investigators, our values for iron and cobalt at the lower temperatures are somewhat lower than previously reported. It was found necessary to hold specimens of these alloys for considerable periods of time to attain substantial equilibrium in the neighborhood of 2000 F. The solubility of aluminum and silicon was higher than expected and justifies their consideration as alloying elements.

The solubility of beryllium was not determined accurately, but it can be placed below 0.1 (weight) per cent at 2000 F with certainty. Unlike carbon, it was found to have a tremendous effect on hardness and therefore will be considered along with the other alloying elements.

The solubility limits for titanium and vanadium have not been established, but a sufficient number of samples were examined metallographically and by x-ray methods to establish that at least 20 per cent titanium and 33 per cent vanadium are soluble in molybdenum at 2000 F. Vanadium is body-centered cubic at room temperature, and it is considered likely that it forms an uninterrupted series of solid solutions with molybdenum. Titanium also is body-centered cubic above 1650 F, and it is quite possible that above this temperature, a continuous series of solid solutions occurs in the titanium-molybdenum system. The solubility of zirconium was found to be between 3 and 5 per cent in the neighborhood of 2000 F.

The problem of vaporization must be taken into account in selecting an alloying element to be used in the vacuum-arc process. Up to the present time, hot-working difficulties have limited the concentrations of the more volatile elements to such an extent that volatilization has not been a serious restriction. However, as hot-working techniques are improved and harder alloys are desired, the question of vapor pressure will become more important. On the basis of vacuum-melting experience, the elements under consideration so far can be divided into two quite distinct classes, those which volatilize excessively and those which do not. Those which volatilize excessively are beryllium, aluminum, silicon, chromium, manganese, iron, cobalt, and nickel. Titanium, vanadium, zirconium, columbium, tantalum, and tungsten cause no difficulty due to volatilization. Except for iron and cobalt, only a few tenths of 1 per cent of the volatile group can be retained on vacuum-melting. Volatilized metal forms a crust on the ingot and may reduce the recovery of sound metal considerably. As stated previously, the solubility and hardness data presented

TABLE 3 HARDNESS OF UNALLOYED MOLYBDENUM

Temperature, F	Condition	Vickers hardness, 10 kg	Dynamic hardness, kg per mm sq
75	As-cast	175	...
75	Cast and annealed	160	...
1500	As-cast	70	...
1500	Cast and annealed	70	280
3000	Cast and annealed	...	300

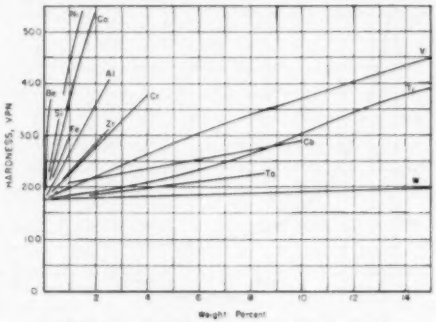

FIG. 8 ROOM-TEMPERATURE HARDNESS OF MOLYBDENUM-BASE ALLOYS AS-CAST

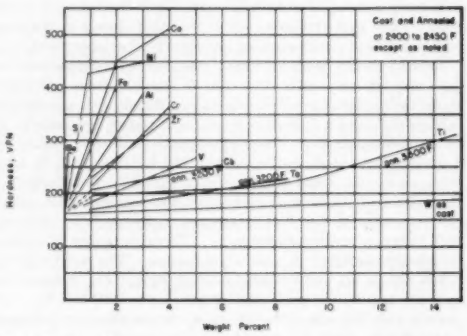

FIG. 9 ROOM-TEMPERATURE HARDNESS OF MOLYBDENUM-BASE ALLOYS

herein for the more concentrated alloys of the volatile group were obtained from ingots melted in argon at 1 atm pressure.

SOLID SOLUTION-HARDENING EFFECTS

A series of curves is presented to show the effects of the various elements on the Vickers hardness of molybdenum measured at room temperature and in the range 1400 to 1600 F, and on the dynamic hardness measured at 3000 F. For comparison, the values characteristic of pure molybdenum are given in Table 3.

All of the data in this section apply to unworked samples. However, in general, the values may be taken to apply to worked and fully annealed samples as well.

Fig. 8 shows the room-temperature Vickers hardness as a function of concentration for various alloys in the cast condition. As would be expected, the less soluble elements increase the hardness most rapidly.

Similar curves are presented in Fig. 9 for alloys annealed and slow-cooled to reduce segregation and to permit precipitation in any supersaturated concentration ranges. Precipitation oc-

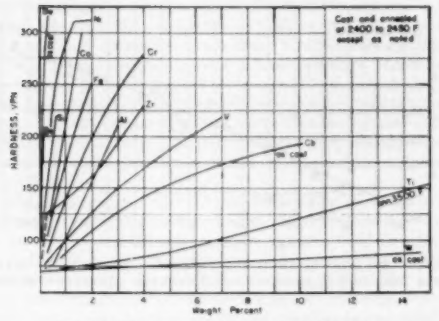

FIG. 10 HARDNESS OF MOLYBDENUM-BASE ALLOYS AT 1400 TO 1600 F

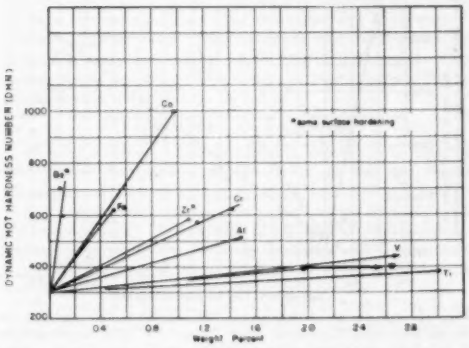

FIG. 11 DYNAMIC HARDNESS OF MOLYBDENUM-BASE ALLOYS AT 3000 F AFTER 1 HR AT 3000 F

curred in the more concentrated beryllium, nickel, and cobalt alloys, causing the curves for these elements to change slope above the solubility limit. Presumably, the inflections would occur at lower concentrations (closer to the solubility limit) if the cooling rate were sufficiently slow. Aside from these effects, the curves lie in nearly the same relative position for the annealed alloys as for the alloys as-cast.

Since curves representing the variation of Vickers hardness with temperature for various alloys indicated practically no change in hardness with temperature changes in the range 1400 to 1600 F, data for Vickers hardness in this temperature range have been combined and are presented in Fig. 10. It may be seen that except for the chromium curve, the slopes of the curves for the various elements lie in the same relative order as those for the room-temperature-hardness curves. The chromium curve for the hot-hardness tests lies above those for aluminum and zirconium, whereas, in the room-temperature tests, it was nearly coincident with the zirconium curve and considerably below the aluminum curve.

Each of the Vickers hardness curves presented represents a large number of hardness readings, the data having been obtained by exploring the hardness of strips cut from graded ingots.

The relative hardness from room temperature to 3000 F was obtained for a number of alloys by applying the dynamic test described previously. Fig. 11 represents the data obtained at 3000 F after holding 1 hr. The hardness differences would be small in terms of Vickers numbers, and each curve is established by only 1 or 2 points derived from the hardness-temperature curves. Titanium and vanadium as well as tungsten seem to have little effect on hardness at this temperature, and the relative potency of aluminum seems to have been decreased considerably compared to that of zirconium and chromium by the change from the 1400 to 1600 F range to 3000 F. Even at 3000 F, beryllium is seen to have a remarkable effect on hardness. Silicon and nickel alloys have not yet been subjected to this test.

CONTROL OF HARDNESS BY HEAT-TREATMENT

Preliminary tests designed to detect precipitation-hardening in binary alloys of molybdenum with beryllium, aluminum, and silicon; and in ternary alloys with titanium and carbon; and with zirconium and carbon, gave negative results. Sykes (8, 9) has shown that precipitation-hardening can be obtained in molybdenum-rich molybdenum-iron and molybdenum-cobalt alloys. However, the amounts of iron or cobalt necessary to obtain this effect are so great as to render the alloys too hard, even in their softest condition, to permit working.

Some very interesting reactions of molybdenum-beryllium alloys to heat-treatment were obtained. Beryllium apparently is retained in supersaturated solution as-cast, for, although the cast metal containing 0.05 per cent or more beryllium is very hard, reheating in the range 2000 to 3000 F and slow-cooling causes precipitation and softens the metal. The hardness is regained by heating again to 3200 F and cooling at a moderate rate. It is evident, therefore, that the hardness of such alloys may be controlled by heat-treatment. The data of Table 4 illustrate these effects.

TABLE 4 EFFECT OF BERYLLIUM ON HARDNESS OF MOLYBDENUM

Beryllium, per cent	Carbon, per cent	Treatment	Vickers hardness
0.10	<0.01	As-cast	351
0.34	0.018	As-cast	380
		(a) 58 hr — 2400 F — slow cool	280
		(a) + 1 hr 2700 F—quench	300
		(a) + 2 hr 2400 F—slow cool	265
0.46	0.018	As-cast	392
		1 hr 3000 F—slow cool	219
0.095	0.077	As-cast	359
		1 hr 3000 F—slow cool	225
0.05	0.064*	As-cast	359
		1 hr 3000 F—slow cool	245
0.12	0.05	(b) 2 hr 3200 F—fast furnace cool	433
		(b) + 1 hr 3000 F—slow cool	224

* Added to charge.

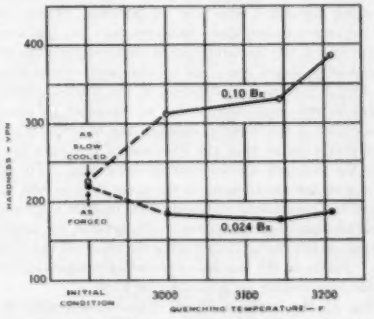

FIG. 12 EFFECT OF QUENCHING ON HARDNESS OF MOLYBDENUM-BERYLLIUM ALLOYS

Fig. 12 shows the increase in hardness obtained as the quenching temperature was raised for a 0.1 per cent beryllium alloy.

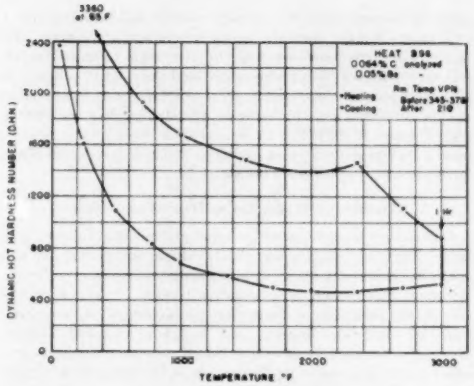

FIG. 13 DYNAMIC HOT HARDNESS OF MO-BE ALLOYS

The lower curve indicates that 0.024 per cent beryllium is insufficient to permit hardening by quenching.

The dynamic hot-hardness test was applied to several molybdenum-beryllium alloys, and Fig. 13 is typical of the results obtained. The softening obtained by reheating is strikingly demonstrated by this curve, beginning at about 2350 F. The alloy was hard originally.

These results indicate that the increase of hardness on quenching is due simply to the retention of beryllium in a supersaturated solid solution, but there remains the possibility that these alloys may be hardened to an even greater extent by precipitation-hardening. This possibility is being explored.

In order to compare the effects of various alloying elements on work-hardening and on the temperatures at which softening and recrystallization take place, a number of alloys were reduced from $1^1/_2$ in. diam to diameters ranging from 0.63 in. to 0.82 in. by impact-extrusion at 2500 to 2600 F. These were then annealed 1 hr at various temperatures, tested for hardness, and examined metallographically to estimate the degree of recrystallization.

Figs. 14, 15, and 16 show hardness and recrystallization-temperature data plotted to compare the effects of the elements on work-hardening and resistance to recrystallization and softening on annealing. The actual amounts of the alloying elements present are not important since the relationships sought comprised those between solid-solution hardness and (*a*) the amount of work-hardening, (*b*) the temperature required to soften the work-hardened alloy 50 per cent, and (*c*) the temperature required to effect 50 per cent recrystallization of the work-hardened alloy. In order to minimize scatter due to variation in composition from one part of the ingot to another, the hardness after full recrystallization rather than the hardness of the ingot as-cast was used as the measure of solid solution-hardening. The effects of variations in size of extrusion in the range 0.63 to 0.83 in. and in extrusion temperature in the range 2500 to 2600 F were found to be small enough to permit general comparisons, yet large enough to discourage fine distinctions among the effects of the various elements. Points on the graphs representing samples of essentially the same composition are joined by tie lines.

In Fig. 14 the hardness of the alloys as extruded is plotted against the hardness after full recrystallization. The difference is a measure of work-hardening and is observed to increase regularly with the amount of solid solution-hardening, regardless of which element is employed—with the exception of carbon. Increasing the carbon content does not increase the work-hardening,

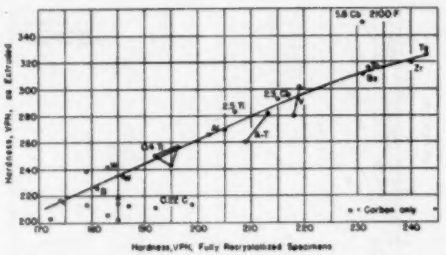

FIG. 14 RELATION OF AMOUNT OF WORK-HARDENING TO AMOUNT OF SOLID SOLUTION-HARDENING FOR EXTRUDED MOLYBDENUM-BASE ALLOYS

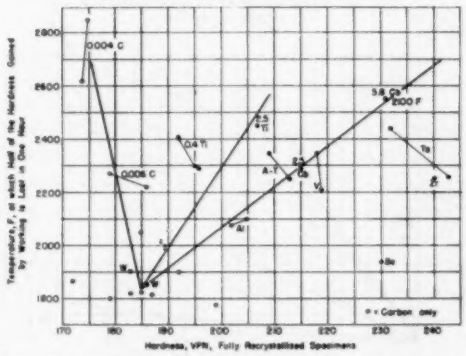
0.004 C
0.006 C
5.8 Cb
2100 F
Temperature, F, at which Half of the Hardness Gained by Working is Lost in One Hour
Hardness, VPN, Fully Recrystallized Specimens
• = Carbon only

FIG. 15 RELATION OF SOFTENING TEMPERATURE TO AMOUNT OF SOLID SOLUTION-HARDENING FOR EXTRUDED MOLYBDENUM-BASE ALLOYS

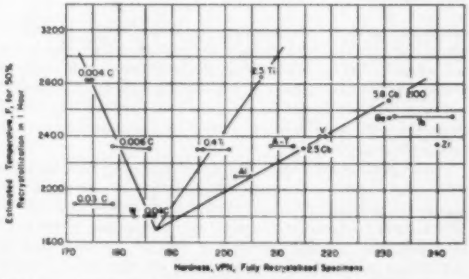

FIG. 16 RELATION OF RECRYSTALLIZATION TEMPERATURE TO AMOUNT OF SOLID SOLUTION-HARDENING FOR EXTRUDED MOLYBDENUM-BASE ALLOYS

since it does not go into solid solution in the concentration range under consideration. The point for columbium lying above the curve represents a sample extruded at 2100 F and is not comparable.

Fig. 15 was derived by selecting, through interpolation, the annealing temperatures necessary to obtain hardnesses halfway between those of the samples as extruded and those of the fully recrystallized samples. These temperatures were then plotted against the hardnesses of the fully recrystallized samples to ob-

tain Fig. 15. Probably this method is sufficiently accurate to establish the superiority of the titanium alloys with respect to retention of work-hardness on annealing. The tantalum and zirconium alloys softened at relatively low temperatures, considering the amount of solid solution-hardening involved, and the beryllium alloy also lost half of its hardness at a relatively low temperature. However, its hardness was higher than that of most of the other alloys as extruded, and reference to the previous section will show that the loss in hardness is due to precipitation as well as release of strain.

The estimated figures for per cent recrystallization were plotted against annealing temperature, and straight lines were drawn between the points. The temperatures at which these lines intersected the 50 per cent line were then plotted against the hardness of the fully recrystallized samples to give Fig. 16. This graph also shows the titanium alloys to be superior with respect to the high temperature required for recrystallization as compared to other alloys with comparable solid solution-hardening. Carbon, in contrast to the other elements, reduces the recrystallization temperature; in fact, the higher-carbon samples are not represented on this graph, since they were more than 50 per cent recrystallized as extruded. Recrystallization of the lower-carbon samples is probably retarded by the presence of oxygen. The tantalum and zirconium alloys appear to have relatively low recrystallization temperatures.

Workability of Alloys

All alloy additions which significantly increased the hardness complicated the problem of fabrication of the cast ingots. Throughout the investigation, evidence was obtained that the lack of hot plasticity was the result of intergranular weakness of the cast structure. The addition of alloying elements appears to increase the difference between granular and intergranular strength by increasing the hardness of the matrix without a corresponding increase in the grain-boundary cohesion.

The hardness of molybdenum is 70 VPN at 1600 F. With the exception of molybdenum-beryllium and molybdenum-zirconium alloys, it has so far been possible to forge only those alloys whose hardnesses at 1600 F do not exceed 90 VPN. However, additions conferring lesser increases in hardness have been found sufficient to raise the degree of work-hardening, and the recrystallization temperature of worked alloys to a useful extent.

Extrusion experiments indicated that greater deformation of the materials was possible by these operations than by hammer-forging. Further intensive study of the factors affecting hot plasticity of the cast aggregates is essential to the development of commercially feasible fabrication methods.

It is indicated that, if suitable dies could be obtained, it would be possible by extrusion to make useful articles from alloys with an initial hardness at 1600 F as high as 180 VPN.

Acknowledgment

The information presented herein has been developed by the Research Laboratory of the Climax Molybdenum Company during an extensive investigation of the metallurgy of molybdenum and molybdenum-base alloys. Much of the information was obtained under Contract N8onr-78700, between the Climax Molybdenum Company of Michigan and the Office of Naval Research, United States Navy. The technical contributions of the personnel of the Research Laboratory, the support and encouragement of the Office of Naval Research, and the valued advice of the Climax administrative and technical supervisory staff are herewith acknowledged.

BIBLIOGRAPHY

1 "The Melting of Molybdenum in the Vacuum Arc," by R. M. Parke and J. L. Ham, Trans. AIME, vol. 171, 1947, pp. 416–430.

2 "Hardness Testing of Metals and Alloys at Elevated Temperatures," by F. P. Bens, Trans. ASM, vol. 38, 1947, pp. 505–516.

3 "The Nature of Solid Solutions," by E. C. Bain, *Chemical and Metallurgical Engineering*, vol. 28, 1923, pp. 21–24.

4 "Structures and Microhardness of Binary and Ternary Systems of the Metals, Columbium, Tantalum, Molybdenum and Tungsten," by Helmut Bückle, *Metallforschung*, vol. 1, 1946, pp. 53–56.

5 "The Systems of Cr With W and Mo," by O. Kubaschewski and A. Schneider, *Zeitschrift für Elektrochemie*, vol. 48, 1942, pp. 671–674.

6 "X-Ray Analysis of Chromium-Molybdenum and Chromium-Tungsten Alloys," by W. Trzebiatowski, H. Ploszek, and J. Lobazowski, *Analytical Chemistry*, vol. 19, 1947, pp. 93–95.

7 "Measurements on the Oxidation-Resistance of High-Melting-Point Alloys," by O. Kubaschewski and A. Schneider, *Journal of the Institute of Metals*, vol. 75, 1949, pp. 403–416.

8 "The Iron-Molybdenum System," by W. P. Sykes, Trans. ASM, vol. 10, 1926, pp. 839–869.

9 "The Cobalt-Molybdenum System," by W. P. Sykes and H. F. Graff, Trans. ASM, vol. 23, 1935, pp. 249–285.

10 "The Nickel-Molybdenum System," by F. H. Ellinger, Trans. ASM, vol. 30, 1942, pp. 607–638.

Discussion

H. H. Hanink.[4] We believe that the author and others in their organization responsible for planning and carrying out the work reported in this paper have done an outstanding job of producing a maximum of necessary information in a relatively short time. This is particularly appreciated by those who see in molybdenum-base alloys one of the most promising solutions to the problem of producing durable components for future gas turbines, ramjets, and rockets, where metal temperatures may start at about 1800 F, and where the lack of adequate materials has been responsible for holding up almost immediate improvements in the efficiency, durability, and output of such engines. The problem is in urgent need of a practical solution, and we are pleased to see the urgency reflected in this effective approach to the utilization of molybdenum as a structural material.

From the specialized point of view of one interested in the application of molybdenum or its alloys to aircraft-engine components, some added emphasis might have been placed on the function of alloying elements in raising the recrystallization temperature independent of hardening action, since even hot-rolled and stress-relieved, pure molybdenum has useful strength but is extremely limited in its application by a low recrystallization temperature.

Because of weight considerations, most aircraft-engine applications of molybdenum will require fabrication of sheet-metal parts by forming and welding. The latter appears to be the only basic problem in this regard, since it is related to the lowered strength of recrystallized material in the welding-heat-affected zone. Here again, while proper welding techniques may minimize this effect, it is expected that the use of alloying elements to retard recrystallization might eventually provide the greatest help. Special brazing techniques also may be applicable to the problem by eliminating the need for welding, in some cases, but some increase in recrystallization temperatures is still required as compared to pure molybdenum.

Work on welding and sheet-metal fabrication by the writer's company, using pure molybdenum, or a tungsten chromium alloy has already shown promise, so that our optimistic outlook for the use of molybdenum in aircraft engines is considered justified.

Author's Closure

The remarks of Mr. Hanink are gratefully received. His interest in the subject is very encouraging. The author concurs

[4] Manager, Materials and Processes Research Division, Wright Aeronautical Corporation, a Division of Curtiss-Wright Corporation, Wood-Ridge, N. J

in the belief that special emphasis should be placed on evaluating the effects of various elements on the recrystallization temperature as well as on evaluation of their effects on hardness.

For the purpose of raising the temperature to which molybdenum can be heated without becoming unmanageably brittle, additional elements should be sought which raise the recrystallization temperature with the least accompanying increase in hardness. Fig. 16 as plotted was intended specifically to determine which elements are preferable in this respect but further studies of this type should be made using samples worked at lower temperatures. It is possible that an addition such as titanium would minimize the brittleness encountered on brazing.

It is believed that in order to avoid brittleness on welding, an element should be sought which will counteract the impurities which presumably cause molybdenum to be brittle as-cast or as-welded. Application of some simple test for evaluation of the room-temperature ductility of cast-molybdenum samples, which contain small percentages of various scavenger-type elements and which have been rolled or severely worked, then welded or reheated to some temperature near the melting point, might point to an addition which would leave molybdenum ductile as-welded.

Experience With Austenitic Steels in High-Temperature Service in Petroleum Industry

By M. E. HOLMBERG,[1] BARTLESVILLE, OKLA.

Experience in the petroleum industry shows there are other factors besides tensile, creep, and stress rupture to consider in the use of austenitic steels in high-temperature service. There is no advantage in using stabilized grades in many applications. A spheroidizing heat-treatment is generally effective where stabilized steel is required. The coefficient of expansion and the thermal conductivity have been important factors in thermal-shock and thermal-fatigue failures in austenitic steels.

Introduction

HIGH temperatures and high pressures, for many years, were associated with improvements in refining processes. In many cases, maximum improvement was impossible because suitable steels were not available to withstand the ever-higher temperatures and pressures. The refineries demanded better high-temperature steels and were quick to use the new alloys developed by the steel industry. It is not surprising, therefore, that the oil industry has a wealth of experience in the use of materials in high-temperature service.

The most severe high-temperature service has been in still tubes, gas-cracking furnaces, and associated piping. Fluid temperatures of 1350 F have not been uncommon. Pressures as high as 5000 psi have been used. Metal temperatures of 1450 F are common. Due to the formation of coke on the inside of tubes, much higher temperatures frequently are encountered unintentionally. Cyclic operations, involving periodic changes in temperatures, have increased the severity of conditions.

This paper is devoted mostly to the austenitic steels because of the recent interest of many in the use of these steels for high-temperature service. Reference is also made to the ferritic steels, which for many purposes have definite advantages. The purpose of the paper is to call attention to factors that should be considered in using austenitic steels in high-temperature service. It is based on performance of materials in service and examinations of material removed from service.

High-Temperature Properties

The importance and relationship of high-temperature strength, creep, and stress rupture are recognized in high-temperature designs. These might be considered the basic high-temperature properties. If high-temperature equipment does not have sufficient strength at temperature to hold together, if it deforms more than the service can tolerate, or if it deforms and then breaks, the material or the design is obviously unsatisfactory.

As a result of work done by the technical societies and industry, these properties are well understood, and there is now a large amount of high-temperature tensile, creep, and stress-rupture data available. These properties have been discussed so thoroughly by others that further attention will not be given to them in this paper. However, in passing over these basic properties so quickly, it is not intended that their importance be depreciated in any way.

If these important properties are recognized so generally, why then do premature failures still occur in high-temperature service? The answer is that, in addition to these basic properties, there are other factors to consider. The operation of pressure piping and other pressure equipment above 900 F is relatively new. It is not surprising, therefore, that in some cases the factor that proved to be the most important was overlooked completely in the original design.

In designing one gas-cracking furnace, adequate provision was made for tensile, creep, and stress-rupture requirements. In fact, the pressures were so low that these requirements were not too serious, even though the fluid temperature was 1350 F. By using 25 Cr-20 Ni, the design requirements were easily met; yet failures occurred in a matter of days. The 25 Cr-20 Ni had the required high-temperature strength called for in the design, but it did not have the necessary high-temperature abrasion resistance, which had not been recognized even as a factor. Experience showed that strength was not the governing factor, but that abrasion resistance was. Experience further showed that the lower-strength 18 Cr-8 Ni was more economical in the service than the 25 Cr-20 Ni.

The intent is not to imply that high-temperature abrasion resistance is a factor that should be considered in every high-temperature application. It probably is of no importance in most cases; but, as in the case cited, it may become the most important consideration. Similarly, experience has shown that certain other factors are important, and those that are likely to prove important in most high-temperature applications will be discussed briefly.

Stabilized Versus Nonstabilized

Should stabilized or nonstabilized steel be used? This is the first question raised when the use of austenitic steels is considered. A check of the literature, and the manufacturers' data show that, if the steel is to be welded or will operate in the temperature range of 750 to 1550 F, the stabilized grades of austenitic steels should be used. This statement is so often made and is so positive that there seems to be little reason to question it. However, it was intended for and applies to corrosive service. Experience has shown that it does not necessarily apply to high-temperature service.

The "stainless" steels, as the name implies, were developed principally for corrosive service. Most people still do not associate them with high-temperature service. This failure to distinguish between the two types of service is responsible for some of the mistakes. To further confuse the matter, it is of course possible to have corrosive conditions and high-temperature conditions existing simultaneously or at different times in the same equipment.

The first large use of austenitic steels by the oil industry was in still tubes. Corrosion was severe from sulphur compounds in the crudes. Operating temperatures were in the carbide-pre-

[1] Phillips Petroleum Company.

Contributed by the Joint ASTM-ASME Committee on Effect of Temperature on the Properties of Metals and presented at the Annual Meeting, New York, N. Y., November 26–December 1, 1950, of The American Society of Mechanical Engineers.

Note: Statements and opinions advanced in papers are to be understood as individual expressions of their authors and not those of the Society. Manuscript received at ASME Headquarters, August 25, 1950. Paper No. 50—A-41.

cipitation range of 750 to 1550 F. It seemed obvious that stabilized tubes should be used, even though no welding was involved. Though titanium-stabilized tubes were used satisfactorily in one installation for approximately 10 years, later experience indicated that plain 18 Cr-8 Ni would have performed equally as well, and possibly even better.

Large tonnages of austenitic steels have been used in gas cracking tubes. Fluid temperatures up to 1350 F and very high heat inputs exist. Fittings were attached to the tubes by welding. Unlike the still tubes, where pressures were as high as 2500 psi, the pressures in the gas-cracking furnaces were less than 60 psi. Again, the conditions indicated stabilized austenitic stainless steel should be used, and it was, originally.

In both still tubes and in gas cracking tubes, the inside surfaces often become carburized. When this was discovered, the logic in using stabilized tubes was immediately questioned. Carburization to depths of $^1/_8$ in. was common, and analyses showed as high as 3 per cent carbon. It was obvious that columbium or titanium in sufficient quantities to satisfy the original carbon content was ineffective when the carbon content increased as much as 30 times. Test installations and replacements with the nonstabilized austenitic steels showed they were entirely satisfactory.

Here was corrosive service—from the sulphur compounds—and operations within the carbide-precipitation range. Why did not intergranular corrosion take place? The hypothesis offered is that an electrolyte is necessary for intergranular corrosion and that the operating temperatures are too high for an electrolyte to exist. On this basis, installations have been made in other services using nonstabilized austenitic steels. For example, a superheater used to superheat a mixture of steam and air to 1200 F was made from 18 Cr-8 Ni (Type 304) tubes. This has been in service since June, 1944, and all indications are that the 18 Cr-8 Ni is satisfactory.

There are precautions to be observed when nonstabilized austenitic steels are used in high-temperature service. Even though intergranular corrosion may not develop while the metal is at the operating temperatures, it might at atmospheric temperatures when the equipment is shut down and out of service. If there is a probability that an electrolyte will be present, either stabilized steel should be used or definite action taken to remove the electrolyte during shutdown periods. In the case of still tubes and gas-cracking tubes, no precautions have been necessary; but in the case of the superheater referred to, care is taken to see that it is drained during any shutdown.

Why should the nonstabilized tubes be considered for high-temperature service if there is even a remote chance that intergranular corrosion might take place? There are several reasons. Primarily, the use of stabilized tubes may not eliminate failures. Mention was made that nonstabilized tubes may perform even better than the stabilized. The reason for this is that the nonstabilized steel is cleaner. Columbium and titanium exist in the steel as nonmetallic inclusions, and the result is essentially a dirty steel. In tubes, these inclusions are elongated into stringers and form surface cracks. Experience has shown that many of the failures in high-temperature service originate at small surface cracks caused by inclusions in the steel (see Fig. 1). Another important reason is cost. The stabilized grades cost approximately 20 per cent more than the nonstabilized grades. Since shortages and restrictions have developed on the use of columbium, it is important that columbium be used only where it is actually needed and not wasted on applications where there is only a remote possibility it will be required.

There are cases where the stabilized grades are required in high-temperature service. For example, it is good practice to use the stabilized grades in the few cases where austenitic steels are required for thermocouple wells. There is usually a temperature gradient over the length of a thermocouple well, and condensation might take place and cause intergranular corrosion. The failure of a thermocouple well can be extremely serious. They are a stock item, and it is undesirable to have too many grades, as it is difficult to control the services in which they will be used. (12 Cr is preferred for thermocouple wells in refinery service as austenitic wells have failed from stress-corrosion cracking where chloride-bearing crudes were being treated.)

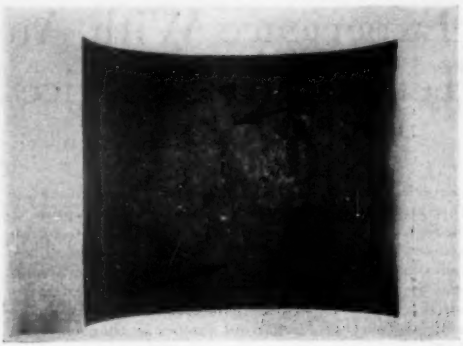

FIG. 1 INSIDE SURFACE OF FAILED 18 CR-8 NI-TI CRACKING-STILL TUBE

(Crack at center penetrated the 5-in-OD × 0.750-in-wall tube after 9 years of service. Many such cracks have been found to originate at inclusions in the steel.)

The use of stabilized grades does not assure freedom from trouble. As is well known, stress-corrosion cracking can take place in the stabilized as well as in the nonstabilized grades. In high-temperature service, some corrosion is almost sure to be present—at least from slight surface intergranular oxidation. Intergranular oxidation frequently has been observed at the edge of welds. This is generally not serious as it is usually only several grains deep as illustrated in Fig. 2. This intergranular oxidation, together with stress concentration, can be enough in severe cases to cause failure, as in the case of a transfer line in which adequate provision had not been made for expansion and contraction. The 18 Cr-8 Ni-Cb piping, exposed to the atmosphere, conducted 1300 F hydrocarbon gas. A failure developed at the outside surface as illustrated in Fig. 3. The failure was along the line of stress concentration at the edge of the weld. Metallographic examination showed intergranular oxidation had been severe on the outside surface in the area of stress concentration. When the same pieces were remachined, rewelded, and put back into identical service—but with adequate provision made for expansion and contraction—no further trouble was experienced. A larger plant was later built using straight 18 Cr-8 Ni and, by making adequate provision to avoid stress concentration, stress-corrosion (oxidation) cracking was not experienced.

Even where temperature and corrosive conditions are such that stabilized grades are desirable, it is often satisfactory to use nonstabilized grades. This can be accomplished by giving the finished assembly a stabilizing heat-treatment. Where service exposes austenitic steel above 750 F, the usual solution heat-treatment (2000 F and quench) will not be satisfactory, as the carbides will precipitate out in service. In such cases, a spheroidizing heat-treatment is to be preferred and is effective, especially in fine-grained steel. This treatment consists of heating to 1525–1650 F for a time long enough to precipitate the carbides along the grain boundaries and for diffusion to spheroidize the carbides

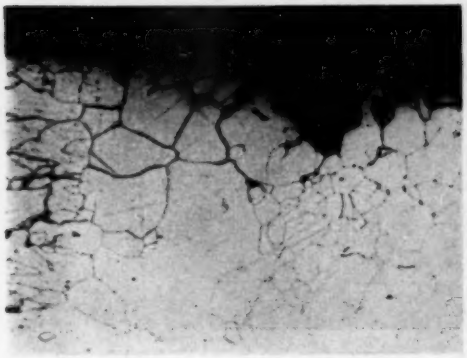

FIG. 2 INTERGRANULAR OXIDATION ON OUTSIDE SURFACE OF 25 CR-20 NI TUBE REMOVED FROM HIGH-TEMPERATURE SERVICE
(Weld metal is at extreme left.)

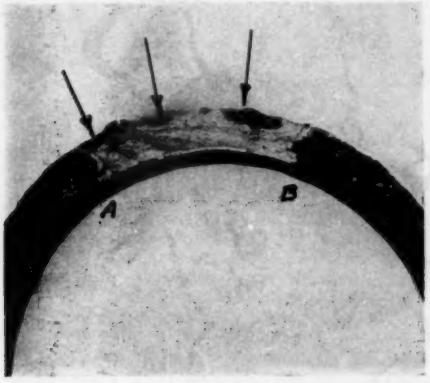

FIG. 3 FRACTURE ALONG EDGE OF WELD IN 18 CR-8 N-CB PIPING EXPOSED TO ATMOSPHERE AT ABOUT 1300 F
(Fracture originated 180 deg from section AB, which did not fail completely but was broken apart by bending. Arrows indicate cracks present on outside surface before complete failure occurred.)

so that they will not form a continuous chain. In addition, the time at temperature permits the chromium to diffuse and replace the chromium in the chromium-depleted zone along the grain boundaries. Eight hours at 1525 F is sufficient. By going to 1650 F the time can be reduced to 2 hr. This heat-treatment is simpler than the solution heat-treatment and has been found to be effective for conditions encountered in the oil industry. Some sigma phase might form, but this is not serious. Sigma phase has been observed in 18 Cr-8 Ni and 25 Cr-20 Ni for 10 years, and no mechanical failure has been observed in austenitic steel that could be attributed to sigma phase.

STRESS-RELIEVING

Stress-relieving the austenitic chromium-nickel steels should not be considered on the same basis as the carbon steels. The two steels are different. The austenitic steels do not pass through a transformation temperature during welding and are not hardenable. Heating the austenitic steels to 750–1550 F results in carbide precipitation, which has an adverse effect on corrosion resistance. Harmful carbide precipitation does not take place in the carbon steels in this manner.

Thermal stress-relieving of carbon steel is beneficial in two ways: (1) it reduces stresses, and (2) by tempering, it improves the physical properties. Brittle steels with low ductility are benefited most by stress-relieving heat-treatment, both by the reduction of stresses and the improvement in physical properties.

The austenitic chromium-nickel steels are extremely tough and very ductile, and therefore do not require the improvement in physical properties so often needed in welded carbon steels. Moreover, stress-relieving does not improve the properties. Instead, if anything, stress-relieving has an adverse effect by precipitating carbides. The only benefit to be derived from stress-relieving the austenitic chromium-nickel steels is a slight reduction in stresses. This reduction for most stress-relieving treatments will be small because of the high elevated-temperature strengths of the austenitic chromium-nickel steels.

If corrosion resistance is a reason for using the austenitic chromium-nickel steel, the loss in corrosion resistance due to carbide precipitation during stress-relieving may be serious enough to make the austenitic steel utterly unsatisfactory for the intended service. The harmful effect of intergranular corrosion may be greater than any benefits derived from a slight reduction in stresses. It should be noted that some carbide precipitation might take place even though the stabilized grades are used.

If, for some reason, the austenitic chromium-nickel steels must be stress-relieved, the stabilizing heat-treatment of 1550–1650 F, previously described, should be considered. This treatment will more effectively relieve stresses than a lower temperature, and will give the additional advantage in that stabilization of carbides will result.

EXPANSION AND CONTRACTION

The austenitic steels have a coefficient of expansion approximately $1^1/_2$ times that of steel. If adequate provision is not made for this added expansion and contraction, failures will develop in high-temperature service. Failures are quite likely to be in the form of stress-corrosion cracking. Reference was made previously to such failures in the discussion of stabilized steels. The high coefficient of expansion may not cause failure in itself, but it does have a great influence on most failures associated with high-temperature service by aggravating and increasing the effects of any other weakness or undesirable property.

In high-temperature service, cracking is often associated with the high coefficient of expansion. Wherever an austenitic steel is tacked down and held in place, cracking is likely to occur whether the material is stabilized or nonstabilized. In one assembly, the tubes were tacked in place. After about 2 years of service, cracks developed on the outside surface at each tack. The tacks were cut loose, the cracks repaired, and the equipment put back into service with the tubes free to distort. No further trouble has been experienced, and the equipment has been in service 4 years since the tacks were cut loose.

HOT SHORTNESS

The strength of steel decreases as the temperature is increased. With the decrease in strength, in ferritic steel, there is an increase in ductility. This is not true with austenitic steel. The ductility of austenitic steel decreases as the temperature is increased to about 1600 F. Between about 1600 and 2200 F there is an improvement in ductility. This difference between ferritic and austenitic steels is illustrated in Fig. 4.

The ductility of austenitic steel at elevated temperatures is misleading. The values look good in spite of the fact that they

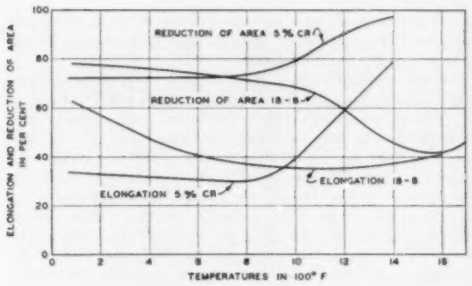
REDUCTION OF AREA 5% CR
REDUCTION OF AREA 18-8
ELONGATION 5% CR
ELONGATION 18-8
ELONGATION AND REDUCTION OF AREA IN PER CENT
TEMPERATURES IN 100° F

FIG. 4 DUCTILITY-TEMPERATURE CURVES FOR 5 CR-MO AND 18 CR-8 NI, ILLUSTRATING DIFFERENCE IN HIGH-TEMPERATURE DUCTILITY BETWEEN FERRITIC AND AUSTENITIC STEELS

(Curves from "Report on the Strength of Wrought Steels at Elevated Temperatures," by R. F. Miller and J. J. Heger.)

FIG. 5 PORTION OF HOT-BENT 18 CR-8 NI TYPE 304 TUBE CONTAINING SURFACE CRACKS

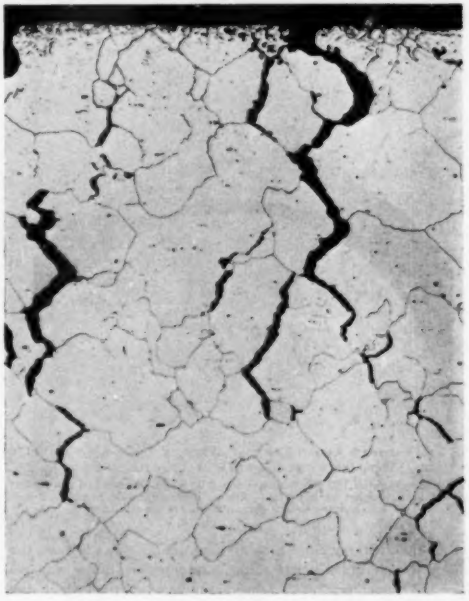

FIG. 6 CROSS SECTION OF CRACKED ZONE SHOWN IN FIG. 5

(Note that many intergranular cracks do not come to surface. In some cases cracks are entirely subsurface. Also note that high temperature used to bend tube developed coring at surface.)

are somewhat lower than the high values for atmospheric temperature. What the curves and data fail to bring out is that, between about 1000 and 1800 F, severe deformation or bending develops intergranular cracks. Furthermore, above about 2200 F the austenitic steels are extremely hot-short. Steel companies and others who regularly hot-form the austenitic steels are aware of these hot-short characteristics. They know that there are only narrow temperature ranges in which these steels can be hot-worked or formed. Most users of austenitic steels and many fabricators do not recognize these hot-short characteristics.

This hot shortness is important. During fabrication it is common practice to heat piping and other shapes prior to bending. Without careful temperature control, there is a danger of forming intergranular cracks (see Figs. 5 and 6). These cracks are usually extremely hard to detect—they may not even reach the surface—with the result that defective material may be put into service. When operating equipment made from austenitic steel in the temperature ranges where intergranular cracks might form, every effort should be made to keep deformation to a minimum. It is suspected that some high-temperature stress cracks may be actually hot-short cracks. In the oil industry there are numerous operations in which carbon is periodically burned off catalyst or metal surfaces. If not controlled properly, temperatures high enough to melt the austenitic steels can be reached. When extremely high temperatures inadvertently develop, any deformation may result in hot-short cracks.

THERMAL CONDUCTIVITY

The thermal conductivity of austenitic steel is low, being about one half to one fourth that of ferritic steel. This results in steep temperature gradients, and uneven heating causes hot spots that tend to be localized. Sudden changes in temperature cause parts to be hot while adjacent parts are cool, and it takes longer for temperatures to become equalized. In passing, it is of interest to note that the low thermal conductivity of the austenitic steels probably accounts for workmen, accustomed to dealing with carbon steel, overheating the austenitic steels. Evidence of the extreme temperature gradients that are so easily developed is illustrated by the coring at the surface in Fig. 6.

In cyclic operations, where equipment is alternately hot and cold, the temperature gradients can be very steep. When a cold valve opens quickly and hot fluid passes through it, the inside surface immediately becomes hot, while the outside is cold and requires some time before it becomes heated. This is particularly true of thick sections such as flanges. Temperature measurements made on an austenitic valve in cyclic service are plotted in Fig. 7. This illustrates the temperature gradients that can develop, and that the temperatures may never reach equilibrium in service.

What are the effects of these temperature gradients? Hot spots or local heating in thin material result in warpage. When the sections are larger and deformation does not occur, stresses are set up. The steeper the temperature gradient, the greater the stresses. Also, the steeper the gradient, the more localized are the high stresses. Again, the high coefficient of expansion of the

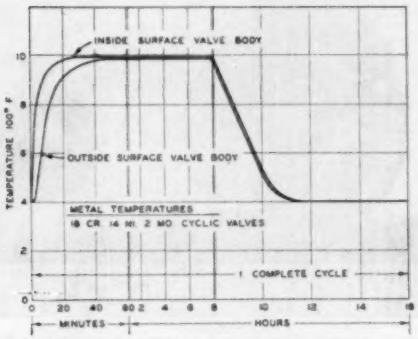

FIG. 7 CURVES SHOWING TEMPERATURES MEASURED NEAR INSIDE AND AT OUTSIDE SURFACE OF AUSTENITIC VALVE

(Temperature of fluid passing through valve when open was 1000 F.)

austenitic steels aggravates the difficulties resulting from the low thermal conductivity.

HEATING AND COOLING

Experience has shown that much of the trouble with high-temperature service occurs during heating or cooling. When equipment is being brought on stream and is heating up, leaks are likely to develop in piping systems. When it cools down, other leaks and even breaks may develop. Less trouble is experienced with equipment that operates steadily at temperature than that which requires shutdowns. Unfortunately, most high-temperature equipment in refineries requires periodic shutdowns—for example, every 90 days—for cleaning or other maintenance operations. As a result, refineries have become conscious of the difficulties associated with heating and cooling.

Within the past 10 years many cyclic processes have been introduced. In these, the equipment operates for a period of time at one set of temperature and pressure conditions, and then for another period at a different set of conditions. In some of these cyclic operations, the high-temperature failures have been almost spectacular and have resulted in frequent reference to such terms as "thermal shock" and "thermal fatigue."

THERMAL SHOCK

Thermal shock is not new. Its effects long have been recognized in the failure of rolling-mill rolls, gun barrels, brake drums, and other equipment subjected to sudden applications of heat. With the advent of thermal cyclic processes, thermal-shock failures have come to be recognized in certain high-temperature piping and fitting installations.

Fig. 8 illustrates a piping assembly in which thermal-shock failures occurred. The piping and flanges were 5 Cr-Mo, but the valves were 18 Cr-12 Ni. For 8 hours valve A was open and B closed. The fluid temperature of the hydrocarbons passing through A was 1150 F. At the end of 8 hours, valve A closed and B opened. Steam and air at 1120 F passed through B for 8 hours and A gradually cooled down. Valve B then closed, valve A opened, and the cycle repeated itself. When this plant was put into operation, at the end of 10 days cracks were found at the flange face of valve A radiating from the bore and extending back into the bore approximately the thickness of the flange. Similar cracks were found in valve B shortly thereafter. These cracks soon extended into the ring groove and are shown in Fig. 9.

The cracks formed as follows: While closed, the valves slowly cool down. When they open, the inside surface is exposed to high-temperature fluid and instantly becomes hot to a shallow depth, while the outside is still cool. The inside surface tends to expand, but is restrained by the cool outer mass of metal. Instead of expanding, the inside is compressed or upset. Then, as the outer mass gradually heats up, the inside is put into tension. It should be noted that the cracks first formed at the flange where the restraining mass of metal and the differences in temperature were greatest. Experience showed that only a few cycles were required to develop cracks in 18 Cr-12 Ni valve flanges, but that the 5 Cr-Mo flanges of the same size and 5 Cr-Mo piping could withstand many identical cycles.

The superiority of the ferritic over the austenitic steel is believed to be due to the differences in thermal conductivity and coefficient of expansion. The higher thermal conductivity of the

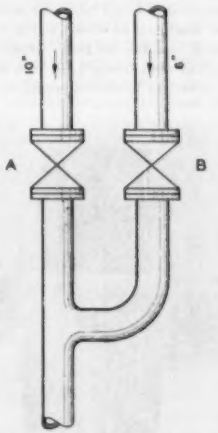

FIG. 8 PIPING ASSEMBLY IN WHICH CRACKS DEVELOPED IN AUSTENITIC VALVES IN 10 DAYS, BUT NOT IN FERRITIC PIPING AND FLANGES

(Valves alternately opened and closed on 8-hr cycle. Temperature of fluids was approximately 1130 F.)

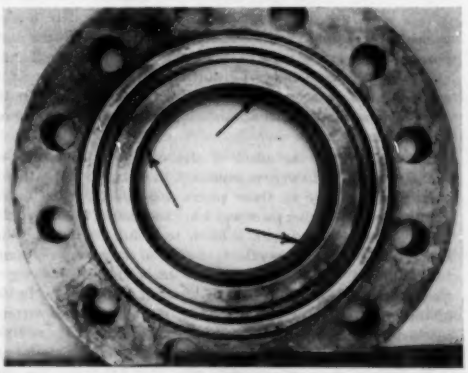

FIG. 9 VIEW OF FLANGE FACE SHOWING SOME OF LARGER CRACKS IN AUSTENITIC VALVES USED IN PIPING ASSEMBLY ILLUSTRATED IN FIG. 8

ferritic steel results in lower temperature differences between the inside and outside surfaces; hence lower stresses. Similarly, the lower coefficient of expansion of the ferritic steel results in lower deformation and less restraint between the two surfaces. Again, the result is—less stress. These two factors combined result in appreciably less stress and longer life in the ferritic than in the austenitic steel. This experience has been confirmed in several installations where ferritic steels have performed better than austenitic steels in thermal cyclic operations. In the case cited, replacement valves made from 9 Cr-Mo gave excellent service.

Thermal-shock failures occur, of course, in ferritic steels as well as in austenitic steels. In the foregoing installations, where austenitic flanges in the valve cracked in 10 days, several small cracks were found in the mating 5 Cr-Mo flanges of the same size at the end of $2^1/_2$ years.

To demonstrate the mechanism of such failures, a simple test was made. Samples of 18 Cr-12 Ni, 12 Cr, and plain carbon (SAE 1035) steels were machined as shown in Fig. 10. The bores were heated with a torch to a dull red heat. Holding the bore at heat, the entire piece was then brought up to a dull red heat. The piece was then cooled to room temperature. At the end of 16

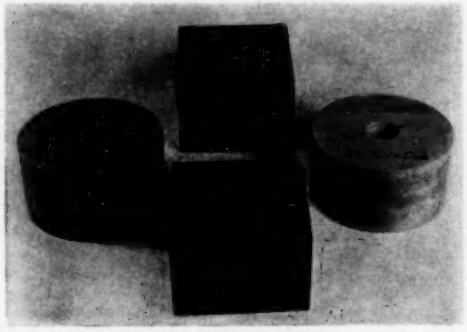

FIG. 10 SAMPLES USED TO SHOW EFFECT OF THERMAL CONDUCTIVITY AND THERMAL COEFFICIENT OF EXPANSION ON CRACK FORMATION

(Upper 18 Cr-12 Ni sample was given stabilizing treatment of 24 hr at 1565 F before being exposed to heating and cooling cycles. Arrows indicate location of cracks in 18 Cr-12 Ni samples.)

cycles, the austenitic 18 Cr-12 Ni had developed cracks at the bore. Ferritic steels, SAE 1035, and 12 Cr, subjected to the same cyclic treatment 32 times did not develop any cracks. At the end of 32 cycles several cracks had formed in 18 Cr-12 Ni that had previously been given a stabilizing heat-treatment of 24 hours at 1565 F.

To demonstrate the effect of size on crack formation, two samples of 5 Cr-Mo were machined as shown in Fig. 11. The diameter of the bore of these pieces was $^1/_2$ in. The outside diameter of the smaller piece was 1 in., and that of the larger, 2 in. The bore was heated with a torch to a dull red heat. While keeping the bore at temperature, the rest of the piece was brought to a dull red heat. The cycle was completed by blowing air through the bore until the bore had lost all visible heat. In view of the inaccuracies of visual control, the temperature extremes reached by this process probably were within the range of 800 to 1300 F. At the end of 50 cycles many small cracks were found in the bore of the larger piece. Even after 100 cycles, the small specimen showed no cracks. The heavier the section, the more readily it cracks.

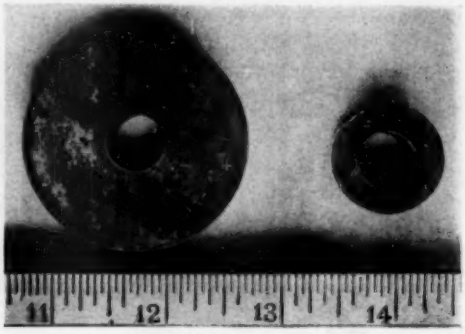

FIG. 11 SAMPLES USED TO SHOW EFFECT OF SIZE ON CRACK FORMATION

(Cracks were in bore of larger sample at end of 50 cycles; none was found in small sample at end of 100 cycles.)

THERMAL FATIGUE

The examples used to illustrate thermal shock might also be considered thermal fatigue, as a number of cycles were required to produce failure. However, since so few cycles were required to produce failure and the rapid heating was such an important factor, they were classified as primarily thermal shock rather than thermal-fatigue failures. Cyclic changes in temperature can cause changes in stress and produce thermal-fatigue failures without thermal shock; but the rate of temperature change is often closely related to the stresses induced.

Fig. 12 shows two methods used to attach vertical tubes to a header. At the bottom of the tube there is a grid, which supports catalyst. The juncture of the tube and the lower header repeatedly goes through a rather complex heating cycle approximately as follows: 1 hour at 1150 F, followed by 1 hour starting at 1050 F and increasing to 1450 F, and finally dropping down to 900 F.

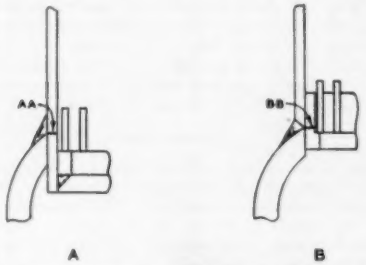

FIG. 12 SKETCH SHOWING DETAILS OF GRID, TUBE, AND HEADER ASSEMBLY

(Failures developed at AA and BB in assemblies made from austenitic steels.)

Serious failures developed in a year at AA in austenitic steel using detail A. Such a failure is shown in Fig. 13. An unimportant, but significant, cracking was found in $2^1/_2$ years at BB in austenitic-steel assemblies using detail B. No failures developed in detail B when the assemblies were made from ferritic steels. Assemblies of 27 Cr and of 7 Cr-Mo both gave good service in so far as detail B was concerned. The 27 Cr became extremely brittle in service and many failures occurred, but they were not

FIG. 13 END OF 25 CR-20 NI TUBE CONTAINING GRID
(Tube failed along AA of Fig. 12.)

associated with the design of the assembly. In making 27 Cr tube replacements, assemblies approaching detail A were used successfully.

The failures in the austenitic steel (25 Cr-20 Ni) have been classified as thermal fatigue. As the equipment passes through the different cycles, the end of the tube protruding into the header expands, is restrained and slightly upset, cools and contracts. The alternate bending results in the formation of cracks and the tube end breaks off. Note that the cracks at BB correspond to the condition at AA. The freedom from failure in the ferritic steels is believed to be due to their higher thermal conductivity and lower coefficient of expansion. It is also suspected that the bending of the austenitic steel in a hot-short temperature range contributes to the failure.

CONCLUSIONS

1 Stabilized austenitic steels are not required for gas-cracking and still tubes.

2 A spheroidising heat-treatment is adequate for many oil-industry applications requiring austenitic steels in the stabilized condition.

3 Stress-relieving austenitic steels can seldom be justified, unless stress-corrosion cracking is known to occur.

4 The hot-short characteristics of austenitic steels should be considered in high-temperature design.

5 The low thermal conductivity and high coefficient of expansion are responsible for many of the failures of austenitic steels in high-temperature service, especially where thermal shock and thermal fatigue are involved.

Discussion

H. D. NEWELL.[2] The author's conclusions are soundly drawn and it would be well for the user to keep them in mind in applying the austenitic stainless steels so as to receive maximum benefits from their use. The difficulties which have been encountered stem in considerable measure from the physical properties of low thermal conductivity and high coefficients of expansion and, since these are inherent properties, they cannot be altered. Therefore design should always allow sufficient freedom for expansion and should strive for uniformity of temperature so as to avoid excessive thermal stresses.

Still tubes of austenitic stainless steel have been used by the refining industry since 1928, and a considerable percentage of the total has been supplied by the company with which the writer is associated. As the author points out, plain unstabilized 18-8 has been used to the greatest extent, and when tubes are manufactured with a fine grain size and heat-stabilized, they are placed in best condition for maximum serviceability. One of the major users, after a number of years of experience, has instituted an arbitrary retirement to more moderate service after 60,000 hr in thermal-cracking service. Other users have used tubes well in excess of 100,000 hr even though handling corrosive stocks and at fairly severe pressures. Ultimate tube life is a function of several factors and includes corrosion from the contained fluid, some slight scaling of the OD, the amount depending upon firing conditions, wear, or loss of metal from mechanical tube cleaning to remove coke, and carburization of the bore of the tube, which ultimately may affect serviceability. In general, tube-metal temperatures are usually limited to not in excess of about 1250 F and most users attempt to restrict the metal temperature to about 1200 F maximum in liquid-phase cracking.

In gas cracking, or reforming, and in vapor-phase operations, 25 per cent Cr 20 per cent Ni is the preferred material except in those cases where abrasion due to coke in the gas stream governs tube life. Where such abrasion occurs, it is more economical to use 18-8, since the wear factor outweighs the difference in scaling rate in these alloys. At lower gas velocities and where the coke in the fluid stream is not a factor, the 25-20 is the superior material, since it is more resistant to scaling and carburization than the 18-8 alloy.

Some stabilized 18-8-Cb and 18-8-Ti alloys have been used in still tubes. In one instance at least, the columbium alloy was selected to offset intercrystalline corrosion which had been encountered when moisture collected on the OD tube surface during shutdown. In the general case, stabilized steels are not necessary. They are more costly, and the possible advantage expected from the stabilized material may be offset largely by carburization of the material when in contact with hydrocarbon fluids at high temperature.

The fine-grained manufacturing practice and stabilizing heat-treatment used on 18-8 still tubes is not applicable to the 25-20 alloy. Production of a fine grain in 25-20 results in a considerable loss in creep and rupture strength and present practice is therefore to heat-treat the alloy so as to obtain a medium-coarse grain of about 3-6 ASTM. Further, recrystallization of cold-worked 25-20 at temperatures below about 1700 F will result in sigma formation which will decrease the ability of the alloy to withstand forming operations, bending, and so forth. The effect of heat-treatment and the depreciating influence of a fine grain size on the high-temperature properties of 25-20 may be noted by reference to the summary of information collected on this alloy and presented in Fig. 14, herewith. A new series of rupture tests just recently completed on 25 per cent Cr 20 per cent Ni alloy, Type 310, stainless steel having a grain size of 4-6 ASTM, resulted in the values shown in Fig. 15.

The author properly has called attention to the trouble which may be experienced during heating and cooling the austenitic steels where leakage at rolled joints may be encountered. This difficulty is associated to some extent with the type of mechanical joint or fitting that is employed and some of the present designs help to reduce such difficulties. Cyclic operations are much more severe than steady-state operation and may lead to thermal fatigue through the mechanism described by the author, resulting from alternating thermal stresses which are due to temperature differences in the metal. This behavior is directly related to the

[2] Chief Metallurgist, The Babcock & Wilcox Tube Company, Beaver Falls, Pa.

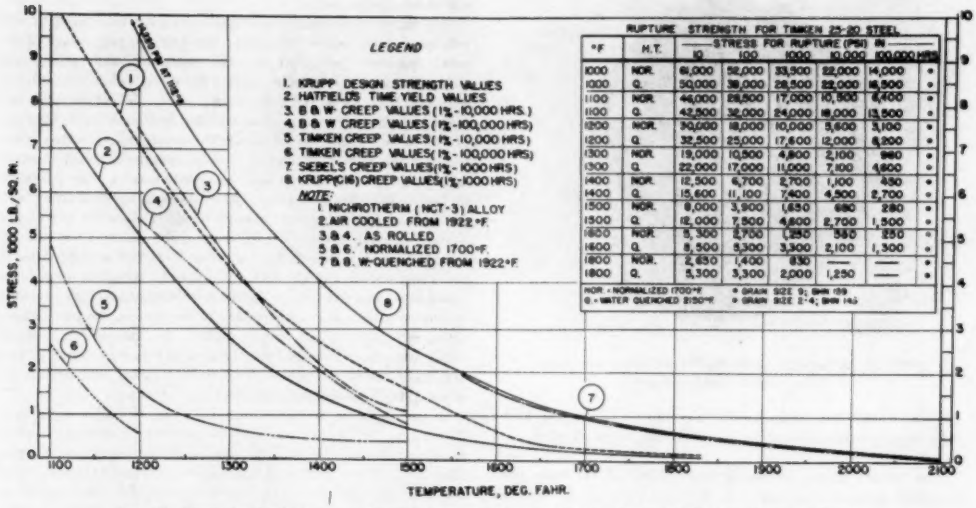
LEGEND
1. KRUPP DESIGN STRENGTH VALUES
2. HATFIELDS TIME YIELD VALUES
3. B & W CREEP VALUES (1% - 10,000 HRS.)
4. B & W CREEP VALUES (1% - 100,000 HRS)
5. TIMKEN CREEP VALUES (1% - 10,000 HRS)
6. TIMKEN CREEP VALUES (1% - 100,000 HRS)
7. SIEBEL'S CREEP VALUES (1% - 1000 HRS)
8. KRUPP (CIS) CREEP VALUES (1% - 1000 HRS)
NOTE:
1. NICHROTHERM (HCT-3) ALLOY
2. AIR COOLED FROM 1922 °F.
3 & 4. AS ROLLED
5 & 6. NORMALIZED 1700 °F.
7 & 8. W: QUENCHED FROM 1922 °F
STRESS, 1000 LB./SQ. IN.
TEMPERATURE, DEG. FAHR.

RUPTURE STRENGTH FOR TIMKEN 25-20 STEEL

°F	H.T.	STRESS FOR RUPTURE (PSI) IN 10	100	1000	10,000	100,000 HRS
1000	NOR.	61,000	52,000	33,500	22,000	14,000 *
1000	Q.	50,000	38,000	28,500	22,000	16,500 *
1100	NOR.	44,000	28,500	17,000	10,500	6,400 *
1100	Q.	42,500	32,000	24,000	18,000	13,500 *
1200	NOR.	30,000	18,000	10,000	5,600	3,100 *
1200	Q.	32,500	25,000	17,600	12,000	8,200 *
1300	NOR.	19,000	10,500	4,800	2,100	980 *
1300	Q.	22,000	17,000	11,000	7,100	4,600 *
1400	NOR.	12,500	6,700	2,700	1,100	450 *
1400	Q.	15,600	11,100	7,400	4,500	2,700 *
1500	NOR.	8,000	3,900	1,650	680	280 *
1500	Q.	12,000	7,500	4,800	2,700	1,500 *
1550	NOR.	5,350	2,750	1,250	560	250 *
1600	Q.	8,500	5,300	3,300	2,100	1,300 *
1800	NOR.	2,650	1,400	830	—	— *
1800	Q.	5,300	3,300	2,000	1,250	— *

NOR. - NORMALIZED 1700 °F * GRAIN SIZE 9; BHN 159
Q. - WATER QUENCHED 2150 °F * GRAIN SIZE 2-4; BHN 143

FIG. 14 SUMMARY OF CREEP AND STRESS-RUPTURE DATA ON 25 PER CENT CR-20 PER CENT NI STEEL

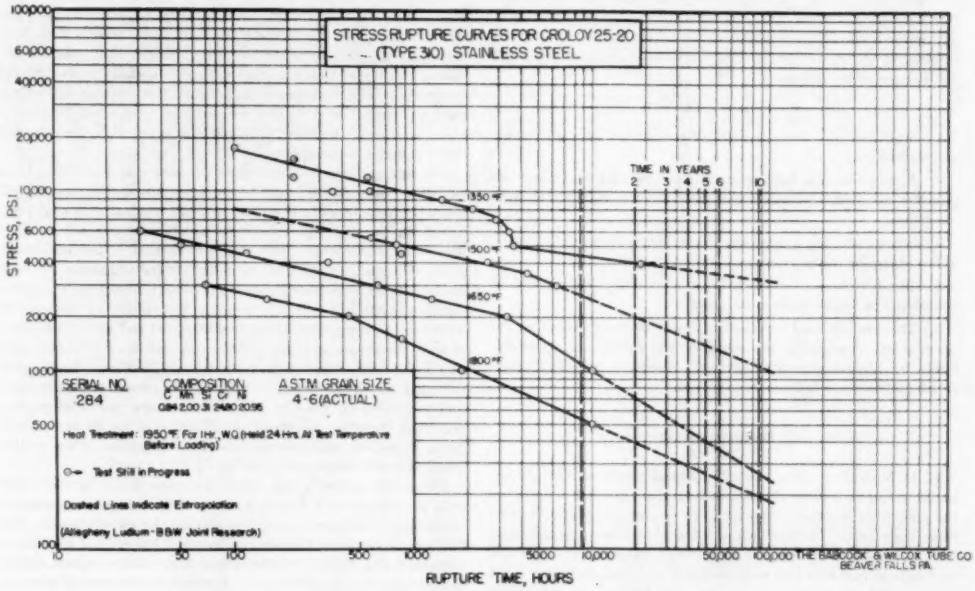
STRESS RUPTURE CURVES FOR CROLOY 25-20
(TYPE 310) STAINLESS STEEL
TIME IN YEARS
1350 °F
1500 °F
1650 °F
1800 °F
SERIAL NO. 284
COMPOSITION C Mn Si Cr Ni 0.04 2.00 .31 24.80 20.95
ASTM GRAIN SIZE 4-6 (ACTUAL)
Heat Treatment: 1950 °F. For 1 Hr., W.Q. (held 24 Hrs. At Test Temperature Before Loading)
Test Still in Progress
Dashed Lines Indicate Extrapolation
(Allegheny Ludlum - B&W Joint Research)
STRESS, PSI
RUPTURE TIME, HOURS
THE BABCOCK & WILCOX TUBE CO. BEAVER FALLS PA.

FIG. 15 STRESS RUPTURE CURVES FOR TYPE 310 STAINLESS STEEL

conductivity and thermal expansion of the stainless steels of austenitic type.

Engineers should thank the author for placing on record the experiences with austenitic steels in high-temperature service in the petroleum industry which he has described in his paper.

P. D. THOMAS.[2] Bataafsche Petroleum Maatschappij, our associates in The Hague, Holland, have commented as follows on the paper:

We wish to congratulate the author of this paper which we feel is a valuable contribution to the knowledge of stainless-steel applications. We wonder, however, if in his further consideration of this problem, he has given some attention to the occurrence of the sigma phase and its relation to failures in stainless-steel equipment.

Our experience indicates that in some cases cracking of stainless steels in service may be aggravated by this hard and brittle constituent and we cite the following cases:

1 We found that the weld (23.0 per cent Cr, 18.0 per cent Ni, and 0.81 per cent Mo) in a 5 per cent Cr, 0.5 per cent Mo Dubbs furnace tube failed after 50,000 hours. X-ray and microscopical examinations revealed the presence of sigma phase and fine carbides. The impact value (Charpy 10 × 10 × 55 mm keyhole notch, depth 3 mm) of the weld metal was 1.9 kg m/cm,[2] which low value cannot be ascribed to the carbide precipitation alone.

2 In another case, a Dubbs furnace tube of 5 per cent Cr, 0.5 per cent Mo steel, welded with 25 per cent Cr, 20 per cent Ni, electrodes cracked after 3200 operating hours. Though the microscope only showed carbide precipitation, x-ray testing revealed sigma formation. The chemical composition of the weld metal was 0.14 per cent C, 23.4 per cent Cr, 18.2 per cent Ni, and 0.18 per cent Mo. Under the prevailing working conditions, this material is susceptible to sigma formation due to the low nickel content with respect to the chromium content. Moreover the molybdenum content is also unfavorable.

Under the heading "Thermal Fatigue," fracturing of tubes near the headers is mentioned and ascribed to cyclic changes in temperature. We wonder whether in this case sigma formation might also be considered an important factor, because the temperature range of 900–1450 F is very critical for the 25 per cent Cr, 20 per cent Ni steel. We found that a steel with 0.1 per cent C, 18.0 per cent Ni, 24.7 per cent Cr, and 1.14 per cent Si had become very brittle after heating for a long time at about 1470 F. Microscopical examination clearly showed the formation of the sigma constituent.

A. B. WILDER.[4] The author has shown that ordinary austenitic steels may be used successfully in certain applications where stablized austenitic steels have been specified previously. This is a significant observation and suggests the possibilities of using ordinary austenitic alloy instead of the more complex alloys for other applications. If the demand for stabilized austenitic alloys was replaced to some extent by ordinary austenitic alloys, the problems encountered in the manufacture and fabrication of seamless tubing would be simplified.

T. MCLEAN JASPER.[5] This paper indicates that the most appropriate method of selecting materials for service is that of actual experience in their use. True, that in order to start a promising new material, the simulating short-time test gives the first impulse to its use. It should be stated here that in addition to the usual metallurgical approach other methods of solving the engineering problem should not be overlooked—such methods as preprocessing the products to be manufactured so that they are less active in attacking the processing equipment.

Corrosion inhibitors that do not interfere with the process are not easily discovered. There is the possibility of valuable returns from the viewpoint of changing the environment. Economic engineering, however, demands that we become as diligent in exploiting this avenue of approach as we have been as metallurgists.

The author of this paper has a unique opportunity in that he is associated with an operating company of the first order which is most progressive in its approach to the problem of reducing the hazards and costs of high-temperature high-stress operations. Some of the author's conclusions are somewhat different from the generally outlined heat-treatments for austenitic steels for high-temperature service in the petroleum industry. This is the result of considerable experience and should be received with due regard to this experience.

The matter of thermal shock in the operation of refinery equipment is too often neglected. This has led to the introduction of methods of testing which are sometimes beside the point in so far as solving the critical problem. Thermal shock can so increase stresses as to be the cause of failures which would not occur if coming on and off stream were more carefully planned. Carelessness in this matter may bring on problems which are just as difficult to overcome as those brought about by the selection of the wrong materials for resisting operating service conditions.

AUTHOR'S CLOSURE

Mr. Newell's review of the use of austenitic steel tubes in oil and gas cracking is appreciated. It is gratifying to see that he confirms the fact that the plain unstabilized grades have been used to the greatest extent and that in general the stabilized grades are not necessary. Mr. Newell calls attention to an important difference between the 18 Cr-8 Ni and 25 Cr-20 Ni—the same fine grain heat stabilizing heat-treatment, which has been so successfully applied to 18 Cr-8 Ni, does not have application to 25 Cr-20 Ni. The disadvantage of fine grain 25 Cr-20 Ni would have been more clearly illustrated in Fig. 14 if the legend had shown the grain size. Incidentally, the legend shows the source of the information and it is understood does not necessarily represent the heat-treatments and grain sizes recommended or used by the different investigators.

Mr. P. D. Thomas and his associates raise the question of sigma phase. About 1939 we first encountered sigma phase in austenitic steels that had been in gas-cracking service. We became very much concerned and did our best to attribute failures to sigma phase; but there were always more obvious reasons for the failures. Later, we made a large installation of 27 Cr. There was no question about the harmful effects of sigma phase. In fact, sigma phase made the 27 Cr so brittle that it was necessary eventually to replace most of the 27 Cr with 25 Cr-20 Ni. It has been our experience that even when large quantities of sigma phase develop in austenitic steels, the steels remain relatively tough. The author does not believe sigma phase alone has been responsible for any of our high-temperature failures in austenitic steels.

Welds made with 25 Cr-20 Ni have been eminently successful. We have been welding 5 Cr-Mo with 25 Cr-20 Ni rods for some time. It was recently estimated in one refinery that in the past ten years more than 10,000 25 Cr-20 Ni welds had been made in retipping Cr-Mo still tubes. Only three weld failures have occurred, while several thousand tubes have been retired and quite a number have failed by rupturing. None of the three weld failures was due to sigma phase.

Mr. Wilder suggests the possibilities of using ordinary austeni-

[2] Asiatic Petroleum Corporation, New York, N. Y.
[4] Chief Metallurgist, National Tube Company, U. S. Steel Corporation Subsidiary, Pittsburgh, Pa.
[5] A. O. Smith Corporation, Milwaukee, Wis.

tic alloys instead of the more complex stabilized grades for other applications than those mentioned in the paper. While this paper was limited to high-temperature service, it might be of interest that during the past two years we have found that in some corrosive services Type 304 18 Cr-8 Ni has given satisfactory service where we originally thought Type 347 would be required. It is believed that many of the failures in plain unstabilized austenitic steels occurred before the lower-carbon grades, such as 304 and 304 ELC were available.

Dr. Jasper calls attention to several interesting factors in the selection of materials. Hindsight is often better than foresight. By studying failures and operating records much valuable information can be obtained concerning the performance and characteristics of materials. Such studies determine the validity of the short-time tests that one must depend upon so often. The use of inhibitors, controlling the environment, and design often offer greater possibilities in solving a material problem than does metallurgy. Where operating conditions can be modified to meet the limitations of the materials, many failures can be avoided as suggested by Dr. Jasper in his reference to thermal shock.

An Investigation of the Role of Aluminum in the Graphitization of Plain Carbon Steel

By A. M. HALL[1] and E. E. FLETCHER,[1] COLUMBUS, OHIO

This investigation was sponsored by Project No. 29 of the Joint ASTM-ASME Committee on the Effect of Temperature on Properties of Metals, and was directed toward casting more light on the role of aluminum in the breakdown of iron carbide in plain carbon steels into iron and graphite at temperatures below the lower critical point of the steel. The approach to the problem was to extract the carbides from several plain carbon steels which had been deoxidized with different amounts of aluminum and had different known degrees of susceptibility to graphitization, and then to examine and analyze the extracted carbides, with particular attention to the amount and form of the aluminum therein. By comparing the aluminum found in the carbide with the aluminum of the original steel, data were obtained on the role which that element appears to play on the graphitization process. The results strongly suggest that a graphitization-resistant plain carbon steel does not differ fundamentally from one which graphitizes readily. It is tentatively concluded that, in order to promote graphitization, the aluminum is either in solid solution in the ferrite matrix, or else fixes the nitrogen as AlN. Which of these forms it takes could not be determined from the results. The results further suggested that any aluminum which might be associated with the carbide phase is not influential in determining the degree of susceptibility to graphite formation.

Introduction

THE phenomenon of graphite formation in cast irons and hypereutectoid steels is well known, and considerable information on the graphitization of these materials is to be found in the technical literature. However, very little interest had been developed in the possibilities of graphite formation in low-carbon steels, either plain or alloyed, prior to January, 1943, except as the phenomenon was related to questions of carbide stability and the low-carbon limits of the so-called double iron-carbon constitution diagram (1, 2, 3).[2] In fact, up until that time only two cases of graphitization of a low-carbon steel were on record (3, 4).

The role of aluminum in the graphitization of plain-carbon steels, while recognized, appears not to have been studied in any detail except by Austin and Fetzer (5, 6), who investigated a series of eighteen 1.00 per cent carbon steels. These authors lean to the idea that it is the presence of nuclei of alumina that promotes graphitization. However, a review of their results shows that other factors may have been important. While three of their more stable steels contained as much as 0.010 per cent acid-soluble aluminum, none of them contained enough acid-soluble aluminum to fix all the nitrogen present as AlN. One half of the unstable steels contained enough acid-soluble aluminum to combine with the nitrogen present as AlN, and half did not. On the other hand, no steel containing more than 0.010 per cent acid-soluble aluminum was resistant to graphitization.

In January, 1943, a welded joint in a carbon-molybdenum steel steam line at the Springdale Station of the West Penn Power Company broke after 5½ years of service at an average temperature of 935 F. Examination of the failure (7, 8) showed that it had occurred in the pipe stock about ⅛ in. from the weld, through a narrow band of segregated graphite. The location of the graphite corresponded to the region in the steel which had been heated to the A_1 temperature during welding. Graphitization here had proceeded to such an extent that this zone was occupied by an almost continuous film of graphite.

As a result of numerous studies, considerable information has been gathered on the graphite-formation process in low-carbon steels. Some idea of the compositions of steels which are resistant and which are susceptible to graphitization has been obtained, as well as which heat-treatments increase and which decrease susceptibility. Some knowledge of the extent to which graphitized welded joints can be rehabilitated has also been gained.

Among plain carbon and carbon-molybdenum steels, it has been found that usually those deoxidized with relatively large amounts of aluminum (1½ or more lb per ton) are susceptible to graphitization, and those deoxidized with small amounts of aluminum (½ lb per ton or less) are resistant to graphite formation, while silicon-killed steels are generally very resistant (9, 10, 11, 12).

In the present investigation, carbide residues were electrolytically extracted from four plain-carbon steels whose graphitization characteristics ranged from "very resistant" to "very susceptible." Two of the steels were studied in two conditions of heat-treatment (normalized and spheroidized), and two in one condition of heat-treatment (spheroidized). The residues obtained were examined spectrographically and petrographically, and were analyzed by wet-chemical, x-ray diffraction, and mineral-separation methods.

Test Materials

Composition. The four steels tested were all low-carbon open-hearth steels, and were received in the form of bars varying from ⅛-in. × ⅝-in. sections to 1⅛-in-diam rounds. Table 1 gives their composition in terms of the usual elements, while the results of determinations of special elements are shown in Table 2. Acid-soluble aluminum and Al_2O_3 were obtained by wet-chemical

---

[1] Battelle Memorial Institute.

[2] Numbers in parentheses refer to the Bibliography at the end of the paper.

Contributed by the Joint ASTM-ASME Committee on Effect of Temperature on the Properties of Metals and presented at the Annual Meeting, New York, N. Y., November 26–December 1, 1950, of The American Society of Mechanical Engineers.

Note: Statements and opinions advanced in papers are to be understood as individual expressions of their authors and not those of the Society. Manuscript received at ASME Headquarters on August 23, 1950. Paper No. 50—A-69.

TABLE 1 TEST STEELS FOR CARBIDE-EXTRACTION PROGRAM

No.	General Graphitization Characteristics	Incubation Period for Graphitization at 1025°F.	Source	Quantity, g.	Composition, Per Cent								
					C	Mn	Si	S	P	Ni	Cr	Mo	Cu
G20	Very susceptible	Probably none	National Tube Co.	3025	0.22	0.35	0.13	0.024	0.010				
5B	Moderately resistant	1000 - 1500 hours	National Tube Co.	10040	0.20	0.57	0.224	0.032	0.011	0.005	0.023	0.004	0.01
K1	Moderately resistant	3000 - 6000 hours	Crane Co.	4330	0.17	0.46	0.02	0.038	0.017	0.04	0.02	0.01	0.03
G21	Resistant	Indefinitely long	National Tube Co.	700	0.27	1.11	0.21	0.019	0.010				

TABLE 2 DETERMINATIONS OF SPECIAL ELEMENTS IN THE TEST STEELS*

Specimen Number	Al added lb. per ton	Soluble Al	Insoluble Al (as Al_2O_3)	Total Al	Al_2O_3	N_2 by General Electric	O_2 by BMI	H_2 by BMI	N_2 by BMI	Graphitization Characteristics	Source of Steel
G20	2	0.020	0.003	0.023	0.006	0.008	0.002	0.00004	0.005	Very Susceptible	BMI
5B	-	0.005	0.002	0.007	0.004	0.006	0.007	0.00004	0.005	Moderately resistant	National Tube Co.
K1	-	0.005	0.009	0.014	0.017	0.0056	0.013	0.00005	0.005	Moderately resistant	Crane Co.
G21	1/2	0.005	0.003	0.008	0.006	0.0079	0.004	0.00009	0.004	Resistant	BMI

* All determinations are reported on a weight per cent basis.

methods (for details see Appendix). The nitrogen analyses, supplied by the General Electric Company, were total nitrogen, determined by the standard Kjeldahl method with the results checked by both titration and colorimetric means. The oxygen, hydrogen, and nitrogen analyses, reported by Battelle, were run by the total-vacuum-fusion method. The precision of the latter determinations was ±0.002 per cent for O_2, ±0.00004 per cent for H_2, and ±0.002 per cent for N_2.

Graphitization Characteristics: G20. This material, originally cut from pipe made by the National Tube Company, has been tested extensively at Battelle since 1943, and the results reported previously (9, 10). About 40 per cent of the carbon in this steel was converted from carbide to graphite after 1500 hr at 1025 F, and was completely graphitized after 10,000 hr at the same temperature. It may be added that in a check test at the Crane Company, steel G20 graphitized extensively after only 500 hr at 1025 F.

5B. The National Tube Company supplied this material and reported (13) some graphite at the low-temperature edge of the weld-heat-affected zone of a bead-welded specimen, as well as in the parent metal, after 10,000 hr at 1050 F. In addition, graphite also was reported in the parent metal of a bead-welded sample of this steel after 10,000 hr at 1200 F. However, its composition seemed to place it with the "resistant" steels. Accordingly, a check graphitization test on an unwelded specimen was run at 1025 F, using the facilities of the Crane Company. After 1000 hr on test, no graphite formed in the steel, but after 1500 hr graphitization had begun. Under the same test conditions, steel G20, the Battelle "very susceptible" steel run for comparison, showed considerable graphite after only 500 hr exposure.

It is concluded, therefore, that while steel 5B certainly does graphitize, it is less susceptible than G20; and, for the purposes of the present investigation, it has been classified as a "moderately resistant" steel.

K1. The Crane Company supplied this test material and reported that single-bead-welded specimens of this steel showed no graphitization after 3000 hr at 1025 F, but did show some after 6000 hr. Steel K1 was, therefore, considered moderately resistant to graphitization.

G21. This steel, also originally from pipe made by the National Tube Company, has been tested extensively at Battelle (9, 10). No graphite was found in this material, either in the parent metal or in the weld-heat-affected zones of bead-welded specimens, after 7700 hr at 1025 F, or 8500 hr at 1125 F. Studies on plain low-carbon steels using chemical kinetics, have shown that 8500 hr at 1125 F is equivalent to about 25,500 hr at 1025 F in so far as general graphite formation is concerned.

This steel was, therefore, considered resistant to graphitization.

Heat-Treatment. Part of each lot of steel was subjected to electrolytic extraction with the carbides in a condition of spheroidization, or at least partial spheroidization. The principal reason for using this condition was to increase carbide-particle size and thus favor high degrees of residue recovery. The heat-treatment used was 8 hr at 1300 F, followed by air-cooling, and the lots so treated were labeled G20S, 5BS, K1S, G21S.

The very susceptible steel, G20, and the moderately resistant steel, 5B, were also tested as normalized. The heat-treatment consisted of holding 2 hr at 1700 F, and air-cooling. The lots were identified as 5BN and G20N.

Photomicrographs of the spheroidized and normalized structures of the various steels at a magnification of 1000 are shown in Figs. 1 through 6.

Experimental Procedure

The electrolytic carbide-extraction method used in this investigation was originally developed by Dr. F. J. Dunkerley and will be described in detail in another publication. Briefly, it involves

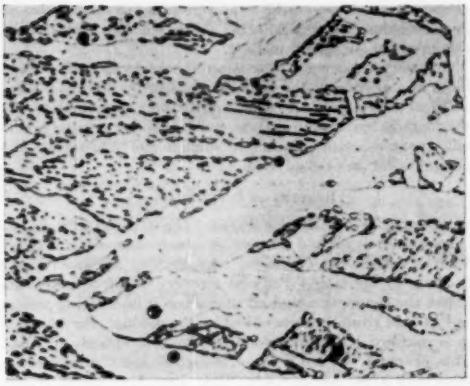

FIG. 1 STEEL G20, PARTIALLY SPHEROIDIZED—G20S
(Nital etch; ×1000.)

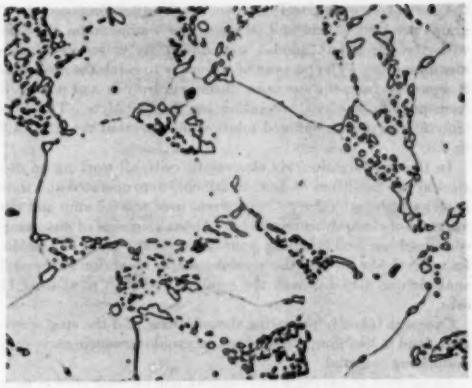

FIG. 2 STEEL 5B AS SPHEROIDIZED—5BS
(Nital etch; ×1000.)

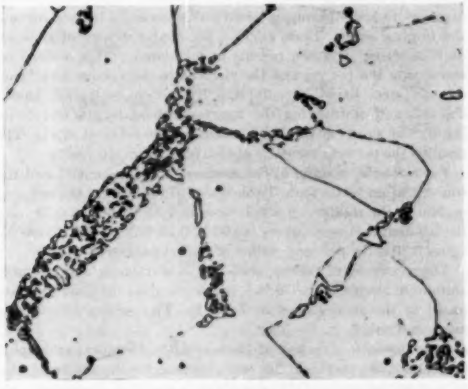

FIG. 3 STEEL K1 AS SPHEROIDIZED—K1S
(Nital etch; ×1000.)

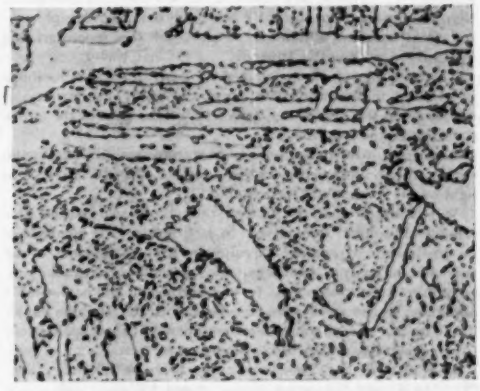

FIG. 4 STEEL G21, PARTIALLY SPHEROIDIZED—G21S
(Nital etch; ×1000.)

FIG. 5 STEEL G20 AS NORMALIZED—G20N
(Nital etch; ×1000.)

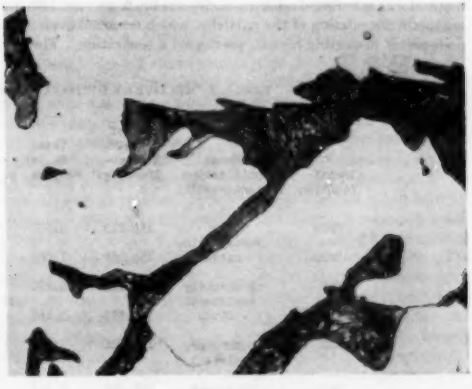

FIG. 6 STEEL 5B AS NORMALIZED—5BN
(Nital etch; ×1000.)

the electrolysis of the steel specimen in a solution composed of 160 grams per l citric acid and 60 grams per l ammonium chloride, with the specimen (anode) surrounded by a semipermeable membrane sac. The purpose of the sac is to catch the residue as it separates from the specimen during electrolysis and protect it from possible chemical alteration by the catholyte. The electrolytic solution is a buffered solution and operated at a pH of 1.8 to 2.8.

In this investigation, six electrolytic cells, all working on one steel in one condition of heat-treatment, were operated at a time in series with each other. The current used was 0.5 amp and the duration of electrolysis was 24 hr. About 13 grams of steel were consumed per cell, yielding approximately 0.3 gram of residue. In general, the size of the residue sample used for study and analysis was 3 to 4 grams, the combined product of at least 12 cells.

Care was taken in preparing the solutions, and the steel specimens, and in handling the residues, to avoid introducing any contaminating material.

Six samples of residue were obtained, one for each steel in each condition of heat-treatment. Each residue was assayed by wet-chemical methods for acid-soluble aluminum, Al_2O_3, carbon, and sulphur. In addition, as a check on the wet-chemical determination, the residue from steel 5BS was analyzed spectrographically for total residual aluminum. Details of the spectrographic analysis are given in the Appendix.

The residues were also examined by x-ray diffraction methods in an effort to obtain information on the mode of occurrence of aluminum in the residue and to determine the form of the major constituent, the iron carbide.

An inspection of some of the residue from steel 5BS was made with a petrographic microscope in a further effort to throw more light on the character of the material.

Wet-chemical analysis showed that both acid-soluble aluminum and sulphur were present in each residue. It would thus be worth while to separate the sulphides from the balance of the residues and analyze them separately for acid-soluble aluminum, to obtain direct evidence as to whether any of the acid-soluble aluminum in the steels were associated with the sulphide phase. Three methods of separation were considered; (*a*) sedimentation, (*b*) magnetic separation, and (*c*) flotation.

The difference in density between the probable sulphide phase, (Fe, Mn)S, and the major phase, shown by x-ray diffraction studies to be Fe_3C was considered sufficient (4.0 to 4.8 against 7.4) for at least a partial separation by sedimentation. This method was attempted on some of the residue from steel 5BS, but magnetic flocculation of the particles, which occurred even in the presence of dispersing agents, prevented a separation. The fineness of the particles and the small percentage of sulphur present in the residue, together with the strong tendency to flocculate, also ruled out a magnetic method.

An attempt was made to separate the sulphides from the carbides in a portion of the residue from 5BS by flotation, using aerofloat as the agent. A "float" and a "sink" were obtained, but the float was too small to analyze, while the sink was found to contain about the same amount of sulphur and acid-soluble aluminum as did the original residue.

Results of Investigation

Recovery Based on Residue Weight. The weights of the six lots of steel electrolyzed and the residues obtained are listed in Table 3. The calculations of the per cent recovery are given in the headings of the table. Per cent recovery based on weight involves the assumption that all the carbon in the steel is present as Fe_3C and keeps the form of Fe_3C in the residue. Furthermore, it is assumed that the residue is composed entirely of Fe_3C. This, of course, was not the case, though Fe and C accounted for more than 90 per cent of residue 5BS. Recovery calculated from weight, then, is approximate, but it is a useful way of handling weight data and inspecting it for trends.

Recovery Based on Assay. Another method, which is direct and involves no assumptions, is based on the assay of the residue and the original steel. From them a per cent recovery of each individual element in the residue is calculated. This is done by converting the per cent of the element in the residue to a "residue on steel basis" by dividing by the concentration factor, Table 3, and multiplying the figure obtained by 100 and dividing by the per cent of that element in the original steel. The result is the per cent recovery of that element in the residue.

For example, residue 5BS contained 7.15 per cent C and the concentration factor from Table 3 was 37.66. Then, the per cent carbon in the residue on steel basis is 7.15/37.66, or 0.19, and the per cent carbon recovery is $100 \times 0.19/0.20$, or 95, where the figure 0.20 is the per cent carbon in the original steel.

The recoveries of carbon, acid-soluble aluminum, and insoluble aluminum are given in Table 4, where the data for aluminum are based on the assays listed in Table 8. The sulphur recovery is given in Table 6.

Spectrographic Analysis of Residue 5BS. The spectrographic laboratory, in checking the wet-chemical results for total aluminum in the residue (acid-soluble plus insoluble aluminum), reported 0.1 to 0.2 per cent. This compares with the figure of 0.18 per cent obtained by wet methods.

X-Ray Diffraction Results. The results of x-ray diffraction studies of samples of the various residues are given in Table 5.

In general, only the phases marked "predominant" could be

TABLE 3 RECOVERY OF TOTAL CARBIDES BASED ON WEIGHT OF RESIDUE

Identification	General Graphitisation Characteristics	Wt. of Steel Electrolized, g. 1	Total Wt. of Residue, g. 2	Conc. Factor 3 = 1÷2	C in Steel, % 4	Theoretical Fe_3C in Steel, % 5	Theoretical Fe_3C in Steel Electrolized, g. 6 = 1 x 5	% Recovery 7 = 2÷6
G2CS	Very susceptible	158.213	3.502	45.18	0.22	3.30	5.22	67
G2CN	ditto	154.459	2.863	53.95	0.22	3.30	5.08	56
5BS	Moderately resistant	167.011	4.434	37.66	0.20	2.99	5.00	89
5BN	ditto	117.573	3.169	37.10	0.20	2.99	3.53	90
K1S	Moderately resistant	159.446	3.849	41.42	0.17	2.55	4.07	95
G2IS	Resistant	156.998	3.861	40.66	0.27	4.04	6.34	61

TABLE 4 RECOVERY OF CARBON AND ALUMINUM IN RESIDUE, BASED ON ANALYSIS

Identification	General graphitization characteristics	Carbon recovery, per cent	Aluminum recovery, per cent Soluble	Insoluble	Total
G20S	Very susceptible	65	15	60	21
G20N	Very susceptible	59	18	67	25
5BS	Moderately resistant	95	58	95	69
5BN	Moderately resistant	84	38	105	57
K1S	Moderately resistant	91	86	19	43
G21S	Resistant	60	70	57	65

TABLE 5 X-RAY DIFFRACTION RESULTS

Material	Condition	Phases identified in residue
G20S	Spheroidized	Fe_3C predominant
G20N	Normalized	Fe_3C predominant Al_2O_3 very faint
5BS	Spheroidized	Fe_3C predominant Al_2O_3 very faint
5BN	Normalized	Fe_3C predominant
K1S	Spheroidized	Fe_3C predominant (Fe or Cr)$_7C_3$ type, very faint
G21S	Spheroidized	Fe_3C only

TABLE 6 SULPHUR ANALYSES AND RECOVERY

Material	General graphitization characteristics	Residue analysis, per cent	Residue on steel basis, per cent	Steel analysis, per cent	Recovery, per cent
G20S	Very susceptible	0.28	0.0062	0.024	26
G20N	Very susceptible	0.66	0.012	0.024	50
5BS	Moderately resistant	0.28	0.0074	0.032	23
5BN	Moderately resistant	0.49	0.013	0.032	41
K1S1	Moderately resistant	0.30	0.0072	0.038	19
G21S	Resistant	0.35	0.0086	0.019	45

TABLE 7 CARBON ANALYSES AND RECOVERY

Material	General graphitization characteristics	Residue analysis, per cent	Residue on steel basis, per cent	Steel analysis, per cent	Recovery, per cent
G20S	Very susceptible	6.4	0.142	0.22	65
G20N	Very susceptible	7.0	0.130	0.22	59
5BS	Moderately resistant	7.15	0.190	0.20	95
5BN	Moderately resistant	6.2	0.167	0.20	84
K1S	Moderately resistant	6.4	0.155	0.17	91
G21S	Resistant	6.6	0.162	0.27	60

TABLE 8 ALUMINUM ANALYSES IN WEIGHT PER CENT

Material	Constituent	Normalized 1	Spheroidized 2	Al in Residue, on Steel Basis: Normalized 3	Spheroidized 4	Al in Steel 5	Acid-Soluble Al not in Residue (Steel Basis): Normalized 6	Spheroidized 7
G20 Very susceptible	Soluble Al	0.20	0.14	0.0037	0.0031	0.020	0.0163	0.0169
	Insoluble Al	0.11	0.08	0.0020	0.0018	0.003		
	Total Al	0.31	0.22	0.0057	0.0049	0.023		
	Al_2O_3	0.20	0.16	0.0037	0.0035	0.006		
5B Moderately resistant	Soluble Al	0.07	0.11	0.0019	0.0029	0.005	0.0031	0.0021
	Insoluble Al	0.08	0.07	0.0021	0.0019	0.002		
	Total Al	0.15	0.18	0.0040	0.0048	0.007		
	Al_2O_3	0.15	0.14	0.0040	0.0037	0.004		
K1 Moderately resistant	Soluble Al		0.18		0.0043	0.005		0.0007
	Insoluble Al		0.07		0.0017	0.009		
	Total Al		0.25		0.0060	0.014		
	Al_2O_3		0.14		0.0034	0.017		
G21 Resistant	Soluble Al		0.14		0.0035	0.005		0.0015
	Insoluble Al		0.07		0.0017	0.003		
	Total Al		0.21		0.0052	0.008		
	Al_2O_3		0.13		0.0032	0.006		

identified with certainty. The indications of the other phases were so weak that the table records only what seem to be the most reasonable possibilities. All of the residues showed faint indications of other phases but it was impossible to identify them.

The small amounts of residues which were examined cannot be relied upon for identifying or detecting the presence of minor amounts of constituents. For example, only occasionally did circumstances permit the detection of Al_2O_3 in the residues, though wet-chemical analysis showed its presence. Evidently, the indications of Al_2O_3 were frequently masked by those of the dominant phase.

Evidence of other aluminum-containing constituents was not found by x-ray diffraction methods.

Petrographic Examination of Residue 5BS. Petrographic examination of a portion of the dried residue 5BS revealed that the major constituent, presumably iron carbide, was black and opaque to transmitted light. It was also highly magnetic and, when suspended in immersion oil, it responded vigorously to an Alnico hand magnet. This residue was difficult to disperse, though nitrobenzene was of some help. The particles were of the order of 2 microns and less in size, which agrees with their appearance in Fig. 2.

A minor quantity of a yellow transparent constituent was observed in addition to the black phase. It was either nonmagnetic or weakly magnetic. Due to their extreme fineness, however, these particles could not be identified by optical means.

Wet-Chemical Assays. The sulphur results for the residues are shown in Table 6, the carbon determinations in Table 7, and the various aluminum determinations are given in Table 8.

Relative to Table 8, the figures in columns 6 and 7 are the per cent of acid-soluble aluminum in the steel not recovered in the residue. They were derived by subtracting the appropriate figures in columns 3 or 4, for the normalized or spheroidized conditions, from the corresponding values in column 5.

Discussion of Results

Recovery. Table 8 shows that neither the total aluminum nor the acid-soluble aluminum in the residue varied in the same direction as did these constituents in the steel. In fact, the per cent recovery of acid-soluble aluminum, as given in Table 4, showed a tendency to change from a high value for the resistant steels (with low total aluminum) to a low for the susceptible steel containing a relatively high amount of total aluminum). Of course the small number of steels studied must be taken into account in evaluating this trend. Nonetheless, it suggests a difference in the mode of occurrence of the acid-soluble aluminum between a resistant and a susceptible plain-carbon steel. The difference might be physical (for example, particle size) or, more likely, it might be chemical. The evidence does not permit a decision on this point. Whatever it was, it appeared to reduce the recovery of acid-soluble aluminum in the residue from the susceptible steel.

The effect of initial carbide-particle size, as a function of the heat-treatment of the steel prior to electrolysis, was also reflected

in the recovery figures. Thus carbon recovery was less when the steels were normalized than when they were spheroidized (see Table 4). The particle size of the carbides in a steel as normalized would be smaller on an average than in the same steel spheroidized, and, consequently, less readily retained as residue. The figures based upon residue weights show the same general tendency but not so definitely. Recovery for 5B was about the same whether normalized or spheroidized; for G20, as expected, the recovery from the normalized lot was less than from the spheroidized lot.

Before leaving the recovery figures, it should be pointed out that one of the recovery values (Table 4, per cent recovery of insoluble aluminum in 5BN) is 105 per cent. This of course is impossible, but it emphasizes the point that residue extraction and analytical work are subject to appreciable error.

Findings Relative to Aluminum. The finding of acid-soluble aluminum in every residue is of first importance to the problem. The pH of the electrolyte was such (1.8 to 2.8) that it could not have been aluminum which had originally been in solid solution in the steel, or aluminum in the form of a simple nitride; that aluminum would have dissolved in the electrolyte. This leaves the possibility that the acid-soluble Al was associated with the sulphides, carbides, or any complex nitrides in the steels which might be insoluble in the electrolyte.

Some indications bearing on possible association of the acid-soluble aluminum in the residue with the sulphide phase were found in the investigation. Recovery of sulphur in steels 5B and G20 as normalized was about twice what it was in the same steels as spheroidized (see Table 6). If much of the acid-soluble aluminum were associated with sulphide, then acid-soluble-aluminum recovery should tend in the same direction as sulphur recovery, and the figures for the normalized steels should be higher than those for the same steels as spheroidized. Reference to Table 8 shows no such trend; in one case, acid-soluble-aluminum recovery was lower in the normalized lot than in the corresponding spheroidized lot, while in the other case the situation was the reverse. It appears, then, that no great amount of the acid-soluble aluminum in the residues was associated with sulphur.

That the acid-soluble aluminum in the residue was not bound up entirely with the carbides is indicated in the recovery figures for carbon and aluminum, shown in Table 4. Aluminum recovery and carbon recovery did not parallel each other as would be expected had all the acid-soluble aluminum in the residue been associated with the carbides. The results, then, do not show exactly how the acid-soluble aluminum in the residue exists, beyond suggesting that its mode of occurrence is complex.

Viewing the aluminum results from the standpoint of the steel, Table 8 shows that some of the acid-soluble aluminum in the steel was insoluble in the electrolyte used for the carbide extractions and some of it was soluble. Correlation of the latter (columns 6 and 7, Table 8) with the graphitization characteristics of the test steels suggests that it is the fraction of the acid-soluble aluminum in the steel, which is also soluble in the electrolyte, that correlates with the degree of susceptibility to graphitization.

By the same token, the data also suggest that any aluminum associated with the carbide phase is not influential in determining susceptibility of the carbide to decomposition into iron and graphite.

Finally, the analytical work reported in Table 2 confirms indications found in other investigations, both at Battelle and elsewhere, that insoluble aluminum (as Al_2O_3) does not take part in graphitization. It is the acid-soluble aluminum to which graphitization susceptibility is related.

Influence of Heat-Treatment. Beyond an influence on carbide recovery in the residue, the heat-treatment of the steel prior to electrolysis had only one other effect observable in the data.

This effect, already touched on, related to sulphur recovery. Normalizing evidently changed the sulphides in a manner rendering them more readily retained as residue than they were in the same steels as spheroidized. Perhaps an agglomeration of sulphide particles took place during normalizing.

Conclusions

The results strongly supported the premise that the difference between a graphitization-resistant and a graphitization-susceptible plain carbon steel is one of degree and not of kind, that a graphitization-resistant plain carbon steel is not an essentially different species from a graphitization-susceptible, plain carbon steel. This philosophy has been expressed in the report of a previous investigation (14) but attention was focused at that time on the incubation period of the graphitization process, and the premise took the form that different steels had incubation periods of different lengths, the susceptible ones having very short incubation periods, and the resistant ones having long incubation periods.

The thought can be put another way. The accumulated information strongly suggests that plain carbon steels cannot be divided into two groups, i.e., those whose carbide phase is stable and those whose carbide phase is unstable. Rather, all plain carbon steels are metastable, but to varying degrees. The readily graphitizable steels are least stable, the resistant ones are most stable; all tend ultimately to be converted from iron and iron carbide to iron and graphite. This conception is consistent with the known thermodynamic information on the iron-carbon system.

The findings which support the philosophy of continuity, differences in behavior being related to differences in degree rather than kind, were that all of the steels tested, whether resistant or susceptible, contained acid-soluble aluminum. No sharp difference in the form or association assumed by the acid-soluble aluminum could be found among the steels. The difference that was found was in the percentage recovery of acid-soluble aluminum in the residues, which varied from high in the resistant steels to low in the susceptible steel. In other words, susceptibility to graphitization appeared to vary with the proportion of acid-soluble aluminum also soluble in the electrolyte. The smaller the percentage of this aluminum in the steel, the more resistant it was to graphitization.

Acknowledgment

The authors wish to express their appreciation to Project No. 29 of the Joint ASTM-ASME Committee on the Effect of Temperature on Properties of Metals for the opportunity to conduct the investigation reported here. They are particularly indebted to the committee for its interest and its constructive suggestions.

BIBLIOGRAPHY

1 "The Free Energy, Entropy and Heat of Formation of Iron Carbide (Fe_3C)," by Chu-Phay Yap and C. L. Liu, Trans. Faraday Society, vol. 28, November, 1932, pp. 788–797.

2 "The Metastability of Cementite," by H. A. Schwartz, Trans. ASM, vol. 23, 1935, p. 126.

3 "Graphitization in High Purity Iron-Carbon Alloys," by Cyril Wells, Trans. ASM, vol. 26, 1938, p. 289.

4 "Graphite in Low Carbon Steel," by A. B. Kinzel and R. W. Moore, Trans. AIME, vol. 116, 1935, p. 318.

5 "Effect of Composition and Steelmaking Practice on Graphitization Below the A_1 of Eighteen One Per Cent Carbon Steels," by C. R. Austin and M. C. Fetzer, AIME T.P. 1228, 1940, 12 pp.

6 "Factors Controlling Graphitization of Carbon Steels at Subcritical Temperatures," by C. R. Austin and M. C. Fetzer, Trans. ASM, vol. 35, 1945, pp. 485–529.

7 "Progress Report No. 1 on Survey of Graphitization of Piping," Edison Electric Institute Bulletin 11, 1943, pp. 307–308 and 318.

8 "Carbide Instability of Carbon-Molybdenum Steel Piping," by R. W. Emerson, ASTM-ASME Symposium on Graphitization, 1943.

9 "Progress Report on Graphitization of Steam Lines," by S. L. Hoyt and R. D. Williams, ASTM-ASME Symposium on Graphitization, 1944.

10 "Summary Report on the Joint EEI-AEIC Investigation of Graphitization," by S. L. Hoyt, R. D. Williams, and A. M. Hall, ASTM-ASME Symposium on Graphitization, 1945.

11 "Graphitization of Low-Carbon and Low-Carbon-Molybdenum Steels," by H. J. Kerr and F. Eberle, ASTM-ASME Symposium on Graphitization, 1944.

12 "Investigation of Graphitization at Detroit," by R. M. Van Duzer, Jr., I. A. Rohrig, and Arthur McCutchan, ASTM-ASME Symposium on Graphitization, 1944.

13 "Graphitization of Steel at Elevated Temperatures," by A. B. Wilder and J. D. Tyson, Trans. ASM, vol. 40, 1948, pp. 233–262.

14 "Further Investigation on the Graphitization of Piping for the EEI and AEIC," by A. M. Hall and S. L. Hoyt, Trans. ASME, vol. 70, 1948, pp. 847–853.

Appendix

Methods of Aluminum Analysis

Spectrographic (Total Aluminum). The sample is first converted to the oxide form and mixed with an equal weight of pure graphite. A 25-mg charge is weighed into a hollow graphite electrode and burned in a direct-current arc at 10 amp for 120 sec using a Baird three-meter spectrograph and a wave-length range of 3050–4460 A. The Al_2O_3 present is compared with two known standards as follows: A National Bureau of Standards iron oxide containing 0.46 per cent Al_2O_3 was mixed with an iron oxide containing 0.0001 per cent Al_2O_3 to give standard samples containing 0.23 per cent and 0.115 per cent Al_2O_3, respectively, with which comparisons were made.

Determinations of Aluminum in Electrolytic Residues: Insoluble Aluminum. Weigh a 0.500-gram sample into a 250-ml beaker. Treat with 50 ml of 1:3 HCl; warm on the side of the hot plate until action ceases. Filter through a Whatman No. 42 paper; wash well with hot 1:9 HCl followed by a final wash of hot water. Reserve the filter for the determination of soluble aluminum.

Ignite the residue in a platinum crucible. Cool, add 8–10 drops of 1:1 H_2SO_4 and 10–15 ml HF. Evaporate to fumes and continue fuming until all of the H_2SO_4 is gone. Fuse this residue in a minimum of potassium bisulphate, cool, leach in about 50 ml of water, add 10 ml concentrated HCl and chill in ice.

Transfer the chilled solution to a separatory funnel, add 15 ml of a 6 per cent solution of cupferron, shake for 10–15 sec, and add 20 ml of ethyl acetate. (Both the cupferron solution and the ethyl acetate must be chilled in ice.) Shake for 30 sec and allow the layers to separate. Allow the lower (aqueous) phase to run into a second separatory funnel and again extract with 20 ml of ethyl acetate. Repeat the extraction a third time, transferring the aqueous phase from the third extraction to a 250-ml beaker.

Add 5 ml 1:1 H_2SO_4 and place on the hot plate. Evaporate the solution to fumes, adding concentrated HNO_3 as needed to destroy organic matter. Fume well after each addition.

Cool, take up in 30–40 ml of water. Adjust the pH of the solution to 4.4 ±0.2 by the addition of 4 N ammonium acetate. A pH meter should be used for this adjustment.

Transfer the solution to a separatory funnel and extract four times with 10-ml portions of chloroform containing 14.4 grams of 8 hydroxyquinoline per liter. Dilute the combined extracts to 100 ml with chloroform and shake well.

Place a portion of the solution in a 1-cm cell of the Beckman spectrophotometer and determine the per cent transmittance at 425 mu using chloroform as a blank. Read milligrams of aluminum from a standard curve prepared by running standard solutions of aluminum through the chloroform-extraction procedure.

Soluble Aluminum. Transfer the filtrate obtained from the first filtration to a 250-ml volumetric flask. Dilute to the mark with water and shake well. Transfer a 100-ml (0.2 gram) aliquot to a 250-ml beaker, warm on the hot plate, and oxidize with a few drops of 2 per cent potassium permanganate solution. Cool in the ice bath and extract with cupferron and ethyl acetate as described under the treatment of the insoluble portion. However, since the iron content is higher in this solution, use 35 ml of cupferron solution and 40 ml of ethyl acetate. Complete the analysis as outlined for the insoluble aluminum.

Determination of Aluminum in Plain Low-Carbon Steel: Insoluble Aluminum. Dissolve 20 grams of drillings in 210 ml of 1.9 H_2SO_4. Digest on the hot plate at a temperature below boiling until action ceases. Filter through a Whatman No. 40 paper with pulp and wash well with hot water. Reserve the filtrate for the determination of soluble aluminum.

Ignite the residue in a platinum crucible. Cool, add 6–8 drops of 1:1 H_2SO_4 and 10–15 ml HF. Evaporate to fumes and continue fuming until all of the H_2SO_4 is gone. Fuse this residue in potassium bisulphate, leach in water, and add enough sulphuric acid to make the solution approximately 0.2 N.

Transfer the solution to a mercury-cathode cell and electrolyze until a test with a 1 per cent ferricyanide solution shows no iron present. Remove from the cell to a 400-ml beaker, heat nearly to boiling, and add NH_4OH from a burette to a methyl red end-point. Digest for ½ hr and filter on a Whatman No. 41 with pulp. Wash well with a 2 per cent solution of ammonium nitrate. Ignite in a tared platinum crucible, treat with HF in the usual manner to eliminate any silica, reignite, and weigh as Al_2O_3.

Soluble Aluminum. Heat the filtrate nearly to boiling and add an 8 per cent solution of sodium bicarbonate from a burette, stirring until a permanent precipitate forms, then 4 ml in excess. Bring the solution to a boil and then remove from the hot plate. When the precipitate has settled, filter as rapidly as possible through a Whatman No. 41 paper with pulp. Do not wash the precipitate.

Return the filter paper and residue to the original beaker. Add 10 ml concentrated H_2SO_4 and 30 ml concentrated HNO_3. When the vigorous action has stopped, place the beaker on the hot plate and evaporate to fumes. If organic matter has not been destroyed, add more HNO_3 and fume again. Adjust the acidity to approximately 0.2 N and transfer to a mercury-cathode cell. Electrolyze until a ferricyanide test shows no iron present. Complete the determination as outlined for insoluble aluminum.

Discussion

A. B. Wilder.[3] In the investigation of the role of aluminum in the graphitization of plain carbon steel, the authors have referred to the influence of nitrogen. Various types of steel with a nitrogen content, varying between 0.005 per cent–0.015 per cent nitrogen, are commercially available. Recently H. F. Beeghly[4] developed a method for determining the aluminum-nitride content of steel which is soluble in certain organic solvents. Heat-treatment has a pronounced effect upon the amount of aluminum nitride determined by this method. In the same steel, a wide range of aluminum-nitride content may be obtained after suitable heat-treatment. Therefore it is now possible to experiment with a series of steels with different nitrogen content

[3] Chief Metallurgist, National Tube Company, U. S. Steel Corporation Subsidiary, Pittsburgh, Pa.

[4] "Determination of Aluminum Nitride Nitrogen in Steel," by H. F. Beeghly, *Analytical Chemistry*, vol. 21, December, 1949, p. 1513.

and varying amounts of aluminum nitride by the organic-solvent method. An investigation conducted along these lines may contribute additional information concerning the role of aluminum in graphitization.

The statement, "All plain carbon steels are metastable but to varying degrees," suggests that if the temperature is sufficiently high and the incubation period long enough, graphite will form. We have observed in certain low-carbon steel that after long periods of incubation the rate thereafter of graphitization may be high. These results again suggest the importance of adding chromium to resist graphitization.

We have observed that some low-carbon steel, made without the use of aluminum for deoxidation, graphitize; and also many steels made with a similar deoxidation practice, are highly resistant to graphitization. Graphitization is apparently not necessarily dependent upon deoxidation practice except when large quantities (2 lb/NT) of aluminum are added to low-carbon steel. In the latter case, the material is almost certain to graphitize under proper conditions of exposure. It may be desirable to experiment, therefore, with low-carbon steels containing small amounts of chromium (0.15 per cent) and melted to coarse-grained deoxidation practice (less 0.5 lb Al/NT). This type of steel, however, would not be commercially desirable due to the coarse-grained deoxidation practice and the very limited demand for the product.

In order to advance our knowledge of the subject, the authors' work suggests that a new approach to the problem be considered. This paper, and the paper by G. V. Smith, J. A. MacMillan, and E. J. Dulis[5] on the mechanics of graphitization are valuable contributions to the literature and have advanced our knowledge of the subject.

Authors' Closure

The authors wish to thank Dr. Wilder for his comments on the paper and for the corroborative information he has supplied. Beeghly's observation that the aluminum nitride content of a steel, as determined by his analytical methods, may vary with the type of heat-treatment given the steel is of great interest. This finding may have an important bearing on the general problem of the relationship of aluminum and nitrogen to the susceptibility of steel toward graphitization.

[5] "Some Aspects of Graphitization in Steel," by G. V. Smith, J. A. MacMillan, and E. J. Dulis, American Society for Metals, Preprint No. 17, 1950.

Nickel-Chromium-Molybdenum Steel Valve Casting After 50,000 Hours of Service at 900 F

By T. N. ARMSTRONG[1] and R. J. GREENE[2]

Extensive tests have indicated that nickel-chromium-molybdenum steel, conforming to the requirements of ASTM Specifications A-217 is very resistant to graphitization under conditions imposed in the laboratory in testing cast valves and fittings of this composition for steam temperatures up to 950 F. Through the co-operation of The Detroit Edison Company a cast-steel valve of approximately WC-4 composition that had been in service over 6 years was made available for study. The paper describes tests made on this valve and the results obtained.

Introduction

THE trend toward increasing efficiencies of steam-power generating units has created the problem of selecting materials which adequately will meet the service requirements imposed by steam at high pressure and at high temperatures. Low-alloy steels have been used for temperatures up to above 1000 F, but there is a limit of temperature, generally considered to be in the neighborhood of 1050 F, beyond which the properties of low-alloy steels no longer are adequate.

Long service at 900 F and above has revealed that some steels which have been considered suitable for the service conditions deteriorate much faster than anticipated, particularly in the vicinity of welds. Certainly, the type of deterioration that has caused greatest concern over the past several years has been graphitization. This subject has been discussed so widely in the recent literature that it is considered unnecessary to add to the general discussion at this time.

Test of Service Material

One of the materials that has been used extensively in cast valves and fittings for steam at temperatures up to 950 F is a nickel-chromium-molybdenum steel, conforming to the requirements of grade WC-4 of ASTM, Specifications A-217. Extensive tests[3] had indicated that this steel was very resistant to graphitization under conditions imposed in the laboratory. It was recognized, however, that no matter how favorable the laboratory data, the most convincing evidence would result from tests of material that had been in active service for a long period. Through the co-operation of The Detroit Edison Company, a cast-steel valve of approximately WC-4 composition that had been in service for slightly over 6 years was made available for study. The valve was performing satisfactorily and probably would have continued in service for an indefinite period had it not been removed for this investigation.

Operating Conditions. The part selected was a 4-in. 900-lb slide valve which had been in continuous operation at a nominal temperature of 900 F for 53,810 hr and at an average pressure of 841 psi. From results of frequent pyrometer readings, it is estimated that the valve operated 90 per cent of the time at temperatures within a range of 885 to 900 F. Maximum temperature reported was 935 F, and the minimum temperature was 855 F.

Welding Practice. Stellite-faced seat rings had been welded into the body by the valve manufacturer. The pipe ends were welded to the body after the valve was received. The welding procedure for the pipe ends consisted of preheating the casting to 400 to 600 F, welding by the metal-arc process, and subsequently stress-relief-annealing at 1200 F, the time at temperature being 2 hr per in. of section.

Chemical Composition and Deoxidation Practice. Chemical analysis of the steel and the limits of analysis specified for grade WC-4 are listed in Table 1. At the time that the casting was made, the present specifications for grade WC-4 cast steel were not in effect but, in general, the casting meets current requirements except for slightly lower molybdenum than now specified.

TABLE 1 CHEMICAL ANALYSIS

	Per cent							
	C	Mn	Si	P	S	Ni	Cr	Mo
Valve casting	0.21	0.62	0.39	0.030	0.017	0.99	0.81	0.37
WC-4 Specs.	0.20 max	0.50/0.80	0.60 max	0.050 max	0.060 max	0.70/1.10	0.50/0.80	0.45/0.65

The melt was produced in the acid-electric furnace and deoxidized in the conventional manner before pouring. Additions of 0.09 per cent calcium-manganese-silicon alloy and 0.12 per cent aluminum were made to the ladle.

Mechanical Properties. The castings had been subjected to the following heat-treatment cycle:

Heated to 1800 F—held 5 hr—cooled in furnace
Reheated to 1550 F—held 5 hr—cooled in air
Reheated to 1200 F—held 5 hr—cooled in air

Results of tensile and impact tests of coupons heat-treated with

---

[1] Development and Research Division, The International Nickel Company, Inc., New York, N. Y.

[2] Research Laboratory, The International Nickel Company, Bayonne, N. J.

Contributed by the Joint ASTM-ASME Committee on Effect of Temperature on the Properties of Metals and presented at the Annual Meeting, New York, N. Y., November 26–December 1, 1950, of The American Society of Mechanical Engineers.

Note: Statements and opinions advanced in papers are to be understood as individual expressions of their authors and not those of the Society. Manuscript received at ASME Headquarters on July 11, 1950. Paper No. 50—A-67.

[3] "Graphitization in Some Cast Steels," by A. J. Smith, J. B. Urban, and J. W. Bolton, Trans. ASME, vol. 68, 1946, pp. 609–624.

TABLE 2 RESULTS OF TENSILE AND IMPACT TESTS

Test no.	Location	Yield strength, psi	Tensile strength, psi	Elong. in 2 in., per cent	Red. of area, per cent	Charpy V impact, ft-lb	Bhn
1[a]	Test coupon	54000	84700	26.2	52.2	32	170
2	Casting	57400	92200	20.5	30.3	22	166
3	Casting	54100	82100	22.0	45.5	21	163
4	Casting	53400	83400	16.5	26.5	24	166
5	Heat-affected zone	...	...	..	..	24	207/240
6	Heat-affected zone	...	...	..	..	43	200/255
	Specifications	40000	70000	20.0	35.0	..	.....

[a] These values reported by the valve manufacturer.

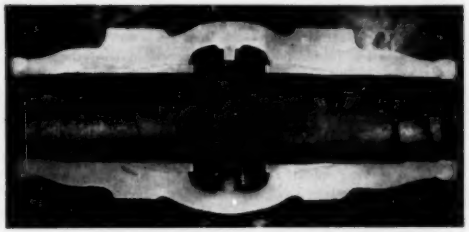

FIG. 1 SPECIMEN OF VALVE CASTING ETCHED TO SHOW LOCATION OF WELD
(About one-sixth actual size.)

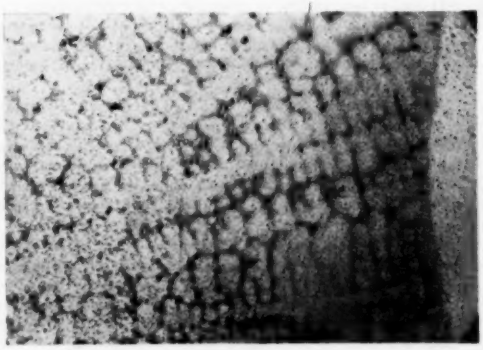

FIG. 2 TYPICAL STRUCTURE IN WELDED AREA OF VALVE CASTING; ×25

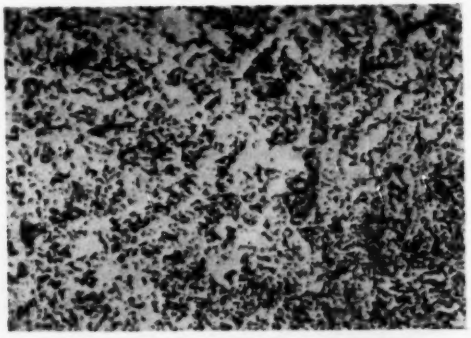

FIG. 3 GRAPHITE-FREE HEAT-AFFECTED ZONE NEAR WELD IN CASTING; ×1000

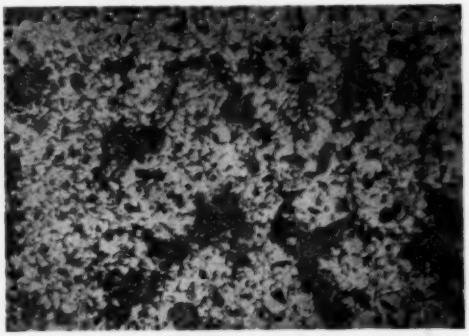

(*a*) ×100

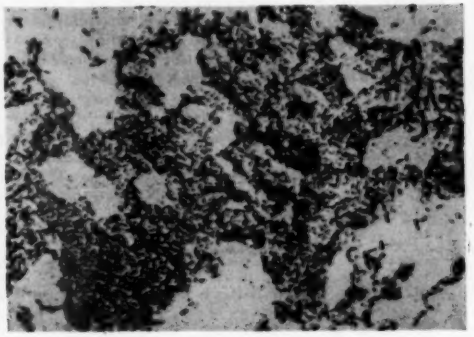

(*b*) ×1000

FIG. 4 STRUCTURE OF CASTING IN AREA UNAFFECTED BY WELDING AS REMOVED FROM SERVICE

the casting are compared in Table 2, with results secured on specimens cut from the valve after it had been withdrawn from service. Three of the specimens from the valve were taken from random areas not affected by welding, and two specimens were taken that included the heat-affected zone adjacent to a weld.

It will be noted that strength values of specimens cut from the casting are in close agreement with the strength values of the test coupon and, although the ductility of the casting specimens is somewhat lower, this is to be expected.[4] The impact properties of the casting specimens are slightly lower, with one exception, than the value for the test coupon, but there is no indication of brittleness. The one high value for the casting is probably due

[4] "Steel Castings Handbook," Steel Founders Society of America, Cleveland, Ohio, 1941, pp. 143–144.

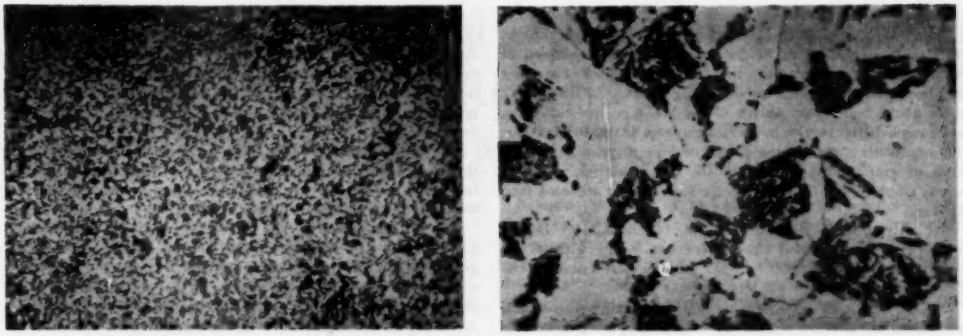

(*a*) ×100 (*b*) ×1000

FIG. 5 STRUCTURE OF CASTING IN AREA UNAFFECTED BY WELDING: RE-HEAT-TREATED AFTER REMOVAL FROM SERVICE

to a preferred microstructure resulting from rapid cooling from high temperature during welding. As impact values in the heat-affected zone usually fall within a wider scatter band than test values in unwelded areas, these results follow the general pattern.

Metallographic Examination. Eight randomly selected welded areas of the casting and two areas removed from welds were examined microscopically. Fig. 2 is typical of the welded areas surveyed and includes the weld metal, the heat-affected zone, and the base metal unaffected by the welding heat. Fig. 3 shows an area of fine spheroidized carbides near the weld, the area generally most susceptible to graphitization. No graphite was detected in any of the areas examined and also, there was no concentration of carbides that might indicate a stage preliminary to graphitization. The small black dots in Fig. 2 are nonmetallic inclusions, principally sulphides.

Although mechanical properties of sections from the casting and metallographic examinations indicated there had been little change in either properties or structure during the service period, there were no control specimens for comparison. An attempt was made to approximate the original microstructure by subjecting a specimen from the casting to the same heat-treating cycle originally employed. Fig. 4 shows the microstructure of the casting as taken from service, and Fig. 5 is of the same section after heat-treatment.

The only difference appears to be a more uniform distribution of carbides in the re-treated sample, but the faster cooling rate of the laboratory-treated sample could account for this difference. No difference could be detected in the form of the carbides.

CONCLUSION

The results of this examination indicate that there has been no loss of strength, no embrittlement, and no occurrence of graphite in the welded valve casting of nickel-chromium-molybdenum steel, of approximately WC-4 grade, after exposure to steam at 900 F for a period of 6 years.

ACKNOWLEDGMENT

The authors wish to acknowledge the co-operation of Mr. Glenn Coley of The Detroit Edison Company, for making the casting available, and of Mr. J. W. Bolton of The Lunkenheimer Company, who supplied the details on the manufacture of the casting.

Discussion

J. J. KANTER.[6] Among the steel-castings compositions which have been studied for graphitization susceptibility by Project No. 29 of the ASTM-ASME Joint Committee on Effect of Temperature on the Properties of Metals are included several heats of the grade WC-4 with which the authors deal.

The Project No. 29 aging studies, as reported to the sponsor societies, have shown that grade WC-4 has not graphitized after more than 40,000 hr of aging at 1025 F and 30,000 hr of aging at 1100 F. However, the same statement can be made of any of the other compositions studied having a chromium content equivalent to that of WC-4. Regardless of what other alloy content a steel casting has, it does not graphitize if it contains chromium.

All of the alloying combinations in steel castings killed with aluminum which have been studied to date show graphitization susceptibility in the absence of a chromium content. The fact that the valve casting reported by the authors showed no graphitization after 50,000 hr of service at 900 F is accounted for by its chromium content.

H. W. WYATT.[6] The paper is a factual report of a valve in actual service. As mentioned, the WC-4 steel was made under the old specifications. The steel that is now being furnished has lower carbon and higher moly content. It might be of interest to know that the present steel possesses higher creep strength.

H. A. WAGNER.[7] We believe the authors recognize, as will those at all familiar with the graphite problem, that the WC-4 analysis is not unique in its ability to resist graphite formation. Other analyses have proved satisfactory. In our opinion, however, the long service hours represented by these results may be of interest and in some measure reassuring in further substantiating laboratory results. The fact that serious graphite formation appears on the pipe side of some of the samples whereas none appears on the casting side of the same sample would seem to be an excellent indication of the resistance of this alloy to graphite formation in service under conditions which produce graphite.

[6] Directing Engineer, Engineering Laboratories, Crane Company, Chicago, Ill. Mem. ASME.

[6] Department Head, Physical Laboratory, The Lunkenheimer Company, Cincinnati, Ohio. Jun. ASME.

[7] Engineering Department, The Detroit Edison Company, Detroit Mich. Mem. ASME.

Because of the appearance of serious graphite in welded joints in both carbon steel at 825 F and carbon-molybdenum pipe at 900 F, a large number of welded joints have been sampled in Detroit Edison power plants. In so doing, a number of samples have been taken of pipe-to-valve casting joints. At the Delray power plant, boiler stop valves of the WC-4 composition have been sampled after service hours ranging from 48,000 to 65,000 hr. This represents a total elapsed time of 7 to 10 years. No evidence of graphite was found in the cast material, although serious graphite was evident in some cases in the adjacent pipe material.

Five valve-to-pipe joints on the No. 14 manifold at Delray power plant were sampled after 12 years in service with 90,000 service hours at about 900 F. No graphite was found in the WC-4 cast material.

At Connors Creek power plant, boiler nonreturn valves and gate valves of the WC-4 analysis have been sampled after service periods up to 109,000 hr at 825 F, without evidence of graphite formation.

Authors' Closure

The authors appreciate the remarks contributed by Messrs. Kanter, Wyatt, and Wagner. As Mr. Wagner mentions, it was not the intent to infer that WC-4 steel is unique in its resistance to graphitization, but rather to submit evidence that this steel under the service conditions described has shown little, if any, deterioration.

Mr. Wyatt's statement that the lower-carbon modification of this steel has superior resistance to creep is of considerable interest and it is hoped that data indicating the superiority of the lower-carbon grade will be presented sometime in the near future.

The authors agree with Mr. Kanter that additions of chromium are most effective in increasing the resistance of ferritic steels to graphitization but to base the resistance of a complex alloy steel such as WC-4 entirely on the chromium content is believed to be an oversimplification. It is known that manganese also has an inhibiting effect on graphite formation and there is some indication that the influence exerted by a single alloy may be altered when present in combination with other alloys.

The General Tensional Relaxation Properties of a Bolting Steel

By D. N. FREY,[1] ANN ARBOR, MICH.

One objective of the investigation reported in the paper was to measure the tensional relaxation properties of a Cr-Mo-Si-Va commercial high-temperature bolting at 1000 F under varying conditions of follow-up by means of the step-down relaxation test. To this end certain necessary assumptions were made relative to high-temperature behavior, which were checked for validity by means of a true relaxation test, with a particular value of elastic follow-up, carried out in a Barr and Bardgett test unit. Comparison of these results with the results of the step-down test at the same value of elastic follow-up gives a partial evaluation of the assumptions inherent in the latter testing method.

INCREASED interest in the phenomenon of relaxation of metals at elevated temperatures has occurred in recent years. This can be attributed to the fact that mechanical equipments designed to operate at these elevated temperatures are becoming more numerous in both type and quantity. Relaxation can occur in those members which have stresses dependent upon one or more of their dimensions (the critical dimension), and which are also operating at least in part, at temperatures high enough for creep to occur under these stresses. If this creep results in changes of the critical dimensions in such a direction as to reduce the dimensionally dependent stresses, relaxation is said to occur. Another way of stating the same thing is to say that the elastic strains in the stressed member are replaced by the plastic strains of creep and, since the stresses of the member are dependent upon its elastic strains, relaxation occurs. A familiar case is a tightened bolt at a high temperature. As it creeps under tensional stress, it gradually relaxes its pressure on the bolted members.

Two cases of relaxation are readily apparent. In the first case the entire stressed member is at a temperature high enough for creep to occur, and the resulting stress relaxation takes place in the fullest amount possible.

For purposes of this discussion this will be called simple relaxation. In the second case only part of the stressed member is at a temperature high enough for creep, and this creep results in smaller stress relaxation than in the former case. The cold sections are not relaxing and tend to maintain the stresses in the hot section. This will be called general relaxation or relaxation with elastic follow-up. The greater the ratio of cold-section length to hot-section length, the greater the elastic follow-up. A constant-load creep test can be considered as a limiting case of general relaxation with an infinitely large value of elastic follow-up.

Even for the case of relaxation under uniaxial tension, little has been done to ascertain clearly the dependence of stress relaxation upon the amount of elastic follow-up. Accordingly, the first objective of this investigation was to measure the tensional relaxation properties of a Cr-Mo-Si-Va commercial high-temperature bolting steel at 1000 F under varying conditions of elastic follow-up by means of the step-down relaxation test.

In order to consider this widely used test method as a true relaxation test, certain assumptions must be made relative to high-temperature behavior. Thus a secondary objective of this investigation was to investigate partially the validity of these assumptions. This was to be done by means of a true relaxation test, with a particular value of elastic follow-up, carried out in a Barr and Bardgett test unit.[2,3] Comparison of these results with the results of the step-down test at the same value of elastic follow-up can give a partial evaluation of the assumptions inherent in the latter testing method.

Basic Analysis[4]

The strain equation of simple relaxation with no elastic follow-up can be written

$$\frac{S(t)}{E} + X = \frac{S_0}{E} \qquad [1]$$

where

$S(t)$ = stress at time, t
S_0 = initial stress
X = plastic deformation
E = tensile modulus at test temperature

In general, three methods of obtaining $S(t)$ are used: (1) The experimental setup can be such that Equation [1] is satisfied continuously and that $S(t)$ can be thus recorded as a function of t (method 1). (2) Equation [1] can be satisfied in a steplike fashion with the increments of $S(t)$ small so that the stepped plot of $S(t)$, as a function of t, can be smoothed to obtain $S(t)$ (method 2). The validity of this method depends on the size of the $S(t)$-increments. This method as well as the one next described has the advantage of being adaptable to conventional creep-test units. (3) Equation [1] can be satisfied again in stepwise fashion and a plot of $(dx)/(dt)$ versus $S(t)$ obtained.

By differentiating Equation [1]

$$\frac{dx}{dt} = -\frac{1}{E}\frac{ds}{dt} \qquad [2]$$

If $(dx)/(dt)$ as a function of S is at hand, a solution of Equation [2] can, at least in principle, be found with the boundary condition that at $t = 0$, $S = S_0$ (method 3). The largest amount of published data for simple tensional relaxation has been obtained with method 3 and with the empirical expression

---

[1] Assistant Professor, Department of Chemical and Metallurgical Engineering, University of Michigan.

Contributed by the Joint ASTM-ASME Committee on Effect of Temperature on the Properties of Metals and presented at the Annual Meeting, New York, N. Y., November 26–December 1, 1950, of The American Society of Mechanical Engineers.

Note: Statements and opinions advanced in papers are to be understood as individual expressions of their authors and not those of the Society. Manuscript received at ASME Headquarters, July 11, 1950. Paper No. 50—A-68.

[2] British Patent Specification 339890, December 18, 1930.

[3] "An Accelerated Test for the Determination of the Limiting Creep Stress of Metals," by W. Barr and W. E. Bardgett, Trans. The Institution of Mechanical Engineers, vol. 122, 1932, pp. 285–297.

[4] This analysis uses as a first approximation the engineering strain, $X = L/L_0$ rather than the true strain, $E = \ln (L/L_0)$.

$$\frac{dx}{dt} = K_1 S^{K_2} \quad [3]$$

i.e., $(dx)/(dt)$ versus S is a straight line on a plot of log $(dx)/(dt)$ versus log S—used to solve Equation [2]. The solution of Equation [2] using Equation [3] can be written

$$S^{K_2-1} = \frac{S_0^{K_2-1}}{K_1 E(K_2-1)\,(S_0^{K_2-1}\,t) + 1} \quad [4]$$

if

$$K_1 E(K_2-1)\,S_0^{K_2-1}\,t + 1 \ll S_0^{K_2-1}\,t\,K_1 E\,(K_2-1)$$

as is usually the case, then Equation [4] can be written

$$S = \sqrt[K_2-1]{\frac{1}{K_1(K_1-1)Et}} \quad [5]$$

Equation [5] appears to give $S(t)$-values independent of S_0, but it has been determined experimentally that both K_1 and K_2 are, in general, functions of S_0. It should be emphasized that Equation [5] holds only when the empirical Expression [3] is used for $(dx)/(dt)$ as a function of S. While Equation [3] fits some of the data obtained, it does not fit all, and some other $(dx)/(dt)$ (S) function may be more accurate. Some data have been obtained for which the expression

$$\frac{dx}{dt} = K_1 e^{K_2 S} \quad [6]$$

has greater validity. With this expression, Equation [5] becomes

$$S = -\ln(K_1 K_2 E t)^{\frac{1}{K_2}}$$

provided

$$K_1 K_2 E t >> \frac{1}{e^{K_2 S_0}} \quad [7]$$

as is usually the case.

As a final comment on methods for obtaining $S(t)$ under conditions of simple relaxation, it would appear that method 3 has little to offer over method 2, as each is subject to the same implied assumptions, namely, that creep rate is a unique function of stress and not of time or prior history, in general. It is obvious that this assumption is ridiculous in the general case, but it may be quite good for small increments of stress relief. It also should be stated that the empirical constants of Equations [3] and [6] are, in the general case, a function of the initial stress, S_0.

As stated, one of the purposes of this investigation was to investigate the validity of the foregoing assumption for the small values of stress relief commonly used in the step-down test. Unfortunately, the equipment at hand allowed the check to be carried out only under the more general condition of relaxation with elastic follow-up. The analysis of relaxation with elastic follow-up follows:

The equation of general relaxation (with elastic follow-up) similar to Equation [1] is

$$(L_e - L)\left(\frac{S(t)}{E_0}\right) + L\left(\frac{S(t)}{E}\right) + LX = (L_e - L)\frac{S_0}{E_0} + L\frac{S_0}{E} \quad [8]$$

where

$S(t)$, S_0, X, and E are as before
E_0 = tensile modulus at ambient temperature
L = creeping section
L_e = total stressed length-creeping section plus cold sections

Dividing through by L and calling $L_e/L = b$, the elasticity ratio, we get

$$(b-1)\left(\frac{S(t)}{E_0}\right) + \frac{S(t)}{E} + X = (b-1)\frac{S_0}{E_0} + \frac{S_0}{E} \quad [9]$$

To obtain $S(t)$, the three methods briefly outlined under simple relaxation, in general, can be still applied with the proviso of course that some means be provided to obtain the effects of elastic follow-up.

A number of years ago, a test was devised by Barr and Bardgett for evaluation of creep properties which was in reality a relaxation test with elastic follow-up.[a,b] Hence this type of test can be used to achieve method 1 for solving Equation [9].

For an approximate solution of Equation [9] by methods 2 and 3, step-down tests can be run. To obtain the effects of elastic follow-up, the elastic contraction following each increment of load removed can be followed by a plastic extension (creep) which is b' times as large, before another increment of stress is removed.[b] To obtain the equivalence between the factor b', associated with the step-down test, and the factor b, associated with an actual relaxation test, the following analysis is made:

For the step-down relaxation test

$$\Delta X = -\left(\frac{\Delta S}{E}\right) b' \quad [10]$$

which for small increments of S may be written

$$dx = -\frac{dS}{E}\,(b') \quad [11]$$

for a true relaxation test with elastic follow-up

$$dx = -\frac{(b-1)}{E_0}\,dS - \frac{1}{E}\,dS = -\frac{dS}{E}\left[\frac{E}{E_0}(b-1) + 1\right] \quad [12]$$

and from this it is evident that

$$b' = \frac{E}{E_0}(b-1) + 1$$

or

$$b = \frac{E_0}{E}(b'-1) + 1 \quad [13]$$

When $E = E_0$, it is further evident that the expression reduces to $b = b'$.

Considering method 2 specifically, the construction of the smoothed $S(t)$-plots is the same as before for simple relaxation tests taking into account the proper values of b or b'. For method 3, step-down tests run with specific b (or b')-factors can be made to yield plots of $(ds)/dt$ versus stress. From these plots the appropriate empirical expression of $(dx)/(dt)$ as a function of S can at least in principle be determined. If Expression [3] applies, the solution to Equation [11] analogous to (S) is

$$S = \sqrt[K_2-1]{\frac{E(b-1) + E_0}{K_1(K_2-1)\,E\,E_0 t}} \quad [14]$$

or if Expression [6] applies

$$S = -\ln\left(\frac{K_1 K_2 E\,E_0 t}{E(b-1) + E_0}\right)^{1/K_2} \quad [15]$$

[b] "The Resistance to Relaxation of Materials at High Temperature," by E. L. Robinson, Trans. ASME, vol. 61, 1939, pp. 543–554.

provided in this case that

$$\frac{K_1 K_2 E E_0 t}{E(b-1)+E_0} >> \frac{1}{e^{K_2 S_0}}$$

General Experimental Method

For all test specimens, rolled $^3/_8$-in. round bar stock from a commercial heat of Cr-Mo-Si-Va steel[4] (17-22A) was used having the following chemical analysis:

	Per cent
Carbon	0.45
Silicon	0.60
Manganese	0.55
Chromium	1.26
Nickel	0.29
Molybdenum	0.52
Vanadium	0.24

This stock was normalized from 1725 F and tempered for 6 hr at 1225 F. The resulting pertinent physical properties are as follows:

0.02 per cent offset yield point at 1000 F—57,500 psi
Tension modulus at 70 F—30.5 × 10^6 psi
Tension modulus at 1000 F—22.5 × 10^6 psi

From the heat-treated stock four ASTM standard 0.505-in-diam creep specimens and three bars required for the Barr and Bardgett test were machined. These latter consisted of two bars 19.5 in. long, 0.500 in. diam, and terminated at both ends with $^3/_8$-in. threads; and one bar 17.5 in. long with the same diameter and thread arrangement at both ends, also containing a $^1/_2$-in-square section near one end.

Step-Down Relaxation Tests

Standard 0.505 creep specimens were placed in conventional beam-loaded creep-testing units equipped with modified Martens optical extensometers. The specimens were brought to temperature and loaded in 4 hr to the desired initial stress, 40,000 psi (roughly $^3/_4$ of the yield strength). The specimens were then allowed to creep an amount equal to b' times the elastic contraction occurring when a stress increment of 1900 psi (the stress due to one weight on the loading system) was removed. This contraction had been calculated previously in terms of the extensometer readings. After this initial creep had taken place, the first stress increment was removed, the same amount of creep allowed to take place, and the whole process repeated for a total testing time of 1000 hr.

Four tests of this type were run at b'-values of 1 (simple relaxation) 3, 6, and 12. From the stress-time and elongation-time records of these tests, Figs. 2 and 3 were prepared.

Barr and Bardgett Test[2,3]

To one of the 19.5-in. bars were attached nine thermocouples, one at the center of the bar; two at either side from the center and 2 in. from the center; 2 more, 1 in. from the preceding pair; 2 more, 1 in. from this pair; and finally two more, 2 in. from the last pair. To the other 19.5-in. bar electrical-resistance strain gages were attached. The three bars were then assembled together by means of heavy nuts, with the bar with the thermocouples in the center. This assembly was next placed in a tensile machine, and stressed to approximately one half the yield stress, with elongation measurements taken from the tensile-machine crosshead. The effect of the two joints was evaluated by calculation of the apparent length of the whole assembly in terms of a continuous bar of 0.500 in. diam from the stress-strain data.

[4] Heat number 15429, was furnished by the Steel and Tube Division of the Timken Roller Bearing Company.

Next, the assembled bars were placed under no stress in the Barr and Bardgett test fixture. This fixture consists essentially of a heavy cast-iron base with two heavy upright bars 5 ft high and approximately $1^1/_2$ ft apart mounted in the base. These uprights are in turn surmounted by a crosshead with a hole in the center. There is also a hole in the center of the base between the two uprights. The test bar or bars are slipped through the holes in the top crosshead and the base, and held in place by nuts over bottom and top ends of the bar or bars, said nuts seating on the bottom side of the base and the top side of the crosshead. The top nut has between itself and the crosshead a thrust bearing, and the test bar is stressed by turning the top nut. As mentioned previously, a squared section is machined on the test bar to keep it from turning during the stressing.

The Barr and Bardgett unit is also equipped with an electrical-resistance furnace suspended between the uprights so as to surround the center of the test bar. The furnace is cylindrical in shape and split into two halves along a plane normal to the cylindrical axis.

By means of previously determined settings on the furnace controls, the center bar was brought to temperature, with as good a temperature distribution along the axis as possible, in 4 hr. The assembled bars were then stressed to the desired initial stress of 40,000 psi by turning the top nut of the Barr and Bardgett fixture. Determination of the stress present was done with the strain-gage readings starting at zero stress.

After starting the relaxation test in the foregoing manner, readings of the strain gages were taken over a 1000-hr period and converted to the equivalent stresses. From these readings the residual-stress curve in Fig. 2 was plotted. In order to check any drift that might have occurred in the strain-gage system during the time period of testing, the test bar was unloaded after 1000 hr, and the reading of the strain gage compared with the zero-stress reading obtained before the initial stressing. The difference between the two quantities was 4 microinches—a negligible quantity.

Results of Step-Down Relaxation Tests

The four step-down tests run at b'-factors of 1, 3, 6, and 12 (b factors of 1, 3, 7, 7.75, and 15.85) gave the stress versus time plots shown in Fig. 2. The curves shown were constructed from the stepwise stress versus time plots obtained from the creep-test units by equalizing the stepped areas above and below the curve as drawn. Accordingly, the method is method 2 in the "Basic Analysis" section. No simple plot of residual stress versus time gave straight lines, although the semilog plot shown gave the best approximation to a straight line.

The creep rate versus stress relationships obtained from the elongation data taken from the creep units are shown in Fig. 3. From the straight lines drawn through the experimental points (admittedly these lines are only approximations), the constants K_1 and K_2 of Equation [6] were determined. By using Equation [14], the residual stresses at 100, 1000, 10,000, and 100,000 hr were obtained. These values are shown in Table 1. The method used to obtain these values can be considered method 3 of the Basic Analysis section.

The calculated 100- and 1000-hr residual-stress values are also shown in Fig. 4 (solid curves), as a function of b. These values checked closely the values obtained from the smoothed stress versus times curves in Fig. 2.

Results of Barr and Bardgett Test

The results of tensile testing the entire bar assembly indicated that the effective length was 62 in. This compared favorably with the actual length of 56.6 in., and the joints were considered to be contributing little deformation under stress.

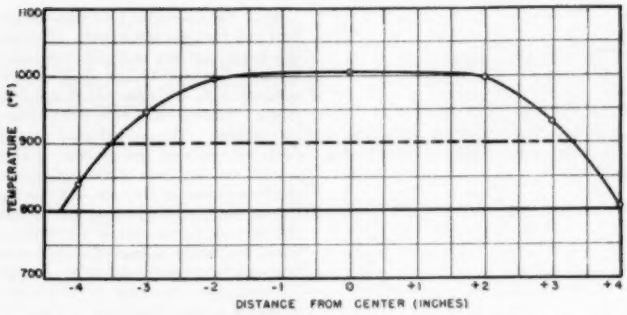

FIG. 1 LONGITUDINAL TEMPERATURE DISTRIBUTION OF BARR-BARDGETT TEST

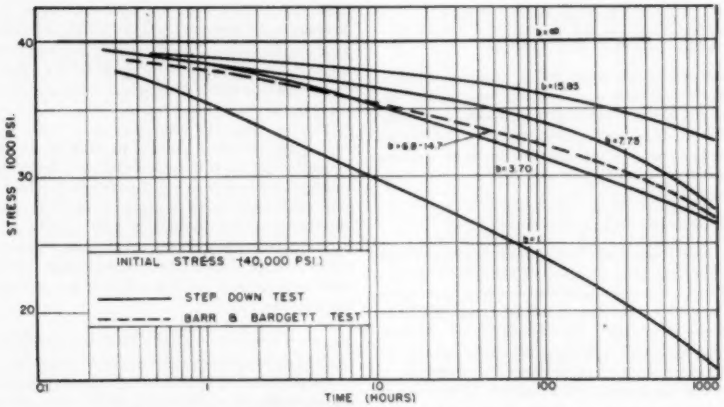

FIG. 2 EFFECT OF ELASTICITY FACTOR ON RESIDUAL STRESS OF 17-22A AT 1000 F

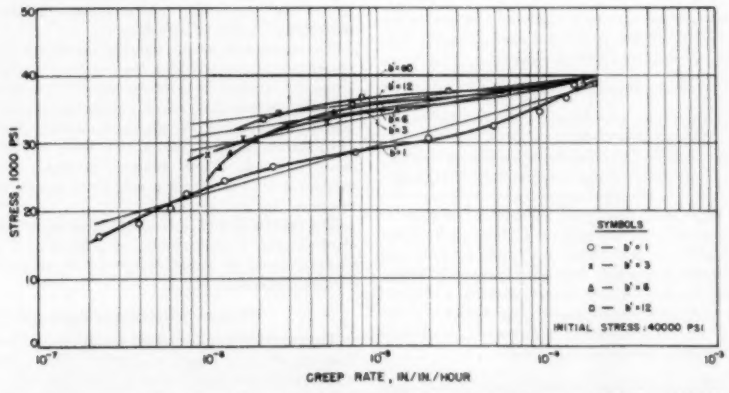

FIG. 3 EFFECT OF ELASTICITY FACTOR ON STRESS-CREEP RATE RELATIONSHIP FOR 17-22A AT 1000 F

TABLE 1 SUMMARY OF RESULTS OF STEP-DOWN RELAXATION TESTING

(Normalized and drawn Cr-Mo-Si-Va steel at 1000 F; Initial stress 40,000 Psi)

b	K_1	K_2	Calculated 100-hr stress, psi	Observed 100-hr stress, psi	Calculated 1000-hr stress, psi	Observed 100-hr stress, psi
1	4.67×10^{-10}	3.36×10^{-4}	23700	24300	16900	15800
3.70	3.4×10^{-13}	5.06×10^{-4}	31300	31300	26700	26400
7.75	2.04×10^{-15}	6.39×10^{-4}	33500	33900	30000	28000
15.85	6.02×10^{-18}	7.80×10^{-4}	35600	36000	32600	32500
∞	....	....	40000	40000	40000	40000

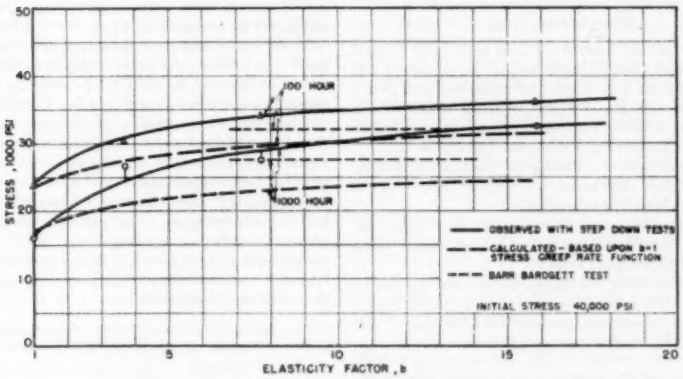

FIG. 4 EFFECT OF ELASTICITY FACTOR ON 100 AND 1000-HR RESIDUAL STRESSES OF 17-22A STEEL AT 1000 F

Temperature distribution along the center bar during the relaxation test was as shown in Fig. 1. As would be expected, the ideal case of a stepwise distribution, with no intermediate temperature zone was not achieved. The problem then is to estimate accurately the relaxing zone and, thus, the elasticity factor under which the test was run. Previous data obtained indicated that Cr-Mo-Si-Va steel does not creep measurably under the stress used here at temperatures below 800 F. Accordingly, those portions of the bar below 800 F can be considered as not relaxing. Thus the relaxing section is between 4 and 8.25 in. in length. This defines the limits of the factor b as 14.1 and 6.8, with the actual value probably closer to 14.1, since relaxation rates are strongly temperature dependent.

Table 1 and Fig. 2 show the residual stresses measured at the strain gages. Unfortunately, no simple straight-line plot of residual stress versus time was possible for ease of extrapolation. The semilog plot in Fig. 2 gave most nearly a straight line.

DISCUSSION OF RESULTS

Examination of Fig. 2 shows that variation of the elasticity factor between 1 and ∞ produces a family of residual-stress curves with the curve for $b = 1$ having the greatest negative slope, and the curve for $b = \infty$ horizontal. When it is recognized that a creep test is a fixed-stress test having effectively an infinite value of the elasticity factor (no relief of stress as the hot section creeps), and that simple relaxation ($b = \infty$) results in the greatest possible relief of stress, then the results are as one would predict on a qualitative basis.

Two other concepts are important in this connection:

(1) Analogous curves of elongation versus time can be constructed. The curve for simple relaxation ($b = 1$) would be horizontal, since it is a constant-strain test, while the curve for infinite elastic follow-up (creep test) would have the greatest positive slopes, and the curves for all intermediate values of elasticity factor would fall in between.

(2) If the initial stress for a series of relaxation tests with varying elastic follow-up were high enough, some of the tests should fracture within periods of time which are functions of the elasticity factor.

For infinite elasticity (creep test), the rupture time would be the shortest possible, and the test would be an ordinary stress-rupture test so familiar in the high-temperature metallurgical field today. With simple relaxation ($b = 1$), run with the same initial stress, the test should theoretically never break, provided the material would elongate before fracture occurs. Tests run with intermediate values of b and the same initial stress, should break at times between those for the foregoing two limiting cases. Thus fracture time should be a uniform and predictable function of the elasticity factor.

It is suggested that these interesting properties of metals at high temperatures have engineering applications and that further research should be done in the general field of relaxation.

Plotted in Fig. 4 are two horizontal lines showing the 100 and 1000-hr residual stresses of the Barr and Bardgett test within the values of b, under which the test must have been run. These stresses are between 5 and 10 per cent lower than the corresponding residual stresses of the step-down tests (solid curves). The fact that the values from the Barr and Bardgett test are lower is probably a result of the assumptions made in the step-down test. However, it appears that the approximation of the step-down tests, at least for the conditions herein studied, do not give residual stresses greatly in error. Certainly, the factors of safety (or ignorance) used in the design of bolts for high-temperature service cover adequately the errors involved.

It is foreseeable that a designer would have available such constants as K_1 and K_2 of Equation [6] only for a single relaxation test ($b = 1$), and for no other value of b, and yet wish to calculate the residual stresses under some condition of elastic follow-up. Using the value of K_1 and K_2 for this step-down test, run under a factor of $b = 1$, 100, and 1000 hr, residual stresses at higher values

of b were calculated by means of Equation [15]. These are shown in Fig. 4 (dotted curves). The values are uniformly lower than the actual values from the various step-down tests and are also lower than values from the one true relaxation test. (Note how the single Barr and Bardgett test falls above the value on the dotted curve.) It appears then that such a design procedure as the foregoing, in the absence of further data, will give conservative values.

Conclusions

1 Approximate residual stresses for time periods up to 1000 hr were obtained experimentally by means of the step-down test for elasticity factors from 1 to 15.85 with normalized and drawn Cr-Mo-Si-Va steel at 1000 F and 40,000 psi initial stress. These residual stresses vary with b in a manner qualitatively predictable when a creep test is considered as a relaxation test at $b = \infty$.

2 Empirical formulas for calculating the residual stresses for longer time periods than 1000 hr are also derived subject to the possible errors of any long-time extrapolation.

3 From the results of a single Barr and Bardgett test it appears that the step-down test gives residual-stress values which are of the order of 5–10 per cent too high.

4 Values of residual stress, calculated for values of the elasticity factor b, higher than 1 from empirical data obtained from a step-down test run under an elastic factor of $b = 1$, are most probably conservative by a factor of the order of 20 per cent.

Discussion

Ernest L. Robinson.[7] This paper is a welcome contribution of test results, together with appropriate analytical interpretation of the behavior of a good modern bolting steel for high-temperature service under conditions where follow-up elasticity has been utilized to prolong the tightness of a joint.

Both smooth and step-down relaxation results are presented and discussed which is just what a designer needs to improve his intelligent use of materials.

The writer's company makes extensive use of the step-down type of test for general creep-testing work using longer steps than would be best for the direct determination of bolting strength, but determining creep rates under a number of steady loads on the same bar from which creep strengths for design can be predicted for conditions where the total allowable strain is limited. Admittedly, the results are not identical with what would be obtained with constant-load tests. However, results on successive constant loads differ among themselves.

It is useful to improve the technique of interpretation for the various methods of running tests. While special relaxation-testing equipment is useful, it is also advantageous to be able to run such tests in ordinary creep furnaces and be able to apply the results with confidence.

[7] Structural Engineer, Turbine Engineering Divisions, General Electric Company, Schenectady, N.Y. Fellow ASME.

Basic Factors in Hot-Machining of Metals

By E. J. KRABACHER[1] and M. E. MERCHANT,[2] CINCINNATI, OHIO

This paper presents the results of research on the influence of basic metal-cutting quantities when machining metals at elevated temperatures. Much of the investigation centered around some of the commoner high-temperature alloys. Studies on the mechanics of cutting at elevated temperatures were made in which such basic quantities as chip friction, shear strength, and machining constant were measured. In addition, tool-chip interface temperatures were calculated. These data were correlated with data obtained from milling tool-life tests on the same materials. Two main factors oppose each other in their effect on tool life in hot-machining. These are the increased ease with which the heat-softened tool material can be abraded away and the decreased ability of the heat-softened chip and workpiece to produce such abrasion. It was found that these two factors can be evaluated roughly from tool-temperature data taken in combination with data on the mechanics of cutting.

Introduction

THERE are three quantities which, in practice, determine how readily a given work material can be machined. These are tool life, tool forces and the accompanying power consumption, and surface finish. In the present investigation of hot-machining, attention has been directed to the first two of these as being the most important. Particular attention has been given the matter of tool life since this is so very important in controlling costs in the machining of such hard-to-machine metals as high-temperature alloys. It is on such metals that hot machining can be used to real advantage.

The use of heat to aid in the machining of metals on production machining operations is a relatively new development. A patent covering the use of induction heating for such an application was issued in 1946, to M. Berliner (1).[3] In 1949 Armitage and Schmidt (2) described milling tests carried out on die blocks heated to red heat. The same year, Tour and Fletcher (3) described the application of heat to turning operations. In all this initial work no data on tool life were reported. However, in 1950, Armstrong, Cosler, and Katz (4) described the results of an extensive study on hot-machining carried out at Battelle Memorial Institute in which tool-life data were obtained. To date, theirs are apparently the only data on tool life which have been reported in the literature. All of these investigators have reported a very considerable reduction in tool forces and power consumption brought about by machining metals at elevated temperatures. However, the basic reasons for lower values of power consumption and tool forces were not investigated. In the case of the tool-life data reported by Armstrong, Cosler, and Katz, it was shown that increasing the temperature of the workpiece does not always result in an increase in tool life. There is an optimum temperature at which tool life will be a maximum. However, in these tool-life studies, as in the case of all the studies on power consumption and tool forces, no investigation was made of the basic factors influencing these important practical quantities. It was the purpose of the present research to study such basic factors.

It is not surprising to find that less power is required to machine metals hot than at room temperature. It is a well-known fact that increasing the temperature of a metal decreases its strength, so that the power required for chip formation, involving deformation of the metal, ought naturally to decrease with increasing temperature. However, the question arises as to whether this is the only factor influencing the power consumption and tool forces as temperature is increased. It was one of the purposes of the research described in this paper to investigate this question.

As regards the fact that increased tool life can sometimes be obtained by heating the workpiece, the question naturally arises as to why this should occur. It is a well-known fact that tool life decreases with increasing tool temperature. Schallbroch, Schaumann, and Wallichs (5) have shown that in the case of cutting tests made with the workpiece at room temperature, with only the cutting speed as a variable, tool life varies inversely as approximately the 20th power of the tool-chip interface temperature, expressed in degrees Centigrade. The action of increased tool temperature is to soften or weaken the tool metal so that it is more readily abraded away by the work material. Therefore it would be expected that if heating the workpiece resulted only in higher temperature at the chip-tool interface, tool life inevitably would be shortened. However, temperature is not the only factor influencing tool life. The ability of the work material to abrade the cutting tool is also an important factor. It is these two factors taken together—the chip-tool interface temperature (which softens the tool and makes it more subject to wear), and the abrading action inflicted by the work material on the tool—which oppose each other in such a way as to result in the peculiar behavior of tool life with increasing workpiece temperature. Therefore increasing the workpiece temperature may result in either an increase or decrease in tool life, depending upon the relative manner in which these two factors change with increasing temperature. It was thus also the purpose of the research described in this paper to attempt a quantitative evaluation of the basic factors which influence tool life in hot-machining.

In order to investigate problems of the type outlined, it is necessary to carry out experimental work and theoretical analyses of three different types, namely, an investigation of the mechanics of cutting, a study of tool temperatures, and an investigation of tool life. In the present research, these three studies were carried out and correlated to obtain an understanding of the basic factors in the hot-machining of metals.

The work materials selected for this research were three of the commoner high-temperature alloys, namely, Inconel X, Timken 16-25-6 and S-816, and an alloy steel, namely, AISI 3145. The three high-temperature alloys are characteristic of the type of hard-to-machine metals on which hot-machining has possibilities of being of most benefit. The 3145 steel was used because it

---

[1] Research Engineer, The Cincinnati Milling Machine Company. Jun. ASME.

[2] Senior Research Physicist, The Cincinnati Milling Machine Company. Mem. ASME.

[3] Numbers in parentheses refer to the Bibliography at the end of the paper.

Contributed by the Research Committees on Metal-Cutting Data and Bibliography, and Cutting Fluids and the Production Engineering Division, and presented at the Annual Meeting, New York, N. Y., November 26–December 1, 1950, of The American Society of Mechanical Engineers.

Note: Statements and opinions advanced in papers are to be understood as individual expressions of their authors and not those of the Society. Manuscript received at ASME Headquarters, October 13, 1950. Paper No. 50—A-92.

could be hardened to a normally unmachinable condition; the results obtained by applying hot machining to the steel in this condition could then be compared with those found from tests on the same steel in the soft, machinable, "as-received" condition. The nominal chemical composition of the high-temperature alloys is given in Table 1.

TABLE 1 NOMINAL CHEMICAL COMPOSITION OF HIGH-TEMPERATURE ALLOYS

	Timken 16–25–6 composition, per cent	Inconel X composition, per cent	S-816 Alloy composition, per cent
Nickel	25.0 aim	70.0 min	20.2
Chromium	16.0 aim	14.00 to 16.00	19.8
Titanium	.....	2.25 to 2.75	..
Columbium	.....	0.70 to 1.25	3.8
Aluminum	.....	0.40 to 1.00	..
Iron	.....	5.00 to 9.00	3.5
Molybdenum	6.0 aim	.....	4.3
Manganese	2.0 max	0.30 to 1.00	1.0
Silicon	1.0 max	0.50 max	0.4
Copper	.....	0.20 max	..
Carbon	0.08 to 0.10	0.08 max	0.4
Sulphur	.....	0.01 max	..
Nitrogen	0.15 aim	.....	..
Tungsten	.....	.....	4.3
Cobalt	.....	.....	42.3

In general, these work materials were used in two different forms. For the studies on the mechanics of cutting and tool temperatures, the workpieces were in the form of a tube having a $^1/_4$-in. wall thickness, which could be machined on the end to provide continuous orthogonal cutting. For the tool-life studies, the workpieces were of rectangular shape and about 1 in. thick so that they could be machined, on edge, in a face-milling operation with a single-tooth cutter. The mechanical properties and important dimensions of these various workpieces are given in Table 2.

A standard grade of steel-cutting sintered carbide was the tool material in all the cutting tests run on the foregoing materials in the present investigation.

The Mechanics of Hot-Machining

Theoretical Background. The mechanics of the metal-cutting process for the case of orthogonal cutting and a simple continuous chip (Type 2) can be analyzed readily by existing methods (6) Under the conditions normally employed for hot-machining, namely, the use of carbide tools and relatively high cutting speeds, chip formation is usually of the simple continuous type (Type 2). Therefore the existing methods of analysis of the mechanics of cutting can be applied readily to this problem. The force system and geometry of cutting for this type of chip formation, when using orthogonal cutting, are as shown in Fig. 1. This force system and accompanying geometry are controlled by three basic factors as follows:

1 The friction angle τ, which is a direct measure of the coefficient of friction μ acting between chip and tool.

2 The mean shear strength S_s of the metal being cut.

3 The machining constant C which, to a first approximation,

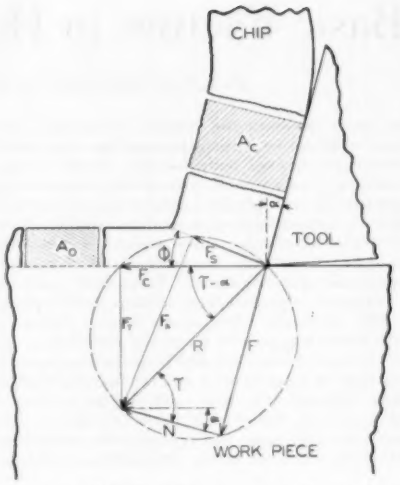

Fig. 1 Geometry of Chip Formation and Force System in Orthogonal Cutting

is a constant of the metal being cut and which, in theory, is related to the rate of change of the shear strength of the metal with applied compressive stress.

The magnitudes of the horizontal and vertical force components F_c (cutting force) and F_t (thrust force) shown in Fig. 1, determine the magnitude and direction of the resultant force R acting between tool and work. These two force components are controlled completely by the three basic quantities, together with the rake angle of the tool and the size of cut being taken. The equations for these force components in terms of these basic quantities are as follows

$$F_c = A_o S_s \left[\tan\left(\frac{C+\tau-\alpha}{2}\right) + \cot\left(\frac{C-\tau+\alpha}{2}\right)\right] \quad [1]$$

$$F_t = A_o S_s \left[\tan\left(\frac{C+\tau-\alpha}{2}\right) \cot\left(\frac{C-\tau+\alpha}{2}\right) - 1\right] \quad [2]$$

where

A_o = cross-sectional area of chip before removal from workpiece, sq in.
C = machining constant as just described, deg
F_c = cutting force; force component acting in direction of motion of tool relative to work, lb
F_t = thrust force; force component acting in a direction perpendicular to F_c and to surface generated, lb

TABLE 2 MECHANICAL PROPERTIES AND DIMENSIONS OF WORKPIECES

Work material	Type of test	Type of workpiece	Brinell hardness, kg per sq mm	Meyer strain hardenability exponent, n	Outside diameter (tube), in.	Wall thickness (tube), in.	Width (flat stock), in.
AISI 3145 "as-received"	Tool dynamometer	Tube	186	2.34	2.159	0.250	..
AISI 3145 "as-received"	Tool life	Flat stock	180	2.33	...	...	1.00
AISI 3145 hardened	Tool life	Flat stock	350	..	...	...	1.00
Timken 16–25–6	Tool dynamometer	Tube	268	2.27	2.159	0.250	..
Timken 16–25–6	Tool life	Flat stock	264	2.27	...	...	1.15
S-816 alloy	Tool life	Flat stock	282	2.34	...	...	1.00
Inconel X	Tool life	Flat stock	203	2.22	...	...	1.00

S_s = mean shear strength of metal on shear plane, psi
α = rake angle of tool as measured in a plane perpendicular to its cutting edge, deg
τ = friction angle, deg (= arc tan μ)
μ = coefficient of friction acting between sliding chip and tool face

The cutting force F_c is responsible for all the power consumed in chip formation. The relationship between the power consumption and the cutting force is as follows

$$P = \frac{F_c}{396{,}000 A_c} \quad [3]$$

where

P = horsepower consumed at tool per cubic inch of metal removed per minute

Equations [1], [2], and [3] indicate that direct measurements of chip friction, shear strength, and machining constant in the hot-machining process will demonstrate the relative part played by each of these three basic factors in the observed changes in tool forces and power consumption which accompany changes in workpiece temperature.

In addition to controlling tool forces and power consumption, the mechanics of cutting plays a very important part in the process of tool wear; it directly affects the abrading action which the work material has on the tool. It is true, of course, that the microstructure of the work material plays a very important part in the abrading action of the work on the tool, apart from the mechanics of cutting. If the work material contains hard, abrasive microconstituents, tool wear will of course be rapid; if all the constituents of the microstructure are relatively soft compared to the tool material, the rate of wear of the tool will of course be low. The part played by the tool-chip interface temperature in softening the tool and thus increasing its rate of wear has also been mentioned. However, for a given work material and microstructure, and for a given tool-chip interface temperature, the abrading action which the work material has on the tool will depend directly on the mechanics of cutting. This abrading action may be expected to depend both on the hardness of metal which is in sliding contact with the tool and on the force or pressure with which that metal is pressed against the tool (both of which will normally decrease with increasing workpiece temperature).

The hardness of the metal which abrades the tool is roughly proportional to the shear strength S_s of the metal on the shear plane. The force or pressure with which the metal is pressed against the tool depends not only on the shear strength S_s but also on the machining constant C and the coefficient of friction μ acting between chip and tool, as explained previously. Thus the abrading action of work on tool (for a given microstructure and interface temperature) depends mainly on the three basic quantities that control the mechanics of cutting.

Experimental Methods and Results. The experimental method used in the present study to measure the basic factors influencing tool forces and power consumption has already been described elsewhere (7). In brief, it consisted of using a workpiece of tubular form and cutting on the end of it with a tool having a single straight cutting edge, so as to obtain continuous orthogonal cutting. The two force components F_s and F_t were measured by means of a two-component mechanical tool dynamometer. The additional measurement necessary to calculate the required basic quantities was that of the shear angle ϕ, Fig. 1. This shear angle was determined from cutting-ratio measurements in the usual manner.

To carry out hot machining with this type of setup, an oxypropane flame was used to heat the end of the tubular workpiece. This was supplied by a multiple-tip flame head mounted just ahead of the cutting tool and moving with it. The over-all setup used for this phase of the research is shown in Fig. 2. With this arrangement it was possible to obtain workpiece temperatures ranging from room temperature to 1500 F. The workpiece temperatures actually used were 80 F, 500 F, 1000 F, and 1500 F. The 500 F and 1000 F temperatures were measured with temperature-indicating pencils and the 1500 F temperature with an optical pyrometer.

In the present research, tests of this type were carried out on the AISI 3145 steel and on the Timken 16–25–6 high-temperature

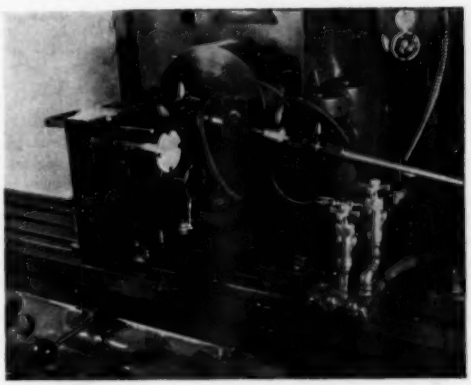

FIG. 2 EXPERIMENTAL HOT-MACHINING SETUP FOR ORTHOGONAL CUTTING WITH A TWO-COMPONENT MECHANICAL TOOL DYNAMOMETER

alloy. A wide variety of cutting conditions were investigated in the case of the 3145 steel, including various feeds, speeds, and rake angles. The results of these tests are summarized in Table 3. In the case of the 16–25–6 alloy only one rake angle and one feed were used, and the cutting speed and workpiece temperature were varied. The results of these tests are shown in Figs. 3 to 7, inclusive.

From the results of both these sets of tests, it is evident that the main factor responsible for the lower tool forces (and corresponding power consumption) at elevated workpiece temperatures is the lowered shear strength of the work material. This quantity decreases consistently with increasing temperature, with but few exceptions. In the case of the AISI 3145 steel, chip friction also decreases fairly regularly with increasing temperature, as seen from Table 3, thus contributing to the lower tool forces when machining hot. However, this is not the case with the 16–25–6 alloy, as seen in Fig. 5. As regards the machining constant, this decreases with increasing workpiece temperature in the case of the 16–25–6 alloy, as seen in Fig. 7. This would tend to offset somewhat the effect of the decreasing shear strength. The machining constant of the 3145 steel shows no regular behavior with increasing temperature; its trend with temperature varies with the cutting conditions.

An interesting exception to some of the foregoing general statements is found in the tests made on the 3145 steel with a 10-deg negative-rake tool at a cutting speed of 462 fpm and feeds of 0.0049 and 0.0080 in. per revolution. Here, as may be seen from Table 3, tool forces and shear strength actually increase when

TABLE 3 TESTS ON MECHANICS OF CUTTING, AISI 3145 STEEL

Workpiece: Tube, 0.25 in. wall; orthogonal cutting
Tool: Sintered carbide, 3-deg relief

Workpiece temperature, deg F	Feed per rev, f, in.	Cutting speed, V_c, fpm	Rake angle, α, deg	Cutting force, F_c, lb	Thrust force, F_t, lb	Coefficient of friction, μ	Shear strength, S_s, psi	Machining constant, C, deg
80	0.0018	462	−10	255	240	0.64	105000	74
500				222	246	0.78	86700	79
1000				175	186	0.74	76700	97
1500				141	126	0.61	66700	79
80	0.0049	462	−10	360	340	0.65	64000	95
500				498	400	0.54	88400	74
1000				381	242	0.62	70700	95
1500				300	207	0.46	66300	87
80	0.0080	462	−10	479	415	0.63	54000	102
500				686	458	0.47	82500	75
1000				510	316	0.40	70000	86
1500				440	260	0.37	61500	80
80	0.0030	72	−10	575	395	0.46	....[a]	....[a]
1500				170	146	0.58	48600	74
80	0.0030	315	−10	350	331	0.64	93500	77
1500				200	168	0.57	62500	79
80	0.0030	605	−10	251	228	0.62	74500	90
1500				196	190	0.57	58400	82
80	0.0018	462	+10	213	186	1.25	100000	78
1500				123	80	0.93	74500	90
80	0.0049	462	+10	439	251	0.82	98000	75
1500				228	112	0.74	55700	76
80	0.0080	462	+10	630	283	0.68	97500	77
1500				332	126	0.58	55000	79
80	0.0030	72	+10	307	168	0.80	....[a]	....[a]
1500				147	70	0.71	58000	73
80	0.0030	315	+10	332	280	1.08	95000	72
1500				147	70	0.71	62500	83
80	0.0030	605	+10	310	190	0.90	107000	74
1500				170	100	0.85	65000	89

[a] Type 3 chip.

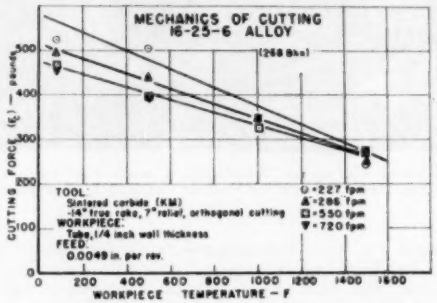

FIG. 3 EFFECT OF WORKPIECE TEMPERATURE ON OBSERVED VALUES OF CUTTING FORCE FOR ORTHOGONAL CUTTING

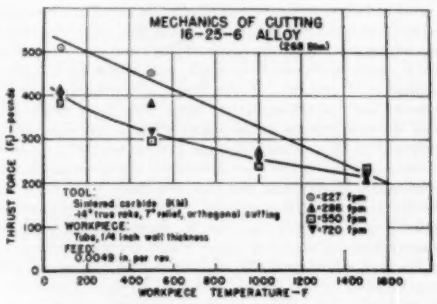

FIG. 4 EFFECT OF WORKPIECE TEMPERATURE ON OBSERVED VALUES OF THRUST FORCE FOR ORTHOGONAL CUTTING

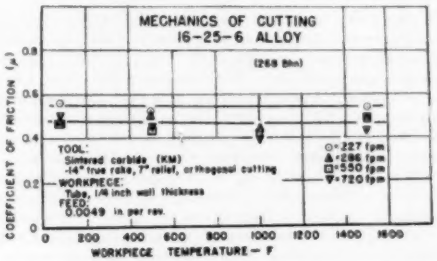

FIG. 5 RELATION BETWEEN WORKPIECE TEMPERATURE AND CHIP FRICTION

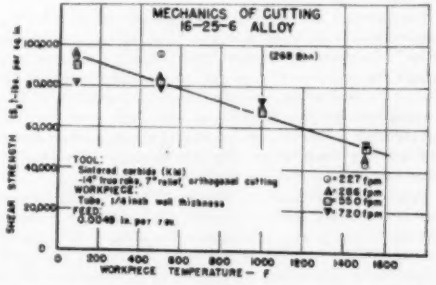

FIG. 6 RELATION BETWEEN WORKPIECE TEMPERATURE AND SHEAR STRENGTH

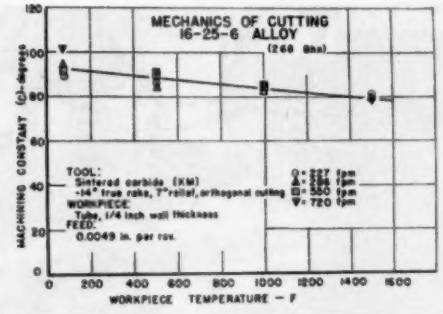

FIG. 7 RELATION BETWEEN WORKPIECE TEMPERATURE AND MACHINING CONSTANT

the workpiece is heated from room temperature to 500 F. While this is surprising, it was found to be an entirely reproducible result. Obviously then, this AISI 3145 steel is less easy to machine (for the foregoing cutting conditions) when it is heated to 500 F than when it is at room temperature.

TOOL TEMPERATURE

In the case of the 16–25–6 alloy, an analytical study was made of tool-chip interface temperatures, using the data obtained in the investigation on the mechanics of cutting, in order to explore the relationship between interface temperature and workpiece temperature. The interface-temperature calculations were based upon the method developed by Trigger and Chao (8). These authors have shown that, for cutting speeds above about 300 fpm, such calculated values agree with actual experimental values to an accuracy of about 5 per cent or better. It was necessary, however, to adapt several equations to take care of the fact that in the present research the workpiece and the cutting tool were at different temperatures. These revised equations are as follows

$$(\theta_s - \theta_w)_{avg} = \frac{A[F_c V_c(1 - B_1) - FV_f]}{JC_p\rho(V_c \times 12)A_s} \quad [4]$$

$$\theta_s + \frac{4}{3(\pi)^{1/2}} \cdot \frac{B_2 q}{K}\left[\frac{km}{V_f}\right]^{1/2} = \theta_c + \frac{4(1 - B_2)ql \times \text{shape factor}}{\pi K_t} \quad [5]$$

where

θ_c = average tool (cutter) temperature, deg F
θ_w = average work temperature, deg F
θ_s = average chip temperature as it leaves shear zone, deg F
q = quantity of heat liberated at tool-chip interface per unit of time, Btu/(in²)(sec)
m = average length of tool-chip contact, in.
l = average width of tool-chip contact (chip width), in.
J = mechanical equivalent of heat, 778 ft-lb/Btu
K = thermal conductivity of heated chip body, Btu/(in.²)(sec)(deg F/in.)
K_t = thermal conductivity of tool, Btu/(in.²)(sec)(deg F/in.)
k = thermal diffusivity of tool material, in.²/sec
V_c = cutting velocity; velocity of tool relative to workpiece, fpm
V_f = chip-flow velocity; velocity of chip relative to cutting tool, fpm
B_1 = fractional part of total heat left in workpiece; 0.10 for present conditions
B_2 = fractional part of interface heat going into chip
F = friction force; force component acting between tool face and sliding chip, lb
C_p = specific heat of heated chip, Btu/(lb)(deg F)
ρ = density of chip material, lb/in.³
A = proportion of energy of deformation which appears as sensible heat in chip, assumed to be 0.95 for present conditions
Shape factor = a quantity depending on ratio (l/m), as defined by Trigger and Chao

and the other quantities are as already defined.

Equation [4] was used to calculate the value of θ_s. This value was inserted in Equation [5], which was then used to calculate the value of B_2. The tool-chip interface temperature θ_t could then be calculated from the equation

$$\theta_t = \theta_s + \frac{B_2}{9(5\pi)^{1/2}} \frac{F}{KJl}\left[\frac{kV_f}{m}\right]^{1/2} \quad [6]$$

Values for the quantities A_s, F_s, F, V_c, and V_f for use in the foregoing equations were obtained from the data observed in the investigation of the mechanics of cutting, where tool forces and shear-angle values had been measured. Values for the quantities l and m were also observed in those orthogonal cutting tests, for the case of the 16–25–6 alloy. The value of l was taken to be equal to the width of cut (i.e., the wall thickness of the tube, 0.25 in. in the present case). The value of m was obtained by direct measurement of the length of the chip-contact area on the face of the tool with a measuring microscope, using the technique described by Trigger and Chao (8).

Mention should be made of the fact that the values for interface temperature resulting from these calculations are for the case of orthogonal cutting with a tool having a single straight cutting edge; there is no corner or nose radius involved. Trigger and Chao pointed out that in such a case the interface temperature will be lower than when cutting on the corner of a tool, but that these lower temperature values will be proportional to those obtained when cutting on a corner under similar conditions.

The calculated tool-chip interface temperatures for the 16–25–6 alloy are shown in Table 4. The reciprocal of these interface-temperature values are shown plotted against the workpiece temperature in Fig. 8. Here it may be seen that the tool-chip interface temperature increases with cutting speed in the usual manner. However, it is interesting to note from either Fig. 8, or Table 4 that, for this material, an optimum interface temperature is obtained not at room temperature, but rather at a work temperature of approximately 500 F. In other words, in this case the interface actually runs cooler when the workpiece is heated to 500 F than it does when the work is at room temperature.

TOOL LIFE

Experimental Methods and Results. Milling tool-life tests were made on the three high-temperature alloys and on the AISI 3145 steel, to determine the effect of elevated work temperature on tool life and to obtain a correlation between tool life and the tool-chip interface temperature and mechanics of cutting.

A knee-and-column-type milling machine, adapted with a vertical milling attachment was used throughout these tests. A 2½-in-diam single-tooth fly-type cutter, tipped with sintered carbide (KM), was used in a face-milling operation. The tool geometry for all tests was —14 deg true rake, 7 deg relief, and 0 deg inclination of the cutting edge. Thus the basic tool angles were the same as those used for the orthogonal cutting tests

TABLE 4 CALCULATED VALUES OF TOOL-CHIP-INTERFACE TEMPERATURE, 16-25-6 ALLOY

Orthogonal cutting (tubular workpiece)
Width of cut: 0.25 in. Tool: Sintered carbide (KM);
Feed per revolution: 0.0049 in. —14-deg true rake, 7-deg relief

Cutting speed, V_c, fpm	Workpiece temperature, θ_w, deg F	Tool-chip-interface temperature, θ_c, deg F
286	80	1654
	500	1685
	1000	1997
	1500	2102
550	80	2124
	500	1650
	1000	2074
	1500	2463
720	80	2324
	500	1935
	1000	2337
	1500	2482

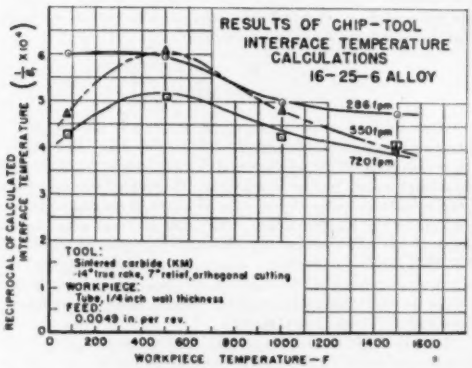

FIG. 8 RELATIONSHIP BETWEEN TOOL-CHIP INTERFACE TEMPERATURE AND WORKPIECE TEMPERATURE SHOWING OPTIMUM CONDITION AT 500 F

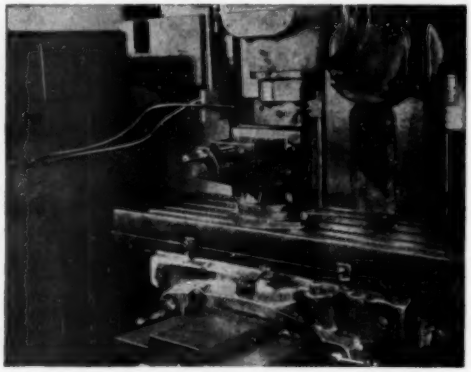

FIG. 9 EXPERIMENTAL INDUCTION HEATING SETUP FOR FACE-MILLING TOOL-LIFE TESTS

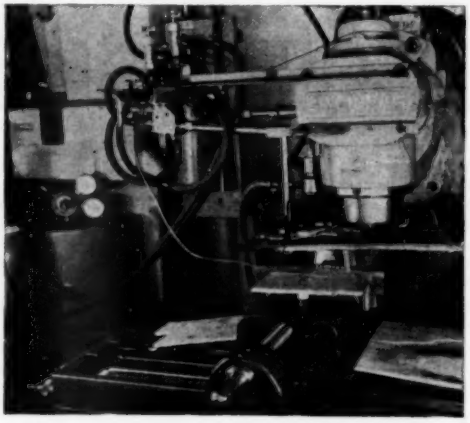

FIG. 10 EXPERIMENTAL FLAME-HEATING SETUP FOR FACE-MILLING TOOL-LIFE TESTS

made to study the mechanics of cutting and interface temperatures. In addition, the milling-cutter tooth had a 30-deg corner angle. In this milling process, cutting was of course done by the corner of the tool, as compared to the single straight cutting edge used for the orthogonal cutting tests. The face-milling tests were made with a 0.010-in. feed per tooth and a 0.050-in. depth of cut. Tool life was measured in terms of the volume of metal removed to produce a wear land on the tool flank of 0.030 in., as is customary in work with carbide tools.

For the tests on the 3145 steel, a high-frequency induction-heating unit was used to heat the workpiece. The experimental setup is shown in Fig. 9. The pancake-type induction-heating coil, made from copper tubing, was mounted immediately ahead of the cutter. The power available from this unit was found to be insufficient for the work with the nonmagnetic high-temperature alloys. For this work a multiple-tip flame head was used, as seen in the experimental setup shown in Fig. 10. The temperature was controlled by correlating the intensity of the flame, rate of table travel, and amount of preheating, and was measured by means of temperature-indicating pencils, and an optical pyrometer.

The data obtained from these tests are shown in Figs. 11 to 14. These curves are a plot of tool life as a function of cutting speed for workpiece temperatures of 80, 500, 1000, and 1500 F. It can be seen that for all the materials tested, the tool-life curves are of the conventional straight-line type at high cutting speeds and, in most cases, show a reversal or "break-back" at low cutting speeds. This reversal is characteristic of cutting-speed versus tool-life curves obtained with carbide tools, particularly on machining operations where the cutting action is intermittent, such as milling. The reversal occurs due to failure of the tool by sudden chipping, rather than by the normal process of smooth, continuous wear such as takes place on the straight-line portion of the curves, at higher speeds. The upper straight-line portion of the tool-life curves is, therefore, of most importance and is given the most consideration in this paper.

In the case of the AISI 3145 steel, it was found that when this material was machined in the "as-received" condition (180 Bhn), the tool life at room temperature was approximately 7 times the tool life at 1500 F, for a cut speed of 1020 fpm. This can be seen in Fig. 11 from the location of the two single plotted points for this case. Tool-life results on this same material, hardened to 350 Bhn by heat-treatment, showed just the opposite behavior. Here the tool life at 1500 F was about 10 times the tool life at room temperature, for cutting speeds above 350 fpm, as seen in Fig. 11. When the hardness of the workpiece, at room

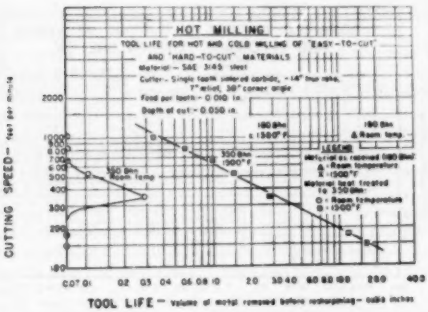
HOT MILLING
TOOL LIFE FOR HOT AND COLD MILLING OF "EASY-TO-CUT" AND "HARD-TO-CUT" MATERIALS
Material — SAE 3145 steel
Cutter — Single tooth sintered carbide, −14° true rake, 7° relief, 30° corner angle
Feed per tooth = 0.010 in.
Depth of cut = 0.050 in.
CUTTING SPEED — feet per minute
TOOL LIFE — volume of metal removed before resharpening — cubic inches

FIG. 11 TOOL-LIFE CURVES FOR FACE-MILLING AISI 3145 STEEL OF TWO DIFFERENT HARDNESSES AT VARIOUS WORKPIECE TEMPERATURES

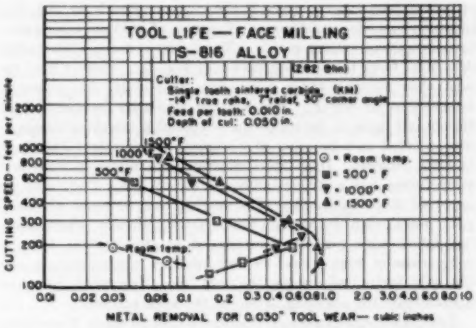
TOOL LIFE — FACE MILLING
S-816 ALLOY
(282 Bhn)
Cutter: Single tooth sintered carbide, (KM) −14° true rake, 7° relief, 30° corner angle
Feed per tooth: 0.010 in.
Depth of cut: 0.050 in.
CUTTING SPEED — feet per minute
METAL REMOVAL FOR 0.030" TOOL WEAR — cubic inches

FIG. 12 TOOL-LIFE CURVES FOR FACE-MILLING S-816 ALLOY AT VARIOUS WORKPIECE TEMPERATURES

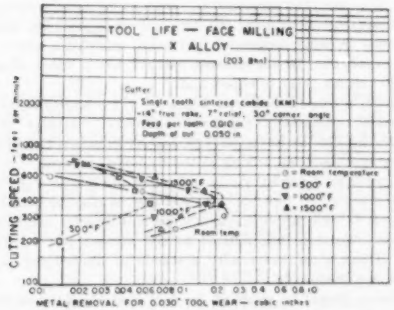
TOOL LIFE — FACE MILLING
X ALLOY
(203 Bhn)
Cutter: Single tooth sintered carbide, (KM) −14° true rake, 7° relief, 30° corner angle
Feed per tooth: 0.010 in.
Depth of cut: 0.050 in.
CUTTING SPEED — feet per minute
METAL REMOVAL FOR 0.030" TOOL WEAR — cubic inches

FIG. 13 TOOL-LIFE CURVES FOR FACE-MILLING INCONEL X ALLOY AT VARIOUS WORKPIECE TEMPERATURES

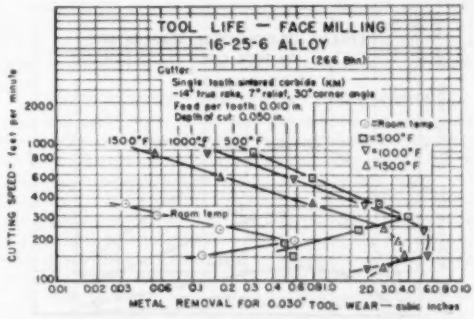
TOOL LIFE — FACE MILLING
16-25-6 ALLOY
(266 Bhn)
Cutter: Single tooth sintered carbide (KM) −14° true rake, 7° relief, 30° corner angle
Feed per tooth 0.010 in.
Depth of cut 0.050 in.
CUTTING SPEED — feet per minute
METAL REMOVAL FOR 0.030" TOOL WEAR — cubic inches

FIG. 14 TOOL-LIFE CURVES FOR FACE-MILLING TIMKEN 16-25-6 ALLOY AT VARIOUS WORKPIECE TEMPERATURES

temperature, was measured at the conclusion of these tests, it was found to have dropped to only 340 Bhn.

The data obtained from the tests on the S-816 alloy are shown in Fig. 12. Here it may be seen that great improvement in tool life was obtained when machining this material at elevated temperatures. The tool life at 500, 1000, and 1500 F is, respectively, 30, 65, and 80 times the tool life obtained at room temperature for a cutting speed of 250 fpm.

Fig. 13 shows the data obtained for the X-alloy. Here also considerable improvement in tool life was obtained at the elevated temperatures. The tool life at 500, 1000, and 1500 F was, respectively, 3, 4, and 5 times the tool life at room temperature, for a cutting speed of 600 fpm.

The data for the tool-life tests on the 16–25–6 alloy are plotted in Fig. 14. Here again it may be seen that the tool life was greatly improved when machining at elevated temperatures. However, the tool life did not continue to improve as the workpiece temperature was increased; rather, an optimum condition was reached at approximately 500 F, where the tool life became a maximum. In this case the tool life at 500 F and 300 fpm cutting speed was approximately 55 times the tool life obtained at room temperature, whereas the tool life at 1000 and 1500 F was, respectively, only 45 and 20 times that at room temperature.

Interpretation. It is apparent that, for any given work material, an optimum temperature range exists at which, for given machining conditions, the tool life will be a maximum. This optimum temperature may lie above, below, or at room temperature. The existence of such an optimum is to be expected in view of the opposing behavior, with rising temperature, of the abrading action of the work material and the abrasion resistance of the cutting tool, as described in the introduction to this paper.

It is also apparent that heating improves the machinability of the particular high-temperature alloys tested during this research. This, however, is not necessarily true for readily machinable steels, as evidenced by the behavior of the AISI 3145 steel in the as-received condition. This is accounted for by the fact that, with such a material, the abrading action on the tool is relatively mild, even at room temperature. An increase in work temperature to 1500 F increases the tool-chip interface temperature to a great extent, and renders the tool more susceptible to abrasion (tool wear), thus more than nullifying the benefits derived from the reduction in the shear strength and hardness of the work material.

As pointed out, in the case of the S-816 and the X-alloy, tool life is progressively improved with increasing workpiece temperature, up to a temperature of at least 1500 F. From this it may be concluded that the optimum temperature ranges for machining these materials are in excess of 1500 F.

The tool-life curves for the 16–25–6 alloy, Fig. 14, show that tool life is greatly improved by heating the workpiece, and that best tool life results at a temperature of about 500 F. This

optimum temperature range is shown more clearly in Fig. 15, in which tool life is plotted as a function of workpiece temperature for various cutting speeds. These curves were plotted using data read from the tool-life curves in Fig. 14. Here it may be seen that for the given machining conditions the optimum temperature is 500 F. The striking similarity between these curves and those of the reciprocal of tool-chip interface temperature, plotted as a function of workpiece temperature, Fig. 8, is at once evident. It is apparent that the tool-chip interface temperature has a strong influence on tool life. This is to be expected since the ability of a cutting tool to resist abrasion goes down with increasing temperature, already emphasized throughout this paper. However, it is also evident from a comparison of Figs. 8 and 15 that interface temperature is not the only factor influencing the tool life. The other factor is undoubtedly the abrading action of the work material.

Tool Life Versus Interface Temperature and Cutting Mechanics. In view of the foregoing findings, a rough quantitative evaluation was attempted of the combined effect on tool life of interface temperature and the abrading action of the work material. As

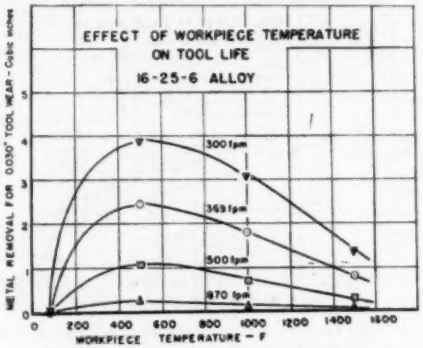

Fig. 15 Relationship Between Tool-Life and Workpiece Temperatures Showing Optimum Condition at 500 F

explained in the discussion of the mechanics of cutting, the abrading action of work on tool (in the case of a given microstructure of the work material) depends mainly on the three basic quantities that control the mechanics of cutting, namely, the coefficient of friction μ, the shear strength S_s, and the machining constant C. Therefore, as a convenient and logical quantity which is dependent on all three of these basic entities (see Equation [2]), the readily measured thrust force F_t was selected as a rough measure of this abrading action of work on tool.

Values of both thrust force and interface temperature in orthogonal cutting were obtained for the 16–25–6 alloy in the present investigation. These values were combined as a simple product and plotted as a function of the tool-life values obtained from the face-milling tests on the 16–25–6 alloy. The results are shown in Fig. 16. The values plotted were read from the curves of thrust force, interface temperature, and tool life for the 16–25–6 alloy, for cutting speeds covering the range from 300 to 700 fpm. It can be seen that a single straight line results for tool-life data obtained over the entire range of workpiece temperatures, and cutting speeds. It appears, therefore, that an approximate relationship exists between thrust force, interface temperature, and tool life of the form

$$F_t \theta_i T^x = C_1 \quad \ldots\ldots\ldots\ldots\ldots\ldots\ldots\ldots [7]$$

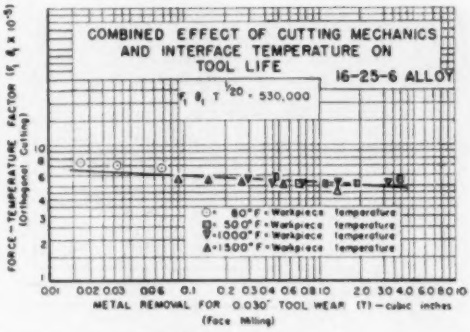

Fig. 16 Relationship Between Force-Temperature Factor and Tool Life

where T is tool life (expressed in terms of metal removal), C_1 is a constant dependent upon the work material (probably strongly influenced by microstructure) and other quantities, and x is a small exponent. In the present case C_1 has a value of about 530,000 and x a value of about 1/20.

It must be emphasized that Equation [7] is approximate and, at present, essentially empirical. However, it does give a quantitative clue as to the part played by interface temperature and the mechanics of cutting in the tool-wear process. As such it can serve as a helpful guide to further analytical and experimental research on tool life. In addition, it may be hoped that Equation [7] will prove to be a valid and broadly useful semi-empirical equation, not limited to the present test conditions only. There is no reason why it should be limited only to the case of hot machining.

Mention should be made of the fact that the data on thrust force and interface temperature, used to plot Fig. 16, came from orthogonal cutting tests, while those on tool life came from face-milling tests. Obviously, the interface-temperature values are not the same for the two cases. However, as previously noted, Trigger and Chao (8) have shown that the temperature values will usually be proportional to each other for the two cases. In addition not the same depth and feed were used for the milling tests as for the orthogonal cutting tests, due to mechanical limitations. However, the smaller feed per revolution used in the case of the orthogonal cutting is offset by the greater width (depth) of cut. Thus, again it can be assumed safely that results in the two cases would be proportional to each other. This being the case, the straight-line relationship of Fig. 16 should not be affected; only the constant C_1 of Equation [7] would be changed in value by correcting for the proportionalities involved.

It is interesting to note that the exponent x of Equation [7] was found to have a value of approximately 1/20. This is in agreement with the empirical finding of Schallbroch, Schaumann, and Wallichs (5), that tool life varies inversely as approximately the 20th power of the interface temperature, when cutting speed is the only variable. In tests where cutting speed is the only variable, the thrust force F_t is essentially a constant, so that Equation [7] actually contains Shallbroch's empirical relationship as a special case.

Conclusion

From the present research it is evident that the lower cutting forces and consequent lower power consumption achieved by hot-machining are due mainly to reduced shear strength of the work material at high temperatures. Although this finding is not

surprising, it does establish as fact what was previously conjecture only.

It does not follow from the foregoing, however, that tool life will always increase with increasing workpiece temperature. Instead, for a given work material, there is a definite temperature range for which tool life will be an optimum. This may be above, below, or at room temperature. For some materials this optimum occurs at a temperature in excess of 1500 F. The tool life obtained with a given work material depends mainly on two factors: (*a*) the tool-chip interface temperature, and (*b*) the abrading action of the work on the tool. Both are controlled by the mechanics of cutting. It appears that the product of thrust force and interface temperature provides a rough quantitative measure of these two factors, as indicated by Equation [7].

Some of the basic factors in the hot-machining of metals have been identified in the course of this research, and their role in the machining process clarified. In particular, a better insight into the factors influencing tool life has been obtained. The findings are thus not limited to the case of hot-machining only. In addition, they suggest further avenues for research in the basic study of machinability.

Acknowledgments

The authors wish to express their thanks to Mr. Hans Ernst, Research Director, for his helpful suggestions and inspiration throughout the course of this research. The authors also thank Mr. Robert Harper and Mr. William Demaree, students in the Training School, for their part in carrying out some of the experimental work, and Miss Sue Hannaford and Miss Margaret McNeill of the Research Department, for their help in the preparation of the manuscript and illustrations.

Bibliography

1 U. S. Patent No. 2412797, by M. Berliner, December 17, 1946.

2 "Influence of Steel Hardness in Face Milling," by J. B. Armitage and A. O. Schmidt, Trans. ASME, vol. 71, 1949, pp. 413–419.

3 "Hot Spot Machining," by Sam Tour and L. S. Fletcher, *Iron Age*, vol. 164, July 21, 1949, pp. 78–89.

4 "Machining of Heated Metals," by E. T. Armstrong, A. S. Cosler, Jr., and E. F. Katz, Trans. ASME, vol. 73, 1951, pp. 35–43.

5 "Testing for Machinability by Measuring Cutting Temperature and Tool Wear," by H. Schallbroch, H. Schaumann, and R. Wallichs, Vortrage der Hauptversammlung 1938 der Deutschen Gesellschaft für Metallkunde, Vereines deutscher Ingenieure Verlag, 1938, pp. 34–38.

6 "Mechanics of the Metal Cutting Process," by M. Eugene Merchant, *Journal of Applied Physics*, vol. 16, 1945, pp. 267–275 and pp. 318–324.

7 "New Methods of Analysis of Machining Processes," by M. Eugene Merchant and N. Zlatin, *Experimental Stress Analysis*, vol. 3, 1946, pp. 4–27.

8 "An Analytical Evaluation of Metal-Cutting Temperatures," by K. J. Trigger and B. T. Chao, Trans. ASME, vol. 73, 1951, pp. 57–68.

Discussion

E. T. Armstrong.[4] In the authors' work, a general-purpose roughing carbide tool was used. Previous work[5] has shown that finishing grades which are hard brittle carbides usually perform better in hot-turning than the comparatively soft, but tougher, roughing carbides. This work has also shown that preferred carbides for hot-turning cannot usually be used successfully in machining very "hard-to-cut" materials at room temperature.

In hot-milling, with very hard brittle carbides, the intermittent cutting action may be so severe as to lead to premature tool failure by chipping with such hard tools. However, it is possible that the use of harder grades of carbides in hot-milling might more fully realize the potentialities of the method. It is hoped that this research can be extended to the evaluation of other tool materials.

In the described research on tool life, a pancake-type induction heating coil was used. From this source it is noted that the available power was inadequate for hot-milling austenitic materials. This emphasizes the view previously[5] expressed that a high-power-density heating means increases the scope of hot-machining practice.

In hot-machining, where the heat is delivered to the work at a low rate, the work-material temperature gradient is low. This means that more heat is required to achieve a specified average chip temperature at low power density than would be required if the heat were supplied at high power density. Thus in the case where a pancake-type induction heating coil is used, it would be expected that considerable heat would diffuse into the work material, and the temperature gradient in the work material would be correspondingly low. In other words, the work-material temperature would be essentially constant over the depth of cut.

In machining AISI 3145 steel at 1500 F, no effect of initial heat-treatment would be expected since the machining temperature exceeds the critical temperature for this material. However, data are reported showing that the tool life differs by a factor of 5 for material hot-milled at 1500 F, quenched and drawn, and normalized. It is also surprising to find that the 350-Bhn workpiece air-hardened to 340 Bhn after hot-machining. It would be interesting to know whether the 180-Bhn stock also air-hardened after hot-machining. In each of these cases, a normalized condition would be expected after air-cooling from 1500 F.

In these particular cases the total actual cutting times were comparatively short. For this reason, measurement of life based on a wear index might be more in error in this range than for greater total cutting times. It is also possible that irreproducible cut interruptions, to make wear measurements, might have disturbed the thermal equilibrium of the tool.

A further possible source of error in short-time tests is the tool temperature starting transient in hot-milling. Note in hot-milling that the principal heat input to the tool from the work occurs over only from 5 per cent to 10 per cent of the total time in each revolution. Under these conditions, the time required to reach thermal equilibrium may be large compared to the total tool life. Tool-life data obtained under these conditions are less representative of hot-machining practice since they correspond to an uneconomically short tool life. For the high-temperature alloys, comparatively short tool life was observed in hot-machining. It seems possible that the reversal or "break-back" of these tool-life cutting-speed data may also be related to the deferred thermal equilibrium attained in the milling tool.

Supplementing the authors' conclusions on one point—understanding and appreciation of the potentialities of hot-machining require consideration of the relative effect of increased temperatures on the work material and the tool material. Full exploitation of the technique requires the use of tool materials particularly suited to high-temperature service. These materials may be useless for conventional machining.

R. S. Hahn.[6] There are some factors not brought out in the paper relating to the validity of plotting force-chip interface tem-

[4] Assistant Supervisor, Battelle Memorial Institute, Columbus, Ohio. Jun. ASME.

[5] Authors' Bibliography (4).

[6] Research Engineer, The Heald Machine Company, Worcester, Mass. Mem. ASME.

perature under orthogonal cutting against tool life in milling as is done in Fig. 16 of the paper.

The authors have used the analysis of Trigger and Chao[7] to calculate the chip-tool interface temperature. Trigger's analysis for the chip-tool interface temperature gives the steady-state temperature. His formula is therefore good for steady orthogonal cutting, but is it good for milling where the cutter is submerged for only short intervals of time? If so, and if the thrust force in milling is taken equal to that in orthogonal cutting, then the ordinate in Fig. 16 of the paper could be thought of as applying to the milling process. Jaeger[8] not only has dealt with the steady-state temperatures under moving heat sources, but also has considered the time required to reach the steady state. In milling is there sufficient time to reach steady state? An estimate can be obtained from Jaeger's paper.[9] We might consider the steady state to be attained at, say, 10 times the time to reach one half steady-state temperature, which has been plotted[9] for a moving square heat source.

In this way we get

$$\frac{V^2 T_{ss}}{2\kappa} = 2.7L$$

where

$$L \equiv \frac{Vl}{2\kappa}$$

which gives for the distance traveled d, to reach steady state ($d = 2.7l$), where l is the half length of the source.

Suppose in milling the chip bears 0.060 in. up the tool face. Then the foregoing equation indicates that thermal equilibrium will be attained in about $^1/_{16}$ in. Therefore, when the cutter is engaged for 1 in. of travel, it is reasonable to consider that a steady state has been attained on the tool face and that the

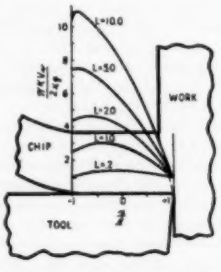

FIG. 17 TEMPERATURE DISTRIBUTION ON TOOL FACE
("Dimensionless temperature" ($\pi KV_s/(2K_q)$ is plotted against X/l, after Jaeger.[9])

authors' results are reasonably valid in this respect. The foregoing moving source corresponds to Trigger's moving source of strength B_{sq}.

The other consideration regarding Fig. 16 of the paper is the irrationality of plotting a variable containing tool-chip interface temperature against tool life, wherein the tool life is measured by wear on the flank or clearance surface of the tool. The temperature under discussion is on the rake surface of the tool, but the wear with which it is supposed to be correlated is on the flank of the tool. If the authors had correlated chip-tool interface temperature with cratering on the tool face, it would have presented a more logical picture.

It is interesting at this point to note that cratering on the tool face takes place in a region slightly behind the cutting edge, and Fig. 17, herewith, shows the temperature distribution on the tool face.[10] It will be seen that as the speed (i.e., L) is increased the point of maximum temperature drifts farther away from the cutting edge. It is in this region where cratering occurs. Consequently, the greatest rate of wear appears to be in a region near the point of maximum temperature, perhaps where the product of sliding stress and temperature is a maximum.

A. O. SCHMIDT[11] AND J. R. ROUBIK.[12] This paper gives additional interesting information on some phases of the hot-machining process and is especially valuable in its attempt to correlate the findings of several experimenters in various laboratories. It should further encourage those engaged in machining very hard materials to make use of this power and tool-saving technique.

The test results obtained when machining AISI 3145 steel of 180 Bhn at elevated temperatures confirm that this type of machining is not indicated as a desirable method when the material can be machined successfully at room temperature. In this case the additional heat of the workpiece caused more tool wear than machining it at room temperatures at higher hardness and strength properties. Heating of the workpiece will be beneficial only when machining at room temperature entails rapid destruction of the tool.

Machining high-strength alloys under application of heat is possible primarily because the carbides and cast alloy or stellite-type tool materials keep sufficient hardness at higher temperatures.

In tool-life tests[12] with heated workpieces it was found that HSS milling cutters would fail very quickly, while those with carbide or cast-alloy teeth stood up much longer under the same conditions. In repeated comparative tests between HSS cutters and cutters with cast-alloy teeth, the HSS cutters machined an average of 60 pieces of SAE 4340 steel, 280 Bhn, 24 in. long, $^3/_4$ in. wide, and 0.200 in. deep, at a cutting speed of 90 fpm and a feed of 6 ipm with the application of a coolant. When the top layer of the piece was preheated with an oxyacetylene flame, a cast alloy-tipped cutter finished an average of 90 pieces at a greatly increased feed of 53 ipm and at a cutting speed of approximately 200 fpm. Since only the top layer of the workpiece was heated, and climb-milling was employed to remove the heated material in the form of chips, the newly generated surface was accurate dimensionally and was unaffected by the heat.

MILTON C. SHAW.[14] The manner in which stress varies with strain in true stress-strain tensile tests is particularly useful in interpreting cutting data obtained under hot-machining condi-

[7] Authors' Bibliography (8).

[8] "Moving Sources of Heat and the Temperature at Sliding Contacts," by J. C. Jaeger, Journal and Proceedings of the Royal Society, of London, vol. 76, 1934, pp. 203–224.

[9] Ibid., Fig. 4.

[10] From reference (8), Fig. 1, for a moving-band source. Actually this temperature distribution is on the underneath side of the chip and assumes the tool to be an insulator. In case the tool is not an insulator there is a fundamental difficulty in deriving the division of heat between two contacting surfaces, and, consequently, the temperature distribution. This occurs because the distribution obtained under a moving source is not the same as that under a stationary source. This difficulty is involved in Trigger's analysis,[7] also Equation [14] of the paper.

[11] Research Engineer, Charge of Metal Cutting, Kearney & Trecker Corporation, Milwaukee, Wis. Mem. ASME.

[12] Junior Machine Designer, Research and Development, Kearney & Trecker Corporation. Jun. ASME.

[13] "Milling Hot Workpieces," by A. O. Schmidt and J. R. Roubik, *Automotive Industries*, vol. 101, November 1, 1949, pp. 29–31 and 67; *The Tool Engineer*, vol. 23, December, 1949, pp. 17–19.

[14] Associate Professor of Mechanical Engineering, Massachusetts Institute of Technology, Cambridge, Mass. Mem. ASME.

tions. When such curves are plotted for a representative steel at different constant temperatures, results such as those shown in Fig. 18, herewith, are obtained.[15] Here the yield point is marked by a circle and the rupture point by X. The increase of stress with strain above the yield point is due to strain-hardening, and the slope of this straight portion of the curve is a measure of the tendency for the metal to strain-harden. This slope (modulus of strain-hardening) will be greatest for materials with a strong tendency to strain-harden, such as the high-temperature alloys. For large plastic strains, the yield stress and the modulus of strain-hardening are the important items in determining the stress resulting from a given strain. The yield stress and modulus of strain-hardening are influenced by changes in test conditions in the following ways:

1 Both the yield stress and modulus of strain-hardening increase with an increase in alloy content.

2 An increase in hardness produced by heat-treatment is accompanied by an increase in both yield point and modulus of strain-hardening.

3 An increase in strain rate causes an increase in the modulus of strain-hardening.

4 The presence of a hydrostatic component of stress (as the normal stress on the shear plane in cutting) produces no change in either modulus of strain-hardening or yield stress, but does cause an increase in the rupture stress if the normal stress is compressive (a decrease if tensile).

The authors state that the reduction in the forces in hot-machining is due to the decrease in shear strength of the metal cut. This statement is misleading, for the word "strength" infers that the material has ruptured during cutting which is not the case, since continuous chips are obtained under the conditions of this paper. The material is, instead, subjected to a stress corresponding to the plastic strain required by the geometry of the process and the particular stress-strain curve obtaining. The name assigned to the stress on the shear plane is a trivial matter provided it does not lead to false concepts such as the quantity C. The quantity C, which the authors call the machining constant, has meaning only when the chip ruptures. It is then a measure of the increase in rupture stress due to the presence of a normal compressive stress on the shear plane in accordance with item 4 of the foregoing conditions. The C that is determined for continuous chips has no significance in the light of the materials tests cited. This explains the fact that the quantity C, as determined by the authors, is frequently greater than 90 deg (see Fig. 7 of the paper), which infers that a compressive stress has caused a "decrease" in shear strength. This would be in contradiction of item 4, were it not for the fact that a flow stress has been interpreted incorrectly as a rupture stress.

The general decrease in the cutting forces in hot-machining is due to a decrease in yield stress and modulus of strain-hardening with increased temperature (see Fig. 18). This results in a lower value of shear stress on the shear plane for a given required strain and hence lower cutting forces. In the case of high-temperature alloys the chief effect of temperature is to decrease the tendency to strain-harden, an item which the authors have ignored in their list of basic factors.

To observe the relative importance of a change in yield point and modulus of strain-hardening with increased temperature, the curves in Fig. 18 of this discussion must be extended to a strain of from 2 to 3, such unusually high strains being possible without rupture due to the presence of the normal stress on the shear plane.

[15] "The True Stress-Strain Tension Test—Its Role in Modern Materials Testing," by C. W. MacGregor, *Journal of The Franklin Institute*, vol. 238, 1944, pp. 111 and 159.

In the case of annealed carbon steels that do not strain-harden nearly as much as the high-temperature alloys, hot-machining may not cause a decrease in the cutting forces. This is illustrated by the authors' results for annealed SAE 3145 steel which actually showed greater forces at 500 F than at room temperature. This is to be expected from the inversion in the temperature effect

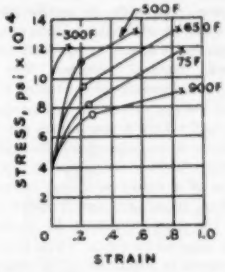

FIG. 18 TRUE STRESS-STRAIN CURVES FOR A STEEL AT SEVERAL TEMPERATURES AND A CONSTANT STRAIN RATE OF 10^{-2} SEC^{-1}

that is usually found in tensile tests as shown in Fig. 18. Here it is evident that the stress-strain curve at room temperature is actually lower than that at 500 F.

Again, it was found that heating annealed SAE 3145 steel to 1500 F before cutting actually caused a decrease in tool life whereas the tool life of the same material when hardened by heat-treatment was improved by hot-machining at 1500 F. The reason for these results is that the harder material has a greater tendency to strain-harden than the annealed steel and hence hot machining is more effective in reducing the tool forces and chip strain-hardening responsible for increased wear in the case of the hardened steel. In general, hot-machining will be most effective on materials that have a high modulus of strain-hardening due to high alloy content or increased hardness due to heat-treatment (but not due to cold work).

The existence of an optimum speed with regard to tool life may be explained by the existence of two types of wear which have different velocity characteristics. Cemented-carbide tools have a strong tendency to form a built-up edge at very low cutting speeds. This tendency is, in fact, so pronounced that the life of a tungsten-carbide tool will generally be less than that of a high-speed-steel tool at very low speeds. The nature of the wear produced by a built-up edge might be described as a chipping action, as noted by the authors, since it is due to very hard particles of built-up edge plowing out microscopic grooves as they pass across the tool and clearance faces. The size and number of built-up edge particles will decrease as the speed is increased and hence the wear due to this cause will decrease with speed. There is, however, another type of wear, namely, that due to transfer. This involves the submicroscopic particles that are pulled from the surface when the minute junctions responsible for friction are broken. The wear surface in this case will be smooth and the rate of wear will increase with an increase in the temperature of the tool face. Since the temperature of a slider increases as $V^{1/2}$, where V is the speed of the slider, the wear due to transfer will increase with cutting speed. We then have two types of wear that are operative in cutting—that due to plowing which decreases with increased speed, and that due to transfer which increases with speed. An optimum speed is to be expected. Below this optimum speed the plowing wear predominates, and the wear surface will be rough, while above the optimum speed the wear surface will be smooth. It would appear that the fore-

going explanation of tool wear is more feasible than that offered by the authors, in which the optimum speed is explained by the inversion in the relative hardness of chip metal and tool material with increased temperature.

Several comments might be made concerning the proposed Equation [7]. This equation is not derived from a clear mechanism of the wear process and hence must be regarded as an empirical expression. As such, its justification must lie in its ability to satisfy experimental data. However, the experimental data that this equation is meant to represent are strangely mixed values for different physical processes. The forces are measured values from a two-dimensional tool taking a "continuous" cut. The temperatures are not measured, but computed values for a two-dimensional tool taking a continuous cut, while the values of tool life are for a three-dimensional fly milling cutter which cuts "intermittently." Now the temperatures, forces, and tool-life characteristics of a cutter operating intermittently are entirely different from those of a cutter which operates continuously and hence the data are not at all compatible. The observation that the slope of the curve in Fig. 16 of the paper corresponds to an exponent in Equation [7] of $^1/_{20}$, which is the tool-life exponent observed by Schallbroch, Schaumann, and Wallichs, appears to be coincidental. A line corresponding to a slope of $^1/_{40}$ fits the plotted points equally well.

SAM TOUR.[16] The authors mention an article by Tour and Fletcher,[17] and state that "in all this initial work no data on tool life were reported," and "the basic reasons for lower values of power consumption and tool forces were not investigated." Neither of these statements is wholly true. They do not mention another article by Tour,[18] which presents and explains the basic reasons for the lower values of power consumption and tool forces encountered in hot-machining and presents the factual data. Neither do they mention additional articles by members[19] of the writer's company.

Attempts to make a mathematical analysis of the conditions obtaining at the point of a cutting tool are laudable. However, all equations to express these conditions must be founded on certain assumptions. Whether or not these assumptions are correct may be debatable. If the equations as set up give results that are not in keeping with known facts, it would appear that the equations are wrong rather than the facts.

We realize that the theoretical background used by the authors in this paper are those that were published about 5 years ago, and since then incorporated in the "Tool Engineers' Handbook." That the applicability of these equations to actual metal cutting has not been challenged seriously in the past does not prove that they are applicable.

A rational study of the calculated data offered by the authors in their Table 3 on AISI 3145 steel, throws considerable doubt on the validity of the so-called basic factors and equations set up by them. They have not proved that their friction angle is a direct measure of the coefficient of friction between chip and steel. They do not explain how they arrive at their values for the mean shear strength S_s in psi of the metal being cut. In Table 3 they present this property of the metal as a variable, although in their Equations [1] and [2] they define it as a constant. Obviously, it should be a constant at any given temperature. They calculate it and arrive at values for shear strength at room temperature that vary from a low of 54,000 psi to a high of 107,000 psi. This is not rational. It is well known that AISI 3145 steel is soft and quite plastic at 1500 F, yet in Table 3 they calculate it to have shear strengths of from 55,000 to 74,500 psi at that temperature. Obviously, the calculated values for shear strength S_s, in Table 3 are incorrect. Equally obvious should be the conclusion that the methods by which those figures were arrived at are incorrect. The formulas as used are not applicable. Equations [1] and [2] must be discarded.

Equation [3] is incorrect since it is based upon the false assumption that all the power consumed in cutting is in the cutting force F_c. If this were true, no power would go into the tool carriage. Since this is contrary to fact, the equation must be discarded.

Table 3 lists calculated coefficients of friction between a chip of AISI 3145 steel and a sintered-carbide tool. At room temperature the spread is from a low of 0.46 to a high of 1.25. At 1500 F, the spread is from a low of 0.37 to a high of 0.93. Such variations of the actual coefficient of friction are irrational. Obviously, the values calculated are not coefficients of friction. What they represent, other than that the equations used are inapplicable, we are unable to state.

Fig. 5 of the paper, for 16–25–6 alloy, shows some of these coefficient-of-friction calculation results plotted against workpiece temperature. Although straight lines have been drawn on the plot, the actual data as plotted show otherwise. The values decrease from room temperature to 500 F, decrease further to 1000 F, and then increase to about original room-temperature values by the time 1500 F is reached. Even had the curves been drawn to fit the points as plotted, the chart would have little significance since the points have been derived in a questionable manner.

Since the shear strengths and the coefficients of friction are incorrect, it follows that the machining constants C, as calculated, are meaningless.

We are not familiar with the paper by Trigger and Chao,[7] so have been unable to study the complex Equations [4] and [5] in their original form or as revised. It seems that the equations as finally used by the authors contain the misunderstood value F_c, a factor J that is not defined, and a friction-force value F not defined. No actual average chip-temperature measurements were taken; values were calculated. Use was made of questionable Equation [4]. The results of such obscure calculations were used in the questionable Equation [5], and those results used in the questionable Equation [6] to arrive at the values presented in Table 4. These questionable values were then used to produce the peculiar curves in Fig. 8. Confusion is compounded by Equation [7] where the previously discarded F_t is brought back to life in combination with the results of Equation [6], and an empirical constant of questionable constancy. This combination is used to produce the straight line in Fig. 16 but proves nothing.

The experimental methods used by the authors to study tool life have yielded data of limited application. Their Fig. 11 indicates that for SAE 3145 at 350 Bhn and for one particular tool and cut condition, the optimum cutting speed for maximum tool life is about 350 fpm at room temperature, but only 150 fpm at 1500 F. However, tool life at optimum speed at 1500 F is 60 times tool life at optimum speed at room temperature. Their Fig. 12 shows that for S-816 alloy for a particular set of tool and cut conditions, the optimum speed is of the order of 200 fpm at elevated temperatures, but below 150 fpm at room temperature. Tool life is maximum at 1500 F. Their Fig. 13 shows that for Inconel X, for one particular set of tool and cut conditions, the optimum speed for maximum tool life is at about 350 fpm at all temperatures. Fig. 14, for 16–25–6 alloy, shows an optimum

[16] Sam Tour & Company, Inc., New York, N. Y.

[17] Authors' Bibliography (3).

[18] "Hot Spot Machining," by Sam Tour, *The Tool Engineer*, vol. 24, May–June, 1950, pp. 32–34.

[19] "Strain Gage Dynamometer for Measuring Cutting Tool Loads," by H. Rottersman, A. J. Bettinger, and W. P. Blake, *Iron Age*, vol. 164, September 29, 1949, pp. 55–61.

"Hot Spot Machining," by L. T. Friedman, *Iron Age*, vol. 165, February 9, 1950, pp. 71–76.

"Tooling for Hot Machining of Hard-to-Cut Metals," by Henry Janes, *Machinery*, vol. 56, April, 1950, pp. 152–157.

speed of 200 fpm for all temperatures, except 500 F, where an optimum of 300 fpm is indicated. Maximum tool life is shown to be obtained at 1000 F work temperature. Fig. 15 is an attempt to compare nonoptimum conditions and has little significance.

The writer's company has done considerable work in this field of hot-machining. Our work was done by the hot-spot machining method. We endeavor to heat a relatively small surface layer of metal ahead of the tool and to machine it off before much of the heat can travel into the body of the workpiece. Most of our work was done on turning 3-in. round bars. We used a standard square insert-type right-hand turning tool. The insert was Kennametal Grade K3H. The tool used was set at the following angles: Back rake —9 deg; side rake —9 deg; end relief 9 deg; side relief 9 deg; end cutting edge 5 deg; side cutting edge 5 deg; and nose radius $^1/_{16}$ in. It should be noted, therefore, that our results are based upon normal turning operations which give conditions that vary somewhat from the limited conditions used in the tests by the authors. Power consumption was measured. Our feeds and depths of cuts were considerably in excess of those reported by them and more in keeping with practical machining operations. Forces on the tool were measured with a tool dynamometer. Complete details of the SR-4 strain-gage dynamometer for this purpose have been published.

One of the steels that we used, Navy Grade V, is a higher-nickel, lower-chromium steel than SAE 3145. The carbon content, 0.41 per cent, was roughly the same. The high-temperature alloy we used was S-816.

We made no effort to measure or to determine mathematically coefficients of friction for the chip. We would expect a lowering of the frictional forces, as with lowered yield strengths the unit pressures which cause deformation of the chip are lowered. We cannot accept the authors' explanation that the coefficient of friction directly affects the force or pressure with which the metal is pressed against the tool. Such forces as are present due to friction will be parallel to the surface. They, therefore, cannot have a component normal to this same surface. It seems to us that there is some confusion as between friction, the effect of friction in changing the chip geometry, and abrasion. This question of friction seems to us to have been very much oversimplified in the paper.

As regards the effect of tool angles, we made one experiment and found that changing the side rake from —7 deg to +7 deg gave a decrease of 6 per cent in power consumption, while changing the back rake from —7 deg to +7 deg gave an increase of 6 per cent in power consumption by the lathe when cutting 3-in. round bars of Grade V steel with a surface temperature of 1000 F at 0.250 in. depth of cut, 0.024 ipr feed, and 136 rpm.

We have great difficulty believing the authors' statement that 16–25–6 alloy has a lower interface temperature when the workpiece is heated to 500 F than when run at room temperature. We note that Table 4 shows this to be true only at the higher cutting speeds. Moreover, this table shows interface temperatures far above the softening temperatures of even carbide tools. Moreover, a temperature of 2400 F is a dazzling white heat and should be readily visible if such temperatures are actually reached.

Our work was done on a lathe. The chip removed was one that might be removed in any shop operation. For a nonmathematical but realistic approach to the basic factors involved in the hot-machining of metals, we prefer to deal in terms of unit pressures of the chip on the tool tip.

Fig 19, herewith, shows an end-cutting tool. Although most lathe work is done with a side-cutting tool, fundamentally the mechanics is the same in either form of tool. The illustration shows the tool and the chip being removed. The different components which consume the power used in machining can be stated in simple words. There are three components as follows:

(*a*) The shear component: As the tool pushes against the work, it shears the steel. The amount of energy consumed in shearing the steel is a direct function of the shear strength of the steel.

(*b*) Energy consumed in deforming the chip as it leaves the edge of the work. The amount of energy consumed in this deformation is an inverse function of the plasticity of the steel.

(*c*) Energy consumed in friction as the chip goes across the surface of the tool.

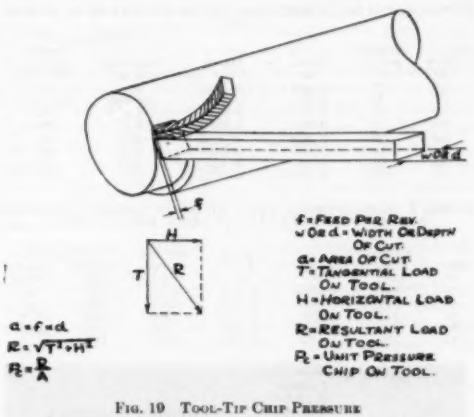
w OR d
f
H
T
R
f = FEED PER REV.
w OR d = WIDTH OR DEPTH OF CUT.
a = AREA OF CUT.
T = TANGENTIAL LOAD ON TOOL.
H = HORIZONTAL LOAD ON TOOL.
R = RESULTANT LOAD ON TOOL.
P_s = UNIT PRESSURE CHIP ON TOOL.
a = f × d
$R = \sqrt{T^2 + H^2}$
$P_s = \frac{R}{A}$

FIG. 19 TOOL-TIP CHIP PRESSURE

Referring again to Fig. 19, it will be seen that the energy consumed in shear, and at least a portion of the energy consumed in deformation of the chip, combine to make up a tangential load on the tool, called *T*. Part of the energy of deformation of the chip and the energy due to friction of the chip across the face of the tool join to make up the horizontal load on the tool, called *H*. Within limits the shear energy involved as a portion of the tangential load *T* will be independent of the feed per revolution. In other words, as the feed is increased, the proportion of the load on the tip of the tool, which is accounted for by deformation of the chip, will increase, although the load due to shearing of steel will remain substantially constant. These combined loads are shown as *T* in Fig. 19. The horizontal load on the tip of the tool, which is due to both deformation of chip and friction on the face of the tool, is shown as *H* in Fig. 19. The resultant load on the tip of the tool shown as *R* is calculated by the formula shown in Fig. 19. This resultant load, divided by the area of the chip, is shown as the unit pressure of the chip on the tool and is designated P_s in Fig. 19. The unit pressure of the chip on the tip of the tool is the most important item in connection with tool failure, and it is directly related to the temperature conditions of machining.

Table 5[10] gives the results obtained on some runs on S-816 alloy. In this connection, it should be noted that in one run at 1500 F we removed in excess of 13 cu in. of material with no evidence of tool failure.

Some of our results on Navy Grade V steel (approximating AISI 3345 steel) are shown in Table 6 for room-temperature cuts, and Table 7 for cuts at 1000 to 1200 F.

Fig. 20, herewith, shows cutting pressures on the tool tip when hot-spot-machining medium-carbon steel at various surface tem-

[10] Authors' Bibliography (7), table XII. Table 6 of this discussion is table IX of the same reference, and table 7, herewith, is table X.

TABLE 5 METAL REMOVAL RATES FOR S-816 ALLOY AT VARIOUS MACHINING TEMPERATURES

Run No.	Heat Source	Spindle Speed, Rpm	Feed, In. per Revolution	Depth of Cut, In.	Temperature, °F		Tool Loads, Lb		Power Consumption, Hp	Metal Removed Cu In. per Min
					Work	Chip	Torque	Thrust		
97	Cold	91	0.015	0.0625	....	....	....	....	2.84	0.88
98	Cold	136	0.010	0.0625	....	....	410	320	....	0.80
99a	Gas	73	0.010	0.110	1260	....	350	250	....	0.78
99b	Gas	73	0.010	0.110	1300	....	230	230	2.01	0.78
99c	Gas	73	0.010	0.110	1500	1000	110	190	1.93	0.78
98	Gas	73	0.015	0.140	1520	1000	....	....	....	1.44
108	Flux	171	0.010	0.187	1500	....	....	....	4.09	3.01
110	Flux	171	0.015	0.187	1500	....	....	....	5.23	4.52

TABLE 6 COLD-CUTTING TEST RUNS ON GRADE V NICKEL STEEL

Run no.	Spindle speed, rpm	Feed, ipr	Depth of cut, in.	Tool loads, lb	
				Tangential (torque)	Longitudinal (thrust)
46	73	0.010	0.0625	420	200
47	73	0.010	0.125	610–680	390–420
48	73	0.005	0.0625	230	130
49	73	0.005	0.125	375	290
50	136	0.010	0.0625	400	195
51	136	0.005	0.0625	235	125
52	136	0.005	0.125	360	270
53	136	0.0025	0.0625	100	140

TABLE 7 HOT-CUTTING TEST RUNS ON GRADE V NICKEL STEEL AT TEMPERATURES FROM 1000 TO 1200 F

Run no.	Spindle speed, rpm	Feed, ipr	Depth of cut, in.	Work surface temp, deg F	Tool loads, lb	
					Tangential	Longitudinal
54	136	0.010	0.125	1100	320	240
61	136	0.015	0.125	1025	440	295
62	136	0.020	0.125	1000	565	330
63	136	0.010	0.156	1150	400	280
64	136	0.010	0.188	1125	480	315

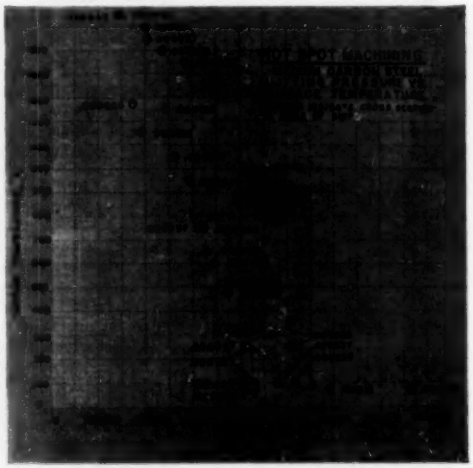

FIG. 20 HOT-SPOT MACHINING MEDIUM-CARBON STEEL

peratures. It should be noted that cutting pressures decrease with increasing cross-sectional area of chip. It should be noted also that for different speeds and ratios of feed to depth of cut there is a difference in cutting pressures at the same surface temperature. Maximum tool life with minimum power consumption can be expected when the conditions selected are such as to give minimum cutting pressures without chip temperatures rising to an excessive degree.

In hot-spot machining, the cutting action is taking place on material that is not at a uniform temperature. The surface of the workpiece may be at 1500 F, while the tip of the tool is working at a depth where the workpiece temperature is only 1100 F. The chip being removed may not have a rectangular cross section. If the steel is in the plastic stage, the chip cross section is of the airfoil type. The chip width may be 50 per cent greater than the depth of cut. The chip thickness may vary from as low as the feed per revolution to as high as several times the feed. The thin edge represents the base of the cut or tip of the tool and the thick edge of the surface of the workpiece.

We agree heartily with the authors in their conclusion that the greatest advantage in hot-spot machining is found in the hard-to-machine and high-temperature alloys. We do feel, however, that useful, though less spectacular, savings may be made in hot-spot machining of many of the common materials.

The authors are to be complimented on their addition to the all too scarce data on this important subject.

AUTHORS' CLOSURE

The authors wish to thank all the discussers for their contributions. The reader should bear in mind, in considering these remarks, that this paper presents the results of research on the influence of basic metal-cutting quantities when machining metals at elevated temperatures. Therefore, it follows that when this work was planned, conditions were chosen which were considered most suitable to the study of these basic quantities, which were not necessarily those best suited to practice.

Mr. Armstrong questions the use of a general-purpose roughing grade of carbide. However, for the purpose of this research, it was desirable to use such a grade of carbide in order that a single tool material might be used for machining at both room and elevated temperatures. The hard brittle grades of carbide would not have held up under conditions of an intermittent cut at room temperature.

In regard to the question concerning the hardness of the AISI 3145 steel after heating, it should be pointed out that in machining this steel, the power density available from the high-frequency induction-heating unit was sufficient to give localized heating of the work surface. Under these conditions the hardened workpiece (350 B) retained its physical properties, despite the brief surface heating above the critical temperature. By the same token the AISI 3145 steel machined in the as-received condition (180 B) did not air-harden because the bulk of the material was never heated above the critical temperature. Mr. Armstrong points out the desirability of tool-life tests with longer actual cutting time and, consequently, greater tool life, mentioning that short-time tests such as employed here are more subject to error. This point was considered. However, in view of the nature of the research, it appeared that the test method used would be the most productive of useful data on a variety of materials. While this test method gave values of tool life which in practice would be uneconomical, it was the relative values of tool life obtained at various cutting speeds and workpiece temperatures with which we were concerned. These data were found to be both reliable and reproducible.

The informative discussion by Dr. Hahn clarifies the question raised by Mr. Armstrong concerning the thermal equilibrium at the tool-chip interface. In his discussion Dr. Hahn substantiates what had been concluded by the authors in setting up this test method, namely, that the tool-chip interface reaches thermal equilibrium very shortly after the tool enters the work during each revolution. Mr. Hahn raises a question regarding the validity of plotting a variable containing tool-chip-interface temperature against tool life, where tool life is measured by wear on the flank of the tool and the interface temperature is measured on the face of the tool. The validity of this method is established if the process of flank wear is understood. The wear land on the flank occurs owing to the breaking down of the cutting edge. As the tool wears the cutting edge recedes back from its original position allowing a triangular section of the tool to be worn away at the tip. In other words, the wear land on the flank is essentially a "taper section" of the actual wear taking place on the tool face at the cutting edge. This removes the clearance from the tool flank for a proportional distance down from the original cutting edge. It is this distance which is measured as the tool wear land on the flank of the tool. From the foregoing it can be seen that the wear land on the flank is a direct measure of the wear (breakdown) of the cutting edge. Also, it can be seen that the tool-chip-interface temperature directly affects the ability of the cutting edge to withstand the specific pressure and abrading action to which it is subjected under cut.

The authors appreciate the supplementary remarks by Dr. Schmidt and Mr. Roubik and are pleased to note that their findings are in agreement with those presented in the paper.

In reference to the point raised by Professor Shaw, the term "shear strength" was of course used synonymously with "yield stress" to describe the conditions necessary to produce plastic flow on the shear plane. However, shear strength (or yield stress) is definitely influenced by compressive stress. This is indicated, for example, by such data as given in Fig. 21 of this closure. This figure plots typical data obtained from tests made on steel using the Bridgman method[21] of testing the effect of compressive loading on the shear strength of a material. Shear strength S_s, is plotted as a function of shearing strain ϵ, for various conditions of compressive stress, S_c. In this particular case the steel was SAE 3150 having a pearlitic structure. It can be seen that for a given value of strain, the shear strength increases with increasing compressive stress. Cutting tests were also made on this same material so that a comparison can be made between values of machining constant C obtained from the torsion-compression test and those obtained from metal cutting. The correlation may be considered good. For example, for a shearing strain of 3.02, the value of machining constant under conditions of metal cutting was found to be 77.1 deg; the value of machining constant obtained from the Bridgman test method for this strain is 74.5 deg. The quantity C, as such, does not change in meaning when rupture occurs on the shear plane. However, it is not in itself a measure of the increase in rupture stress due to applied compressive stress. Instead, a quantity K (as defined by Field and Merchant[22]) is the measure of the latter.

It was not the intention of the authors to give the impression that they attribute the existence of an optimum speed (with regard to tool life) to an inversion in the relative hardness of chip and tool. The reason for this optimum speed is explained by the authors in the fourth paragraph of the section of the paper entitled "Tool Life," and is the same as that given by Professor Shaw.

Equation [7] is admittedly based on a mixture of data from two different types of tests, as clearly stated in the paper. As such, the authors point out, further work is needed to indicate its degree of usefulness. However, the two sets of data which are mixed empirically in arriving at the equation are not incompatible for the reason set forth in the paper. Further evidence to this effect is set forth by Dr. Hahn in his discussion.

The discussion by Mr. Tour discards the various basic equations governing the mechanics of cutting which are fundamental to this paper. This is done without presenting any facts, substantiated or otherwise, to prove these equations incorrect or invalid. The only explanation given is, "if the equations as set up give results that are not in keeping with known facts, it would appear that the equations are wrong rather than the facts." These equations, however, have been published now for more than

[21] "On Torsion Combined With Compression," by P. W. Bridgman, *Journal of Applied Physics*, vol. 14, 1943, pp. 273–283.

[22] "Mechanics of Formation of the Discontinuous Chip in Metal Cutting," by Michael Field and M. E. Merchant, Trans. ASME, vol. 71, 1949, pp. 421–430.

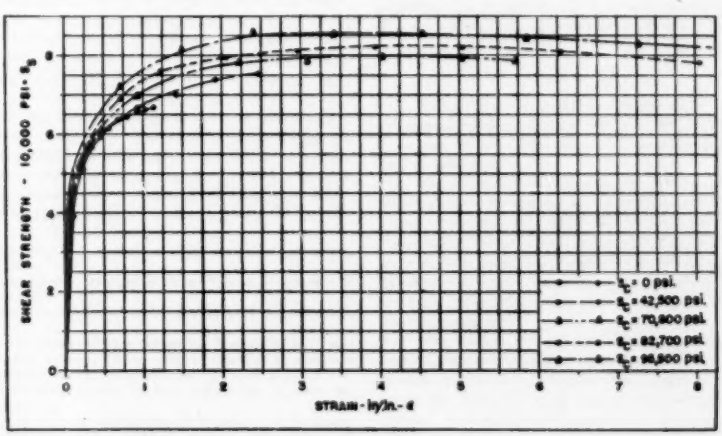

FIG. 21 STRESS-STRAIN DIAGRAM FOR SAE 3150 STEEL UNDER VARIABLE COMPRESSIVE LOADS

5 years.[23] In that time, they have been found to be in agreement with the facts regarding "machining operations" by numerous independent investigators in various parts of the world. It seems logical then that these equations must have some merit and, therefore, should not be discarded casually. Obviously, it was not the purpose of this paper to present the scientific background for these various equations (which has been done elsewhere[24]), but rather once again to apply them to the basic study of a particular machining problem.

Mr. Tour has questioned the values of S_s, as given in Table 3 of the paper. The fact that these values of S_s vary over a considerable range for a given workpiece temperature, and the fact that values of S_s, ranging from 55,000 to 74,500 psi, are obtained for AISI 3145 steel when machining at 1500 F are the sole reasons given for discarding Equations [1] and [2]. The authors, however, have defined the shear-strength value S_s as the mean shear strength of the metal on the shear plane, "in machining." The value S_s is not at all the same as the bulk shear strength of the metal, as determined from mechanical tests on bulk specimens, and as assumed by Mr. Tour. This distinction must be kept clearly in mind. The nature of the obvious differences between the quantity S_s and bulk shear strength, has been well discussed by various authors[23,24,25] in the metal-cutting literature, so that a recapitulation seems quite unnecessary here.

In Mr. Tour's discussion Equation [3] was discarded without presenting any facts in support of this action. The cutting force F_c determines the power consumed in "chip formation." The thrust force F_t only affects the power required for feeding the tool. As an example of the relative power consumed in these two processes, take a turning operation. If a tool with 0-deg side-cutting-edge angle is assumed, the longitudinal (feeding) force would equal the thrust force F_t. To be on the safe side the value of F_t may be chosen equal to F_c (it isn't usually this large). If the stock being turned had a mean circumference, in the cut, of 10 in., and the feed per revolution was 0.010 in., then the power consumed in the cut by F_t would be only 0.1 per cent of the net power consumed in chip formation. For all practical purposes then, F_t may be ignored in making power calculations, as is the general practice.

The relationship between the friction angle and the coefficient of friction, which has been questioned by Mr. Tour, has already been established. Proof of this has been published in the literature, and reference has been made to that literature by the authors in this paper. The presentation of Fig. 5, to which Mr. Tour refers, was intended to point out that workpiece temperature has no appreciable effect on the coefficient of friction. This would have been just as obvious if the curves had been drawn exactly through every experimental point as by drawing the average straight line actually presented.

Mr. Tour also states, "since the shear strengths and coefficients of friction are incorrect, it follows that the machining constants C, as calculated, are meaningless." No facts have been presented to substantiate this statement.

It is unfortunate that Mr. Tour did not familiarize himself with the paper of Trigger and Chao[26] to which he refers, so that he might have studied the "complex Equations [4] and [5]." It does not seem reasonable to discredit the work of the authors concerned on the basis of what is termed "a misunderstood value F_c, a factor J which is not defined, and a friction-force value F, not defined." Actually, the friction force F was defined in the paper following Equation [5]. Definition of the common quantity J (mechanical equivalent of heat), unfortunately, was omitted from the preprint.

Mr. Tour's remarks directed at the remaining equations, tables, and curves of this paper stem from an unfortunate misunderstanding of Equations [4] and [5]. Each of the nonempirical equations presented by the authors in this paper and elsewhere is based on a sound mathematical analysis using fundamental engineering concepts. They can be proved invalid only if controverted by the presentation of new facts, similarly based upon sound engineering principles.

[23] Authors' Bibliography (6) and "Basic Mechanics of the Metal-Cutting Process," by M. E. Merchant, *Journal of Applied Mechanics*, Trans. ASME, vol. 66, 1944, pp. A-168 to A-175.

[24] "Correlation of Plastic Deformation During Metal Cutting With Tensile Properties of the Work Material," by J. T. Lapsley, Jr., R. C. Grassi, and E. G. Thomsen, Trans. ASME, vol. 72, 1950, pp. 979–986.

[25] "A Quantized Theory of Strain Hardening as Applied to the Cutting of Metals," by M. C. Shaw, *Journal of Applied Physics*, vol. 21, 1950, pp. 599–606.

[26] Authors' Bibliography (8).

Cutting Temperatures and Metal-Cutting Phenomena

By B. T. CHAO[1] and K. J. TRIGGER,[2] URBANA, ILL.

This paper considers some important findings which resulted from an investigation on the mechanism of heat generation during metal-cutting operations. It has been found that many changes during the cutting of metals are due to the change in tool-chip interface temperature through its influence on tool-chip friction. The paper is divided into two parts, the first of which pertains to the cutting forces and cutting temperatures observed during conventional turning and orthogonal cutting under otherwise identical conditions. The higher heat-dissipating capacity of the tool in orthogonal cutting operations was found to be fundamentally responsible for the observed differences. In the second part of the paper, the role of tool-chip contact area on interface temperatures is further investigated. This study has been of value in the interpretation of tool-chip interface temperature data and other phenomena heretofore inexplicable.

1 TOOL-CHIP INTERFACE TEMPERATURE

An Important Factor in Modifying Chip Geometry and Force Relationships

ANALYSIS of the basic mechanics of the metal-cutting process (1)[3] reveals that tool-chip interface friction plays an important role in the mechanism of chip formation. While the nature of static friction between clean metallic surfaces has been fairly well known (2, 3), the laws governing the behavior of tool-chip interface friction, where excessive sliding under high pressure and temperature takes place, remain to be studied. From the consideration of the interaction of surface-force fields as well as the interlocking of surface irregularities, Ernst and Merchant have shown that the coefficient of static friction is expressible as the ratio S/H, S being the force per unit area necessary to cause slip or shear of the contact area, and H, the compressive force per unit area of actual contact (which is the mean pressure hardness of the softer of the two contacting solids). Among other things both S and H are functions of temperature at the contact area.

In order to study the effect of change in interface temperature upon chip formation, tests were conducted for both orthogonal cutting and conventional turning operations under otherwise identical conditions. After investigating the mechanism of heat generation during cutting, it was revealed (4) that the main difference between the two operations lies in the fact that, in the case of orthogonal cutting where only a small portion of the side cutting edge is active, the tool will have greater capability to conduct the interface (frictional) heat away from where it is generated, i.e., the interface contact area. Another difference is that in conventional turning a slightly larger proportion of the total energy consumed in cutting will be conducted back into the workpiece. This, however, depends to a certain extent on the relative size of cut and the work diameter. Little investigation has been done on the subject, and, in so far as the interface temperature is concerned, its influence is presumably only of secondary importance. Hence this effect of size will be ignored in the following discussion.

A decrease of interface temperature (commonly referred to as cutting temperature) results in an increase in the coefficient of sliding friction at the tool-chip contact area which, in turn, decreases the shear angle and thereby the chip-thickness ratio. A lower chip-thickness ratio is usually accompanied by a harder and thicker chip[4] which, consequently, increases the tool-chip contact area—an important factor in influencing cutting temperature. These are borne out by tests to be described in the following sections.

Test Procedure

The general method of testing was the same as that reported in a previous paper (4). The orthogonal cutting was done at the end of a tube employing a tool set with its cutting edge perpendicular to the direction of relative motion of tool and workpiece and fed in the direction of the rotating axis of the tube. The tube was bored out from the same bar stock (NE 9445, mill-annealed 183 Bhn) used in the conventional turning study. The mean diameter was 4.123 in. and the wall thickness was 0.102 in.

Cutting was done at the mid-portion of the side cutting edge of the same tool used in conventional turning. Other test conditions were identical in both cases. The speeds were such that a type 2 chip was obtained in all tests except in one instance as shown by the dotted line in Fig. 1.

Test Results

1 Results of cutting speed-cutting temperature tests for both orthogonal cutting and conventional turning have been reported in a previous paper (4). They are reproduced in Fig. 1 for convenient reference.

2 Results for both components of cutting force and chip-thickness ratio at various cutting speeds are summarized in Figs. 2 and 3, respectively. Note that in the case of orthogonal cutting, a higher thrust force F_t is experienced, while the cutting force F_c is slightly lower than obtains in conventional turning. The differences in F_c are small, however. The chip-thickness ratio is lower for orthogonal cutting but the difference becomes small at low cutting speeds.

3 The change in both tool-chip contact area and length of contact with cutting speed is illustrated in Fig. 4. The decrease in contact area with increased cutting speeds is a significant factor in the higher cutting temperatures experienced at greater speeds. At a specified cutting speed, the larger contact area ob-

---

[1] Research Associate, Department of Mechanical Engineering, University of Illinois.

[2] Professor, Department of Mechanical Engineering, University of Illinois. Mem. ASME.

[3] Numbers in parentheses refer to the Bibliography at the end of the paper.

Contributed by the Research Committees on Metal Cutting Data and Bibliography, and Cutting Fluids, and Production Engineering Division and presented at the Annual Meeting, New York, N. Y., November 26–December 1, 1950, of The American Society of Mechanical Engineers.

Note: Statements and opinions advanced in papers are to be understood as individual expressions of their authors and not those of the Society. Manuscript received at ASME Headquarters on August 24, 1950. Paper No. 50—A-43.

[4] This is true for most machining operations on ferrous and non ferrous materials where type 2 chip is formed.

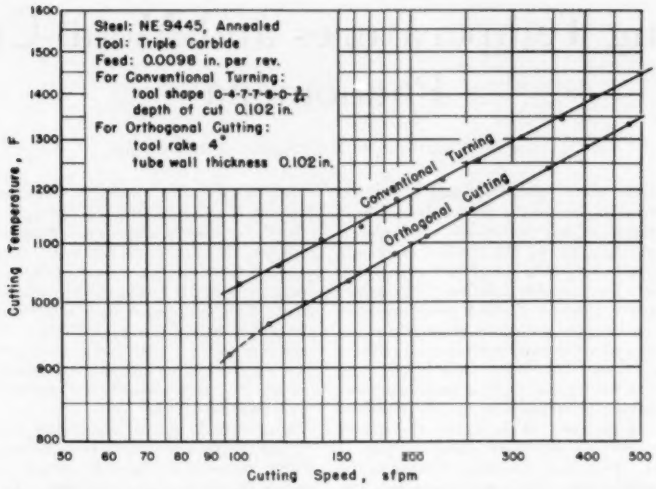

FIG. 1 CUTTING SPEED-CUTTING TEMPERATURE RELATIONSHIPS FOR CONVENTIONAL TURNING AND ORTHOGONAL CUTTING OPERATIONS

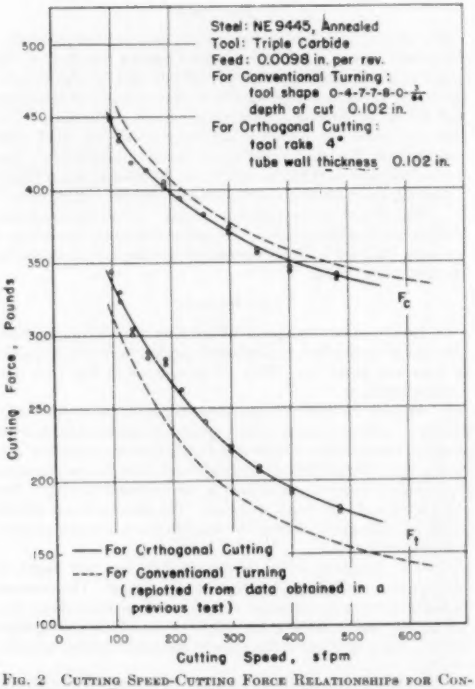

FIG. 2 CUTTING SPEED-CUTTING FORCE RELATIONSHIPS FOR CONVENTIONAL TURNING AND ORTHOGONAL CUTTING OPERATIONS

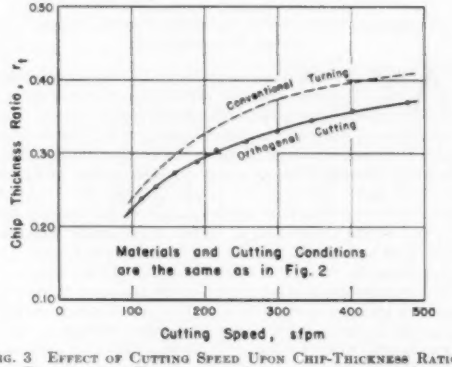
Conventional Turning
Orthogonal Cutting
Materials and Cutting Conditions are the same as in Fig. 2
Chip Thickness Ratio, r
Cutting Speed, sfpm

FIG. 3 EFFECT OF CUTTING SPEED UPON CHIP-THICKNESS RATIO FOR CONVENTIONAL TURNING AND ORTHOGONAL CUTTING OPERATIONS

served in orthogonal cutting is associated with a lower interface temperature than that in conventional turning under identical test conditions. This is true in spite of the fact that a higher coefficient of friction and larger frictional force are encountered in orthogonal cutting. The role of tool-chip contact area in influencing cutting temperature and chip geometry will be further illustrated in Part 2 of this paper.

4 Fig. 5 shows the relationship between tool-chip contact area and chip-thickness ratio. The values were obtained from Figs. 3 and 4, at equal cutting speeds. Within the limits of this investigation, it is evident that there exists a linear relationship between the contact area and thickness of the chip. The two straight lines are almost exactly parallel to each other. For a given chip-thickness ratio, a slightly larger value (approximately 5 per cent) of contact area is observed in orthogonal cutting. This suggests that for a given work-tool combination, the chip-thickness ratio plays a major part in the tool-chip contact area.

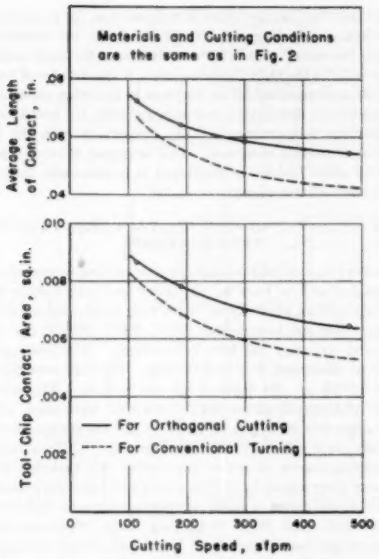

FIG. 4 EFFECT OF CUTTING SPEED ON TOOL-CHIP CONTACT AREA

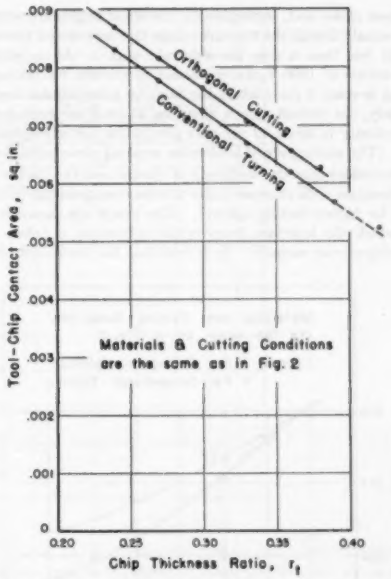

FIG. 5 RELATIONSHIP BETWEEN CHIP-THICKNESS RATIO AND TOOL-CHIP CONTACT AREA

However, there apparently are other minor factors which have an effect on the change. Further investigation will be necessary to clarify this point.

If the interface temperature is the major factor influencing the mechanism of chip formation, then the coefficient of friction at the interface calculated for both orthogonal cutting and conventional turning on the basis of equal cutting temperature should be approximately the same. According to Merchant (1), the shear angle ϕ, the friction angle τ (the tangent of which is the coefficient of friction at the interface) and the rake angle of the tool α are connected by a simple approximate relationship, namely

$$2\phi + \tau - \alpha = C \quad \ldots\ldots\ldots\ldots\ldots\ldots [1]$$

where C is (to a good degree of approximation[5]) a constant of the material being machined. From studies on chip geometry, he also derived an expression for chip-thickness ratio

$$r_t = \frac{\sin \phi}{\cos (\phi - \alpha)} \quad \ldots\ldots\ldots\ldots\ldots\ldots [2]$$

On the basis of these relationships it is evident that for a given value of τ, ϕ and r_t are fixed accordingly. Thus the values of μ, ϕ and r_t should be in close agreement when compared at the same cutting temperatures. The various quantities are shown in Table 1.

The agreement between the various quantities at any selected cutting temperature is fair considering the necessary approximations in the analysis. Apparently, the best over-all agreement is obtained at cutting temperatures of 1200 or 1250 F. The chip-

[5] The variation in C, as evaluated by Equation [1] was about 5 per cent for the orthogonal cutting tests reported herein.

TABLE 1 COMPARISON OF CUTTING PHENOMENA FOR CONVENTIONAL TURNING AND ORTHOGONAL CUTTING AT THE SAME INTERFACE TEMPERATURE

Work material: NE9445 steel, mill-annealed, 183 Bhn
Tool material: Triple carbide

Cutting temperature, deg F	Corresponding cutting speed, sfpm	Cutting forces, lb F_c	F_t	Chip-thickness ratio, r_t	Chip velocity, V_f, fpm	Tool-chip contact area, in.^{2} × 10^{-3}	Coeff. of friction, μ	Shear angle ϕ
CONVENTIONAL TURNING								
	Tool shape: 0-4-7-7-8-0-3/64			Depth of cut: 0.102 in.		Feed: 0.0098 ipr		
1050	112	459	308	0.25	27.6	8.1	0.77	14.4
1100	139	437	278	0.28	38.9	7.6	0.74	15.9
1150	172	419	253	0.31	52.8	7.1	0.71	17.5
1200	209	404	229	0.33	69.4	6.65	0.66	18.8
1250	254	390	207	0.35	90.3	6.25	0.63	20.0
1300	304	377	191	0.37	114.1	5.95	0.60	21.1
1350	364	384	176	0.39	142.3	5.65	0.57	21.9
ORTHOGONAL CUTTING								
		Rake angle: 4 deg			Tube-wall thickness: 0.102 in.			
1050	166	411	286	0.28	46.2	8.05	0.80	15.7
1100	204	398	264	0.30	60.8	7.7	0.76	16.9
1150	249	384	242	0.32	79.0	7.32	0.73	17.9
1200	298	371	222	0.33	99.0	7.02	0.68	18.8
1250	360	358	203	0.35	125.2	6.75	0.65	19.7
1300	428	347	188	0.36	155.0	6.50	0.63	20.6
1350	504	338	176	0.38	189.0	6.35	0.61	21.2

thickness ratios and, consequently, the shear angles are substantially equal (though the true rake angle in conventional turning is slightly less than 4 deg, the side rake angle). At an interface temperature of 1200 F the coefficient of friction for orthogonal cutting is some 3 per cent higher than for conventional turning. Similarly, the contact area is increased about 5 per cent, and the chip velocity is about 42 per cent greater for the orthogonal cutting. (The cutting speed is likewise some 42 per cent higher.)

It is evident that the coefficient of friction and the contact area both decrease with increase in the interface temperature (brought about by higher cutting speeds). The trends are shown in Fig. 6 in which the interface temperature arbitrarily is taken to be the independent variable. It is seen that the coefficient of friction (type 2 chip) decreases almost linearly with increase in the tool-chip interface temperature. The coefficient of friction is higher for orthogonal cutting though the difference is not great. Since both the cutting speed and chip sliding velocity with orthogonal cutting are higher for a given interface temperature, it appears that the cutting speed has little effect per se on the coefficient of friction. Its principal influence is through the effect on the rate of heat generation and, therefore, the interface temperature. The coefficient of friction undoubtedly is influenced by the tendency to adhesion of the tool and the chip. This factor is affected by the composition and properties of the tool and the workpiece, and by the surface-contact conditions. However, it is thought that with a given combination of tool and work material, a major factor is the temperature of the contact surface.

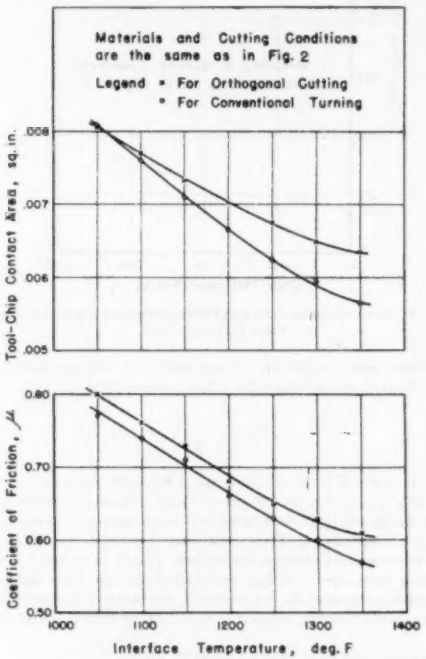

FIG. 6 RELATIONSHIP BETWEEN INTERFACE TEMPERATURE, COEFFICIENT OF FRICTION, AND TOOL-CHIP CONTACT AREA

If the interface temperature is reduced (as, for example, by a greater heat-conducting capacity of the tool), the coefficient of friction is increased. This, in turn, decreases the shear angle and thereby reduces the chip-thickness ratio, a lower value of which is invariably accompanied by an increase in tool-chip contact area. Since the heat is distributed over a larger area, the resultant tool-chip interface temperature is lower, consistent with the higher coefficient of friction observed. This sequence of events, accompanied by other factors, is illustrated in a schematic diagram in the summary of this paper.

2 THE ROLE OF TOOL-CHIP CONTACT AREA IN CUTTING TEMPERATURES

The effect of tool-chip contact area on cutting temperature has been pointed out in Part 1. In order to study further its influence on cutting phenomena, tests were conducted on NE9445 steel, quenched and tempered at 850 F, 950 F, 1050 F, and 1150 F to 401, 352, 311, and 283 Bhn, respectively. The test logs were about 3 in. diam and $1^1/_2$ to 2 ft long. The feed was held constant at 0.0098 ipr; the depth of cut was 0.102 in. Triple-carbide tools of ASA specifications 0-4-7-7-8-0-3/64 were used, and the setting angle was 90 deg in all tests. Only conventional turning tests were made and they were all done dry. Cutting temperatures, cutting forces, chip-thickness ratios, and tool-chip contact areas were determined by the same method heretofore used.

In the second series of tests, cutting was done on mill-annealed NE9445 steel (183 Bhn) employing both triple-carbide and straight tungsten-carbide tools. The triple carbide was a standard steel-cutting grade, while the tungsten carbide was recommended primarily for cast iron, magnesium, and other relatively brittle materials. Otherwise, the cutting conditions were identical.

RESULTS OF TESTS

On Quenched and Tempered Steels:

1 Results of cutting speed-cutting temperature tests on the various quenched and tempered NE9445 steels had been reported by one of the authors (5). The relationships are plotted on logarithmic co-ordinates as shown in Fig. 7. At any selected speed, a higher cutting temperature is observed with an increase in workpiece hardness.

The cutting-temperature equations for the various conditions of the steel are as follows:

Steel condition	Equation
Mill-annealed, 183 Bhn	$T = 387\ V^{0.212}$
Q and T, 1150 F, 283 Bhn	$T = 418\ V^{0.205}$
Q and T, 1050 F, 311 Bhn	$T = 459\ V^{0.193}$
Q and T, 950 F, 352 Bhn	$T = 466\ V^{0.197}$
Q and T, 850 F, 401 Bhn	$T = 499\ V^{0.188}$

wherein T is interface temperature, deg F, and V is cutting speed, sfpm. The effect of workpiece hardness upon chip thickness and chip hardness has been discussed quite extensively in the reference paper.

2 Fig. 8 shows the effect of workpiece hardness upon the relationship between both components of cutting forces and cutting speed. Similar to the annealed steel (spheroidized), an increase in cutting speed results in a decrease in the forces. At a given speed, however, somewhat lower forces were observed in the harder materials. This result is the antithesis of the commonly expected trend since cutting temperatures have been found to be higher for harder steels. The solution to this paradox lies in the effect of work-material hardness upon tool-chip contact area. This aspect will be discussed further in subsequent sections of this investigation.

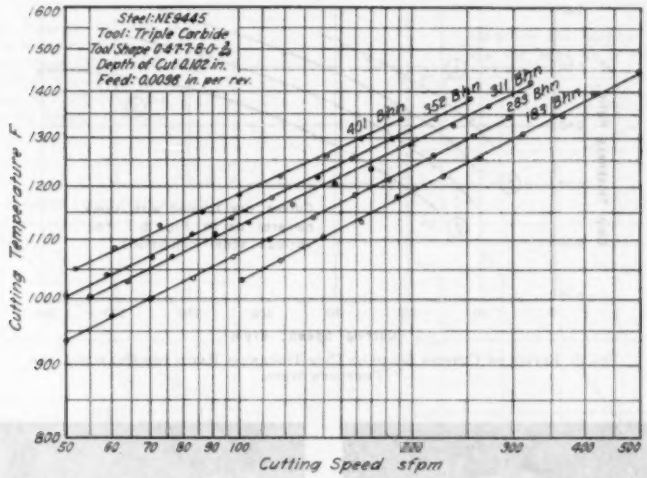

FIG. 7 EFFECT OF STEEL HARDNESS UPON THE CUTTING SPEED-CUTTING TEMPERATURE RELATIONSHIP

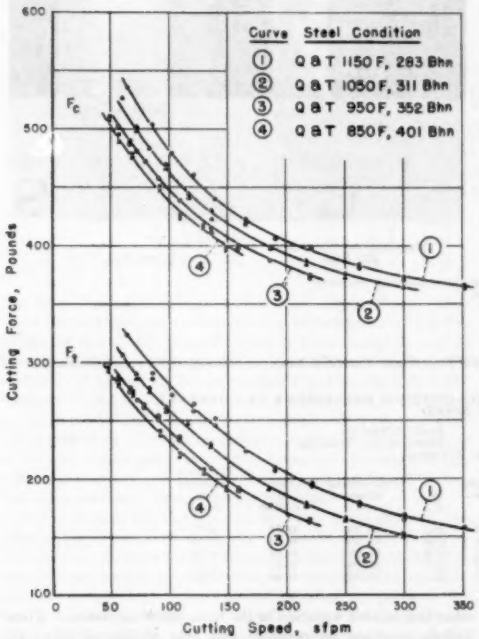
Curve Steel Condition
1 Q & T 1150 F, 283 Bhn
2 Q & T 1050 F, 311 Bhn
3 Q & T 950 F, 352 Bhn
4 Q & T 850 F, 401 Bhn
Fc
Ft
Cutting Force, Pounds
Cutting Speed, sfpm

FIG. 8 CUTTING SPEED-CUTTING FORCE RELATIONSHIPS FOR QUENCHED AND TEMPERED STEEL
(Cutting condition same as in Fig. 7.)

3 Variations of chip-thickness ratio with cutting speed are given in Fig. 9. All steels tested showed trends similar to those observed for the annealed steel, i.e., the increase in chip-thickness ratio is more rapid at the lower speed ranges and then increases at a slower rate as the speed becomes greater. At any specified speed, harder materials have higher values of chip-thickness ratio, i.e., the chip becomes thinner.

4 Illustrations of the contact areas for the various quenched and tempered steels are shown in Fig. 10. In this series of tests, cutting conditions were constant, and the workpiece diameter was the same for all of the steels tested. The contact areas were measured by a planimeter, and their relationships with workpiece hardness are plotted in Fig. 11. The cutting speed was 121 sfpm, a condition common to all test bars.

A part of the curve is shown dotted, since it is questionable that the hardness - contact area relationship for the annealed steel is a continuation of that existing among the quenched and tempered steels. The annealed structure consists of spheroidized carbides in ferrite whereas the microstructures of the quenched and tempered steels are all of the same kind, namely, tempered martensite.

The effect of workpiece hardness upon tool-chip contact area, unit "sliding" stress, coefficient of friction, and tool-chip interface temperature is shown in Table 2. It is evident that an increase in workpiece hardness results in a decrease in the contact area. It is this decrease which is largely responsible for the higher cutting temperature experienced when harder steels are cut. The tool-chip interface temperature is higher because the heat is concentrated on less tool area. It is this concentration of heat at the tool contact area which causes tool wear and failure and which thereby limits the cutting speeds for the harder materials.

It is also seen that the cutting forces (at constant speed) are less for harder materials (which is the equivalent of saying that the total work done in cutting is less). As noted in Table 2 and shown in Fig. 12, the coefficient of friction (at constant cutting speed) decreases as the workpiece hardness increases. This reduction in the coefficient of friction is associated with the higher cutting temperatures, coincident with reduced contact areas, observed in the harder materials. Another possible factor is the higher chip velocity caused by an increase in chip thickness ratio with harder materials. This aspect will be enlarged upon in a succeeding section.

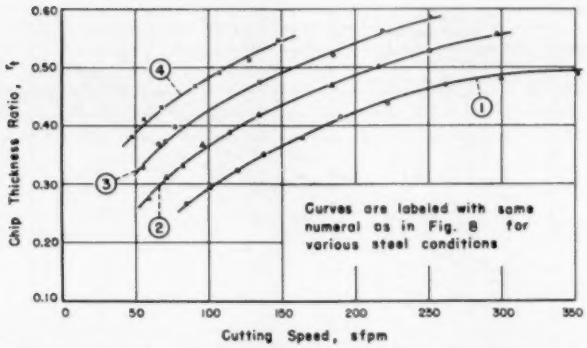

FIG. 9 EFFECT OF CUTTING SPEED ON CHIP-THICKNESS RATIO FOR QUENCHED AND TEMPERED STEEL

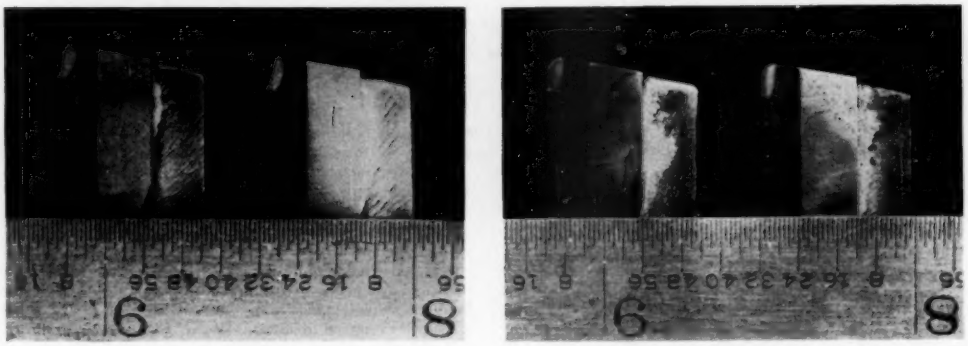

Magnification: × 2.28
Work material hardness: 283 Bhn

311 Bhn

Magnification: × 2.20
352 Bhn

401 Bhn

Work material: NE9445 steel, quenched and tempered
Tool material: Triple carbide
Tool shape: 0-4-7-7-8-0-3/64
Depth of cut: 0.102 in.
Feed: 0.0098 in. per rev
Cutting speed: 121 sfpm

FIG. 10 EFFECT OF HEAT-TREATMENT OF WORK MATERIAL ON TOOL-CHIP CONTACT AREA AT CONSTANT CUTTING SPEED

TABLE 2 EFFECT OF STEEL HARDNESS UPON CUTTING PHENOMENA AT CONSTANT CUTTING SPEED

Tool material: Triple carbide — Feed: 0.0098 ipr
Tool shape: 0-4-7-7-8-0-3/64 — Depth of cut: 0.102 in.
Cutting speed: 121 sfpm

Steel condition	Tool-chip contact area, $in.^2 \times 10^{-3}$	Relative area per cent	Cutting forces, lb F_c	lb F_t	Unit sliding stress, psi	Coeff. of friction	Interface temperature, deg F
Mill-annealed, 183 Bhn	7.97	100.0	448	293	40,700	0.76	1070
Q & T, 283 Bhn	6.34	79.6	456	258	45,650	0.66	1118
Q & T, 311 Bhn	5.76	72.3	440	238	46,650	0.64	1170
Q & T, 352 Bhn	5.25	65.9	427	221	47,700	0.61	1197
Q & T, 401 Bhn	4.82	60.4	418	212	50,000	0.60	1220

Referring to Fig. 12, it is seen that the unit frictional force increases with an increase in workpiece hardness. This so-called sliding or shearing stress appears to have nearly a linear relationship with work-material hardness. Even though the thrust force F_t (the principal factor in the frictional force for small rake angles) is reduced with harder materials, the unit sliding stress increases since the contact area is reduced at a greater rate.

It is evident that, in addition to workpiece hardness, there are other interrelated variables in the tests under discussion. These include interface temperature and chip sliding velocity, V_f. The relative effect of these variables upon the coefficient of friction may be studied by comparing all of the work materials at several constant interface temperatures.

The results for temperatures of 1100, 1200, and 1300 F are shown in Table 3. It is seen that the coefficient of friction decreases with increase in workpiece hardness. This is shown in

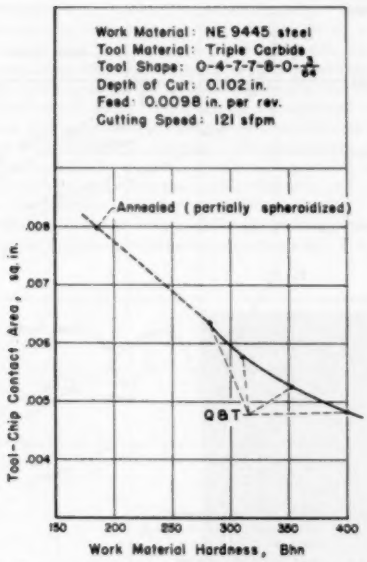

FIG. 11 EFFECT OF WORK-MATERIAL HARDNESS UPON TOOL-CHIP CONTACT AREA

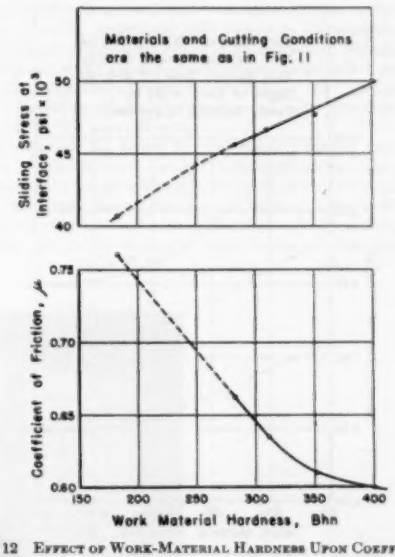

FIG. 12 EFFECT OF WORK-MATERIAL HARDNESS UPON COEFFICIENT OF FRICTION AND SLIDING STRESS AT CONSTANT CUTTING SPEED

TABLE 3 EFFECT OF STEEL HARDNESS UPON CUTTING PHENOMENA AT CONSTANT INTERFACE TEMPERATURE

Tool material: Triple carbide Feed: 0.0098 ipr
Tool shape: 0-4-7-7-8-0-3/64 Depth of cut: 0.102 in.

Steel condition	Tool-chip interface temperature: 1100 F			1200 F			1300 F		
	Corresponding, sfpm	Chip vel., fpm	Coeff. of frict.	Corresponding, sfpm	Chip vel., fpm	Coeff. of frict.	Corresponding, sfpm	Chip vel., fpm	Coeff. of frict.
Mill-annealed, 183 Bhn	138	38.6	0.74	207	68.3	0.67	303	113.6	0.60
Q & T, 283 Bhn	111	34.2	0.67	171	67.1	0.63	252	117.0	0.56
Q & T, 311 Bhn	88	30.2	0.66	137	57.3	0.62	207	102.0	0.56
Q & T, 352 Bhn	78	30.1	0.65	122	55.8	0.61	182	95.5	0.55
Q & T, 401 Bhn	67	28.6	0.65	106	52.2	0.61	162	90.3	0.55

Fig. 13 at the indicated constant interface temperatures. It is noted that the coefficient of friction is nearly constant for the two harder steels and that there is relatively little change for any of the quenched and tempered steels. The difference between the coefficient of friction for the annealed steel and that quenched and tempered to 283 Bhn is from $2^1/_2$ to 3 times as much as the difference between the 283 Bhn and 401 Bhn steels. The effect of interface temperature upon the coefficient of friction is clearly evident in Fig. 13. There seems to be little doubt but that the interface temperature is a major factor influencing the coefficient of friction for a particular tool-workpiece combination.

Further examination of the data in Table 3 reveals that chip velocity has little effect upon the coefficient of friction of the quenched and tempered steels (the annealed steel is excluded since the structure is different), provided the tool-chip interface temperature is constant. At a constant interface temperature the variation in the coefficient of friction is between the approximate limits of $2^1/_2$ and 3 per cent whereas the corresponding variation in chip velocity is from approximately 20 to 30 per cent. The respective variation in cutting speed (the commonly measured quantity) is from 45 to 60 per cent. Apparently, chip velocity has little effect upon the coefficient of friction.

The results for these quenched and tempered steels present a useful idea of the effect of heat-treatment of work materials upon cutting phenomena. However, it must be recognized that such heat-treatment has a definite effect on the so-called machining constant C. An increase in steel hardness raises the value of C, the variation of which has been found to be from 11 to 18 per cent for the range of quenched and tempered steels in this investigation. The change in C has not been isolated in the present analysis though further work is in progress.

On Annealed Steel Using Tungsten-Carbide and Triple-Carbide Tools

Cutting temperature and chip views for annealed NE9445 steel using tungsten-carbide and triple-carbide tools at various speeds have been reported by one of the authors (5). Under identical cutting conditions, lower temperatures result with tungsten-carbide tools which exhibit a greater tendency to adhesion of the chip and, consequently, a rough chip surface. Cutting-force, chip-thickness ratio, and cutting-speed relationships were determined in this series of tests and the results are shown plotted in Figs. 14 and 15.

With reference to these figures it is noted that for cutting speeds below approximately 200 sfpm, there are no appreciable differences in the cutting forces or chip thickness using the two tools. However, at higher speeds there are abrupt changes in both the forces and chip thickness obtained with the tungsten-

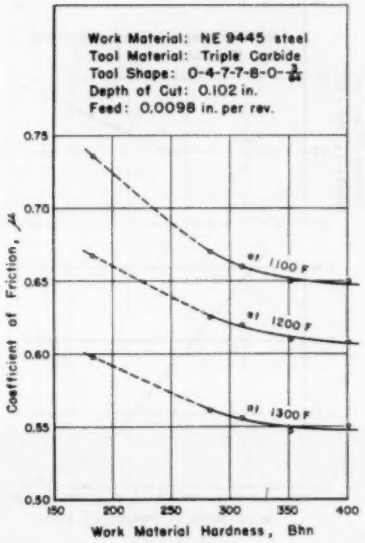

FIG. 13 EFFECT OF WORK-MATERIAL HARDNESS UPON COEFFICIENT OF FRICTION AT CONSTANT INTERFACE TEMPERATURES

carbide tools. F_c and particularly F_t increase abruptly as the cutting speed is increased to about 250 sfpm. Further increase in speed results in decreased cutting forces though the trend may be complicated by tool-cratering which becomes evident at about 325 sfpm. For tungsten-carbide tools the cutting force F_c is some 12 to 17 per cent higher, and the thrust force F_t is in the range of 30 to 35 per cent higher for speeds of 250 to 400 sfpm.

The abrupt change in the cutting forces appears to be due to some aspect of the friction phenomenon of the sliding contact at high temperature and contact stress. The basic factor is thought to be the tendency to adhesion of the chip and the tool. The adhesion temperature is the temperature of incipient welding-on of the chip and the tool. If, at the points of contact of the chip and the tool, the temperature is sufficient to cause "welding," and if the time of contact is sufficient to permit it, this phenomenon would have an effect upon the cutting forces.

Dawihl (6) has reported on the adhesion temperatures for various combinations of tool materials and steels of different physical properties. It has been found that the adhesion temperature for cemented-carbide tools depends upon the amount of cobalt up to 5 per cent, and thereafter is independent of the amount at least up to 20 per cent. Dawihl also found that the adhesion temperature for a given tool-work combination increases as the hardness and strength of the steel become greater. Some of his results are shown in Table 4.

TABLE 4 RESULTS OF DAWIHL'S TESTS

Cemented-carbide composition	Adhesion temperature, deg F — Steel, 85,400 psi tensile strength	Steel, 156,500 psi tensile strength
WC with 5 per cent cobalt	1155	1380
WC with 15 per cent TiC + 5 per cent cobalt	1425	1560

The tungsten-carbide tool used in this investigation had a nominal cobalt content of 6 per cent and the annealed steel a tensile strength of 90,000 psi. The tool-work conditions are therefore substantially the same as those in Dawihl's tests on tungsten-carbide tools.

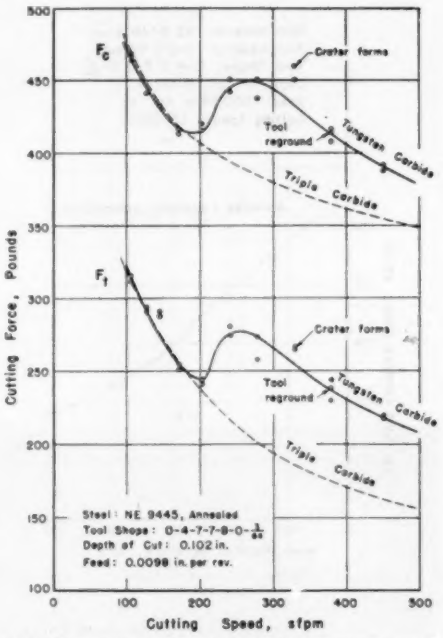

FIG. 14 CUTTING SPEED-CUTTING FORCE RELATIONSHIPS FOR DIFFERENT TOOL MATERIALS

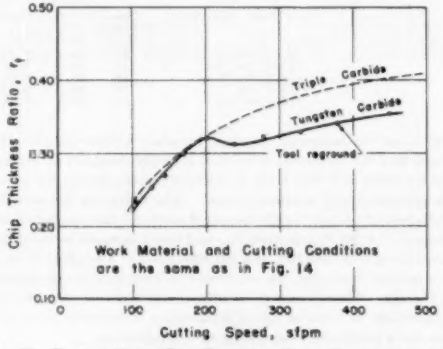
Chip Thickness Ratio, r_c
Triple Carbide
Tungsten Carbide
Tool reground
Work Material and Cutting Conditions are the same as in Fig. 14
Cutting Speed, sfpm

FIG. 15 CUTTING SPEED-CHIP THICKNESS RATIO RELATIONSHIP FOR DIFFERENT TOOL MATERIALS

It is noted in Fig. 14 that the force curves for the tungsten-carbide tool change abruptly between successive tests at 200 and 240 sfpm and that they peak at about 250 sfpm. The respective interface temperatures are 1112 F, 1170 F, and 1180 F (5), or within a few degrees of the adhesion temperature reported by Dawihl for similar tool-work materials. In these tests, however, there is relative motion between the chip and the tool

whereas Dawihl's values were determined statically. If the time for adhesion to occur is short (and it is thought to be), it seems that Dawihl's data may be applied with reasonable assurance. Coincidentally or otherwise, it appears as if the abrupt change in the force curves is due to the adhesion of the chip and the tool. Further increases in speed bring about the characteristic decrease in cutting forces, though the data revealed considerable scatter and some variation due to cratering. The same abrupt changes were observed with the tungsten-carbide tool in cutting tests on NE9445 quenched and tempered to 352 Bhn and on two mill-annealed 8640 steels, one of which was sulphite-treated.

The triple-carbide tool used in this study contained tantalum and titanium carbides in addition to tungsten carbide and cobalt. It was different from the tungsten carbide - titanium carbide tool used by Dawihl, particularly with respect to the tantalum, and the adhesion temperature is thought to be higher. The interface temperature at the maximum cutting speed was 1445 F and apparently below the adhesion temperature of the triple-carbide tool. No discontinuities were observed with the triple-carbide tool in this series of tests.

Even though the forces for the tungsten-carbide tool were higher, above 200 sfpm, the interface temperatures were lower. The answer to this paradox again lies in the effect of tool material upon the contact area of the chip and the tool. Fig. 16 shows a series of views of the tool-chip contact area on both the tungsten-carbide and the triple-carbide tools taken at three different

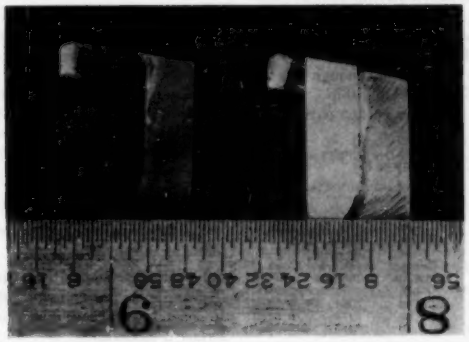

Tungsten carbide Triple carbide
Tool-chip
Contact area 12.16×10^{-3} in.^{2} 8.12×10^{-3} in.^{2}
Magnification: × 2.22
Cutting speed: 118 sfpm

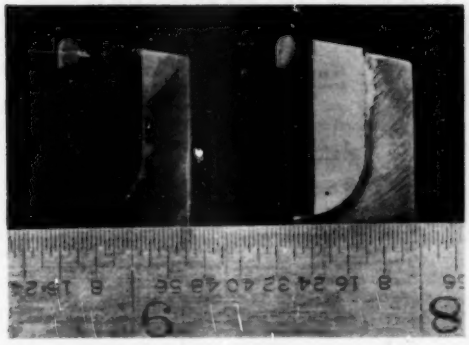

Tungsten carbide Triple carbide
Tool-chip
Contact area 8.85×10^{-3} in.^{2} 6.22×10^{-3} in.^{2}
Magnification: × 2.14
Cutting speed: 276 sfpm

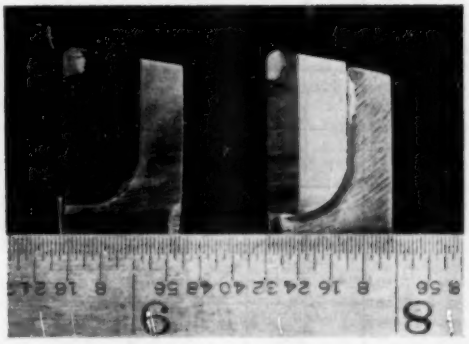

Tungsten carbide Triple carbide
7.83×10^{-3} in.^{2} 5.26×10^{-3} in.^{2}
Magnification: × 1.95
Cutting speed: 413 sfpm

Work material: NE9445 steel, mill-annealed
Tool shape: 0-4-7-7-8-0-3/64
Depth of cut: 0.102 in.
Feed: 0.0098 in. per rev

FIG. 16 EFFECT OF TOOL MATERIAL ON TOOL-CHIP CONTACT AREA

speeds. The propensity to adhesion of the steel chip on the tungsten-carbide tool is evident from these pictures. It is this adhesion which causes the early formation of crater and thereby premature tool failure of the tungsten-carbide tools when used for cutting steel. For all three speeds tested, the contact area on the tungsten-carbide tool is about 40 to 50 per cent larger than that observed on the triple-carbide tools under the same cutting conditions.

The cutting characteristics of the two tools are listed in Table 5. The coefficient of friction for the tungsten-carbide tool is higher in all tests though the difference is small at the lowest cutting speed. Of particular interest is the lower interface temperatures observed with tungsten-carbide tools, especially in view of the higher forces and friction. The relationship of contact area to interface temperature is shown in Fig. 17 for the three speeds in this series of tests. The triple-carbide tools exhibited no built-up edge for any of the three speeds, and it is evident that a higher tool-chip interface temperature is associated with a lower contact area. The same general trend is shown for the tungsten-carbide tools; part of the curve is shown broken since not enough data are available to show an accurate trace of the relationship. It is expected that the trend will follow the same abrupt pattern observed in forces and chip thicknesses. The test at the lowest speed resulted in a distinct built-up edge which probably affected the contact area.

TABLE 5 EFFECT OF TOOL TYPE UPON CUTTING PHENOMENA AT SEVERAL SPEEDS

Work material: NE9445 steel, mill-annealed, 183 Bhn — Depth of cut: 0.102 in. Feed: 0.0098 ipr

Tool shape: 0-4-7-7-8-0-3/64

	—Tungsten-carbide tools—			—Triple-carbide tools—		
Cutting speed, sfpm	Contact area, in.^{2} × 10^{-3}	Tool-chip interface temp, deg F	Coeff. of friction	Contact area, in.^{2} × 10^{-3}	Tool-chip interface temp, deg F	Coeff. of friction
118	12.17	995[a]	0.77	8.12	1064	0.76
276	8.85	1205	0.71	6.22	1273	0.63
413	7.83	1322	0.66	5.26	1387	0.55

[a] Depends upon built-up edge; the more pronounced it is the lower the indicated temperature.

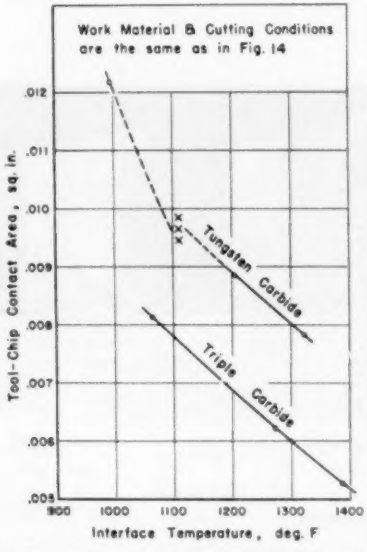

FIG. 17 RELATIONSHIP OF INTERFACE TEMPERATURE TO CONTACT AREA FOR DIFFERENT TOOL MATERIALS

It has been suggested that the main cause of the lower tool-chip interface temperatures with tungsten-carbide tools is the higher thermal conductivity (nearly twice that of the triple-carbide used) of such tools. There is little question but that the higher conductivity has some effect similar to the case of orthogonal cutting as compared to conventional turning in the matter of the greater heat-dissipating capacity of the former. However, from this investigation it is evident that the principal cause is more likely the much larger contact area observed with the tungsten-carbide tool. Examination of Fig. 16 or Table 5 will confirm this contention

SUMMARY

This analysis of several factors in metal cutting suggests a chart to visualize the effects of changes in tool shape, workpiece hardness, and tool material on cutting phenomena. The schematic diagrams in Figs. 18, 19, and 20, respectively, are presented for each set of conditions discussed in this paper. All are compared on the basis of equal cutting speed, feed, and depth of cut. In the charts the heavy lines show principal relationships, light lines show secondary relationships, and dotted lines indicate probable relationships.

CONCLUSIONS

The following conclusions are based upon conditions within the limits of this investigation.

1 Cutting temperature, through its influence on interface friction, is the major factor affecting metal-cutting phenomena. In general, coefficient of friction decreases with an increase in interface temperature.

2 Cutting speed has little effect per se upon the coefficient of friction. Its principal influence is on the rate of heat generation and, therefore, the tool-chip interface temperature.

3 The tool-chip contact area is an important factor influencing interface temperatures. A decrease in contact area is associated with an increase in interface temperature.

4 The tool-chip contact area decreases with an increase in cutting speed. With cutting speed the only variable there is a linear relationship between tool-chip contact area and chip thick-

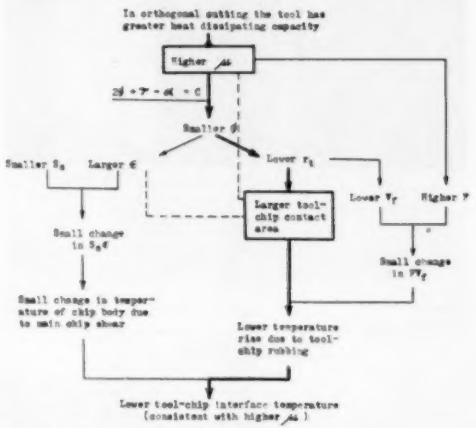

FIG. 18 CONVENTIONAL TURNING VERSUS ORTHOGONAL CUTTING

ness ratio. The thicker the chip (lower chip-thickness ratio), the greater the contact area.

5 The tool-chip contact area is larger in orthogonal cutting than in conventional turning at constant cutting speed. The basic cause is the greater heat-dissipating capacity of the tool under orthogonal cutting conditions.

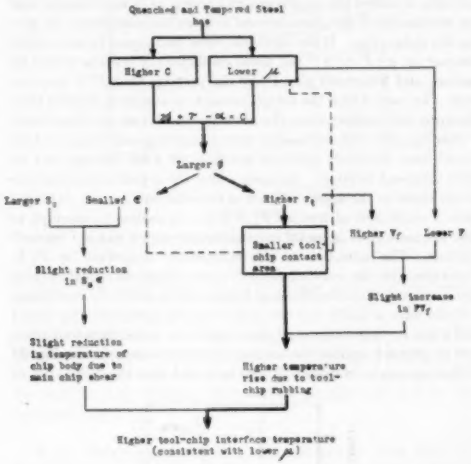

FIG. 19 ANNEALED STEEL VERSUS QUENCHED AND TEMPERED STEEL

6 An increase in workpiece hardness results in a slight decrease in cutting forces with other cutting conditions constant.

7 At constant cutting speed the tool-chip contact area decreases as the workpiece hardness is increased. This is due to a lower coefficient of friction and a higher value of the machining constant, both of which are associated with harder work materials. The interface temperature is higher because the heat is concentrated on less tool area.

8 When used for cutting steel, tungsten-carbide tools show abrupt changes in cutting forces and chip-thickness ratios. The cause is thought to be due to tool-chip adhesion.

9 Similarly, when cutting steel, tungsten-carbide tools cause higher cutting forces, higher coefficient of friction, larger tool-chip contact area, and lower interface temperatures than triple-carbide tools under otherwise constant cutting conditions.

BIBLIOGRAPHY

1 "Basic Mechanics of the Metal-Cutting Process," by M. E. Merchant, *Journal of Applied Mechanics*, Trans. ASME, vol. 66, 1944, p. A-168.

2 "The Mechanism of Static Friction," by M. E. Merchant, *Journal of Applied Physics*, vol. 11, 1940, p. 230.

3 "Surface Friction of Clean Metals—A Basic Factor in the Metal Cutting Process," by H. Ernst and M. E. Merchant, Proceedings of the Special Summer Conference on Friction and Surface Finish, M.I.T., Cambridge, Mass., June, 1940.

4 "An Analytical Evaluation of Metal-Cutting Temperatures," by K. J. Trigger and B. T. Chao; Paper No. 50—SA-1, presented at the Semi-Annual Meeting, St. Louis, Mo., June 19–23, 1950, of THE AMERICAN SOCIETY OF MECHANICAL ENGINEERS.

5 "Progress Report No. 2 on Tool-Chip Interface Temperatures," by K. J. Trigger, Trans. ASME, vol. 71, 1949, pp. 163–174.

6 "Investigation of the Process in the Wear of Cemented Carbide Tools," by Walter Dawihl, *Zeitschrift für Technische Physik*, vol. 21, 1940, pp. 337–345.

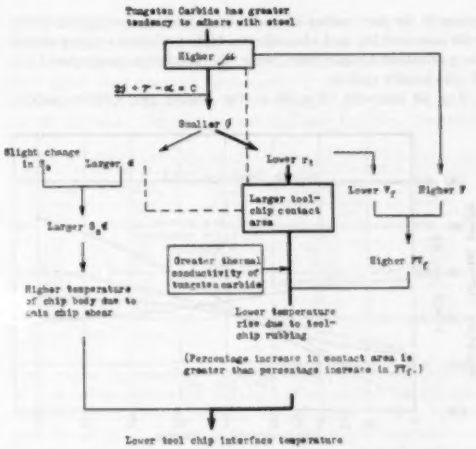
Tungsten Carbide has greater tendency to adhere with steel
Higher
Smaller ϕ
Slight change in
Larger
Lower
Larger tool-chip contact area
Lower
Higher
Larger
Greater thermal conductivity of tungsten carbide
Higher
Higher temperature of chip body due to main chip shear
Lower temperature rise due to tool-chip rubbing
(Percentage increase in contact area is greater than percentage increase in
Lower tool chip interface temperature

FIG. 20 TRIPLE-CARBIDE VERSUS TUNGSTEN CARBIDE

Discussion

W. W. GILBERT.[6] In the comparison of orthogonal cutting and conventional turning, it is stated that the main reason for the lower cutting temperature with orthogonal cutting is that the tool has a greater capacity to conduct the interface heat away from where it is generated. It should be pointed out, however, that in conventional turning the end cutting edge is also active, whereas in orthogonal cutting, only the side cutting edge is active. The additional length of the active end cutting edge amounts to an increase of at least 10 per cent. The temperatures for conventional turning are stated as approximately 10 per cent higher than for orthogonal cutting, as shown in Fig. 1 of the paper. This is probably due to the added heat from the end cutting-edge angle. Undoubtedly, the ability of the tool to conduct the heat away from the interface has some influence in reducing the temperature.

The section of the paper, "The Role of Tool-Chip Contact Area in Cutting Temperature," shows why the machinability, as measured by a tool-force dynamometer, will not always agree with the machinability of a material, measured by temperatures or tool life. Figs. 7 and 8 show clearly that the cutting force F_c, may be lower for harder materials, but the cutting temperature is higher due to the smaller chip contact area and higher unit stress upon this area. It would be desirable if the authors could continue this work to show the tool life at the various hardnesses of the material cut. There undoubtedly would be a much better correlation between tool life and cutting temperatures than between tool life and cutting force.

The writer has made a similar comparison of cutting forces, temperature, and tool life.[7] In the tests reported, a 0.61 per cent carbon steel was cut with high-speed-steel tools, but many of the results were similar to the values obtained by the present authors when using sintered carbide to cut NE9445 steel. Fig. 21 herewith (Fig. 15 in the Boston and Gilbert paper,[7]) shows that an in-

[6] Professor, Metal Processing Department, University of Michigan, Ann Arbor, Mich. Mem. ASME.

[7] "Relations Between Cutting Force, Temperatures, and Tool Life in Cutting Steel With Single-Point Tools," by O. W. Boston and W. W. Gilbert, presented at the Annual Meeting, New York, N. Y., December 5, 1934, of THE AMERICAN SOCIETY OF MECHANICAL ENGINEERS.

crease in the nose radius allowed higher relative cutting speeds for a 60-min tool life and also allowed higher relative cutting speeds for a constant temperature, while the maximum tangential force F_t was hardly varied.

Fig. 22 herewith (Fig. 25 in the Boston and Gilbert paper[7])

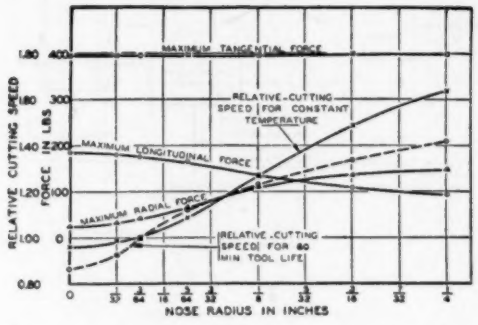
MAXIMUM TANGENTIAL FORCE
RELATIVE-CUTTING SPEED FOR CONSTANT TEMPERATURE
MAXIMUM LONGITUDINAL FORCE
MAXIMUM RADIAL FORCE
RELATIVE CUTTING SPEED FOR 60 MIN TOOL LIFE
RELATIVE CUTTING SPEED
FORCE IN LBS
NOSE RADIUS IN INCHES

FIG. 21 FORCES, LIFE, AND TEMPERATURE FOR VARYING NOSE RADII

(Turning 0.61 per cent C, 207 Bhn steel with high-speed-steel tool of the shape 8, 14, 6, 6, 6, 0, var R. Depth 0.100 in.; feed 0.0125 ipr cutting dry.)

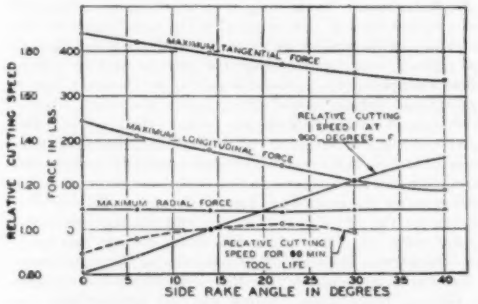
MAXIMUM TANGENTIAL FORCE
MAXIMUM LONGITUDINAL FORCE
RELATIVE CUTTING SPEED AT 900 DEGREES F
MAXIMUM RADIAL FORCE
RELATIVE CUTTING SPEED FOR 60 MIN TOOL LIFE
RELATIVE CUTTING SPEED
FORCE IN LBS
SIDE RAKE ANGLE IN DEGREES

FIG. 22 FORCES, LIFE, AND TEMPERATURE FOR VARYING SIDE RAKE ANGLES

(Tool shape 8—var S R—6, 6, 6, 0, 3/64. Other conditions same as Fig. 21.)

showed that increasing the side rake angle to an optimum value of approximately 22 deg gave the longest tool life, whereas the cutting temperature was progressively decreased up to 40 deg side rake angle. The combination of the decreasing tangential force together with an increasing chip contact area would account for the relative decrease in cutting temperature or the relative increase in cutting speed at 900 F. However, the decrease in tool life for angles larger than 22 deg must be accounted for by the difference in the stress concentration at the chip-interface area. At higher rake angles, the load was concentrated closer to the cutting edge and caused accelerated wear on the cutting edge and on the flank under the cutting edge.

This paper shows clearly the importance of cutting temperature, and its correlation with cutting forces and chip thickness ratios. The authors have nicely pointed out the relationship between coefficient of friction, contact area, sliding stress, and the interface temperature. They are to be commended on their worthy addition to metal-cutting science, and it is hoped they will extend their work in the future.

R. S. HAHN.[8] There are several interesting features about the data which the authors did not bring out. Before mentioning these features, however, let us consider the coefficient of friction.

In general, for two bodies pressed together, it is found that the frictional force is "proportional" to the normal load and independent of the apparent contact area. The constant of proportionality is called the coefficient of friction as is well known, and the mechanics of the phenomenon is described completely by giving the value of μ. If the frictional force had varied in some other manner (e. g., $F \sim N^2$) the usual coefficient of friction would be useless, and we would give F/N^2 the prestige that F/N now enjoys. In cases where the actual contact area is much smaller than the apparent contact area, the actual contact area increases more or less linearly with increasing normal loading and thus the frictional force increases more or less linearly with loading, and we have Coulomb friction. In cases where the actual contact area is about equal to the apparent area as in metal cutting, we no longer have a coefficient of friction F/N and it is useless to attempt to give the ratio F/N in metal cutting the prestige it has in Coulomb friction. The situation is not completely described by F/N. Consequently, the coefficient of friction should be omitted from metal-cutting considerations as being useless and only confusing.

If the data in Table 1 of the paper for orthogonal cutting is used and if the average tangential shearing stress at the chip-tool interface be plotted against the average interface temperature, Fig. 23 of this discussion results. It will be noted that the falling off of

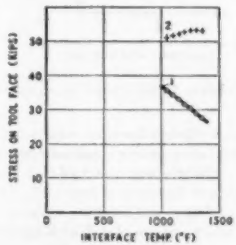

FIG. 23 AVERAGE FRICTIONAL SHEARING STRESS AND NORMAL STRESS AT TOOL-CHIP INTERFACE VERSUS AVERAGE INTERFACE TEMPERATURE

(Curve 1, frictional shearing stress. Curve 2, normal stress.)

stress with temperature lies more or less in a range that is usual for steel, and suggests that the frictional force is caused by shearing of a more or less continuous bond between chip and tool, perhaps on an atomic scale of an alloy formed between tool and chip. The normal stress at the chip-tool interface is also shown and to a first approximation is constant.

It might be suspected that the tool-chip shearing stress is being influenced by changes occurring on the shear plane as the speed is increased. Fig. 24, herewith, shows shear stress, and normal stress on the shear plane plotted against speed. In addition, the temperature on the shear plane has been calculated,[9] and it is seen that both stress and average temperature remain essentially constant as the speed is increased. It might seem incorrect for the temperature to remain constant with increasing speed but it should be remembered that, as the speeds were increased, the shear angle ϕ increased, which has a "quenching effect" on shear-plane temperatures, i. e., the steeper the shear plane the more it is quenched by the oncoming cold metal. Furthermore,

[8] Research Engineer, The Heald Machine Company, Worcester, Mass. Mem. ASME.

[9] "On the Temperature Developed at the Shear Plane in the Metal-Cutting Process," by R. S. Hahn (to be published).

it is shown[9] that a definite ceiling exists above which the temperature will not rise no matter how high the speed is raised.

In view of the foregoing it appears that the falling off of the tool-chip shear stress is associated with increasing tool-chip temperatures and is not caused by changes occurring on the shear plane. Furthermore, the frictional shearing stress acting over a known area appears to be of more fundamental importance than the coefficient of friction, which has no prestige unless F is "proportional" to N.

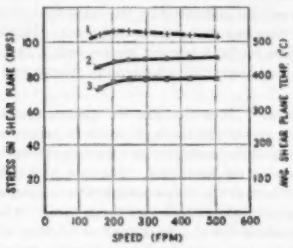

FIG. 24 SHEAR PLANE STRESSES AND TEMPERATURE VERSUS CUTTING SPEED

(Curve 1, normal stress on shear plane versus speed. Curve 2, shear stress on shear plane versus speed. Curve 3, average shear-plane temperature versus speed.)

M. E. MERCHANT[10] AND E. J. KRABACHER.[11] The quality of the research described in the present paper is reflected in the high degree of precision and reproducibility in the experimental results recorded there; such precision is not easily attained in metal-cutting tests.

The authors clearly demonstrate the importance of the tool-chip contact area in influencing cutting temperatures and related quantities. However, as a result, the reader is led to wonder what factors control the size of that contact area. While additional theoretical work remains to be done, a few facts regarding this problem can be stated at this time.

It should be pointed out that the tool-chip contact area referred to by the authors is an apparent contact area only, since the tool and chip are never in contact over 100 per cent of this area at any one instant. The microscopic areas of actual contact between chip and tool are more or less uniformly distributed over this apparent contact area and are constantly shifting as the chip slides on the tool face. The size of the area of "apparent" contact is determined essentially by the "elastic" deformation of the curved chip surface and the flat tool face as they are pressed together under load. The magnitude of the area of "actual" contact is determined essentially by the local "plastic" deformation of the chip surface at the contacting high spots on the tool-chip interface. Details regarding this latter fact are given in references (2) and (3) in the Bibliography cited by the authors. However, the main idea involved is that the area of actual contact is equal to the normal force on the tool face (N) divided by the hardness of the chip metal (expressed as mean pressure or "Meyer" hardness, which is approximately equal to Brinell hardness).

As yet the details of the mathematical relationships determining the area of apparent contact (elastic contact) have not been worked out. It is known, though, that this area depends on the normal force (N) and the radius of curl of the chip. This suggests, therefore, that the area of apparent contact may be, roughly, proportional to the area of actual contact, or, in other words, that the apparent contact pressure may be approximately a constant for a given work material, dependent only on the work-material hardness. This supposition is borne out by the data presented by the authors. The last column of Table 6 of this discussion

TABLE 6 APPARENT CONTACT PRESSURE AT TOOL-CHIP INTERFACE FROM DATA OF TABLE 1[a] ORTHOGONAL CUTTING

Cutting speed, fpm	Cutting force, F_c, lb	Thrust force, F_t, lb	Tool-chip contact area, in^2 × 10^3	Apparent contact pressure, psi
166	411	286	8.05	48500
204	398	264	7.70	49200
249	384	242	7.32	50100
298	371	222	7.02	50500
380	358	203	6.75	50800
428	347	188	6.50	51200
504	338	176	6.35	51200

[a] From authors' paper.

gives values for apparent contact pressure, calculated from the data on orthogonal cutting of Table 1 of the paper, by dividing the normal force N by the tool-chip contact area. It may be seen that the apparent contact pressure is essentially constant over the range of force and contact-area values observed under the given test conditions. Since the apparent contact pressure for these conditions is about 50,000 psi and the mean pressure hardness[12] of the work material is 193 kg per mm^2 (274,000 psi), it may be concluded that the apparent contact area is, roughly, 6 times as great as the actual contact area. Fig. 25, herewith, illustrates the effect of workpiece hardness on the apparent contact pressure; the plotted values of contact pressure were calculated from the data of Table 2 of the paper.

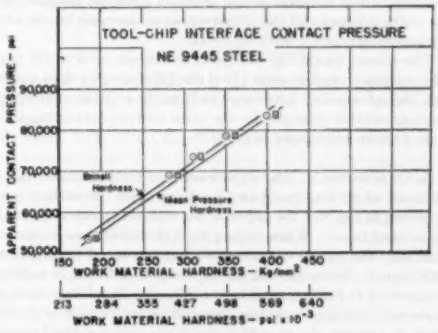

FIG. 25

It can be seen that the apparent contact pressure is, roughly, proportional to the work-material hardness over the range of hardnesses investigated by the authors. The apparent contact pressure remains roughly 1/6 the mean pressure hardness throughout, so that again it may be concluded that, under these test conditions, the apparent contact area is, roughly, 6 times the actual. It appears likely, then, that the foregoing rough rule of thumb (i.e., that the apparent contact pressure is, roughly, a constant for a given work material) may prove to be satisfactory for use in making quick approximate estimates of (apparent) tool-chip contact areas for use in interface temperature calculations and related studies.

Further data are needed, however, to determine the degree of

[9] Research Physicist, Research Department, The Cincinnati Milling Machine Company, Cincinnati, Ohio. Mem. ASME.

[11] Research Engineer, Research Department, The Cincinnati, Milling Machine Company. Jun. ASME.

[12] Based on the hardness value of 183 Bhn given in the paper.

usefulness of this approximation. Meanwhile we recommend to the authors the desirability of working out the details of the quantitative relationships governing the elastic contact between chip and tool, so that exact calculations of tool-chip contact areas can eventually be made.

In general, the reader of this paper might get the impression that high chip friction is desirable because it increases the tool-chip contact area and therefore may reduce the tool-chip interface temperature. While it is true that in the three cases presented in the paper, an increase in chip friction did result in a decrease in interface temperature, this is not always the case. As may be seen from the charts given in Figs. 18, 19, and 20 of the paper, this will be the case only if the mechanisms associated with the tool-chip contact area, represented on the right-hand side of the diagrams, are predominant as they were here. In other cases the changes in FV_f and $S_s\epsilon$ may predominate. For example, the addition of "free machining" additives (such as sulphur and lead) to steel generally results in both lowered chip friction and lower interface temperature. The application of an effective cutting fluid lowers both chip-friction and interface temperature. Thus, although the examples given by the authors are instructive and useful, they should not be generalized.

The authors, in their first conclusion, express the conviction that cutting temperature is the major factor affecting metal-cutting phenomena. While the paper ably demonstrates the importance of cutting temperature, it should be borne in mind that at times other factors may overshadow this quantity in importance. This is particularly true with respect to tool life in metal cutting where, for a given interface temperature, large differences in tool life may occur, depending upon the severity of the abrasive action to which the tool is subjected by the chip and workpiece. The severity of this abrasive action depends upon the magnitudes of the cutting forces and the abrasiveness of the constituents of the microstructure of the work material.

The writers would like to correct one minor error in the paper. The reference cited as item (1) of the Bibliography does not contain the information attributed to it in the context of the paper. A more suitable reference by the same author, containing the required information, may be cited.[13]

A. O. Schmidt.[14] Our experience and tests indicate that the influence of cutting speed and hardness upon the cutting forces, as shown in Fig. 8 of the paper, is not representative of the majority of conditions. When milling steel, the tool forces remain substantially the same even when the cutting speed is extended to 1200 fpm.[15] However, one factor which is different in milling in comparison to turning must be considered. In milling, the tool is in contact with the workpiece material for only a part of the time, while, in turning, the nascent metal of the chip is pressed continuously against the tool point and, as can be observed readily, frequently causes the chip to weld to the tool tip and thus change the cutting forces. Cooling and oxidizing of the milling-cutter-tooth surface, while it is intermittently exposed to the air, provides a coating which probably serves to counteract some welding tendencies between chip and tool. That the authors have listed the composition of the tool used in determining the cutting forces given in Fig. 8, will be of value for comparison of results in future investigations. It may be that under certain conditions the interaction of the tool and workpiece material, due to their specific composition, could cause a decrease of cutting forces at higher cutting speeds.

The values of cutting forces in Table 2 of the paper for the same workpiece material of about 300 and 400 Bhn, instead of 183 Bhn, may also have been influenced by the same kind of welding action between the chip material and the tool point. Harder steel workpiece materials in the foregoing ranges entail, in general, somewhat higher tool forces and considerably shorter tool life.[16]

M. C. Shaw.[17] It is the writer's opinion that the data presented in this and in the authors' previous papers on the subject represent some of the most precise experimental cutting data that are to be found in the literature. The new idea that is put forth in this paper is that the chip-tool interface area plays the major role in the generation of tool-face temperature, which in turn is mainly responsible for the coefficient of friction which obtains. Velocity is held to play a secondary role in the process. The fact that temperature has an insignificant effect upon friction in the case of one body sliding over another[18] has led the writer to seek other interpretations which are not at variance with fundamental experiments. An alternative explanation of the authors' data will be presented, which also explains the unusually steep velocity-force curves obtained, the observed effect of specimen hardness on temperatures and forces, and the discontinuity shown in Figs. 14 and 15 of the paper.

In experiments performed in the Metal Cutting Research Laboratory at M.I.T. it has been found that carbide tools operate with unusually high friction at low speeds when cutting steel and, in fact, have inferior tool life to high-speed-steel tools at speeds below about 50 fpm. It has also been found difficult to obtain data at low speeds without a large built-up edge being present and, in this connection, it is of interest to note that the authors report a visible built-up edge at a cutting speed of 118 fpm in Table 5. The large built-up edge which is present at low speeds is believed to be associated with the observed poor low-speed tool life of carbides.[19] In the following discussion it will be shown that the data presented can be explained in terms of a built-up edge which decreases in size with increased speed.

The principal forces (horizontal and vertical components), which act upon a metal-cutting tool when cutting a given metal, are influenced by two main considerations; these are the coefficient of friction between the chip and the tool and the geometry of the process. The rake angle is the chief item which controls the geometry. If the rake angle is large, the shear angle in general will be large, and the strain in the chip correspondingly small. The decreased strain in the chip results in a reduced shear stress on the shear plane, and the increased shear angle results in a smaller shear area. Both of these effects cause a decrease in the cutting forces with increased rake angle. The coefficient of friction in turn generally has two components. In the absence of a built-up edge, the friction force is that required to shear the many minute junctions that are formed when the surface asperities of tool and chip adhere to each other. When a built-up edge is present, another important contribution to friction is that due to the plowing action on the tool face of small very hard pieces of

[13] "Mechanics of the Metal Cutting Process II. Plasticity Conditions in Orthogonal Cutting," by M. E. Merchant, *Journal of Applied Physics*, vol. 16, 1945, pp. 318–324.

[14] Research Engineer, Kearney & Trecker Corporation, Milwaukee, Wis. Mem. ASME.

[15] "An Investigation of Radial Rake Angles in Face Milling," by J. B. Armitage and A. O. Schmidt, Trans. ASME, vol. 66, 1944, pp. 633–643; *Western Metals*, vol. 3, July, 1945, pp. 11–16; August, 1945, pp. 9–13.

[16] "Influence of Steel Hardness in Face-Milling," by J. B. Armitage and A. O. Schmidt, Trans. ASME, vol. 71, 1949, pp. 413–419; *American Machinist*, vol. 93, February 10, 1949, pp. 98–99.

[17] Associate Professor of Mechanical Engineering, Massachusetts Institute of Technology, Cambridge, Mass. Mem. ASME.

[18] "The Friction and Lubrication of Solids," by F. P. Bowden and D. Tabor, Oxford-Clarendon Press, New York, N. Y., 1950.

[19] For an analysis of the types of wear which occur with carbide tools, see the writer's discussion of the paper, "Basic Factors in the Hot-Machining of Metals," by E. J. Krabacher and M. E. Merchant, in this issue of Transactions, pp. 761–776.

built-up edge, as they pass off periodically with the chip. In general, both the adhesion and plowing components of friction are operative, the plowing term being the dominant one when cutting with a large amount of built-up edge, while the adhesion term will be the most important when the built-up edge is small.

In addition to its influence upon friction on the tool face, a built-up edge also alters the geometry at the tool point. The characteristic shape of the built-up edge is such as to cause an increase in the effective rake angle, and even a small built-up edge will be effective in this connection. Thus a built-up edge has two opposing influences upon the cutting forces. Its presence will cause an increase in friction owing to the plowing action as portions of it escape, while at the same time the effective rake angle will be so altered as to produce a decrease in the cutting forces. When a large amount of built-up edge is involved in cutting (i.e., when cutting with carbides below about 50 fpm), the plowing effect will predominate whereas the effect on the rake angle will be most pronounced with a small built-up edge. As the cutting speed is increased, the tendency to form a built-up edge decreases. Thus, when cutting with a built-up edge, the cutting forces will be higher than normal (i. e., without a built-up edge) for slow cutting speeds (due to the friction effect being predominant) but lower than normal when the cutting speed is high (due to the rake-angle effect being predominant). It has been observed in the writer's laboratory that the rate of change of the principal cutting forces with cutting speed is much greater when a built-up edge is known to be present than when cutting is accomplished with a built-up edge that cannot be detected. The unusually steep slope[20] of the authors' curves of force versus speed, Fig. 2, suggest the presence of a built-up edge.

The sudden change in the force curves in Fig. 14 of the paper may also be explained in terms of the built-up edge. This change is observed to occur at a speed of about 250 fpm, where the built-up edge if present will be small; its main influence being associated with an increase in the effective rake angle. If the small built-up edge on the tungsten-carbide tool were to become unstable at about 250 fpm, its leaving would be accompanied by a decrease in the effective rake angle, but an increase in the principal forces, coefficient of friction, chip-tool area, and cutting temperature. However, if the built-up edge on the triple carbide continued to be stable at higher speeds, its characteristics would continue uninterrupted along the same curve. The foregoing explanation of Fig. 14 of the paper is directly opposite that of the authors in which they suggest an increased tendency toward adhesion between tungsten carbide and steel with increased speed (and hence temperature), rather than the decreased tendency that is in keeping with the general characteristics of a built-up edge.

It should be noted that the foregoing mechanism of cutting with a built-up edge is in agreement with the observed independence of the coefficient of friction of a slider with temperature. It would appear that the variation in the coefficient of friction with speed is mainly a matter of the variation in the plowing component of friction. The temperature is observed to increase with speed due mainly to the increased rate of dissipating energy with increased speed and despite the decreased coefficient of friction with speed. Thus the variation of the coefficient of friction does not appear to be due to an increased temperature but rather due to the extent of the built-up edge which in turn is primarily influenced by speed.

The results obtained for steels of varying hardness (Fig. 7, 8, and 9 of the paper), also may be explained in terms of a built-up edge. The cutting of steels of higher hardness involve lower forces since the adhesion component of friction is less for a harder metal. The decreased friction results in less strain (greater shear angle) which tends to affect the increased shear stress (which accompanies an increase in material hardness) corresponding to a given strain. There would be much less decrease in the cutting forces with hardness than that shown in Fig. 8 for a metal having a lower modulus of strain hardening than that for NE9445 steel. The increased temperature with material hardness appears to be due to the smaller contact area that exists when hard metals are cut, as the authors have indicated. This decreased area is really due to the decrease in the coefficient of friction which in turn causes an increased shear angle and hence a smaller area of contact. The effect of the decreased frictional energy with increased hardness is more than offset by the decrease in area over which this energy is dissipated, resulting in a net increase in cutting temperature.

In conclusion, it should be acknowledged that it is usually difficult to differentiate between cause and effect in any process that is as complex as metal cutting. However, the authors' data would seem to indicate that the cutting speed is an important variable, which controls the size of the built-up edge which in turn gives the observed variations in forces, tool temperature, and contact area as a result of two characteristics of the built-up edge which vary with speed. At low speeds, the resulting large built-up edge appears to contribute to the process primarily via the plowing friction component, whereas at high speeds the characteristically smaller and less easily detected built-up edge has its greatest effect in decreasing the effective rake angle. Tool-face area and temperature would appear to play secondary roles in the mechanism of cutting compared with the influence of cutting speed and the built-up edge. However, tool-face area and temperature will play primary roles with regard to tool life.

[20] Dr. A. O. Schmidt of the Kearney and Trecker Corporation, Milwaukee, Wis., has obtained velocity force curves with considerably less slope under conditions similar to those used by the authors.

Authors' Closure

The authors greatly appreciate the many helpful comments and thought-provoking suggestions brought up by the several discussers.

Professor Gilbert has suggested that the higher cutting temperatures encountered in conventional turning, as compared to orthogonal cutting under otherwise identical conditions, is due to the added length of active cutting edge. This suggestion is not valid and contrary to observed results. Several years ago, during the early stages of the authors' investigation on cutting temperatures, it was observed that a decrease in the nose radius from $^1/_{16}$ in. to $^1/_{64}$ in. caused an appreciable increase in indicated tool-chip-interface temperature.

The experimental results presented by Professor Gilbert likewise refute his suggestion. Fig. 21 of his discussion (Fig. 15 in the Boston and Gilbert paper),[7] shows that the relative cutting speed for a given constant cutting temperature increases with an increase in nose radius; that is, as the length of active cutting edge is increased, the cutting temperature is decreased (under otherwise constant cutting conditions).

The range of cutting speeds used in the series of investigations cited by Professor Gilbert was relatively low, being 8 to 85 sfpm. Under these conditions, our experience shows that the effect of built-up edge would be very significant. All the test results reported in the present paper were obtained with cemented-carbide tools operating at sufficiently high cutting speeds so that a type 2 chip was obtained. The desirability of an extension of the investigation to tool-life study has been considered, and it is hoped that work can be continued along that line before long.

The authors appreciate Mr. Hahn's constructive criticism with reference to the use of the term "coefficient of friction" in the conventional sense. The real significance of the term is expressed in

the breakdown into its components, namely, the frictional shearing stress or sliding stress and the normal stress. In both cases these should be qualified further as "apparent" stresses, since the actual and apparent contact areas are not the same although they may be in reasonably close agreement. For convenience in use, coefficient of friction has its advantages in predicting specific power consumption, surface finish, relative machinability, and so forth. It can be easily calculated from cutting-force dynamometer readings without resort to the determination of the contact area between the chip and the tool.

It should be pointed out that the simple relationship $\mu = F/N$ is written down merely by definition. It is not necessary to have a constant proportionality between F and N.

The decrease in the sliding stress with increase in interface temperatures, Fig. 23 of Mr. Hahn's discussion, does indeed suggest the possibility of a continuous bonding between the tool and the chip surface. Whether this takes the nature of an "alloy" or is in the realm of interatomic attraction is speculative. A slightly oxidized tool surface (steel-cutting grade of carbide containing titanium) causes a difference in tool-chip adhesion which manifests itself in reduced forces. It appears likely that the reaction is on an atomic scale under conditions quite different from that of ordinary boundary lubrication.

With cutting speed as the only variable, the bulk temperature of the chip decreases slightly with increasing speed for NE9445 steel, when a continuous chip with little or no built-up edge is produced (4). As Mr. Hahn correctly indicates, the falling off of the tool-chip shear stress is associated with increasing tool-chip temperature and is not caused by change occurring in the shear zone. The constancy of the dynamic shear stress at the shear plane has been discussed in more detail in another paper[21] by one of the authors.

Mr. Hahn's use of the term "quenching effect" of the oncoming steel is not clear. Apparently, reference is being made to cooling by heat flow from the shear zone to the uncut stock. If this is a correct interpretation, then low speeds with corresponding longer time for heat transfer, smaller shear angle ϕ and a longer shear zone permit more heat to flow to the uncut stock. An increase in cutting speed, increases ϕ, decreases both path of shear and time available for heat flow. As a consequence, the quenching effect at high speed with increased ϕ is much less than at low speed. The effect of cutting speed on surface temperature of the cut stock has been investigated thoroughly by Schmidt, Boston, and Gilbert.[22]

The authors are indebted to Dr. Merchant and Mr. Krabacher not only for their kind remarks, but also for the thought-provoking questions which they have raised.

That the actual contact area is less than the apparent contact area is not questioned here. The problem has been under study for some time, and it appears that the intensity of the contact stress varies from zero at the point of departure from the face of the tool to a maximum over a large part of the area, then decreases as the cutting edge is approached. This is perhaps most clearly shown in the extreme right view of Fig. 10 of the paper. The apparent contact stress, as shown in the right-hand column of Table 6, is caused by the thin surface layer of hot plastic material bearing on the tool surface. This plastic film at 1050 to 1350 F is supported by the bulk of the chip which has been heated to the range of 700 to 850 by main chip shear. It is the bulk hardness of the chip at these latter temperatures which is important in evaluating the actual contact area. However, the question concerning contact area cannot be answered completely at present. If it were true, as Dr. Merchant and Mr. Krabacher contend, that the apparent contact pressure depends only on the work-material hardness, things will be very much simplified. It has been observed that this apparent tool-chip contact stress can be modified to a significant extent by varying the chemical composition of the tool material alone. If one refers to Fig. 14 of the paper, it can be seen that at a cutting speed of 118 sfpm, little difference in the components of cutting force exists when the straight tungsten-carbide tool is substituted for the triple-carbide tool. At the same cutting speed, an appreciable change in the size of apparent contact area is observed as indicated in the top view of Fig. 16. This fact alone suggests that any quantitative relationship governing the area of apparent contact, without taking into consideration the "adhesion" behavior between the sliding chip material and the tool material, necessarily will be incomplete. The authors believe that this marks one of the basic differences between the nature of "elastic" or "plastic" contacts under dynamic as compared to static conditions.

The authors did not intend to imply that a high coefficient of friction was desirable because it increased—or was associated with—the large contact area. From the standpoint of tool life it might be definitely desirable to distribute the cutting force over greater area, with its associated higher friction, than to strive for reduced friction, a high chip-thickness ratio, and, consequently, reduced tool-chip contact area.

The authors agree with Dr. Merchant and Mr. Krabacher that, besides cutting temperature, tool life depends also on the severity of the abrasive action of the fast moving chip; on the magnitude of the cutting forces and the abrasiveness of the microconstituents of the work material, and the adhesion behavior between the tool and work material at elevated temperatures.

As noted in the presentation of the paper, the authors prefer to state that cutting temperature is a major factor affecting metal-cutting phenomena. Admittedly, at times, other factors may overshadow it in importance.

A possible explanation for the difference in the trend of cutting force with speed for milling and for turning is given by Dr. Schmidt. Much more work has to be done, however, before this complex milling operation which is "unsteady" can be better understood.

There was no evidence of any welding action, as shown by a built-up edge, in any of the tests reported in Table 2 of the paper. Using the annealed steel, 183 Bhn, as a datum, the cutting force decreased nearly 7 per cent, the thrust force decreased 28 per cent, while the contact area decreased 40 per cent, over the full range of hardness shown. Even though total forces decreased, the unit stresses both normal and frictional, are higher since the area of contact has decreased in greater proportion than the forces. It is this concentration of forces that leads to early tool failure with harder steels.

The authors appreciate Professor Shaw's comments concerning the dependability of their cutting data as well as his very pertinent questions regarding the mechanism of solid friction and the significance of the built-up edge.

Professor Shaw has proposed an entirely different explanation from that of the authors for the force-speed characteristics observed. The effect of velocity on the extent of the built-up edge is held to be fundamentally responsible for all of the changes. His discussion is based on the observation that temperature has an insignificant effect upon sliding friction between solids.

Bowden and Tabor[23] have shown that the decrease in the co-

[21] "The Effect of Speed and Feed on the Mechanics of Metal Cutting," by B. T. Chao and G. H. Bisacre, The Institution of Mechanical Engineers, London, England, advance copy, 1951.

[22] "Measurements of Temperatures in Metal Cutting," by A. O. Schmidt, O. W. Boston, and W. W. Gilbert, Trans. ASME, vol. 68, 1946, pp. 47–49.

[23] "Friction and Lubrication," Report Nos. 1 and 2, by F. P. Bowden and D. Tabor, Bulletins Nos. 145 and 155, Australia Council for Scientific and Industrial Research, 1942.

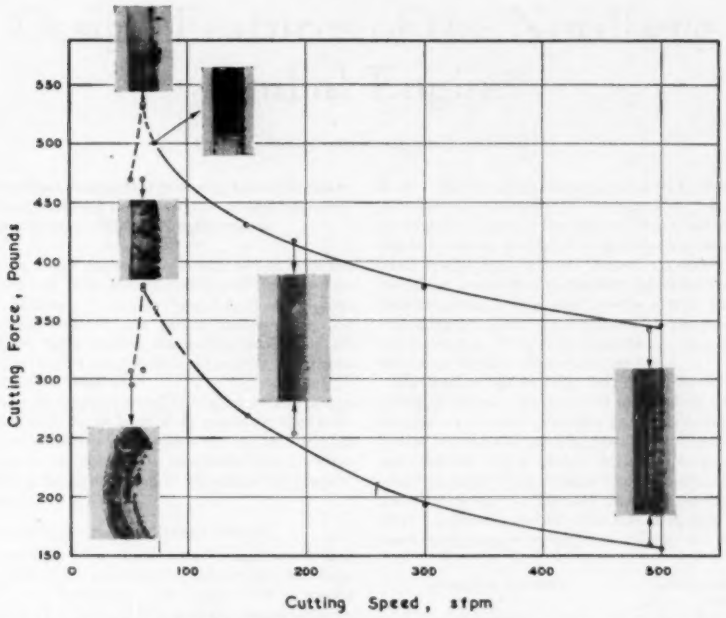

FIG. 26 CUTTING SPEED-CUTTING FORCE RELATIONSHIP AS INFLUENCED BY BUILT-UP EDGE
(Cutting conditions same as Fig. 2 for conventional turning.)

efficient of friction for most metallic pairs is small over a wide range of temperature, provided the temperature involved is not close to the melting point. The velocity of sliding in their experiments ranged from 0.005 cm per sec to 1 cm per sec, or approximately 0.01 fpm to 2 fpm. Under such slow velocity of sliding, the temperature gradient at the sliding contact is small and may be ignored, with the result that both the mean pressure hardness of the metals and the shear strength of the metallic junction decrease simultaneously with increase of temperature. The friction of clean metals under this nearly "isothermal" condition is not markedly dependent on temperature. On the other hand, with the range of cutting speeds reported by the authors, the velocity of sliding (the chip flow velocity) varies from about 23 fpm to 200 fpm. There exists an extremely steep temperature gradient at the interface, perpendicular to the direction of sliding. While the shear strength of the metallic junction probably depends on the interface temperature, the mean pressure hardness depends on that of the bulk of the chip. That friction cannot be regarded as a surface effect only has been discussed quite extensively by Bowden and Tabor. Careful study of the basic mechanism of solid metallic friction reveals that one has to differentiate between "isothermal" and "nonisothermal" conditions if the effect of temperature on sliding friction is to be correctly applied.

The decrease in both components of cutting force with increase in cutting speed cannot be explained in terms of the built-up edge. Under the cutting conditions reported in this paper, there was no built-up edge present. Absence of a built-up edge is best evidenced by the smooth shiny separating surface of the chip as contrasted to the ragged severely torn surface when a built-up edge is present.

In answer to the question of the effect of built-up edge on cutting forces, a supplementary cutting test was recently conducted in the author's laboratory. The results are presented in Fig. 26 of this closure.

At a cutting speed of 52 sfpm, a large built-up edge exists, while the forces are relatively low as compared with those at slightly higher speeds. When cutting at 62 sfpm, the chip produced in the early stages shows the presence of a built-up edge as evidenced by the torn rough chip surface. The built-up edge gradually diminishes with time until it nearly disappears. This change is accompanied by a simultaneous increase of cutting forces. This is illustrated by chip views and leaders in Fig. 26. The dynamometer indicated a steady reading when the chip was clean—a manifestation of the essentially complete removal of the built-up edge. Further increase in cutting speeds produces a strict type 2 chip and results in a decrease in forces as heretofore presented. Therefore the evidence is that, at low cutting speeds when a type 3 chip is produced, an increase of cutting speed will result in a decrease of built-up edge accompanied by an increase in cutting forces—not a decrease as contended by Professor Shaw.

With reference to the adhesion temperatures of steel and cemented carbide tools, Dr. Dawihl has recently stated in a private communication concerning the subject paper: "It was especially interesting to me that the temperatures as measured by you for adhesion on the metal surfaces are in surprisingly close agreement with the temperatures as measured by myself and collaborators in static tests. Based on other tests, I had already anticipated that the difference between dynamic and static determinations of the adhesion temperature might not be very great." Apparently then, Dawihl's values of adhesion temperature may be applied to dynamic conditions with reasonable assurance.

Design Features of the Nordberg Radial Engine

By D. I. BOHN[1] and EMIL GRIESHABER[2]

The paper describes design features and inherent characteristics of the Nordberg radial engine, a new impulse-type ignition system and different applications.

THE Nordberg radial engine is built with eleven cylinders of 14-in. bore and 16-in. stroke, and at 400 rpm develops 1800 hp or 1250 kw. It is of the two-cycle type with port scavenging and port exhaust, the piston undercovering the ports in the cylinder walls thereby eliminating intake and exhaust valves. It is built as a spark-fired gas engine, as a Diesel unit, and as a "Duafuel" engine.

The motor-driven scavenging blower, lube-oil and water pumps can be connected directly to the leads of the generator, thus making a self-contained automatic unit, with a net capacity of 1150 kw; or power may be supplied to the auxiliaries from a station bus bar and utilizing the gross output of the engine for pump or compressor drives.

Advantages of Radial-Engine Design

The basic advantages of a radial-engine design result in a simple, compact, and sturdy arrangement, lightweight, minimum foundations, and small floor space. This engine with its welded base is a little over 12 ft wide, 9 ft 4 in. high, weighs approximately 85,000 lb, and can be shipped by rail as an assembled unit.

Since the cylinders fire one after the other in clockwise rotation, the piston loads are transmitted to the crankpin at an even sequence; consequently the torque variations are small in magnitude. Opposite pistons counteract the peak cylinder pressures, and, therefore, the resulting loads on the crankpin and the two main bearings are greatly reduced and of small variation. This effect, together with a small number of bearings, reduces friction and improves the mechanical efficiency of the engine.

The radial arrangement of the cylinders makes possible a perfect static and dynamic balance of the engine. The first-order inertia force to be balanced equals the sum of the inertia force of the rotating and $^1/_2$ of that of the reciprocating masses of all cylinders. This force, acting in the direction of the crank throw, can be balanced completely by counterweights as there are no free forces or moments transmitted to the foundation of the engine. All the higher-order inertia forces are inherently completely balanced without any counterweights except 11th, 22nd, 33rd, etc., orders which are of negligible magnitudes. Thus the engine is free of vibrations and requires only a light foundation.

The problem of torsional vibrations is greatly simplified since the stiff single-throw crankshaft results in a high natural frequency. Most of the orders that are so familiar to designers of in-line engines are eliminated in this engine due to the radial attachment of the moving parts of the cylinders to a single crank throw. The resulting exciting torque of all cylinders is zero for all orders except for the 11th, 22nd, 33rd, etc., order critical speeds. Of these torques, only the 11th order is of any appreciable magnitude and it can readily be located above normal operating speed on short shaft installations. Smooth operation, free of torsional vibrations, is achieved throughout the entire range. In applications requiring a long shaft, where several modes of torsional vibrations are possible, the number of critical speeds is reduced to a minimum; this greatly simplifies the elimination of torsional vibrations within a wide operating range.

The load on the crankpin bearing can be determined by combining graphically the resultant forces along the connecting-rod axis due to cylinder pressures and the centrifugal force of the master bearing and rotating parts of the connecting rods. The main-bearing load is merely the graphical sum of the cylinder pressures, since the centrifugal forces are completely balanced by the counterweights. The load diagrams are shown in Fig. 1, the force S indicating the direction and magnitude of the load for a given crank angle with respect to cylinder No. 1.

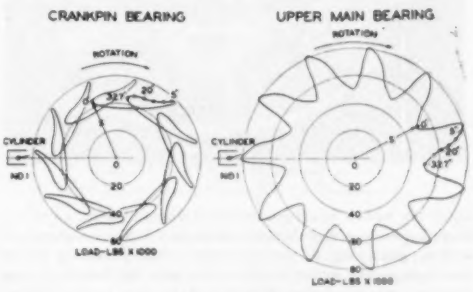

Fig. 1 Bearing-Load Diagram

In all radial engines the rotation of the crankpin bearing, upon which the connecting rods are mounted, must be prevented in order to obtain constrained motion of the connecting-rod crank end. This is usually accomplished by use of a master connecting rod. A newly designed patented method is used in the Nordberg radial engine whereby the master crankpin bearing is prevented from rotating by the use of a planetary gear train which connects the master-bearing gear to the stationary crankcase cover. This gear train consists of four gears shown in Fig. 2. The stationary gear 1 is fastened to the underside of the crankcase cover and is connected through a unit consisting of the small pinion 2, drive shaft and larger drive gear 3 to the gear teeth of the master bearing 4. The connecting gear unit is mounted in the upper counterweight of the crankshaft opposite the crank throw.

It can readily be seen from the schematic diagram, Fig. 3, that if the gear ratio N_1 to N_3 and N_2 to N_4 are equal, as is the case in this gear train, the gears 1 and 4 must have the same angular velocity because pinion 2 and drive gear 3 revolve as a unit. Since gear 1 is stationary, gear 4 cannot revolve with respect to the stationary part of the engine. The position of the crankpin on

[1] Chief Electrical Engineer, Aluminum Company of America, Pittsburgh, Pa.

[2] Chief Engineer, Nordberg Manufacturing Company, Milwaukee, Wis. Mem. ASME.

Presented at the Oil and Gas Power Conference, Baltimore, Md., June 12–16, 1950, of The American Society of Mechanical Engineers.

Note: Statements and opinions advanced in papers are to be understood as individual expressions of their authors and not those of the Society. Manuscript received at ASME Headquarters, April 7, 1950. Paper No. 50—OGP-1.

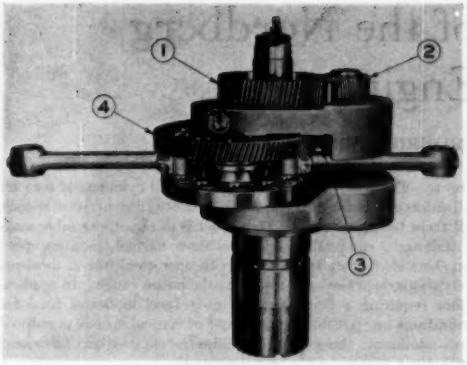

FIG. 2 CRANKSHAFT ASSEMBLY

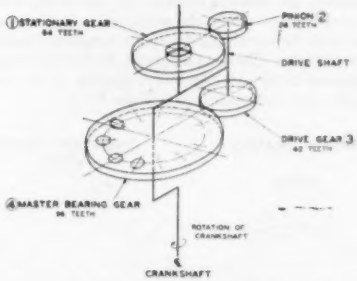

FIG. 3 SCHEMATIC GEAR-TRAIN DIAGRAM

which the master bearing is mounted merely take care of the larger center-to-center distance of gears 3 and 4, as compared with the gears 1 and 2; thus the master bearing revolves at $-N$ rpm with respect to the crank, if the crank revolves at N rpm with respect to the stationary part of the engine. In other words, the resultant angular velocity of the master bearing with respect to the stationary part of the engine is zero, and the master bearing is merely translated by the rotation of the crank.

This type of motion of the master bearing has great practical advantages. Since the center of the master bearing is moving along a circular path, every point on the bearing moves along circles of equal diameters. Therefore the knuckle pins which correspond to crankpins in the connecting-rod - crank mechanism, describe identical circles, thus making the moving parts of every cylinder kinematically identical. Consequently, interchangeable parts can be used in all cylinders and the timing of the engine is greatly simplified and identical for all cylinders.

MATHEMATICAL CONSIDERATIONS

The forces acting on the crank mechanism of the radial engine are shown in Fig. 4. Starting with the actual indicator card and the inertial forces, the net reciprocating force P acting on the piston can be determined. Since the design eliminates the master rod and articulated rods, and, since all moving parts of each cylinder follow the same path, the displacement, velocity, acceleration, and thus the inertia forces of each piston are identical, and Fig. 4 applies to all cylinders. The net reciprocating force P at any crank angle α can be resolved into the following

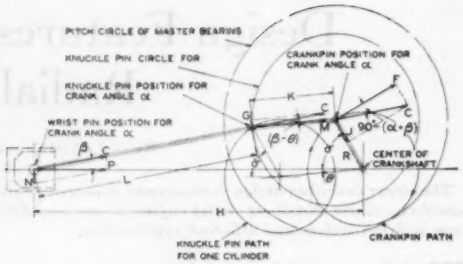
PITCH CIRCLE OF MASTER BEARING
KNUCKLE PIN CIRCLE FOR
KNUCKLE PIN POSITION FOR CRANK ANGLE α
CRANKPIN POSITION FOR CRANK ANGLE α
WRIST PIN POSITION FOR CRANK ANGLE α
CENTER OF CRANKSHAFT
KNUCKLE PIN PATH FOR ONE CYLINDER
CRANKPIN PATH

FIG. 4 FORCES ACTING ON CRANK MECHANISM

$$C = P/\cos\beta \quad [1]$$

$$N = P\tan\beta \quad [2]$$

where

C = connecting-rod force, lb
N = force normal to cylinder wall, lb
β = connecting-rod angle, deg

Transferring the connecting-rod force C to the master-bearing knuckle pin and the crankpin, it can be resolved into the following

$$G = C[\sin(\beta - \theta)] \quad [3]$$

$$M = C[\cos(\beta - \theta)] \quad [4]$$

$$F = C\{\cos[90 - (\alpha + \beta)]\}$$
$$= C[\sin(\alpha + \beta)] \quad [5]$$

$$J = C\{\sin[90 - (\alpha + \beta)]\}$$
$$= C[\cos(\alpha + \beta)] \quad [6]$$

where

G = tangential force on master bearing, lb
θ = master-bearing lag angle, deg
M = radial force on master bearing, lb
F = tangential force on crankpin, lb
J = radial force on crankpin, lb

Torque on Crank Chain. From the fundamental force Equations [1] to [4], we can determine the corresponding torque on the cylinder wall, master bearing, and crankpin or engine crankshaft.

Cylinder-wall torque:

$$= N \times H$$
$$= P\tan\beta\, H$$
$$= P\tan\beta[L\cos\beta + R\cos\alpha + K\cos\theta]$$
$$= P[L\sin\beta + R\tan\beta\cos\alpha + K\tan\beta\cos\theta] \quad [7]$$

where

H = distance from L wrist pin to L crankshaft, in.
$H = L\cos\beta + R\cos\alpha + K\cos\theta$
L = connecting-rod center length, in.
R = crank radius, in.
K = knuckle-pin radius, in.

Master-bearing torque:

$$= G \times K$$
$$= C\,[\sin(\beta - \theta)]\,K \text{ (from Equation [3])}$$
$$= C\,[\sin\beta\cos\theta - \cos\beta\sin\theta]K$$
$$= \frac{P}{\cos\beta}\left[(\sin\beta\cos\theta - \cos\beta\sin\theta)\right]K \text{ (from Equation [1])}$$
$$= PK\,[\tan\beta\cos\theta - \sin\theta] \quad [8]$$

Crankshaft torque:

$$= F \times R$$
$$= C\,[\sin(\alpha + \beta)]R \text{ (from Equation [5])}$$
$$= \frac{P}{\cos\beta}\left[\sin\alpha\cos\beta + \sin\beta\cos\alpha\right]R$$
$$= PR\,[\sin\alpha + \tan\beta\cos\alpha] \quad [9]$$

The relationship between these torques can be shown as follows Since

$$R\sin\alpha = L\sin\beta + K\sin\theta$$

Equation [9] becomes

$$FR = P[L\sin\beta + K\sin\theta + R\tan\beta\cos\alpha]$$

and as

$$G = P[\tan\beta\cos\theta - \sin\theta] \text{ (from Equation [8])}$$

or

$$\sin\theta = \tan\beta\cos\theta - \frac{G}{P}$$

$$FR = P[L\sin\beta + R\tan\beta\cos\alpha + K\tan\beta\cos\theta] - GK$$

or

$$FR = NH - GK \quad [10]$$

which states that the crankshaft torque is equal to the cylinder-wall torque minus master-bearing torque.

It is obvious from the discussion of the gear train, that the torque on the stationary gear is of identical magnitude and direction to that of the master-bearing gear, which is shown in Fig. 5, for various operating conditions.

From these torques the tooth loads on the different gears can be determined. Due to their smaller pitch diameters the loading of the pinion and stationary gear will be greater than that of drive gear and master-bearing gear, and may be found from the following relationship

$$G_p = 2GK/D_s \quad [11]$$

where

G_p = pinion and stationary-gear tooth load, lb

D_s = pitch diameter of stationary gear, in.

As is evident from the curves of the master-bearing torque, Fig. 5, the tooth-loading changes noticeably with a change in master-bearing lag angle. As an example, for the gas cycle with a lag angle of zero degrees, the tooth loading at full load equals a maximum of 11,500 lb whereas with 2 deg lag angle the load is reduced to 4000 lb.

The vertical thrust loading on the bearings supporting the pinion, drive gear, and connecting shaft is reduced to a minimum by the proper choice of the helix angle and the hand of the gears.

Gas-Burning Radial Engine

The Nordberg radial engine, when arranged for gas burning, Fig. 6, operates on spark ignition about 260 psig compression and 650 psi firing pressure. In each cylinder is a gas inlet valve, located above the scavenging ports. These valves are actuated by

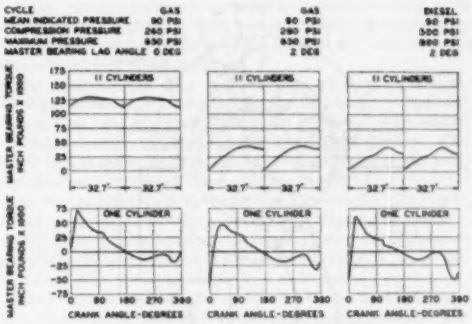

Fig. 5 Master-Bearing Torque Curves

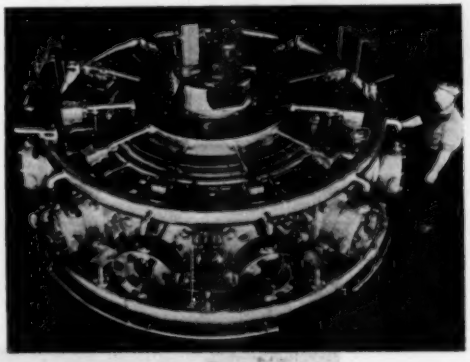

Fig. 6 Gas-Burning Radial Engine

rocker arms and push rods from a cam located on the upper portion of the crankshaft. They introduce the gas at low pressure in the cylinders into the path of the incoming scavenging air to assure thorough mixing. Two spark plugs are in a vertical plane and fire at different crank angles before top dead center. The amount of gas delivered to the cylinders is varied in accordance with the load on the engine by means of a valve inserted in the gas header and connected to the governor. The volume of scavenging air is also controlled proportionately to the load by throttling on the blower suction.

The engine is equipped with a new type of ignition system designed to operate for indefinitely long periods of time without attention or maintenance, and also to insure a very low rate of spark-plug-electrode erosion.

Ignition energy is supplied by a special impulse generator whose output, at the plugs, consists of accurately timed, unidirectional impulses, similar to an individual half cycle of a conventional alternating-current wave. This generator involves no cams, breaker points, brushes, collector rings, or rotor windings.

The general construction, as shown in Fig. 7, involves a four-element rotor, each element of which consists of a permanent-magnet assembly, magnetically distinct from the other elements and equally spaced. The stator consists of laminated punchings, as shown, with four windings. The generator operates at $2^3/_4$ times engine speed, or 990 rpm, so that the generator rotor makes

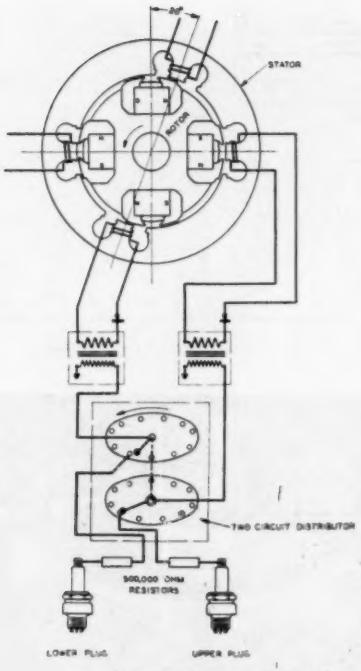

FIG. 7 IGNITION-WIRING DIAGRAM

$^1/_4$ revolution for each $^1/_{11}$ revolution of the engine. Although the permanent-magnet rotor elements are equally spaced, the stator coils are displaced in pairs by 20 deg, as shown. This is done to provide a firing differential of about $7^1/_4$ engine deg between the two plugs in each cylinder. The lower plug fires 15 deg BTDC, and the upper plug fires later at approximately 8 deg BTDC. Experiments indicate that improved smoothness of operation and reduced pressure peaks result from this differential firing.

Normally, either a single stator coil or a pair connected in parallel is employed to supply one ignition circuit of one set of 11 plugs. A single stator coil provides ample energy for this purpose at half speed or above, and, when ignition must be supplied at low starting speeds, such as one quarter of normal, a switch may be employed to connect the two opposite coils in series for the starting period.

The transformer differs from an ordinary spark coil in that the iron circuit is complete as in a conventional transformer. For this engine, it is designed to provide a maximum peak voltage of 25 kv, which is ample for the compression used.

The high-tension distributor, operating at engine speed, is conventional except that it is made for two-circuit operation with connections to each of the 22 spark plugs.

Fig. 8 shows an oscillogram of the output of one generator coil, with and without the selenium rectifier With the selenium rectifier in circuit, the two small positive impulses are eliminated and a single unidirectional impulse results.

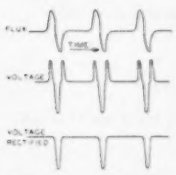

FIG. 8 GENERATOR-COIL OUTPUT OSCILLOGRAM

A special 500,000-ohm resistor is connected in series with each spark plug and located at each plug. This resistor is effective in preventing the harmful effects and rapid spark-plug erosion normally resulting from the

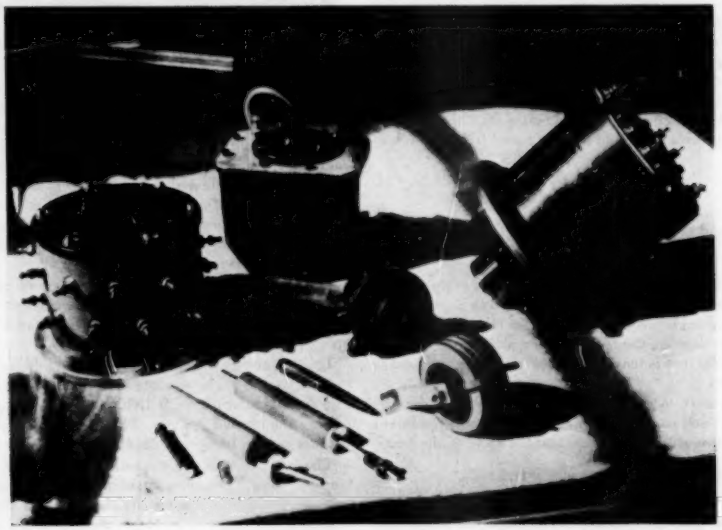

FIG. 9 ELEMENTS OF IGNITION SYSTEM

capacitative energy stored in long high-tension leads. In addition, the fact that all impulses to each plug are unidirectional is conducive to low spark-plug-electrode erosion. The polarity relationship of the various elements is so arranged that the center spark-plug electrode is negative, thus concentrating the erosion on the multiple and cool grounded electrodes.

Fig. 9 shows the various elements of this ignition system, being the impulse generator, one of the two transformers, the two-circuit distributor, and one of the spark-plug resistors and its enclosure which is mounted at each plug.

These engines when operating on natural gas with a high heat value of 1003 and low heat value of 910 Btu per cu ft showed a fuel consumption of 11.4 cu ft per gross kwhr or 12.42 cu ft per net kw corresponding to 7970 Btu per net bhphr.

Installation Experience

In the reduction plant of the Aluminum Company of America at Point Comfort, Texas, 120 of these spark-ignition, gas-burning, radial engines are installed. They operate on natural gas and are connected to 1150-kw direct-current generators running at 360 rpm.

These engines are placed in three buildings with two rows of 20 engines in each building and have a total net capacity of 126,000 kw. Fig. 10 shows one half of an engine bay.

in higher injection pressures for very small quantities and a more even pressure rise over the whole capacity range of the fuel pump. Shifting from one fuel to the other can be done without interrupting the operation of the engine.

The cross section of a spark-ignition gas-burning engine, driving a generator, is shown in Fig. 12. The engine is mounted on a welded base which also carries the generator and a steady bearing and supports the scavenging and exhaust headers. The whole unit is self-contained, can be erected quickly in the field, and requires only a small and simple foundation.

Another application is shown in Fig. 13 where a radial engine drives a centrifugal pump or a compressor. The engine rests on a short subbase which also carries the step-up gear. The high-speed shaft extends downward to the driven unit which is below and separated from the prime mover by a tight floor.

The cylinders are lubricated by forced feed, the bearings, gears, and other moving parts by a continuous pressure system. The lube oil enters through the main bearing into the crankshaft and, by means of passages, is distributed to moving parts throughout the engine. The oil used for cooling the pistons enters and leaves the pistons through rifle drills in the connecting rods, returning to the lower part of the crankcase. From there it drains, together with the balance of the returned lube oil, to a sump tank to be strained, cooled, and recirculated.

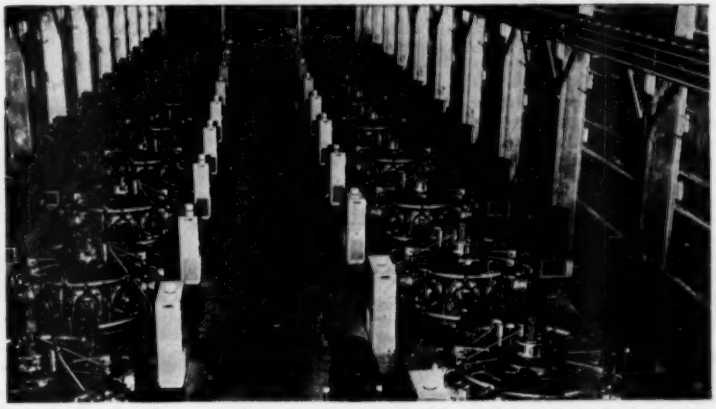

Fig. 10 View of Engine Bay

When the engine burns oil, Fig. 11, it operates on the Diesel cycle with normal compression and mechanical injection of the fuel. It is started by compressed air admitted through a rotary distributor to a starting valve in each cylinder head. The fuel pumps, one for each cylinder, are located in a horizontal plane above the crankcase cover and are actuated by a cam on the crankshaft. The fuel-injection nozzles are centrally located in the cylinder heads, and all fuel lines are the same length. The load and speed of the engine are controlled by a hydraulic governor acting directly on the fuel pumps.

As a "Duafuel" engine, it operates with pilot-oil injection. The fuel pump has a double-helix plunger and variable-retraction valve. The flat helix measures the pilot oil for gas operation and the steep helix is brought into action when operating on fuel oil. The displacer piston of the discharge valve is so arranged that the retraction volume varies from zero to a maximum in proportion to the amount of fuel discharged per pump stroke. This results

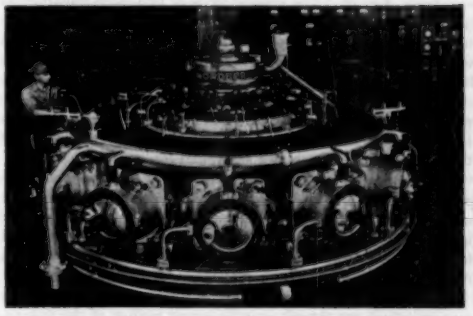

Fig. 11 Diesel Oil-Burning Radial Engine

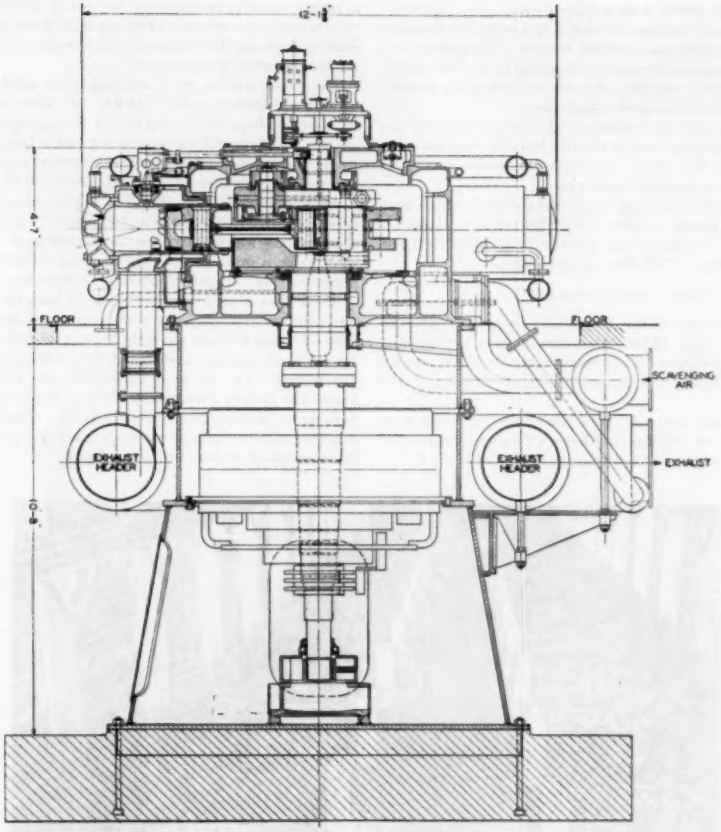

FIG. 12 ENGINE CROSS SECTION

The unusual design of the crankshaft can be seen from the engine cross section, Fig. 12, the illustration of the crankshaft assembly with two connecting rods, Fig. 2, and the top view of the crankcase, Fig. 14. The crankshaft is of two-piece construction and made of high-tensile cast iron. It has two bearings of the babbitted-bronze shell type, the lower one being in the central hub of the crankcase, the upper one in the crankcase cover. The lower section of the crankshaft comprises the short, sturdy shaft, lower counterweight, and crankpin. The underside of the counterweight has a polished thrust face which rides on the eight tilting pads of the thrust bearing which supports the weight of the shaft assembly, generator shaft, and rotor.

The upper section of the shaft consists of the upper counterweight and the upper shaft journal. The drive gear and pinion are attached to the upper counterweight. With the master gear in position on the crankpin, the upper section is then attached to the lower section by doweling and clamping, thus making a rigid assembly.

The pistons are aluminum-alloy forgings and so are the ring carriers, which are shrunk over the upper portion of the pistons. They carry the piston rings and also provide passages for the piston-cooling oil. The wrist pins are of the floating type. The connecting rods are one-piece drop forgings. The knuckle pins are tightly clamped into the crank end eyes of the rods and are carried in two bearings located in the two flanges of the master gear. All bearings are of the one-piece bronze-bushing type, no split shells being used.

Many elements of this engine are of conventional design, others were modified to suit the radial arrangement. No particular effort was made to produce a lightweight engine. The moderate weight in comparison to other engine types of like duty is inherent to the radial design.

Discussion

R. L. BOYER.[3] There are clever design features in this engine, and there are still more clever engineering features of installation in the plant in which these engines have been installed. For all of these features the authors are to be congratulated.

[3] Vice-President and Chief Engineer, The Cooper-Bessemer Corporation, Mt. Vernon, Ohio.

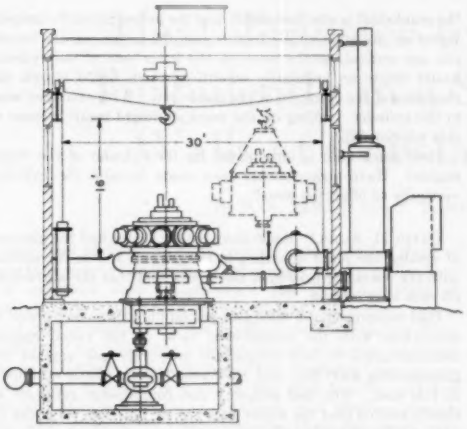

FIG. 13 RADIAL ENGINE ARRANGED FOR PUMP DRIVE

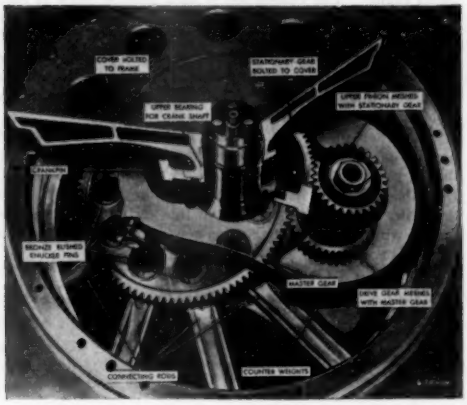

FIG. 14 TOP VIEW OF CRANKCASE

On the other hand, the radial engine is just another way of building an engine. The writer's company designed a radial locomotive engine in 1930, and gave its production very serious consideration. Since then we have on several occasions given further consideration to the radial design as compared to other types, but in no case has that consideration gone further than the layout stages, simply because in each and every case we found that we could accomplish our purposes better in another way. A given design of an engine almost always has some features in its favor, but also certain features which are unfavorable. It becomes a matter of balancing the pros and cons to decide which type of design best fits the job.

When it comes to mechanical balance, on which subject the authors spent considerable time, there is no doubt that the radial represents almost perfection. The in-line or "V" 4-cycle engine with 6 and 8 crank throws is also near perfection and represents no more external forces than does the radial. We are now building the V-engine in 6 and 8 cylinders and, by means of geared balance weights, gain the same precision as in the larger number of cylinders. In other words, the writer sees no advantage in the radial design from the balance standpoint.

There can be no doubt that the radial engine presents a comparatively simple torsional solution. In all fairness, it must be said that we must be more careful of an in-line or V-engine from this angle, yet each and every engine is checked for critical speeds, and we can say definitely that for generator sets in particular, torsional vibration has long ceased to be a problem. Here the radial engine has a slight advantage, however, in that it should require less calculating attention, but not that it will perform any better from this angle.

The paper deals at some length with a new and novel ignition system. We were familiar with this development from its inception and made the first trial of it on an experimental engine. We know that a great deal of original thinking was given to this feature, and it is a clever system. It should be noted, however, that its application is not peculiar to a radial engine.

We do not like the necessity of motor-driving all auxiliaries. It is true that some auxiliaries can just as well be motor-driven, but certainly when it comes to a large auxiliary load such as scavenging blowers, this becomes a handicap. It seems a little far-fetched to have to motor-drive the lubricating-oil pump and even the cylinder lubricators. The radial engine simply does not lend itself well to the driving of auxiliaries.

Of all of the possible power uses of a radial engine, it is probably best adapted to generator drive, than any other, since it makes no particular difference whether the shaft is vertical or horizontal. Owing to the fact that auxiliaries must all be motor-driven, this generator becomes a special one, however, and, except in quantities such as where used in the plant so far built, it would seem that the generator could be expected to cost considerably more. Other than generator drive the radial is at a handicap, for most equipment is best adapted to and is designed for horizontal drive.

The paper states that the basic advantages of a radial-engine design result in a simple, compact, and sturdy arrangement, light weight, minimum foundation, and small floor space.

As to simplicity, the writer can see very little difference whether the engine is radial, or of more conventional design. The greater part of the simplicity of this particular engine would appear to arise from the fact that it is a simple ported 2-cycle engine. We do not choose to use that type of engine for any wide application of generator drives, although we have them in heavy production for other purposes. From the standpoint of the radial design, however, it is not apparent wherein it is particularly more simple than any other type. It is true that it has just one connecting-rod bearing where we might use eight. Bearings, however, are of no particular problem to us. Just reducing the number of bearings to one, while it sounds like simplicity, sounds none too simple when we consider that we are expecting one bearing to absorb the horsepower of six or eight bearings. It has yet to be determined what life can be expected from a bearing under such circumstances. The design of the radial connecting-rod system certainly is not simple. Here again, we have the give-and-take proposition of some items being more simple and some not so much so.

As to compactness, we find this engine has essentially the same cubic feet per horsepower as a V-engine of the same output. It may be interesting to note here that we ship our 3700-hp V-engine in one piece, fully assembled. It of course requires special handling equipment at destination, but even that cost is infinitesimal compared to doing any assembling on the job.

It is claimed the radial engine is basically a lightweight engine. Here we must consider the actual rating. We find a great deal of confusion as to what is the rating, because of the heavy auxiliary load, and whether the rating given is net or gross. The paper states that it is 1800 hp, and we would assume that surely the authors refer to a net horsepower. This doesn't agree with the

net horsepower used in the plant already built, since there the kilowatt output is 1000, representing perhaps 1450 hp. It is true that those engines turn 360 rpm, whereas the paper now refers to 400 rpm. Even that of course falls far short in accounting for the 1800 hp. If, however, we use the 1800 hp and the 85,000 lb weight, we have a specific weight of 47.2 lb per hp. Our 3700-hp 4-cycle V-engine weighs 199,000 lb complete and is, therefore, 53.8 lb per hp. When one realizes that our engine has more than twice the capacity and that larger engines always weigh more per horsepower, it would appear that the V-engine is actually lighter in spite of the fact that it turns only 327 rpm, whereas the radial turns 400 rpm. A V-engine of 1800 hp definitely weighs considerably less than 47.2 lb per hp.

The other basic claim is that the radial engine occupies a small amount of floor space. The building which houses 40 of these engines is actually nearly 600 ft long, and the writer's best estimate is that it has a width of 55 ft minimum. Some length of this building is taken on each end, one for a railroad siding, and one for a repair shop. The writer is not sure of the net floor space occupied by these engines. Some calculations from the actual size of the engine show that a minimum net length of about 440 ft must be required. If we use 440 ft with a 55 ft width, we have a floor space of 24,200 sq ft. Into this area of floor space, using our standard spacing, we will put 28 of our 3700-hp V-engines, totaling, therefore, 103,000 hp. This compares to 58,000 hp in the present installation and compares to 72,000 hp if we accept the 1800-hp rating now proposed. Taking the latter, it is obvious that the V-engine permits 43 per cent more generating capacity in a given space.

T. M. Robie.[4] Ordinarily, if we think of a radial engine, such as used in an airplane, we would have the arrangement here turned 90 deg. In other words, the center line of the cylinders would be vertical and the crankshaft would be horizontal, so that there would be no gravity wear on the walls of most of the cylinders. In this case, each piston rests on the lower wall of the cylinder, which might occasion a certain amount of wear.

In a conventional horizontal-type engine, with a single cylinder, the crankshaft is also horizontal, and the piston pin and crankpin, therefore, are horizontal. In this case the piston pin and crankpin are vertical, so the wear on the lower side of the cylinder would create an angularity condition which would absorb the clearance of the crankpin or the piston pin. With excessive wear in the cylinder, binding on the crankpin might result because of this relationship.

How much wear is anticipated for the cylinder of the radial engine? Have arrangements been made to raise the cylinder vertically to offset the wear?

David M. Salls.[5] Some time ago the writer had the pleasure of visiting the plant described in the paper; and in discussions with the operating personnel there, was told that the spark-plug life was over 5000 hr.

Fuel consumption of 8000 Btu per bhp hour was mentioned in connection with the compression ratio of the radial engine. Manufacturers of two comparable two-cycle gas engines are guaranteeing 8500 Btu, and 8000 would seem a little optimistic in this case. The fuel economy and compression ratio are so closely related that the writer does not see how this value can be as low as mentioned.

We were very much impressed by the ignition system on the radial engine. The elimination of such ignition parts as cams, condensers, and points should reduce the number of engine shutdowns appreciably.

As to the slab foundation, we thought it was a very small foundation when compared to the usual large blocks required for engines of this horsepower. This seems particularly attractive under present-day construction costs.

The writer would like to learn more about the peak firing pressure of this engine. It seems very high—650 pounds—but that is possibly due to the large spark advance of 15 deg btc. Does this high peak have any bad effect on the engine? When the writer watched the operator of this engine, it seemed very smooth with very little combustion noise when compared to other two-cycle engines.

[4] Manager, General Diesel Sales Divison, Fairbanks, Morse & Company, Chicago, Ill. Mem. ASME.

[5] Efficiency Engineer, Texas Eastern Transmission Corporation, Shreveport, La. Jun. ASME.

Heat Transfer to a Fluid Flowing Turbulently in a Smooth Pipe With Walls at Constant Temperature

By R. A. SEBAN[1] and T. T. SHIMAZAKI,[2] BERKELEY, CALIF.

The case of heat transfer to an incompressible fluid of constant properties flowing turbulently within a pipe having constant wall temperature has been investigated analytically. Heat-transfer coefficients have been evaluated and compared to the coefficients obtained by Martinelli (1)[3] for the same flow conditions in a pipe having a linear variation of wall temperature obtained from a constant heat-transfer rate along the pipe length. At low Prandtl numbers, such as obtained with molten metals, the ratio between the coefficients for these two cases may become as low as 0.73, with the coefficient for the constant-wall-temperature case being the smaller of the two. A simple equation of the Lyon type is indicated for the correlation of the present results.

Nomenclature

The following nomenclature is used in the paper:

α = thermal diffusivity of fluid, sq ft per sec
c = heat capacity of fluid, Btu/lb deg F
D = diameter of pipe, ft
h = heat-transfer coefficient between pipe wall and fluid, Btu/hr ft² deg F
k = thermal conductivity of fluid, Btu/hr ft² deg F/ft
p = pressure, lb per sq ft
q = rate of radial heat flow through unit area at radius r, Btu/ft² hr
r = radius, ft
T = temperature at any point r, deg F
T_m = mixed mean fluid temperature, deg F
u = velocity in x-direction at any point r, fps
u_m = mean bulk velocity, fps
$u_\tau = \sqrt{\frac{\tau_0}{\rho}}$, friction velocity, fps
$y = r_0 - r$ = distance from pipe wall, ft
x = distance along pipe axis, ft
γ = weight density of fluid, lb per cu ft
ϵ_H = eddy diffusivity for heat, ft²/sec
ϵ_M = eddy diffusivity for momentum, ft²/sec
ν = kinematic viscosity of fluid, ft² sec
ρ = mass density of fluid, lb sec²/ft⁴
τ_0 = shear stress at the wall, lb per sq ft

Dimensionless Groups:

$\frac{hD}{k}$ = Nusselt number

$\frac{u_m D}{\alpha} = \left(\frac{\nu}{\alpha}\right)\left(\frac{u_m D}{\nu}\right)$ = Peclet number

$\frac{u_m D}{\nu}$ = Reynolds number

$\frac{\nu}{\alpha}$ = Prandtl number

$y^+ = \frac{y\sqrt{\frac{\tau_0}{\rho}}}{\nu}$ = dimensionless distance parameter

Subscripts:

c = at the pipe center line
0 = at the pipe wall
q = constant heat rate
T = constant wall temperature

Introduction

The use of analogy methods for the calculation of heat-transfer coefficients for the flow of all fluids, including those of low Prandtl number, in circular pipes has been presented by Martinelli (1). That analysis yielded results for the case of a linear variation of wall temperature with pipe length.

The effect of constant wall temperature as contrasted to linear variation of the wall temperature was first noted by Reichardt (2) who, however, confined his attention to fluids of Prandtl number greater than 0.70 and found only small variations of the heat-transfer coefficient due to changes in the wall-temperature profile.

This paper presents results comparing heat-transfer coefficients as obtained under conditions of constant wall temperature and linear variation of wall temperature, and it is shown that for fluids of low Prandtl number the effect of the wall-temperature profile is significant. Because of the length of the calculations the results are presented only for flow in a smooth circular pipe.

The present results are obtained analytically by means of an iterative method in which the results of Martinelli are used as a first approximation.

Analysis

Variation of Fluid Temperature With Pipe Length. The system considered is that of an incompressible fluid of constant properties flowing turbulently in a circular pipe. It is assumed that both the velocity and temperature distributions are fully developed, and that in consequence there exists a generalized temperature distribution which is invariable in the direction of flow. This assumption can be expressed as

$$\frac{\partial}{\partial x}\left(\frac{T_0 - T}{T_0 - T_m}\right) = 0 \qquad [1]$$

---

[1] Associate Professor of Mechanical Engineering, University of California. Mem. ASME.

[2] North American Aviation Corporation, Downey, Calif. Jun. ASME.

[3] Numbers in parentheses refer to the Bibliography at the end of the paper.

Contributed by the Heat Transfer Division and presented at the Annual Meeting, New York, N. Y., November 26–December 1, 1950, of The American Society of Mechanical Engineers.

Note: Statements and opinions advanced in papers are to be understood as individual expressions of their authors and not those of the Society. Manuscript received at ASME Headquarters, April 3, 1950. Paper No. 50—A-128.

Carrying out the indicated differentiation, there is obtained

$$\frac{1}{T_0 - T_m}\frac{\partial T_0}{\partial x} - \frac{1}{T_0 - T_m}\frac{\partial T}{\partial x} - \frac{T_0 - T}{(T_0 - T_m)^2} \times \left[\frac{\partial T_0}{\partial x} - \frac{\partial T_m}{\partial x}\right] = 0 \quad [2]$$

In virtue of the specified character of flow, the heat-transfer coefficient will be independent of pipe length and, if the rate of heat transfer is constant with respect to length, then, since

$$q_0 = h(T_0 - T_m)$$

the third term of Equation [2] is seen to be zero. Further, since for this case $\partial T_m/\partial x$ is a constant, the wall temperature varies linearly with x. Equation [2] then becomes

$$\frac{\partial T}{\partial x} = \frac{\partial T_0}{\partial x} \text{ which is also } \frac{\partial T_m}{\partial x}$$

Thus for the case of constant heat rate, the quantity $\partial T/\partial x$ is independent of the radial position in the pipe.

If, however, the wall temperature is constant ($\partial T_0/\partial x = 0$), Equation [2] yields

$$\frac{\partial T}{\partial x} = \frac{T_0 - T}{T_0 - T_m}\frac{\partial T_m}{\partial x} \quad [3]$$

In this case the axial temperature gradient depends upon the radial position in the pipe.

Calculation of Temperature Distribution. For the fully developed flow considered, the equations of momentum and energy can be written (with flow-dissipation effects neglected) as

$$\frac{1}{\rho}\frac{\partial p}{\partial x} = \frac{1}{r}\frac{\partial}{\partial r}\left[r(\epsilon_M + \nu)\frac{\partial u}{\partial r}\right] \quad [4]$$

$$u\frac{\partial T}{\partial x} = \frac{1}{r}\frac{\partial}{\partial r}\left[r(\epsilon_H + \alpha)\frac{\partial T}{\partial r}\right] \quad [5]$$

The temperature distribution satisfying Equation [5] for the case of constant wall temperature is the solution desired.

The radial distribution of the heat rate is given by one integration of Equation [5]

$$\int_0^r u\frac{\partial T}{\partial x}\,r\,dr = \int_0^r d\left[r(\epsilon_H + \alpha)\frac{\partial T}{\partial r}\right] \quad [6]$$

or

$$\int_0^r u\frac{\partial T}{\partial x}\,r\,dr = \frac{rq}{\gamma c}$$

since q is zero at $r = 0$.

In the case that the wall temperature varies linearly, $\partial T/\partial x$ is not a function of the radius. Martinelli (1) made the assumption that the velocity u was equal to the mean velocity and by this further assumption of invariance of velocity with radius removed the product $u(\partial T/\partial x)$ from within the integral sign. Formal integration of the left side of Equation [6] is then possible, and it is seen that these conditions dictate a linear variation of the heat rate q with the pipe radius r.

Lyon (3), retaining the assumption of linear variation of the wall temperature, accounted for the actual variation of the velocity by performing this and subsequent integrations graphically. His results demonstrate that this modification reduces the heat-transfer coefficient by an average of 4 per cent in the Reynolds number range of 20,000 to 1,000,000.

For the case of constant wall temperature, the use of Equation [3] to eliminate $\partial T/\partial x$ in Equation [6] yields the expression

$$\frac{\partial T_m}{\partial x}\int_0^r u\left(\frac{T_0 - T}{T_0 - T_m}\right) r\,dr = \int_0^r d\left[r(\epsilon_H + \alpha)\frac{\partial T}{\partial r}\right]$$

or

$$\frac{r_0^2 u_m}{T_0 - T_m}\frac{\partial T_m}{\partial x}(T_0 - T_c)\int_0^{\frac{r}{r_0}} \frac{u}{u_m}\frac{T_0 - T}{T_0 - T_c}\frac{r}{r_0}\,d\left(\frac{r}{r_0}\right) = r(\epsilon_H + \alpha)\frac{\partial T}{\partial r} \quad [7]$$

For subsequent simplification let

$$\phi\left(\frac{r}{r_0}\right) = \int_0^{\frac{r}{r_0}} \frac{u}{u_m}\frac{T_0 - T}{T_0 - T_c}\frac{r}{r_0}\,d\left(\frac{r}{r_0}\right) = f\left(\frac{u_m D}{\nu}, \frac{\nu}{\alpha}\right) \quad [8]$$

The evaluation of $\phi(r/r_0)$ is seen to require knowledge of the very temperature distribution being sought. An iterative procedure is therefore employed, in which the results of Martinelli for the case of constant heat rate are used for a first approximation to the generalized radial temperature distribution

$$(T_0 - T)/(T_0 - T_c)$$

The function $\phi(r/r_0)$ is seen to depend upon the Reynolds and Prandtl numbers of the flow.

Equation [7] is now integrated again to yield an expression for the radial temperature distribution

$$\frac{r_0^2 u_m}{T_0 - T_m}\frac{\partial T_m}{\partial x}(T_0 - T_c)\int_0^{\frac{r}{r_0}} \frac{\phi\left(\frac{r}{r_0}\right)d\left(\frac{r}{r_0}\right)}{\frac{r}{r_0}(\epsilon_H + \alpha)} = T - T_c \quad [9]$$

To evaluate the integral the radial variation of the eddy diffusivity for heat ϵ_H is required and this is obtained by assuming it equal to the eddy diffusivity for momentum ϵ_M. The diffusivity for momentum is obtained for the turbulent core from the Prandtl-Nikuradse velocity distribution, and the specified linear variation of shear with pipe radius. Thus in the turbulent region, $y^+ > 30$

$$\frac{u}{u_\tau} = 5.5 + 2.5\log_e y^+$$

which yields for the diffusivity

$$\epsilon_M = \frac{\frac{\tau_0}{\rho}\left(1 - \frac{y}{r_0}\right)}{\frac{du}{dy}} - \nu \quad [10]$$

and with ν neglected

$$\epsilon_M = \frac{u_\tau r_0}{2.5}\left(\frac{r}{r_0}\right)\left(1 - \frac{r}{r_0}\right) \quad [11]$$

In the buffer layer, $y^+ = 5$ to $y^+ = 30$, the velocity distribution is taken as

$$\frac{u}{u_\tau} = -3.05 + 5.0\log_e y^+$$

and this yields for the diffusivity

$$\epsilon_M = \frac{u_\tau r_0}{5.0}\left(\frac{r}{r_0}\right)\left(1 - \frac{r}{r_0}\right) - \nu \quad \ldots\ldots [12]$$

In the laminar region, $y^+ = 0$ to $y^+ = 5$, the eddy diffusivity is zero.

The temperature distribution with respect to radius can now be obtained from Equation [9] since the specification of the diffusivities enables the evaluation of the integral in that equation. That integral can be stated as

$$\psi\left(\frac{r}{r_0}\right) = \int_0^{\frac{r}{r_0}} \frac{\phi\left(\frac{r}{r_0}\right) d\left(\frac{r}{r_0}\right)}{\frac{r}{r_0}\left(\frac{\epsilon_H + \alpha}{\nu}\right)} \quad \ldots\ldots [13]$$

and, with this definition Equation [9] can be restated as

$$\frac{r_0^2 u_m}{T_0 - T_m}\frac{\partial T_m}{\partial x}\frac{1}{\nu}(T_0 - T_c)\psi\left(\frac{r}{r_0}\right) = T - T_c \quad \ldots\ldots [14]$$

The generalized radial temperature distribution can be obtained from Equation [14] in the form

$$\frac{T_0 - T}{T_0 - T_c} = 1 - \frac{T - T_c}{T_0 - T_c} = 1 - \frac{\psi\left(\frac{r}{r_0}\right)}{\psi(1)} \quad \ldots\ldots [15]$$

This distribution, used in Equation [8], serves as the next approximation in the iterative procedure by which all the calculations are repeated and a new magnitude is obtained for the temperature distribution given by Equation [15]. When sufficient convergence of the results is obtained, the heat-transfer coefficient is obtained from Equation [14]. It is first noted that

$$\frac{u_m \frac{\partial T_m}{\partial x}}{T_0 - T_m} = \frac{h}{\frac{D}{4}\gamma c}$$

Then, from Equation [14]

$$\frac{hD}{k} = \frac{\nu}{\alpha}\frac{1}{\psi(1)} \quad \ldots\ldots [16]$$

The results obtained herein were calculated according to the foregoing procedure, with two iterations being used to determine the function ψ of Equation [13], that is, the temperature distribution given by Equation [15], obtained by substituting into Equation [8] the temperature distribution given by Martinelli, was used in Equation [8] to obtain a second value of the function ψ. For three conditions this procedure was done once again to obtain an additional approximation so as to check the convergence of the results.

Results

Table 1 gives the results of the calculations. Because of the substantial amount of numerical work involved only a limited number of conditions have been considered but these are adequate to demonstrate the effect. The additional approximation made for three conditions reveals close correspondence with the preceding approximation.

Fig. 1 reveals the predicted Nusselt numbers for a Prandtl number of 0.01 in comparison to the constant-heat-rate solution.

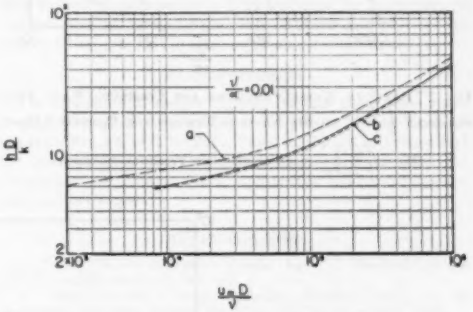

Fig. 1 Nusselt Number for Flow in a Smooth Pipe for Prandtl Number of 0.01

(a, For constant heat rate. b, For constant wall temperature. c, Position of next approximation for constant wall temperature.)

Discussion

Fig. 2 reveals the comparison of the present solution for constant wall temperature to that of Martinelli for constant heat rate (linear variation of wall temperature), the basis of comparison being the ratio of the Nusselt numbers for the two solutions for the same flow conditions.

As the Prandtl number becomes large, the Nusselt-number values tend to become equal. Since, for the same heat-transfer rate, the heat-transfer coefficient depends on the difference between wall and mean-temperature values, the difference in the heat-transfer coefficients for the cases considered depends upon the magnitude of this temperature difference. For fluids of large Prandtl number, the change in temperature between wall and fluid is localized in the sublayer region immediately adjacent to the wall, and the temperature is almost constant across the entire turbulent core. Thus the magnitude of the mean temperature is but insignificantly affected by variation in the temperature of the wall.

TABLE 1 CALCULATED NUSSELT NUMBERS FOR SMOOTH PIPES

$\frac{u_m D}{\nu}$	$\frac{r}{r_0}$	$\frac{u_m D}{\alpha}$	$\left(\frac{hD}{k}\right)_q$ constant heat rate	$\left(\frac{hD}{k}\right)_T$ constant wall temp	Constant wall temp (next approximation)	$\frac{\left(\frac{hD}{k}\right)_T}{\left(\frac{hD}{k}\right)_q}$
2×10^3	0.46	9.2×10^1	10.1	8.95		0.89
10^4	1.0	10^2	36.7	35.4		0.96
	0.46	4.6×10^2	27.3	25.0		0.92
	0.1	10^3	14.0	11.9		0.85
	0.01	10^2	7.97	5.97	6.07	0.75
	0.001	10	7.08	5.14		0.73
10^5	1.0	10^3	217	209		0.96
	0.1	10^4	53.0	46.0		0.87
	0.01	10^3	14.5	11.6	11.7	0.80
	0.001	10^2	8.06	5.93		0.74
10^6	1.0	10^4	1416	1360		0.96
	0.1	10^5	271	256		0.94
	0.01	10^4	48.7	43.1	43.3	0.88
	0.001	10^3	13.3	10.6		0.80

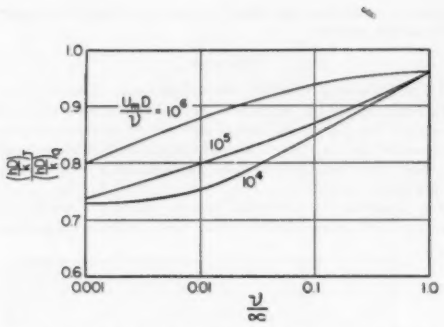

FIG. 2 RATIO OF NUSSELT NUMBER FOR CONSTANT WALL TEMPERATURE $\left(\frac{hD}{k}\right)_T$ TO THE NUSSELT NUMBER FOR CONSTANT HEAT RATE $\left(\frac{hD}{k}\right)_q$ AS A FUNCTION OF PRANDTL NUMBER

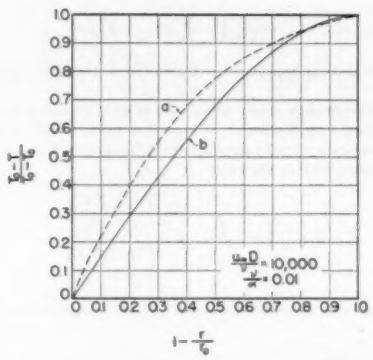

FIG. 3 TEMPERATURE DISTRIBUTION IN A PIPE FOR CONSTANT WALL TEMPERATURE AND CONSTANT HEAT RATE
(Reynolds number 10,000; Prandtl number 0.01; *a*, Constant heat rate; *b*, Constant wall temperature.)

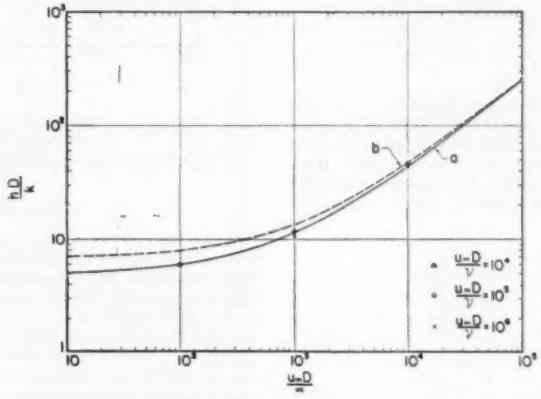

FIG. 4 NUSSELT NUMBER AS A FUNCTION OF THE PECLET NUMBER
(Curve *a* represents Equation 17; the points are the results from Table 1. Curve *b* represents Lyon's expression, $\frac{hD}{k} = 7 + 0.025\left(\frac{u_m D}{\alpha}\right)^{0.8}$, for constant heat rate.)

At Prandtl numbers below unity the difference between the two cases becomes appreciable and is dependent in magnitude on the Reynolds number. For very low Prandtl numbers, the ratio of the Nusselt numbers tends to a limit as conduction becomes the predominant transfer mechanism in the turbulent core. This lower limit is difficult to specify briefly since it depends on the velocity distribution and so upon the effective Reynolds number. Considering conduction only, the typical magnitudes by Norris (4) are given in Table 2.

TABLE 2 NUSSELT NUMBERS

	Const. wall temp	Const. heat rate	Ratio
Parabolic velocity distribution.....	3.66	4.36	0.84
Constant velocity (plug flow).....	5.80	8	0.72

Since for turbulent flow the constant-velocity case is a somewhat better approximation to the actual velocity distribution than is the parabolic case, the minimum value of 0.73 for the ratio of Nusselt numbers as indicated in Table 1 appears to be in agreement with the limiting values as obtained from the analytical solution based on conduction alone.

The difference in temperature distributions indicated by the analysis of Martinelli for constant heat rate and by the present analysis for constant wall temperature is shown in Fig. 3. It is seen that for the same wall to center line temperature difference the heat-transfer rate is substantially less for the case of constant wall temperature. This does not exactly reflect the difference in the heat-transfer coefficients since the mean-temperature magnitudes are also different for the two solutions.

It has been demonstrated by Lyon (3) that for low Prandtl numbers, an equation of the type

$$\frac{hD}{k} = A + B\left(\frac{u_m D}{\alpha}\right)^n$$

with A, B, and n being arbitrary constants, serves as a fair correlation for the analytical results. Because of its simple form, it is a preferred working equation. Fig. 4 reveals the Nusselt numbers predicted by the present analysis compared to the equation

$$\frac{hD}{k} = 5.0 + 0.025\left(\frac{u_m D}{\alpha}\right)^{0.8} \quad \ldots\ldots\ldots\ldots [17]$$

The use of this equation for Prandtl numbers of less than $^1/_{10}$ provides Nusselt numbers agreeing with the theory within ±6 per cent.

The evaluation of the present analytical results by comparison with experimental data is rendered difficult since the effect is significant only for fluids of low Prandtl number, for which the available experimental data are meager.

Colburn and Coghlan (5) have reported heat-transfer coefficients for hydrogen-nitrogen mixtures under constant-wall-temperature conditions. Fig. 5 reveals these data in comparison to the predicted heat-transfer coefficients for constant wall temperature and constant heat rate, for a Prandtl number of 0.46.

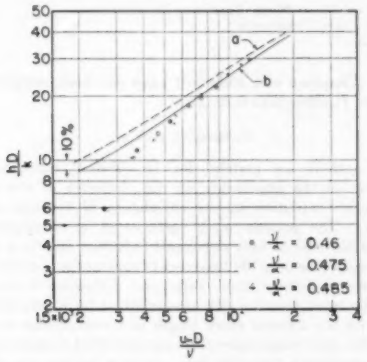

FIG. 5 NUSSELT NUMBER AS A FUNCTION OF REYNOLDS NUMBER FOR PRANDTL NUMBER 0.46

(a. For constant heat rate. b. For constant wall temperature, present analysis. The experimental results are those of reference 5.)

Good correspondence is obtained with the predicted Nusselt-number values for constant wall temperature for Reynolds numbers in excess of 6000. Below this the data depart from the predicted curve and this departure may perhaps be ascribed to transition effects.

A more critical test of the theory would be its comparison with data for fluids of very low Prandtl number, such as molten metals. Unfortunately, presently available data are not suitable for a critical comparison. The data of Styrikovich and Semenovker (6) for mercury were obtained for approximately constant heat-rate conditions but are far below the prediction of Martinelli (1). Musser and Page (7) present data in mercury, taken under conditions approximating an isothermal wall, but these data are also less than the prediction of the present theory. While the results of Styrikovich and Semenovker are higher than those of Musser and Page, this can hardly be construed as a check on the theory in view of the discrepancy between predicted and experimental heat-transfer coefficients.

CONCLUSIONS

1 The case of heat transfer to a fluid flowing turbulently in a smooth pipe with walls at constant temperature has been considered, and heat-transfer coefficients for fluids of Prandtl number less than 1.0 for this case have been shown to be significantly different from the case of constant heat rate as presented by Martinelli.

2 The Nusselt numbers obtained for the case considered can be obtained with an accuracy of ±6 per cent from the empirical equation

$$\frac{hD}{k} = 5.0 + 0.025\left(\frac{u_m D}{\alpha}\right)^{0.8}$$

for Prandtl numbers less than $^1/_{10}$.

3 The present results are in agreement with experimental data for a Prandtl number of 0.46 but data for lower Prandtl numbers are too meager to allow a discrimination between the constant-heat-rate and constant-wall-temperature cases.

ACKNOWLEDGMENT

The analysis and results reported in this paper were made possible through the sponsorship of the Office of Naval Research under Contract N7-ONR-29523, Phase 2, which is concerned with the investigation of heat transfer to molten metals. The contribution of the Office of Naval Research in this regard is gratefully acknowledged.

BIBLIOGRAPHY

1 "Heat Transfer to Molten Metals," by R. C. Martinelli, Trans. ASME, vol. 69, 1947, pp. 947–959.

2 "Heat Transfer Through Turbulent Friction Layers," by H. Reichardt, Technical Memo. No. 1047, NACA, September, 1943.

3 "Heat Transfer at High Fluxes in Confined Spaces," by R. N. Lyon, PhD thesis, University of Michigan, Ann Arbor, Mich., 1949.

4 "Laminar-Flow Heat-Transfer Coefficients for Ducts," by R. H. Norris and D. D. Streid, Trans. ASME, vol. 62, 1940, pp. 525–533.

5 "Heat Transfer to Hydrogen-Nitrogen Mixtures Inside Tubes," by A. P. Colburn and C. A. Coghlan, Trans. ASME, vol. 63, 1941, pp. 561–566.

6 "Heat Transfer to Fluids With Small Prandtl Moduli," by M. A. Styrikovich and I. E. Semenovker, *Journal of Technical Physics* (USSR), vol. 10, 1940, pp. 1324–1330.

7 "Heat Transfer to Mercury," by R. G. Musser and W. R. Page, MS thesis, Massachusetts Institute of Technology, Cambridge, Mass., 1947.

Discussion

MYRON TRIBUS.[4] This paper, together with others of which references[5,6] are suitable examples, emphasizes the importance of describing fully the nature of the surface temperature distribution in the flow direction when reporting heat-transfer data. The effects of surface temperature variation for the case of turbulent flow in a pipe are shown by the authors to be relatively small. However, it does not necessarily follow that similar results will occur for flow in a turbulent boundary layer over a flat plate. The authors' comments on this matter would be helpful.

In the case of a laminar boundary layer over a flat plate, the results of Chapman and Rubesin's analysis may be interpolated to show that the value of the unit thermal conductance (k_c) will be 13.5 per cent higher in the case of a constant heating rate,

[4] Assistant Professor of Engineering, University of California, Los Angeles, Calif.; Consultant in Heat Transfer to the General Electric Company, Aircraft Gas Turbine Division, Lynn, Mass. Jun. ASME.

[5] "Temperature and Velocity Profiles in the Compressible Laminar Boundary Layer With Arbitrary Distribution of Surface Temperature," by D. R. Chapman and M. W. Rubesin, *Journal of the Aeronautical Sciences*, vol. 16, September, 1949, p. 547.

[6] "Contributions to the Theory of Heat Transfer Through a Laminar Boundary Layer," by M. J. Lighthill, Proceedings of the Royal Society of London, series A, vol. 202, August 7, 1950, p. 1070.

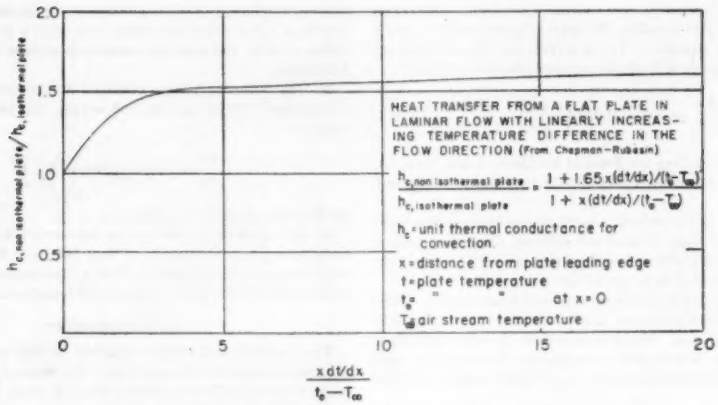

FIG. 6 HEAT TRANSFER FROM A FLAT PLATE IN LAMINAR FLOW WITH LINEARLY INCREASING TEMPERATURE DIFFERENCE IN THE FLOW DIRECTION
(From Chapman-Rubesin.)

as compared to an isothermal surface. Norris and Streid (authors' reference 4) compute a difference of 12 per cent for laminar flow in a pipe for constant wall temperature compared to constant heating rate.

Quite often end effects cause heat conduction and resulting nonuniform temperatures in the vicinity of the leading edge of experimental apparatus. In such cases the measured value of h_c may be radically affected because of the temperature gradient. Fig. 6, herewith, shows a graph which illustrates this effect for the case of the flat plate in laminar flow and having a linear temperature variation with distance from the leading edge.

The plate temperature is taken as

$$t = t_0 + \left(\frac{dt}{dx}\right)x$$

where

(dt/dx) = plate temperature gradient = const
t_0 = plate temperature at $x = 0$

The analysis of Chapman and Rubesin[5] leads to

$$q = -\frac{k}{2x}\mathbf{R}_x^{1/2}\left[Y_0'(0)(t_0 - T_\infty) + Y_1'(0)\left(\frac{dt}{dx}\right)x\right]$$

If the plate were at uniform temperature, t_0

$$q = -\frac{k}{2x}\mathbf{R}_x^{1/2}Y_0'(0)(t_0 - T_\infty)$$

If the unit thermal conductance is defined everywhere by

$$h_c = q/(t - t_\infty)$$

then

$$\frac{h_{c,\text{nonisothermal}}}{h_{c,\text{isothermal}}} = \frac{1 + \dfrac{Y_1'(0)}{Y_0'(0)}\dfrac{x}{t_0 - T_\infty}\dfrac{dt}{dx}}{1 + \dfrac{x}{t_0 - T_\infty}\dfrac{dt}{dx}}$$

Using Chapman and Rubesin's results for $Y_0'(0)$ and $Y_1'(0)$ Fig. 6 was constructed. Unfortunately, the equations for $Y_1'(0)$ (Chapman and Rubesin[5]) have not been integrated for values of P_r other than 0.72 (air).

AUTHORS' CLOSURE

The authors are grateful for Dr. Tribus' comments and emphasis on the importance of the character of the surface temperature variation in the calculation of the rate of heat transfer. The present work endeavored to emphasize this effect in the case of fully developed turbulent flow in a circular pipe, considering only the two cases of constant wall temperature and linear wall-temperature variation. Extension of this work would be most conveniently accomplished by superposition of results for the thermal entry length under conditions of a unit rise in the wall temperature from the zero fluid temperature, for a fully developed turbulent flow. In this manner the effect of an arbitrary variation in the wall temperature might be considered. Unfortunately, solutions of this type must be evaluated numerically and are not widely available.

The comparison of the results for pipe flow with those for the boundary layer upon a flat plate does not appear to be too fruitful because of the essential difference in the constancy of the temperature at the outer edge of the boundary layer and the variability of the center-line temperature in a pipe flow. Further, the flow conditions in the pipe are essentially related to the conditions at one fixed point on the plate, only for turbulent flow, and it does not appear that similar results are expected for the two systems. For example, for a Prandtl number near unity, the present analysis indicates but a slight difference between the heat-transfer coefficient for constant and linearly varying pipe-wall temperature. For the turbulent boundary layer on the plate, the superposition of the results for the effect of a step function in the wall temperature as given by Rubesin,[7] indicates that the local heat-transfer coefficient for a linear variation in wall temperature should be 20 per cent higher than that obtaining for a constant wall temperature. A similar effect obtains in laminar flow, where as noted, the local heat-transfer coefficient for flow in a pipe with linear variation of the wall temperature

[7] "An Analytical Investigation of Convective Heat Transfer From a Flat Plate Having a Stepwise Discontinuous Surface Temperature," by M. W. Rubesin, (Abstract) *Mechanical Engineering*, vol. 71, January, 1949, p. 46.

exceeds that for constant wall temperature by 12 per cent, whereas on the plate the coefficient for a linear variation of wall temperature exceeds that for constant wall temperature by 65 per cent, as illustrated by the asymptotic behavior of the curve of Fig. 6.

As noted, this comparison of pipe and plate is hardly significant except to indicate the general effect of wall temperature variation on the heat-transfer rate. The difference between the boundary layer and pipe flow is further emphasized in that the linear wall-temperature variation as just considered produces a constant wall heat rate for the pipe flow but not for the boundary-layer flows.

Basic Study for a Generating Station

By G. R. MILNE,[1] NEW YORK, N. Y.

This paper gives the results of cost studies made to determine the most economical size and type of boiler and turbogenerator unit to be used in a new generating station for the Consolidated Edison Company of New York, Incorporated. Some of the factors considered include the economical capacity of the unit; single boiler versus two boilers per turbine; unit-type design versus a common steam-header system and reheat versus nonreheat units. Related factors were the number and type of feedwater heaters and alternate arrangements of boiler feed pumps.

THE Consolidated Edison system experienced a 1-hr net peak load of 2241 megawatts during the summer of 1950 and will have a winter peak in the same year of about 2620 megawatts. To provide for the rapidly expanding load, the company is initiating the development of a new generating station on the East River in the Borough of Queens with an ultimate capacity of about 1000 megawatts. A cost study was made to determine the economical size and type of boiler, turbogenerator and related equipment for this station, and the results of this study as given herein may prove of interest to others. However, before a final comparison can be made with the results of studies on other systems, consideration must be given to the differences in system load and load factor and to both fuel and construction costs in the area in which the plant is located.

Equipment Factors Studied

The following factors are reported herein:

1 Size of turbogenerator unit. Three sizes of unit were studied, namely, units of 80, 110, and 160 megawatts maximum rated capability. Units larger than 160 megawatts were not considered because the system already had some units of this capacity, and units of materially increased rating would be burdened with a higher system reserve.

2 Single boiler versus two boilers per unit. In the case of the 160-megawatt units operating on the unit-type system with no reheat, arrangements were estimated for both single boiler and two boiler per turbine combinations. The operating complications using reheat cycles on multiple boilers per turbine or on steam-header systems are such as to make such arrangements impractical and they were not estimated.

3 Tandem versus cross-compound units. The 80-megawatt and 110-megawatt units studied were all tandem-compound whereas proposals were obtained for both tandem and cross-compound units in the 160-megawatt capacity.

4 Nonreheat cycles, unit system, single boiler per unit. For nonreheat units operating at 1050 degrees F, 1450 psi was considered the upper limit of pressure as this cycle produces about 12.5 per cent moisture at the exhaust of the turbine. This cycle was compared with the 1250-psi 950 F cycle for a number of boiler arrangements.

5 Common steam-header versus unit-type design. In order to make cost comparisons between arrangements using a common steam header and the unit-type design, two variations of the steam header were studied. In one arrangement all boilers were made oversize, so that upon the outage of one boiler the remaining boilers would be paralleled on the header so as to operate all of the turbogenerators with the remaining boilers operating at maximum rated capability. The alternate arrangement provides a spare boiler of the same size as the other units together with a header of the transfer type so that segregated operation can continue even during the outage of a boiler. At the higher temperatures and pressures being considered, segregated operation of the units is preferable whenever this is possible.

6 Reheat versus nonreheat units. Sufficient cases were estimated on nonreheat units operating at throttle pressure from 1250 to 1450 psi and temperatures from 950 to 1050 F to enable comparison with reheat units ranging in pressure from 1450 to 2200 psi and in temperature from 950 to 1050 F. Comparisons were made for fuel costs of 30 cents and also 40 cents per million Btu but only the latter are reported herein. In addition, for the reheat cycles the cost of fuel necessary over the life of the equipment to justify the installation of the higher pressures and temperatures are also shown.

7 Feedwater heating arrangements. The installed cost and relative economy of five, six, seven, and eight stages of feedwater heating were considered with one of these stages always being a deaerator. Both open and closed-type heaters below the deaerator were studied. In addition, parallel trains of closed heaters above the deaerator were compared with arrangements having a single train of closed heaters with one additional heater in the train and with individual by-passes around each heater or a single by-pass around the entire group.

8 Boiler feed pumping arrangements. The arrangement employing a single boiler feed pump with all closed heaters above the deaerator operating at boiler pressure was compared to the combination of booster pumps ahead of the boiler feed pumps with the closed heaters in between these pumps so as to operate the heaters at relatively low pressure.

Basic Assumptions

In order to simplify the studies and reduce the number of cases to be studied to a practical figure, the following assumptions were made to determine items 1 to 6 in the foregoing.

1 Feedwater temperature entering boiler was assumed to be 450 F.

2 Feed heating would be done in six stages with approximately equal increments of enthalpy.

3 Use of condensate for oil coolers, air-ejector condensers, and gas coolers would not be considered in the comparative studies because of their negligible effect on the differential heat rates.

4 From study of a recent unit, 1 in. Hg back pressure with 45 F circulating water was assumed to be economical.

5 Motor-driven auxiliaries would be used throughout, and condensate and feed pumps would be provided with a stand-by pump.

6 Auxiliary power requirements were initially assumed at 7 per cent of the gross generated output for computation of heat rates.

7 After discussion with the boiler and turbine manufacturers

[1] Mechanical Engineer, Consolidated Edison Company of New York, Inc. Mem. ASME.

Contributed by the Power Division and presented at the Annual Meeting, New York, N. Y., November 26–December 1, 1950, of The American Society of Mechanical Engineers.

Note: Statements and opinions advanced in papers are to be understood as individual expressions of their authors and not those of the Society. Manuscript received at ASME Headquarters on September 19, 1950. Paper No. 50—A-87.

as to the availability, cost, and present practicability of units for operation at 1100 and 1200 F, it was decided to limit the study to maximum steam temperatures of 1050 F.

Data Considered

Performance data, dimensions, and prices were obtained from the manufacturers on boilers, the various sizes and types of turbogenerators, condensers, boiler feed pumps, closed feedwater heaters, direct-contact heaters, deaerators, forced and induced-draft fans, and fly-ash precipitators for the various cases. In addition to these data, the other variable cost items estimated were main and reheat steam piping, boiler feed piping, building, building foundations, equipment foundations and supports, electric drives, electric auxiliary supply, and high-tension connections. Items common to all cases, or of comparatively equal cost, were not considered and are not included in the estimates. Such items are dock facilities, coal and ash-handling equipment, building services and service building, stacks, flues, low-pressure piping, condensate pumps, and cranes.

Evaluation of Heat Rates

For evaluation of heat-rate differences, fuel was assumed to cost 30 cents, and also 40 cents per million Btu, but only the latter figure will be reported herein. The load factor of the system would permit the initial annual loading of this unit as follows:

Full load	5000 hr
3/4 load	1500 hr
1/2 load	1000 hr

To capitalize the fuel savings the first year's fuel cost was multiplied by the factor 6.25.

Cost of Variable Items

In addition to equipment prices obtained from the manufacturers, diagrams of steam and high-pressure feedwater piping with estimated sizes, lengths, and costs were made. Also a number of plant-arrangement drawings were prepared showing in plans and elevations the relative location of equipment and thereby space required for the alternative cases so as to give relative building costs.

Operating Labor Differentials

The general-arrangement drawings were submitted to the company's operating group so that they might estimate the operating labor requirements for each case. Because of the proposed arrangement of equipment and the liberal use of alarms and remote indications, the number of fixed-post operators was reduced to a minimum. This report indicates that operating labor differential is influenced only by the number of turbogenerators and boilers.

Maintenance Differentials

As no plants have been operated at 1050 F and at the extreme high pressures for any long period, no background of maintenance experience is available for some of the cases studied. However, a study of the maintenance costs on high-pressure boilers and turbine generators operated by this company, as well as other utilities, leads to the following assumptions:

1 A two-boiler installation will require 50 per cent more boiler-plant maintenance, including auxiliaries, than will a one-boiler installation for the same steam conditions and total capacity.

2 Turbine-generator maintenance will vary as follows:

80 megawatt, tandem compound, 100 per cent
110 megawatt, tandem compound, 105 per cent
160 megawatt, tandem compound, 110 per cent
160 megawatt, cross-compound, 125 per cent

3 A boiler and turbine operating at 1250 psi 950 F will not result in any savings in maintenance as compared to units using cycles at higher temperatures and pressures.

4 Subject to the foregoing variations, maintenance costs for the turbogenerators were based upon 2 cents per year per lb of throttle flow. For the boiler plant, the maintenance costs were based upon heat input to the boiler, with cost of 9 cents per year per lb of steam output for a single nonreheat boiler being taken as standard. Of the 9 cents per year per lb of steam flow, 4.2 cents is for the boiler and 4.8 cents for related boiler equipment. Since no data were available on the relative maintenance costs of reheat versus nonreheat boilers, it was assumed that a reheat boiler would require 10 per cent more maintenance than a nonreheat boiler. In the case of the turbine no difference in maintenance costs was assumed between reheat or nonreheat units as the extra complication of the reheat arrangements would be offset by lower maintenance resulting from relatively drier steam at the exhaust end. Electrical maintenance costs were estimated for the electric auxiliaries and the generator high-tension connections, including the 13.8-kv to 132-kv transformers.

Electrical Demand and Capitalized Energy Charges

The cost of power for the various cases was estimated using a capitalized energy charge of $134 and a demand charge of $150 per hp.

Reserve Capacity Costs

The arrangement of plant, i.e., size of turbogenerators, size and number of boilers, and whether a unit or steam-header-type system is used, determines the amount of additional system reserve which should be installed for the ultimate plant, and the cost of this reserve is a justified charge against each scheme. However, the additional installed reserve capacity is available the greater part of the year for economical generation, and each scheme is credited with the fuel savings resulting from this reserve capacity and based upon the difference between its own heat rate and the average system heat rate for that period of operation. The reserve-capacity requirements are given in Table 2.

To evaluate items 1 to 6 mentioned previously, only a limited number of cases were studied for each item. Even with this limitation, thirty-two arrangements were calculated and estimated, and the results are shown in Table 1. This table gives the calculated station heat rate for each case, the capitalized value of the heat rate, the variable costs of installed equipment, the variable operating-labor costs, the variable maintenance costs, the capitalized costs of electric auxiliary power both energy and demand, the net reserve-capacity costs, and the total evaluated costs which are the sums of the previous items.

Results

For the purpose of placing the differentials on a percentage basis, the estimated installed cost of the completed plant, including coal-handling and burning facilities, would approximate $200 per kw of installed capacity based upon present-day prices. The data in Table 1 show the following:

Size of Turbogenerator. Comparing cases 5 and 6 against 17 and 18, the cost differentials in favor of 160-megawatt units range from 5 to 6 1/2 per cent when compared to 110-megawatt units. Comparing cases 5 and 6 with cases 19 and 20, the differentials in favor of the 160-megawatt as against the 80-megawatt units is about 12 per cent.

TABLE 1 SUMMARY OF COST DIFFERENTIALS

				Heat rate, Btu per kwhr	Heat Rate differences, $ per kw	*Cost of installed equipment $ per kw	*Estimated operating labor costs, $ per kw	Estimated maintenance costs $ per kw	*Estimated electrical demand and capitalized energy charges		Net reserve capacity costs, $ per kw	*Compilation of costs, $ per kw	Cost differentials, $ per kw
									Demand charges, $ per kw	Energy charges, $ per kw			
Case 1	160 Mw XC 1800 psi	1050 F—1000 F—1 boiler per unit		9283	1.09	161.63	3.65	5.47	9.87	8.94	14.53	205.18	1.50
Case 2	160 Mw XC 2000 psi	1050 F—1000 F—1 boiler per unit		9222	.08	164.19	3.65	5.42	9.87	8.94	14.53	206.68	3.00
Case 3	160 Mw TC 1800 psi	1050 F—1000 F—1 boiler per unit		9278	1.01	165.96	3.65	5.36	9.87	8.94	14.53	209.32	5.64
Case 4	160 Mw TC 2000 psi	1050 F—1000 F—1 boiler per unit		9217	0	168.90	3.65	5.32	9.87	8.94	14.53	211.21	7.53
Case 5	160 Mw XC 1450 psi	1050 F—	1 boiler per unit	9758	8.96	160.82	3.65	5.68	9.84	8.94	14.95	212.84	9.16
Case 6	160 Mw XC 1250 psi	950 F—	1 boiler per unit	10108	14.76	158.43	3.65	5.92	9.84	8.94	15.32	216.86	13.18
Case 7	160 Mw TC 1450 psi	1050 F—	1 boiler per unit	9820	9.99	165.00	3.65	5.56	9.84	8.94	14.95	217.93	14.25
Case 8	160 Mw TC 1250 psi	950 F—	1 boiler per unit	10205	16.36	161.73	3.65	5.81	9.84	8.94	15.32	221.65	17.97
Case 9	160 Mw XC 1450 psi	1050 F—	2 boilers per unit	9758	8.96	177.67	3.65	7.80	9.80	8.87	10.89	227.64	23.96
Case 10	160 Mw XC 1250 psi	950 F—	2 boilers per unit	10108	14.76	174.56	3.65	8.11	9.80	8.87	11.08	230.83	27.15
Case 11	160 Mw TC 1450 psi	1050 F—	2 boilers per unit	9820	9.99	174.02	3.65	7.69	9.80	8.87	10.89	224.91	21.23
Case 12	160 Mw TC 1250 psi	950 F—	2 boilers per unit	10205	16.36	170.74	3.65	8.02	9.80	8.87	11.08	228.52	24.84
Case 13	160 Mw XC 1450 psi	1050 F—	2 oversized boilers per unit on header	9758	8.96	184.72	3.65	7.80	9.80	8.87	—0.08	223.72	20.04
Case 14	160 Mw XC 1250 psi	950 F—	2 oversized boilers per unit on header	10108	14.76	179.41	3.65	8.07	9.80	8.87	—0.07	224.49	20.81
Case 15	160 Mw TC 1450 psi	1050 F—	2 oversized boilers per unit on header	9820	9.99	177.13	3.65	7.69	9.80	8.87	—0.08	217.05	13.37
Case 16	160 Mw TC 1250 psi	950 F—	2 oversized boilers per unit on header	10205	16.36	175.48	3.65	8.02	9.80	8.87	—0.07	222.11	18.43
Case 17	110 Mw TC 1450 psi	1050 F—	1 boiler per unit	9976	12.57	174.70	4.29	7.33	10.35	9.38	7.45	226.07	22.39
Case 18	110 Mw TC 1250 psi	950 F—	1 boiler per unit	10386	19.36	168.34	4.29	7.66	10.35	9.38	7.59	226.97	23.29
Case 19	80 Mw TC 1450 psi	1050 F—	1 boiler per unit	10178	15.92	181.55	5.53	9.42	10.31	9.35	6.15	238.23	34.55
Case 20	80 Mw TC 1250 psi	950 F—	1 boiler per unit	10598	22.87	176.74	5.53	9.86	10.31	9.35	6.15	240.81	37.13
Case 21	160 Mw XC 1450 psi	1050 F—	1 oversized boiler per unit on header	9758	8.96	170.98	3.65	5.68	9.84	8.94	0.25	208.30	4.62
Case 22	160 Mw XC 1250 psi	950 F—	1 oversized boiler per unit on header	10108	14.76	168.16	3.65	5.92	9.84	8.94	0.28	211.55	7.87
Case 23	160 Mw TC 1450 psi	1050 F—	1 oversized boiler per unit on header	9820	9.99	174.54	3.65	5.56	9.84	8.94	0.25	212.77	9.09
Case 24	160 Mw TC 1250 psi	950 F—	1 oversized boiler per unit on header	10205	16.36	171.69	3.65	5.81	9.84	8.94	0.28	216.57	12.89
Case 25	160 Mw XC 1450 psi	1050 F—	1 boiler per unit with add'l b'l'r on h'd'r	9758	8.96	174.92	3.65	6.38	9.84	8.94	0.09	212.78	9.10
Case 26	160 Mw XC 1450 psi	1050 F—	2 boilers per unit, add'l b'l'r on h'd'r	9758	8.96	186.22	3.65	8.32	9.80	8.87	0.09	225.91	22.23
Case 27	160 Mw XC 1450 psi	1050 F—1000 F—1 boiler per unit		9415	3.28	159.95	3.65	5.61	9.87	8.94	14.71	206.01	2.33
Case 28	160 Mw XC 1450 psi	1000 F—1000 F—1 boiler per unit		9476	4.29	158.11	3.65	5.63	9.87	8.94	14.71	205.20	1.52
Case 29	160 Mw XC 1450 psi	950 F— 950 F—1 boiler per unit		9611	6.53	155.21	3.65	5.64	9.87	8.94	14.84	204.68	1.00
Case 30	160 Mw XC 1800 psi	1000 F—1000 F—1 boiler per unit		9335	1.95	159.12	3.65	5.55	9.87	8.94	14.60	203.68	0
Case 31	160 Mw XC 1650 psi	1000 F—1000 F—1 boiler per unit		9425	3.45	158.69	3.65	5.60	9.87	8.94	14.71	204.91	1.23
Case 32	160 Mw XC 2200 psi	1050 F—1000 F—1 boiler per unit		9138	—1.31	166.23	3.65	5.44	9.87	8.94	14.36	207 08	3.40

Notes:
Fuel cost—$0.40 per million Btu
Operation—6625 hr per year at full load (weighted)
Capitalization factor—6.25

All cases 1 in. Hg back pressure
XC, cross-compound
TC, tandem-compound

* Cost items common to all cases are omitted.

TABLE 2 RESERVE CAPACITY REQUIRED

	Group		Cases 1 to 8 Cases 27 to 32 6 Units 6 Boilers	Cases 21 to 24, inclusive 6 Units 6 Oversized boilers on common header	Case 25 6 Units 7 Boilers on common header	Cases 9 to 12, inclusive 6 Units 12 Boilers	Cases 13 to 16, inclusive 6 Units 12 Oversized boilers on common header	Cases 17 and 18 9 Units 9 Boilers	Cases 19 and 20 12 Units 12 Boiler
1	Proposed plant capacity	Mw	960	960	960	960	960	990	960
2	Required system reserve capacity	Mw	554	502	501	529	500	520	500
3	Reserve capacity added to system by installation	Mw	109	57	56	84	55	73	55
4	Increase in peak demand provided by installation	Mw	851	903	904	876	905	915	905
5	Outage for scheduled overhaul:								
	(a) Turbines—6 weeks/year on 5-year schedule	Mw-Mos	265.8	265.8	265.8	265.8	265.8	274.2	265.8
	(b) Boilers—2 weeks/year on yearly schedule	Mw-Mos	354.5	0	0	354.5	0	365.5	354.5
	(c) Total	Mw-Mos	620.3	265.8	265.8	620.3	265.8	639.7	620.3
	(d) Equivalent annual capacity	Mw	51.7	22.2	22.2	51.7	22.2	53.3	51.7
6	Equivalent peak demand provided by installation	Mw	799.3	880.8	881.8	824.3	882.8	861.7	853.3
7	Equivalent plant capacity required for equal peak demand and service reliability	Mw	1043.4	962.0	961.0	1018.5	960.0	1011.	989.5
8	Equivalent annual generation	10^6 Kwhr	6487	6174	6168	6331	6162	6285	6151

NOTE: Based on forced outage rate of 2 per cent.

TABLE 3 COMPARISON OF BREAK-EVEN FUEL COST FOR REHEAT CYCLES

				Net station heat rate Btu per kwhr	Evaluated costs without fuel	Break-even fuel cost-cents/10^6 Btu
Case 29	160Mw XC 1450 psi	950 F-950 F	1 in. Hg 1 boiler per unit	9611	198.15	...
Case 30	160Mw XC 1800 psi	1000 F-1000 F	1 in. Hg 1 boiler per unit	9335	201.72	31.2
Case 31	160Mw XC 1650 psi	1000 F-1000 F	1 in. Hg 1 boiler per unit	9425	201.45	42.8
Case 1	160Mw XC 1800 psi	1050 F-1000 F	1 in. Hg 1 boiler per unit	9283	204.09	43.7
Case 28	160Mw XC 1450 psi	1000 F-1000 F	1 in. Hg 1 boiler per unit	9476	200.91	49.4
Case 32	160Mw XC 2200 psi	1050 F-1000 F	1 in. Hg 1 boiler per unit	9138	208.38	52.2
Case 2	160Mw XC 2000 psi	1050 F-1000 F	1 in. Hg 1 boiler per unit	9222	206.60	52.5
Case 27	160Mw XC 1450 psi	1050 F-1000 F	1 in. Hg 1 boiler per unit	9415	202.73	56.4

Single Boiler Versus Two Boilers per Unit. Comparing case 5 with 9, 6 with 10, 7 with 11, and 8 with 12 shows the single-boiler per unit arrangement to be lower in evaluated costs by differentials ranging from 3.5 to 7.5 per cent.

Cross-Compound Versus Tandem-Compound Units. Comparing 5 and 6 with 7 and 8, the differentials in favor of the cross-compound unit, based upon single boiler per turbine arrangement are of the order of $2^1/_2$ per cent of the station cost. However, even at the same total evaluated costs, cross-compound units of this size having a quadruple exhaust would be preferred to the tandem-compound units which have a triple exhaust, since the former is more likely to provide a higher overload capacity.

Nonreheat Cycles Unit System Single Boiler per Turbine. Comparing case 5 with 6, 9 with 10, 7 with 8, and 11 with 12 shows differentials of 1.5 to 2 per cent in favor of the 1450-psi 1050-F cycle, and hence this cycle was used for comparison with steam-header-type systems and also with the reheat cycles.

Common Steam-Header Versus Unit-Type Systems. Comparing case 5 with case 30 shows that the most economical nonreheat cycle is about $4^1/_2$ per cent higher on evaluated cost than this reheat cycle. Again comparing case 30 with cases 21, 22, and 25 shows differentials against the header-type system of about $2^1/_2$ to 4 per cent if oversize boilers are used and about $4^1/_2$ per cent if a spare boiler is employed. Even though the header system were equal in cost to a unit system, the latter would be preferred. Since a period of years would elapse between the installation of the first and last units, the adoption of the unit-type system would permit taking advantage of the improvement of the art in the interim. Again the station reliability provided by a header system of reasonable cost can approach but would not exceed that of a unit system.

Most Desirable Reheat Cycle. Having found that a reheat cycle is justified, the determination as to how high to go on pressure and temperature in the choice of a reheat cycle to meet the operating conditions of a system will depend in part on the assumption as to what the future average fuel costs will be over the life of the equipment in the area where the unit is to be installed. For our system we have assumed this fuel cost to be 40 cents per million Btu. In Table 3 there is given the break-even fuel cost for the various reheat cycles studied, using the reheat cycle of lowest first cost and highest relative heat rate as base, namely, the 1450-psi, 950 F–950 F cycle. With an assumed fuel cost of 40 cents per million Btu, it follows that the 1800-psi, 1000 F–1000 F cycle was selected. Therefore the arrangement finally selected was a 160-megawatt, 3600/3600-rpm cross-compound unit, operating on a unit-type system with a single boiler per turbine and with a reheat cycle using 1800-psi, 1000 F steam at the throttle and 1000 F for reheat temperature. The unit will have equal division of load at maximum rating, between the high and low-pressure shafts, will be designed with a quadruple exhaust, and will have duplicate and interchangeable generators.

Feedwater-Heating Arrangements. After the basic cycle had been determined, the economics of feedwater-heating arrangements were investigated using differing numbers of heaters of both the open and closed type as shown in Table 4.

TABLE 4 FEEDWATER-HEATING ARRANGEMENTS

No. of heaters	High-pressure closed heaters	Deaerator	Low-pressure heaters	Heat rate 3 deg F TD*	Heat rate 6 deg F TD	Heat rate 10 deg F TD
5	2 pairs	1	2 open	9264	...	...
6	2 pairs	1	3 open	9237	...	...
7	2 pairs	1	4 open	9218	...	...
8	3 pairs	1	4 open	9203	...	...
5	2 pairs	1	2 closed	...	9274	9288
6	2 pairs	1	3 closed	...	9250	9267
7	2 pairs	1	4 closed	...	9232	9250
8	3 pairs	1	4 closed	...	9218	9237

* TD = terminal difference.

Fig. 1 gives the results of this study. Based upon fuel at 40 cents per million Btu and 6 F terminal difference in the closed heaters, the cycle using seven stages of heating with closed heaters both above and below the deaerator is justified. However, if 10 F terminal difference is assumed, the cycles employing 6 and 7 heaters with open heaters below the deaerators are equal in cost and are about 7 per cent less in cost than the 7-heater cycle using all closed heaters. In the foregoing costs, closed heaters have been included having 30 per cent more transfer surface than the normal heater, in order to keep the terminal difference low in service. Because of this fact and because of their operating simplicity, it was decided to use a 7-heater arrangement with all heaters above and below the deaerator of the closed type.

Boiler-Feed-Pumping Arrangements. A comparison was made between an arrangement having a single set of boiler feed pumps with the heaters above the deaerator operating at boiler pressure versus an arrangement using booster pumps to pass the water through the heaters, followed by boiler feed pumps. Alternate arrangement of heaters above the deaerator were studied using two sets of two heaters each in series without any by-pass, one set of three heaters in series with individual heater by-passes and one set of three heaters with one by-pass around all the heaters. The results are shown in Table 5.

Since the arrangement using two sets of boiler feed pumps with heaters operating at low pressure was about 26 to 30 per cent higher in evaluated cost, as compared to the arrangement using high-pressure heaters and a single set of boiler feed pumps, the latter arrangement was selected. The lower cost is due primarily to the smaller amount of power required for pumping when all pumping is done at the lower temperature. As regards the arrangement of the 2200-psi heaters, the single by-pass around all heaters did not save sufficient money to justify its operating disadvantages with one heater defective. Since the parallel heater arrangement is slightly less costly than the three-heater arrangement with individual by-pass, it was decided to continue our previous practice of using parallel trains above the deaerator.

TABLE 5 SUMMARY OF COSTS OF PUMPS AND HEATERS

	500-psi heaters, $/kw: 2 pairs in parallel	500-psi heaters, $/kw: 3 single, individ. heater by-pass	500-psi heaters, $/kw: 3 single, by-pass around all htrs	2200-psi heaters, $/kw: 2 pairs in parallel	2200-psi heaters, $/kw: 3 single, individ. heater by-pass	2200-psi heaters, $/kw: 3 single, by-pass around all htrs
Installed cost	4.51	4.75	4.59	4.69	5.16	4.90
Added pump power	1.76	1.76	1.76	...	...	...
Capitalized maintenance:						
Booster pump	0.16	0.16	0.16	...	...	...
Heaters	0.06	0.05	0.05	0.13	0.09	0.09
Acid cleaning	0.16	0.12	0.12	0.16	0.12	0.12
Heat rate	0.31	...	...	0.31	...	...
Total costs	6.96	6.84	6.68	5.29	5.37	5.11

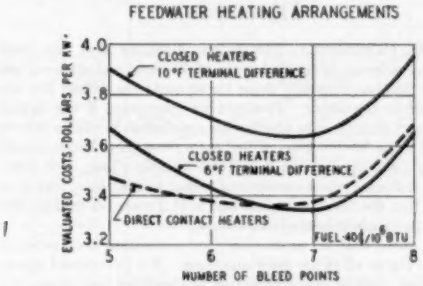

Fig. 1 Comparison of Evaluated Costs

Arrangement Selected

The cycle selected for the new station is shown in Fig. 2. This cycle has a theoretical net heat rate of 9335 Btu per kwhr, excluding certain losses. When these station losses including blowdown,

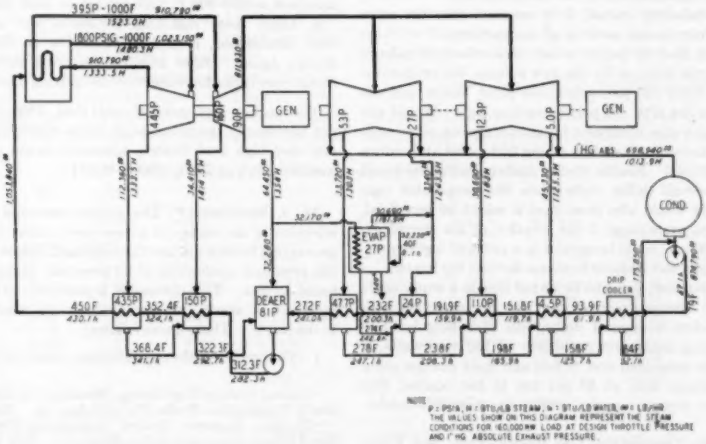

Fig. 2 Heat-Balance Diagram

steam for atomizing oil burners, general building services are considered, the actual net station heat rate should approximate 9700 Btu per kwhr.

ACKNOWLEDGMENTS

Because of the large number of contributors to this study, space does not permit individual listing, but the author wishes to thank the many manufacturers for the complete and extensive data furnished, and also the various departments of the Consolidated Edison Company for the help they gave in the preparation of these data.

Discussion

R. C. DANNETTEL.[3] The author indicates that his comparisons were made for fuel costs of 30 cents and 40 cents per million Btu but that only those for 40 cents per million Btu are reported in the paper. It would be interesting if the author would give an idea as to whether his conclusions would have been altered if the 30-cent level of fuel costs per million Btu had been used to make the decision. In Table 3 of the paper, such selection is indicated when considering reheat cycles alone, and it is shown that the break-even fuel cost is 31.2 cents per million Btu for the particular reheat cycle selected.

It is noted that the author has used a constant back pressure of 1 in. Hg in all of his determinations. For year-round operation, there may be some reduction in the differences shown between the cross-compound quadruple-flow machines and the tandem-compound triple-flow machines because of the lessening of the effect of leaving loss as back pressure increases, it being assumed that a back pressure of 1 in. Hg cannot be maintained during the entire year. This further assumes, of course, that the last-row bucket or blade lengths are the same in both types of machines.

It is also noted that in all cases, operation was equivalent to 6625 hr per year at full load which would approximate 75 to 76 per cent annual load factor. In similar studies made for the Baltimore system, a much lower load factor of about 57 per cent was used. It is no doubt true that the high load factor assumed in the author's studies would obtain over the early years of operation but it seems a little doubtful as to whether such a high average would be maintained over the life of the unit.

Although not definitely stated, it is assumed that the same over-all boiler efficiency was used for all comparisons.

Referring to Fig. 2 of the paper, which shows the heat-balance diagram for the cycle selected for the new station, the evaporator is supplied with third (90 psi) extraction-point steam and delivers its vapor to the fifth (27 psi) extraction line. Would not the use of an evaporator condenser be advantageous, since such procedure would increase extraction at the fifth point and reduce it at the fourth (53 psi)? Similar studies made in Baltimore would indicate lower over-all dollar costs when the evaporator condenser is used. It would also seem that it might be beneficial, steam temperature permitting, if the location of the second extraction point (160 psi) could be moved to a point of higher pressure so as to give a better balance between the two top heaters.

As a matter of interest, it might be stated that in a study made for the Baltimore system about a year ago in connection with 80-megawatt tandem-compound units with 23-in-long last-row buckets, and having maximum capability of 100 megawatts, it was found that the combined cost of fuel and fixed charges using 13,000-Btu per pound coal, at $7 per ton in the bunker, was a stand-off when comparing the 1450-psig 1050 F straight-condensing design with 1450-psig 1000 F/1000 F reheat design. With coal at $8.35 per ton the reheat job showed a savings of 0.3 per cent and, for $10.00 coal, about 0.54 per cent. In these studies a generation of 500 million kwhr per year average over the life of the machine was used and was weighted for variable-load operation. This would give about 57 per cent average annual load factor over the life of the unit. Fixed charges of 15 per cent were used in the studies. In view of the very small advantage for the reheat design, and applying considered judgment that maintenance costs and operating complication would be less than for a reheat design, it was decided to proceed with the 1450-psig, 1050-F straight-condensing arrangement.

It would be interesting to have the author give some idea as to the number of men who were kept busy, and for how long, in making this very excellent study in connection with capacity additions to the Consolidated Edison System. Such determinations are painstaking and necessitate considerable effort and co-operation on the part of the investigator and manufacturers alike if the results are to be worthy of the time expended.

H. R. REESE.[3] The author has done considerable work in compiling a vast amount of data which should be found very valuable to designers of central-station power plants. Of particular interest is the column of cost differentials in Table 1, where one can quickly compare the influence of steam conditions, turbine size, and boiler arrangement.

We agree with the author's selection of 1800–1000 F–1000 F steam conditions for the following reasons:

1 Steam temperature of 1000 F is about as high as is practical to go with ferritic materials which are relatively easily procured.

2 Also, there are about 15 years of experience in the handling of ferritic materials. Steam conditions of 1800–1000 F–1000 F ease the problems from a material standpoint, although we can point to satisfactory operation of 1050-F machines using austenitic material.

3 If higher steam conditions can be justified, austenitic materials are required. With columbium already restricted, the use of the austenitic material will be limited.

4 We believe that 1800–1000 F–1000 F should be given consideration for the next higher steam conditions for the standardized unit. This pressure and temperature seems to be as well matched as 850–900 F, 1250–950 F, or 1450–1000 F.

5 Once these matching pressures and temperatures have been established, it is unnecessary to go through engineering studies again. Other utilities can order turbines to the same steam conditions knowing they are getting a balanced design.

The author has pointed out that 1800–1000 F–1000 F is not necessarily the ultimate in steam conditions. For high fuel cost and high load factors, advanced steam conditions may be justified, such as 2300–1100 F–1050 F.

M. J. STEINBERG.[4] The author describes the basis for the selection of the design of a new power plant to be added to the generating facilities of the Consolidated Edison System, involving the economic evaluation of 32 proposals grouped under 7 major basic designs. This discussion is presented to provide additional information about two items which are mentioned but briefly in the paper. These are as follows:

1 Derivation of the capitalization factor of 6.25.

[2] Senior Engineer, Consolidated Gas Electric Light and Power Company of Baltimore. Mem. ASME.

[3] Central Station Engineering, Westinghouse Electric Corporation, South Philadelphia Works, Philadelphia, Pa. Mem. ASME.

[4] Division Engineer, System Engineering Department, Consolidated Edison Company of New York, Inc., New York, N. Y. Mem. ASME.

2 Effect of design on differential reserve-capacity requirements.

The derivation of the capitalization factor of 6.25 is presented in Table 6 of this discussion. Annual generation was estimated on the basis of past experience projected into the future, taking into account the load characteristics of the system. These are tabulated in column 2 in terms of annual capacity factors for a period of 50 years which is the amortization period or life assumed. The tabular values in this column correspond to a life capacity factor of 42 per cent. Annual savings relative to the savings in the first full year of operation are shown in column 4. These were calculated on the basis that the relative annual savings would be proportional to the corresponding annual capacity factors in the ratios indicated in column 3. The latter are judgment values introduced to compensate for the loss of efficiency of equipment with age, notwithstanding adequate maintenance, and as a factor of conservatism against the uncertainties which are inherent in long-range predictions into the future.

The nonuniform annual savings which result from this procedure are converted into equivalent uniform annual values, using the appropriate compound-interest formulas with interest at 6 per cent compounded annually. The equivalent uniform annual savings are indicated in column 7 to be 0.72784 times the savings in the first year of operation, and this is capitalized at the fixed-charge rate of 11.478 per cent, to a value of 6.341 times the savings in the first year of operation or to a rounded value of 6.25.

The total fixed-charge rate, expressed in per cent of initial investment or book cost, consists of the following items:

	Per cent
Depreciation (50-year life)	2.000
6 per cent return on average book value	4.344
Earnings tax	2.084
Property taxes	3.000
Insurance	0.050
Total	11.478

Columns 9 and 10 have been included in Table 6 to show the rate of capital recovery with age. It will be noted that approximately 94 per cent of the initial investment justified by the annual savings is recovered in the first half of the estimated life or amortization period. Therefore a wide variation in the savings estimated for the second half of the amortization period will not affect materially the value of the capitalization factor.

It is interesting to note that with the recent increase of the income-tax rate from 38 to 45 per cent, the fixed-charge rate is now 12.15 per cent and the capitalization factor is 6.

Reserve-capacity requirements and equivalent generation during the first full year of operation are shown in Table 2 of the paper for each design group. The required system reserve capacities indicated by item 2 of the table were calculated by the application of statistical probabilities, using an average forced outage rate of 2 per cent per year for each boiler and turbine-generator unit. The results of these calculations are shown graphically in Fig. 3 of this discussion. A standard of service reliability, as measured by the loss of load equivalent to an average duration of 1 day in 7 years, was adopted. This conforms, in general, with the standard adopted for other electric systems which employ statistical probabilities for the same purpose.

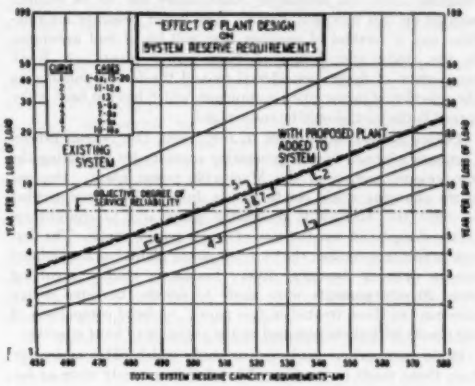
EFFECT OF PLANT DESIGN ON SYSTEM RESERVE REQUIREMENTS
CURVE
CASES
EXISTING SYSTEM
WITH PROPOSED PLANT ADDED TO SYSTEM
OBJECTIVE DEGREE OF SERVICE RELIABILITY
YEAR PER DAY LOSS OF LOAD
TOTAL SYSTEM RESERVE CAPACITY REQUIREMENTS-MW

FIG. 3 EFFECT OF PLANT DESIGN ON SYSTEM RESERVE REQUIREMENTS

The effect of plant design on system-reserve-capacity requirements is shown by item 3 in Table 2 of the paper. In addition, the effect of design on availability of capacity during outages of boilers and turbine generators for scheduled overhaul is indicated in the table by item 5(*d*). The effective increase in system peak demand which each design provides is given by item 6, which is obviously equal to the installed capacity (item 1) less the sum of items 3 and 5d, the requirements for reserve and overhaul.

For evaluation of the designs on a common basis, item 7 indicates the capacity that would be required so that all designs would provide for the same increase in system peak demand with the same degree of service reliability referred to the design which provides for the largest increase in system peak demand. Numerical values for item 7 are obtained from the following:

$$\text{Item (7)} = \text{item (1)} + [882.8 - \text{item (6)}]$$

Equivalent generation in the first year of operation (item 8) is based on the capacity requirements of item 7 for the same num-

TABLE 6 DERIVATION OF CAPITALIZATION FACTOR OF 6.25

(1) Year	(2) Annual capacity factor	(3) Annual savings proportionality factor	(4) Ratio of annual savings to savings in first year	(5) Present worth factor	(6) Present worth of annual savings	(7) Equivalent uniform annual savings for 50 years	(8) Capitalized value of annual savings at 11.478 per cent	(9) —Capital recovery, per cent— During period	(10) Cumulative to end of period
1–5	0.75	1.00	1.0000	4.21236	4.21236	0.26725	2.328	36.71	36.71
6–10	0.70	0.95	0.8867	3.14773	2.79109	0.17708	1.543	24.33	61.04
11–15	0.65	0.90	0.7800	2.35214	1.83467	0.11640	1.014	16.00	77.04
16–20	0.60	0.85	0.6800	1.75769	1.19523	0.07583	0.661	10.42	87.46
21–25	0.50	0.80	0.5333	1.31341	0.70044	0.04444	0.387	6.10	93.56
26–30	0.40	0.80	0.4267	0.98148	0.41880	0.02657	0.231	3.64	97.20
31–50	0.15	0.80	0.1600	1.99702	0.31952	0.02027	0.177	2.80	100.00
				Total	11.47211	0.72784	6.341	100.00	100.00
						Rounded to	6.25		

Col. (4) = (2) × (3)/0.75
Col. (6) = (4) × (5)
Col. (7) = (6) $\left[\frac{0.06(1.06)^{50}}{(1.06)^{50}-1}\right]$ = 0.063444 × col. (6)
Col. (8) = (7)/0.11478
Interest rate at 6 per cent

ber of boiler and turbine-generator units, and generation at capacity for 75 per cent of the available time. In equation form, the values are given by

$$\text{Item 8} = \text{item 7} \times 8760 \times 0.75 \left[1 - \frac{\text{item 5}(d)}{\text{item (1)}}\right] \times 10^{-3}$$

R. W. HARTWELL[5] AND H. A. WAGNER.[6] The author, his company, and the numerous contributors are to be complimented on this excellent paper. The paper presents information, and a method of analysis that will be of real assistance in the study and design of large power plants. A frank comparison of design considerations and the factors influencing the selection of power-plant equipment, which has not been widespread in the past, should be encouraged.

During the year July, 1949, to July, 1950, The Detroit Edison Company planned to add generating capacity by rebuilding the low-pressure section of the Marysville power plant. Because of the changing world conditions, in July, 1950, it was decided to defer the Marysville rebuilding plans and to concentrate on the design and construction of a new power plant. The first unit in this new station, the St. Clair power plant, has a scheduled service date of January, 1953. Economic studies involving some 20 arrangements were made to decide the same design questions as those treated in this paper. A brief comparison of our results with those reported by the author may be of interest.

Basic assumptions made in our study which differ materially from those made in the Consolidated Edison study were as follows:

1 Long-range coal cost—26 cents per million Btu, as compared to 30 or 40.

2 Turbine-generator annual plant factor, 62 per cent for an anticipated 35-year life as compared to about 75 per cent.

3 Annual fixed charges on investment—10 per cent instead of 16 per cent.

4 In selecting the turbine generators and boilers, only established designs were considered, due to the shortage of development and study time.

5 Throttle steam temperatures limited to 950 and 1000 F.

6 Deaeration of all feedwater and drains accomplished in the condenser and therefore all feedwater heaters will be the closed type.

The factors considered in our study were as follows:

Size of Turbine Generator. Units of 125,000 kw and 156,250 kw maximum rated capability were studied.

Single Boiler Versus Two Boilers per Unit. The multiple-boiler arrangement was considered only for the nonreheat units. The single-boiler arrangements included unit system with a crossover and unit system without a crossover. All reheat units were assumed to be supplied by a single boiler, no crossover. In the case of the unit system with crossover, boilers in a four boiler—four turbine plant were sized so that any three would carry name-plate rating on four turbines.

Tandem Versus Cross-Compound Units. The 125-mw units were all tandem-compound whereas both cross-compound and tandem-compound 156-mw units were included in the analysis.

1800-Rpm Versus 3600-Rpm Machines. 1800-rpm and 3600-rpm tandem-compound machines were studied as were 3600/1800-rpm and 3600/3600-rpm cross-compound units.

Reheat Versus Nonreheat Throttle Conditions Studied:

Nonreheat	Reheat
1300 psi–950 F	1450 psi-1000 F–1000 F
1450 psi–1000 F	1800 psi-1000 F–1000 F

Feedwater-Heating Arrangement. An economic comparison of six versus seven stages of feedwater heating for the 1800 psi-1000 F-1000 F reheat condition was made.

It is interesting that the arrangement selected on the basis of these studies is similar in many respects to the Consolidated Edison turbine and cycle choice. Our results led to the selection of a 125,000-kw name plate, 156,250-kw maximum rated capability, 3600/1800 rpm cross-compound turbine-generator. Each machine will operate on a unit system with a single boiler per turbine and with a reheat cycle using 1800 psi–1000 F throttle steam and 1000 F reheat steam.

Although there are material differences in basic assumptions in our study as compared to the author's, some of these differences tend to equalize. For instance, the author's higher plant factor and higher fuel cost result in greater annual savings for the more efficient cycles, but they are capitalized by multiplying by 6.25, representing fixed charges of 16 per cent. Our lesser savings based on a lower plant factor and cheaper coal are multiplied by 10 representing fixed charges of 10 per cent, thus tending to provide comparable results. It was not indicated how the fixed-charge rate of 16 per cent was derived, and whether this included allowances for income taxes.

We agree with the author's provisions of reserve-capacity costs in comparing the several schemes. It is our observation that such an allowance is neglected or overlooked in many studies of this type.

Our heat-balance calculations showed that seven stages of feedwater heating were justified economically. However, after selecting a turbine design that was established and set in some respects, difficulty was encountered in locating low-pressure extraction stages to assure positive drainage of heaters at low loads. This problem led to a final decision to install six stages of feedwater heating. Four heaters are located on the suction side of the boiler feed pump, while two are on the pump discharge. Feedwater temperature entering the boiler will be about 465 F at a turbine-generator load of 156,250 kw. High-pressure heaters will be installed in parallel as indicated also by the author.

H. WEISBERG.[7] The author correctly cautions against the use of the results given for other systems without consideration of differences in basic conditions. The observation should be added that installed cost differentials vary considerably with plant arrangement, with different designs offered by the various equipment manufacturers, and with time. In connection with the last of these factors, the history of power generation is that steam conditions are continually moving toward higher and higher pressures and temperatures. This comes about as a result of development of the art and better ways of doing the job. There is constant change, and no solution will stand for any length of time. In a study of this kind, therefore, it is the writer's opinion that the figures should not be taken too literally but rather be used only as a guide and be tempered with a good deal of judgment. The more efficient plant should be favored, providing reliability is not jeopardized. The equipment is purchased at the time of installation, but the fuel will be purchased during the entire life of the unit, possibly 30 to 40 years for utility installations, and, with inflation predicted on all sides, the chances are that fuel costs will continue to rise.

[5] Engineering Department, The Detroit Edison Company, Detroit, Mich. Jun. ASME.

[6] Engineering Department, The Detroit Edison Company, Detroit, Mich. Mem. ASME.

[7] Public Service Electric and Gas Company, Newark, N. J. Mem. ASME.

We have been in the habit of evaluating heat rate on the basis of 60 per cent capacity factor, representing the average over the life of the unit, fixed charges at 11 per cent, and recently, fuel at 33 cents per million Btu. This results in about 5 to 12 per cent lower capitalized value for differences in efficiency than given in this paper.

In evaluations of auxiliary power, we use a lower demand charge than mentioned in the paper. Since our recent installations include separate auxiliary power generators which are oversize, in order to withstand motor-starting currents with acceptable voltage drop, the capacity of the main unit is not affected by reasonable differences in auxiliary-power demand. The effect on boiler capacity is somewhat theoretical. We generally use $100 per kw demand charge for auxiliary power. It is not clear how the auxiliary-power evaluations given in the paper are applied in the cost comparisons.

A question with regard to the comparison between cross-compound and tandem units: It is surprising to find that the installation cost of the cross-compound arrangement of the turbine is less than that of the tandem compound. Would it be possible to present more detail on the basic reasons for this? Is the cross-compound turbine-generator unit itself lower in cost, or is there some other factor which makes the two-generator arrangement less costly than one?

Another question is in regard to the separate deaerator. Are there any basic operating results or test data which indicate that deaeration cannot be accomplished satisfactorily in the condenser?

Author's Closure

Replying to Mr. Dannettel; as mentioned in the paper, the comparative costs of the various arrangements based upon a fuel price of 30 cents per million Btu were not included in order to conserve space but the entire table is available to anyone who desires the data. This comparison indicated that a reheat cycle with steam conditions 1450 psi, 950–950 F, was lowest in evaluated cost at a fuel price of 30 cents per million Btu, as compared to the 1800 psi, 1000–1000 F cycle which is the most economical with a fuel price of 40 cents per million Btu.

It is true that a back pressure as low as 1 in. Hg cannot be maintained the year round. However, this factor was not a major consideration in our decision between tandem and cross-compound units, all operating at 3600 rpm. With the present limitation of a 23-in. blade length, turning at 3600 rpm, the author thinks there is substantial agreement in the industry that about 50,000 kw per exhaust end represents the economical limit, whereas we are planning to use units in excess of 150,000-kw capacity. This would require a quadruple exhaust which is not a desirable construction for a tandem unit. In addition, it is not desirable to use 3600-rpm generators of the size required by a tandem unit in excess of 150,000 kw, until more operating experience is available with generators of less capacity turning at this speed.

As regards load factor, the 75 per cent figure applies only for the first 5 years of service and, in the author's previous presentation, it was stated that the annual load factor over the life of the equipment was calculated at 42 per cent, which is considerably less than the 57 per cent used for the study on the Baltimore system.

The same over-all boiler efficiency of 89 per cent was used in all comparisons. The use of an evaporator condenser produced such small advantage that its addition was not in our opinion justified. As regards the location of the second extraction point, heat rates for the final cycle chosen were calculated with the second extraction point at 150, 155, 160, 165, and 180 psi, and the results showed 160 psi to provide the lowest heat rate. The choice of this point is of course affected by the fact that reheat is used rather than a straight-through cycle.

In reply to the question as to the number of men kept busy in making the study, an estimate had been made including time spent by engineers, draftsmen, typists, and was found to be the equivalent of 61 man-weeks. This was considered well justified in view of the magnitude of the project.

Mr. Reese's comments are in agreement with the conclusions reached in the paper, and therefore, require no further comment.

The data given by Mr. Steinberg provide the supporting details for various features used in the paper and are, therefore, supplementary data agreeing wholly with the conclusions reached in the paper itself and are to be considered a part thereof.

The independent study referred to by Messrs. Hartwell and Wagner, which was made on the Detroit Edison system at the same time the author made the study for the Consolidated Edison system, gave remarkably similar results, and led to the same basic decision as regards the use of reheat and the choice of steam pressure and temperatures.

In response to Mr. Weisberg's comments, the final choice of a steam cycle depends in large part upon the assumption as to what future fuel costs will be. Since, obviously, there can be no definite information as to these costs, the matter rests solely in the judgment of the engineer making the decision as to how much additional money should be spent on the installations now being made in order to take advantage of savings which would result from higher future fuel costs.

Fireside Deposits on Steam Generators Minimized Through Humidification of Combustion Air

By PAUL MURPHY, JR.,[1] J. D. PIPER,[2] and C. R. SCHMANSKY,[3] DETROIT, MICH.

Increasing the humidity of combustion air to at least 16 lb of water per 1000 lb of dry air has been found to reduce greatly fireside-deposit troubles in stoker-fired steam generators at the Delray Plant of The Detroit Edison Company. It is believed that by keeping the heating surfaces cleaner than normal, humidification will improve average boiler efficiency sufficiently to compensate thermally for the water added to the combustion air, leaving a pronounced gain in availability and lower maintenance. Humidification appears to decrease volatilization from the fuel bed, particularly of silicon compounds.

As stated in a preliminary announcement (1)[4] The Detroit Edison Company, after many years of combating fireside deposits in its stoker-fired steam generators, has found a simple method of minimizing the rate at which they form. The method consists of increasing the humidity of the combustion air that is fed through the fuel bed.

The authors recognize that many cases have been on record for years where water or steam has been introduced through the fuel bed of furnaces for diverse purposes. At least 40 U. S. patents have been issued since 1876, dealing with the introduction of water or steam into fires for purposes other than to put the fire out. Many of those claim that soot is eliminated because the hot carbon particles are consumed in the water-gas reaction. In addition to claiming the reduction of soot formation, Johnson (2) stated that by injecting water directly into the firebox "there is less dirt, and the flues or tubes of the furnace are free of troublesome honeycombing." A more recent claim that moisture can prevent the formation of noncombustible deposits, has reportedly (3) been made by Wetzel. According to the brief report, slag as well as soot deposits have been minimized on the fireside of boiler, superheater, economizer, and air-heater surfaces of the steamship *Mount Greylock* through the use of jets of superheated steam directed into the fire, apparently oil-fed.

In so far as the authors are aware, the present work is the first instance in which combustion air has been humidified for the specific purpose of reducing the formation of high-temperature deposits in large steam generators and for which proof is given that humidification accomplishes that purpose. Presently, it is not known whether humidification of combustion air will help solve fireside-deposit troubles in other steam generators. From the information obtained to date, it is believed that humidification should be helpful for cases involving volatilization of constituents of ash from the fuel bed.

The present paper is a progress report. It shows (*a*) the need that existed for some method of reducing high-temperature deposit troubles in the company with which the authors are connected, and (*b*) the origin of the humidification method, including its relationship to existing theories of fireside-deposit formation. The paper then shows from both operating and probe-test data the extent to which the method is effective and explains in part the manner in which it functions. Further work is in progress.

Troubles From Fireside Deposits at Delray

Of The Detroit Edison Company's steam generators, three at the Delray Plant have been plagued the most by fireside-deposit troubles, particularly in the superheaters. Characteristics of these steam generators have been described by Benjamin (4). Table 1 gives the features that are of the most significance to the present discussion. Two of these steam generators were placed in operation in 1938, and the third in 1939.

TABLE 1 SUMMARY OF SIGNIFICANT DESIGN FEATURES OF DELRAY STEAM GENERATORS, NO. 7, 8, AND 10 (4)

	Normal full load	Emergency maximum load
Steam output, lb per hr	344000	424000
Steam pressure, psig	865	865
Steam temperature, deg F	910	910
Coal burning rate, lb per hr	34000	44000
Gas temperature leaving superheater deg F	1080	1160
Gas temperature at boiler outlet, deg F	1036	1105
Gas temperature leaving economizer, deg F	498	530
Gas temperature leaving air preheater, deg F	315	337
Air temperature leaving air preheater, deg F	334	357
Heat release rate, Btu per cu ft	15800	
Extended grate area, sq ft	611	
Effective area of heating surfaces, sq ft:		
Waterwalls	4622	
Convection boiler	7035	
Superheater	11275	
Economizer	17760	
Air preheater (vertical-tube type)	28008	
Furnace volume, cu ft	27500	
Stoker: Single-ended Taylor underfeed, 15 retorts wide and 57 standard tuyeres long. Actually use 52 thinner tuyères.		
Superheater: Front three loops chrome molybdenum alloy steel. Tubes on 3.3-in. centers; OD 2 1/2 in., except in front loops in which tubes are swaged down to 1 3/4 in.		

Within a few days after being placed in operation the front loops of the superheaters became fouled with sponge ash and shortly thereafter with hard deposits. Early efforts to overcome deposit troubles have been described by Benjamin (5). Briefly, these consisted of damper and baffle changes, changing the nozzles of integral soot blowers to pass twice the original amount of steam, changing from saturated to superheated steam in these blowers, and using telescopic soot blowers in the superheater

[1] Boiler Room Engineer, Delray Plant, The Detroit Edison Company. Jun. ASME.

[2] Chemical Supervisor, Research Department, The Detroit Edison Company. Jun. ASME.

[3] Superintendent, Delray Plant, The Detroit Edison Company. Mem. ASME.

[4] Numbers in parentheses refer to the Bibliography at the end of the paper.

Contributed by the Power Division and presented at the Annual Meeting, New York, N. Y., November 26–December 1, 1950, of The American Society of Mechanical Engineers.

Note: Statements and opinions advanced in papers are to be understood as individual expressions of their authors and not those of the Society. Manuscript received at ASME Headquarters, September 22, 1950. Paper No. 50—A-86.

area. None of these measures corrected the situation. Use of the integral soot blowers, which were fastened in fixed positions (4), was discontinued in 1940, because their use seemed to erode the tubes.

Four additional steam generators, similar to the three described except that the 2½-in. front superheater tubes were on 7-in. centers instead of 3.3 in., and that the effective area was increased from 11,275 to 12,575 sq ft, were placed in operation between 1940 and 1942. The wider spacing reduced the tendency for "bridging-over" to occur but otherwise did not affect deposit formation. Even when the telescopic soot blowers were used once during an 8-hr shift, periods of availability were short for all seven steam generators, often less than 30 days in winter but sometimes 2 to 3 months in summer. In addition to superheater fouling, considerable fouling also occurred in the economizers and air preheaters.

Until recent years, three other troubles aggravated and confused the problem of fireside deposits. One of these was the interruption of coal fed over the stoker when wet coal was being used in winter, often causing blowholes through the fire. Another was secondary combustion in the superheater region, and the third was superheater-tube wastage. Samples of deposit removed from a superheater in 1945 were found by Reid (6), using x-ray diffraction analyses, to contain $K_3Fe(SO_4)_3$, as well as solid solutions of sodium and potassium sulphates. According to Reid, formation of $K_3Fe(SO_4)_3$ is a characteristic of tube wastage. Chemical analyses had shown the deposits to be rich in SO_3, K_2O, Na_2O, and SiO_2.

Two experiments, designed primarily to try to overcome the problems of secondary combustion and superheater-tube wastage, but having a bearing on the fireside-deposit problem, were carried out in 1944 to 1945. In one experiment, use of overfire air practically eliminated secondary combustion but did not reduce deposition of solids. Less sponge ash was found on the superheater tubes, but a very heavy scale formed, plugging the superheater. In the other experiment, superheated-steam jets were used above the fuel bed in one half of a furnace to improve turbulence. Use of the steam reduced but did not eliminate secondary combustion. It reduced deposition of solids to a minor degree. The section of the superheater in the half of the furnace in which the steam was used was noticeably cleaner than the other. Slight improvement was also noticed in the economizer. The improvement, though, was not considered sufficient to justify the cost of the steam.

Gradually the problems of secondary combustion, superheater-tube wastage, and stoker blocking by wet coal were partially eliminated. Troubles from fireside deposits, however, remained as a vicious cycle in which fouled heating surfaces caused higher preheated-air temperatures, which in turn caused stoker-iron burning and increased fouling. Many possible solutions were tried and many others were considered. Murphy (7) reported the failure of the use of lime both as a solid additive to the fire and as a slurry to cover cleaned heating surfaces as advocated by Walsh (8). Small-scale experiments with coatings of graphite and aluminum, applied as paints to superheater tubes, showed these materials also to be ineffective in preventing formation of superheater deposits or in facilitating their removal. The only improvement in boiler availability came through better cleaning using a combination of scraping, blowing, sandblasting, and alkaline-water washing, the latter patterned after the method described by Walsh (8). Improvement in availability was only slight.

Evolution of Humidification Method

Early in 1949 the decision was made to attack more systematically the problem of fireside deposits at Delray. The investigation proceeded along two lines. One dealt with the relationship between the problem as it existed at Delray and experiences of others with fireside deposits. The other line of investigation dealt with the evaluation of a suggestion first made in 1944, that humidification of combustion air might reduce fireside-deposit troubles.

Theories of Others and Their Relationship to the Delray Problem. Chemical analyses of deposits removed from the superheaters of Delray steam generators early in 1949, showed that the deposits could be classified as being of the alkali-matrix type, according to Crossley's descriptions (9). Published literature seems fairly well agreed that alkali-matrix deposits are more prone to form in stoker-fired plants than in pulverized-fuel-fired plants. Sodium, potassium, and sometimes lithium compounds (10) reportedly volatilize or are carried on flames (10) from the fuel bed, and condense upon cooler surfaces, particularly the superheater tubes. There, these compounds react with sulphur trioxide to form, at superheater temperatures, sticky, semifluid sulphates, bisulphates, and pyrosulphates.

Volatilization of solid-forming materials appears not to be limited to alkali-metal and sulphur compounds. Lange (11) and Lessnig (12) showed that some compound of silicon must also volatilize, Lange concluding that it is the sulphide. Crossley (9), also recognizing that some silicon compound volatilized, expressed the belief that it is silicon monoxide, citing the work of Whittingham (13). There is also evidence that certain compounds of phosphorus, boron, and vanadium are selectively volatilized from the fuel bed.

Because the most troublesome deposits at Delray were in the superheater and those deposits appeared to be of the alkali-matrix type, means for combating that type of deposit were sought from the literature. According to The British Boiler Availability Committee (14) one of the best methods of combating alkali-matrix deposits is to clean all heating surfaces thoroughly when the steam generator is shut down. Steam soaking (14, 15) and steam-and-ammonia soaking (16) have been advocated for loosening alkali-matrix deposits. Small-scale experiments showed these methods to have little if any advantage over alkali-water washing for removing deposits in Delray superheaters.

A second method advocated by The British Boiler Availability Committee to combat alkali-matrix-type deposits in stoker-fired plants, was directed toward reducing volatilization of alkali salts. The method consisted of using only those coals in which the concentration of alkali halides was low—less than 0.15 per cent chloride (9). The coals used at Delray met that requirement. Moreover, they were low in both sulphur and phosphorus, according to Crossley's classification.

A third method, also designed to minimize volatilization, was to keep the fuel-bed temperatures as low as possible. Marskell (17) stated, "if the fuel bed is burned so that the rate of combustion approaches the rate of ignition, the depth of the active fuel bed is much less and the temperatures in the fuel bed are considerably lower." Both he and Whittingham (18) pointed out that the greatest volatilization occurred in regions where the coke was burning. Several British operators expressed, privately, the belief that the burning rate should not exceed approximately 40 lb of coal per sq ft of grate area, in contrast to the 56 or 72 lb per sq ft at Delray for normal full load and maximum emergency load, respectively.

Still another method is based upon the theory of Harlow (19) that the primary cause of all fireside deposits is the catalytic production of sulphur trioxide. According to his theory, sulphur dioxide is oxidized to sulphur trioxide on superheater and boiler tubes that are coated with ferric oxide. The sulphur trioxide unites with water and condenses on the air preheater, economizer, and sometimes on the last bank of boiler tubes. His solution to the problem is to minimize catalysis either by limiting the tem-

perature of the heating surfaces or by using noncatalytic materials. Harlow's work and Tolley's (20) have shown that the catalytic activity of steel surfaces is temporarily lessened by coatings of Fe_2O_3, lime, soda, carbon, aluminum, and pulverized-fuel fly ash. Whittingham (13) has shown that silicon monoxide or active-silica smokes markedly reduce the oxidation of sulphur dioxide to trioxide in aerated coal-gas flames. The work of Harlow, Tolley, Whittingham, and of others, cited by Crossley (9), all indicate that the presence of silica dust helps to prevent deposition of alkali-matrix type of deposits.

From the theories reviewed it seemed evident that the formation of alkali-matrix type of deposits on superheaters could be eliminated if either of the following could be prevented:

1 Formation of SO_3.
2 Volatilization of sodium and potassium compounds.

Because the first possibility was already under extensive investigation by Harlow, it seemed more advisable to pursue the second.

Possibilities for Minimizing Volatilization of Sodium and Potassium Compounds. To minimize volatilization of any material, several courses are open. One is to add a reactant that will render the product less volatile than the original material. Another is to reduce the time or temperature of heating. For a stoker-fired installation that is already constructed, the time of heating cannot be shortened materially. The possibility exists, however, that an endothermic reaction, notably the water-gas reaction, may be caused to take place in the fuel bed. The heat thus absorbed should be recoverable when the products of the reaction burn. If the burning takes place above the fuel bed, away from the ash, volatilization of ash constituents should be diminished. The further possibility is believed to exist that the moisture may serve as a reactant to decrease volatilization through hydrolysis reactions.

Correlation Between Atmospheric Humidity and Steam-Generator Behavior. For many years it had been known that superheater deposits formed more rapidly in winter than in summer at Delray. This phenomenon was often ascribed to the stoker troubles caused by the wet coal encountered in winter. In 1944 a suggestion was made that the difference between winter and summer behavior might be related to the difference in the amount of moisture in the combustion air of these two seasons. An early attempt to correlate the amount of moisture in combustion air with steam-generator behavior was unfruitful. In 1949, however, the possibility of correlation was carefully analyzed. As shown in Fig. 1 for a steaming rate of 325,000 lb per hr, the amount of water vapor per hour entering the fuel bed with the combustion air, for the years 1948 and 1949, was computed from U. S. Weather Bureau data. The average value for each month was compared, as shown in Fig. 2, with the corresponding average monthly air-preheater outlet-gas temperature for the seven steam generators under discussion and also with the average monthly efficiency of the entire boiler room which includes five other steam generators that operate at 700 F and 400 psig. Correlation was striking as shown, especially for the 1949 data for which the periods of high humidity coincided with periods of low stack-gas temperature and high efficiency. Conversely, the periods of low humidity coincided with the periods of high stack-gas temperature and low efficiency. Moreover, computation, such as is summarized in Table 2, showed that the amount of water vapor passing through the fuel bed in summer is sufficient to react with an appreciable percentage of the carbon on the fuel bed, provided the water actually does react with the carbon. In winter the amount of carbon that could react with the small amount of water present seems to be nearly negligible.

Conditions Selected for Humidification. Instead of first attempting to determine the extent to which the water-gas reaction takes place and whether heat is actually absorbed from the fuel bed, the decision was made to try a humidification run on Delray steam generator No. 7. This steam generator has the close superheater-tube spacing. The total input of moisture was arbitrarily set at nearly the maximum for summer conditions as given in Fig. 1, namely, 7000 lb per hr for a steaming rate of 325,000 lb per hr, that is, approximately 16.4 lb per 1000 lb of dry air. Because the mount of moisture in the atmospheric air changes rapidly, flexible control was provided for the experiment so that the amount of added moisture could be adjusted every hour to compensate for changes in the absolute humidity of the outdoor air.

TABLE 2 EXTREMES IN MOISTURE CONTENT OF COMBUSTION AIR FOR 1949, AND POSSIBLE EXTENT OF REACTION WITH COAL ON FUEL BED

		Jan 30		July 9
(a)	Average wt of water per 1000 lb dry air, lb	0.979		17.50
(b)	Assumed load, lb steam per hr		325000	
(c)	Coal consumption, lb per hr		32800	
(d)	Carbon consumption, lb per hr		24300	
(e)	Air supply, lb per hr		427000	
(f)	Water with air, lb per hr	418		7470
(g)	Carbon used if water reacts quantitatively, lb per hr	278		4980
(h)	Possible percentage of carbon reacting with water (g/d)	1.14		20.5

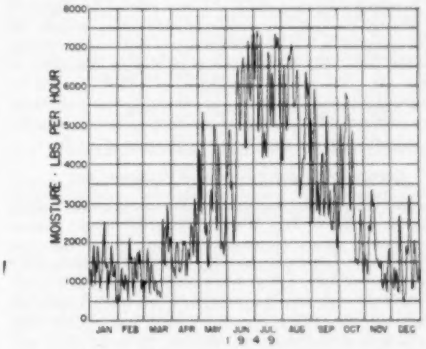

FIG. 1 AMOUNT OF MOISTURE PER HOUR ENTERING FUEL BED WITH COMBUSTION AIR
(Daily average for 1949 for 325,000 lb per hr steaming rate.)

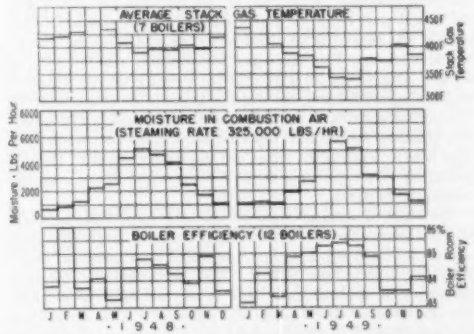

FIG. 2 CORRELATION BETWEEN AMOUNT OF MOISTURE IN COMBUSTION AIR; AND STACK-GAS TEMPERATURES AND BOILER-ROOM EFFICIENCIES

The moisture was introduced into the preheated air as saturated steam.[4] The amount of moisture so added was adjusted for each 25,000 lb per hr change in steaming rate.

When No. 7 steam generator was shut down for installation of the humidification equipment, the external heating surfaces were given a routine scraping and alkali-water washing. However, they were not sandblasted. The economizer and air-preheater surfaces were fairly well cleaned but the less accessible superheater surfaces held the usual residual blue-gray deposits that are so difficult to remove.

The humidification test on No. 7 was started December 3, 1949. Shortly thereafter a similar humidification system was placed in operation in No. 10, which is nearly identical except that part of the time blast-furnace gas is burned as described by Benjamin (4). The second installation provided a means for studying variables of operation without jeopardizing the long-time run on No. 7. Except during the study periods, air to No. 10 was humidified to the same degree as was that to No. 7.

Effect of Humidification on Performance

The effect of humidification on the performance of No. 7 steam generator is shown in Figs. 3 to 7, inclusive. Under normal winter operation, without humidification, illustrated by the upper curve in Fig. 3, the stack-gas temperature rose from 300 to 400 F in 5 days from February 1, and then continued to rise at a slower rate to 450 F or more over the period in which it was possible to keep the steam generator in operation, which was a better than average 53 days in that case. In contrast, the same steam generator, humidified, ran 133 days from December 3 to April 15, with the average stack-gas temperature increasing only approximately 10 F as shown. In accordance with general practice, No. 7 was banked for 3 to 4 hr every 4 or 5 days during these operating periods. At the end of the 133 days the steam generator was shut down for stoker repairs. Without other alterations it was thereafter returned to service and operated without humidification. The stack-gas temperature rose rapidly as shown. During the 29 days that the steam generator operated without humidification, the average input of moisture from the outdoor air was 2090 lb per hr for the 325,000 lb per hr rating used as a standard for the tests reported upon in the curves shown in Figs. 3 to 5. During the entire run the temperatures of the preheated air were approximately 25 F above those of the stack-gas temperatures shown.

The effect of humidification on the boiler-outlet gas temperature is shown in Fig. 4. Without humidification, the temperature rose from 740 to 960 F within 5 days and then increased in another few days to over 1000 F. With humidification, the temperature rose approximately 50 F in the first 60 days of operation and then remained essentially constant. After humidification was shut off, the boiler-outlet gas temperature rose to over 1000 F within 21 days as shown.

During the entire 133 days of operation with humidification, the steam generator was capable of steaming 400,000 lb per hr; after 24 days without humidification the maximum steaming rate obtainable was 300,000 lb per hr.

Fig. 5 shows the draft losses through the steam generator, and the current requirements for the induced-draft-fan motor during the 133-day humidification test, and the 29 days following without humidification. During the 133 days, the draft loss through the superheater (boiler-outlet draft) increased approximately 2 in. There was no increase through the economizer but approximately 1½ in. through the air preheater as shown. Operating without humidification, the draft losses through the superheater, economizer, and air preheater would have increased approximately 2¾, 2, and 2 in., respectively, over a period of 28 days of winter operation as estimated from previous operating data.

Observations made during the course of the test and at its conclusion showed that after 133 days with humidification, there was less deposit on the front rows of superheater tubes than would have been deposited in 30 to 50 days without humidification.

[4] Other methods for humidification are also on trial. Engineering features of the several systems will be reported later.

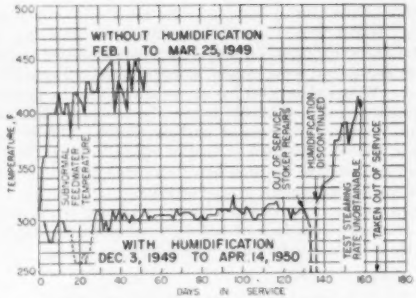

Fig. 3 Effect of Humidification on Stack-Gas Temperatures (Temperatures measured at air-preheater outlet. Steaming rate 325,000 lb per hr.)

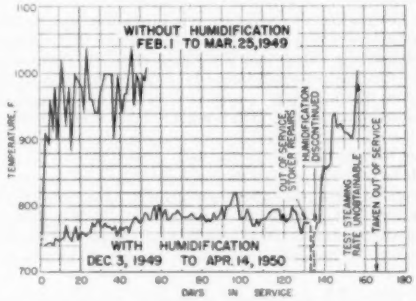

Fig. 4 Effect of Humidification on Boiler-Outlet Gas Temperatures (Steaming rate 325,000 lb per hr.)

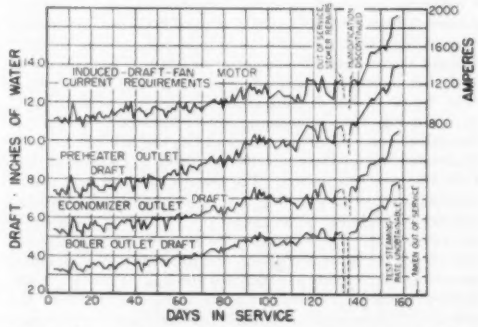

Fig. 5 Draft Performance During Humidification Test (Steaming rate 325,000 lb per hr.)

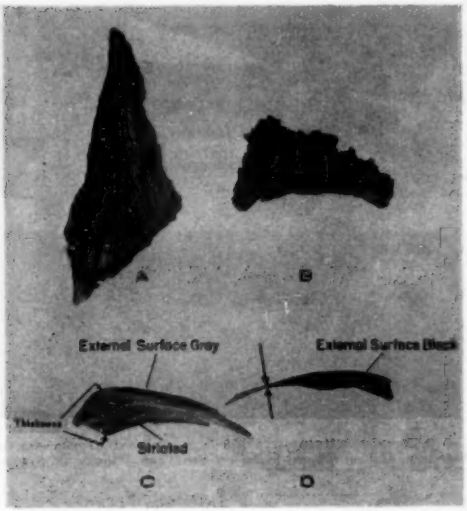

A Superheater deposit, no humidification last 29 days of test.
B Superheater deposit, after 133 days with humidification.
C Economizer deposit after 40 days, no humidification. (Steam generator No. 10) Stratified structure retouched.
D Economizer deposit after 133 days with humidification. Note thinness shown by arrows. Entire specimen same thickness; portions of internal and external surfaces visible.

FIG. 6 CONTRAST IN APPEARANCE OF SUPERHEATER AND ECONOMIZER DEPOSITS WITHOUT AND WITH HUMIDIFICATION

Beyond the fifth row the amount of deposit was negligible with humidification. The economizer was remarkably clean, much of the surface holding no deposit at all and parts where gas velocities were low holding only a very thin layer. The waterwalls and boiler tubes remained remarkably free of the white deposit that normally accumulates. The condition of the air preheater after the 133 days was approximately the same as would be found after 30 to 50 days without humidification.

During the 29 days without humidification, following the 133-day run with humidification, the superheater fouled rapidly. Fig. 6 contrasts the typical appearance of superheater deposits removed at the end of the respective tests. The economizer, however, fouled at less than the normal rate for unhumidified conditions, becoming only moderately dirty. The economizer deposit shown in Fig. 6, to represent unhumidified behavior, was taken from steam generator No. 10 after operating 40 days beginning December 14, 1949.

Efficiency tests were made after 125 days of the 133-day humidification run, after 23 days without humidification, and after the steam generator had been thoroughly cleaned, including sandblasting, during the annual inspection period. The results of the tests are shown in Fig. 7. The several heat losses from which the efficiencies were computed are enumerated in that figure. They include the charge for stoker and fan-power requirements but do not include the charge for humidification. According to information available to date, the humidification requirements for Detroit climate will be 1.3 per cent of the steaming rate when averaged over an entire year. During the coldest part of the winter the requirements may be approximately 2 per cent.

It should be pointed out that further data will have to be obtained before the effect of humidification on boiler efficiency can be evaluated adequately. The top curve in Fig. 7 is believed to represent fairly well the efficiency of the clean steam generator operating with humidification. The center curve, representing the humidified steam generator after 125 days, may be low for two reasons: (a) The heating surfaces of the waterwalls, boiler, and superheater were not well cleaned before the start of the run; (b) the total carbon in the stack dust was unusually high during the course of the efficiency test, thus lowering the computed efficiency. Ash and sulphur concentrations in the coal used for that test were higher than for the other two tests. The values shown by the bottom curve are probably too high to be typical of a nonhumidified steam generator.

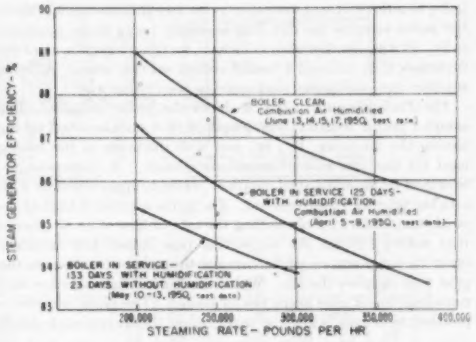

FIG. 7 STEAM-GENERATOR EFFICIENCY DURING HUMIDIFICATION TESTS ON NO. 7 BOILER

(Efficiency computed from following losses using ASME Test Code for Steam Generators: Incomplete combustion loss; unburned-carbon loss; radiation and convection losses; sensible-heat loss in dry flue gas; moisture losses; auxiliary-power requirements.)

As previously stated, the superheater was fouled to some extent after 133 days of operation with humidification, while the economizer was remarkably clean. The accumulation that rapidly developed on the superheater, after the humidification was discontinued, apparently collected the materials that normally would have deposited in the economizer and air preheater. This would have the effect of producing lower air-preheater-outlet flue-gas temperatures than normally would have obtained during an operating period without humidification, and, consequently, an abnormally high efficiency.

Until such time as more data are available, it seems probable that humidification, through keeping heating surfaces cleaner, will improve average efficiency at least enough to compensate for the cost of its use, thus leaving a distinct gain through better availability and lower maintenance. The economic and engineering aspects of the problem are being studied further.

PROBE TESTS

In order to determine the effect of any variable on rate of deposition, on composition, or on properties of materials that deposit on the various heat-transfer surfaces of steam generators, it seemed desirable to employ a probe operating under conditions existing at the surface being investigated. One of the objects of using a probe was to obtain the materials as they first deposited, before they had a chance to undergo extensive reactions that would obscure the initial phenomena. Inasmuch as volatilization of sodium and potassium compounds from the fuel bed, subsequent condensation of these compounds on superheater tubes, and reaction with sulphur trioxide were held, by the theories reviewed, to be the source of the binder that causes fly-ash par-

ticles to adhere, it was desirable to try to eliminate from some of the probe samples the dirt that is simply being borne mechanically. It was also desirable to include, for other samples, all of the materials that ordinarily would collect on the tubes. A probe sampler was constructed that could be used either way.

The Probe Sampler. Fig. 8 shows the probe sampler. The sampler proper is an $11^1/_2$-in. length of 18–8 stainless-steel tubing having the diameter, $1^3/_4$ in., and wall thickness of the tubing used for the first row of superheater tubes. A thermocouple, sheathed by stainless-steel capillary, extends approximately 4 in. into the tube wall from one end. The probe sampler is kept at desired temperature by controlling the rate of flow of an air stream that enters through the supporting pipe shown and impinges upon the inner surface of the sampler through perforations in the pipe that supplies the air. Water flowing through a jacket surrounding the air pipe keeps the air cooled. The probe sampler is polished with metallographic paper before the start of each determination. For those samples for which elimination of mechanically borne ash is desired, a semicircular shield is used, oriented to face the slip stream of gases and dirt.

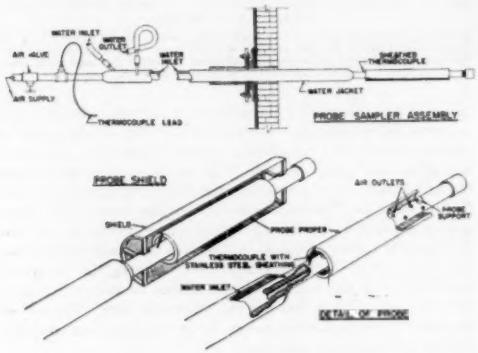

FIG. 8 PROBE SAMPLER

Effect of Humidification on Superheater Deposits. The first probe tests were made to compare the rate of deposition in the superheater of No. 7 steam generator, which at that time had been running 37 days on humidified air, with that of No. 10, which had been running 12 days without humidification. It was intended that all determinations be made at a rating of 350,000 lb of steam per hr. No. 10 was so dirty, however, that a rating of only 335,000 lb per hr could be obtained. The results of the test are shown in Fig. 9 which shows that the rate of initial deposition was much less for the humidified steam generator and the deposit was much darker. These deposits, as well as each of the other superheater probe samples described in this paper, were collected in 1 hr. Shortly after the tests were made, No. 10 was cleaned, equipped for humidification as previously stated, and used for short-time experimentation of many variables.

Fig. 10 shows the amounts of deposit that have collected in all the shielded-probe tests that have been made to date (June 2, 1950), and Fig. 11 shows the amounts for the unshielded probes. For some of the unshielded-probe samples the part on the upstream side of the probe was removed separately from the part on the downstream side. Figs. 10 and 11 both show that use of humidification has a greater effect on rate of deposition in the superheater region than has any of the other variables studied. Those variables include different steam-output rates within the normal range in which the steam generator operates, rapid changes in steam output, grinding and dumping ash, different thicknesses of fuel bed, and use or not of blast-furnace gas as auxiliary fuel. Only by placing the unhumidified steam generator on bank was it possible to reduce the rate of deposition below that of the humidified steam generator operating under normal load. Variation in the amounts of deposits collected reveals, however, that some unknown variable exerts a significant influence on rate of deposition even though it is small as compared with the influence of humidity.

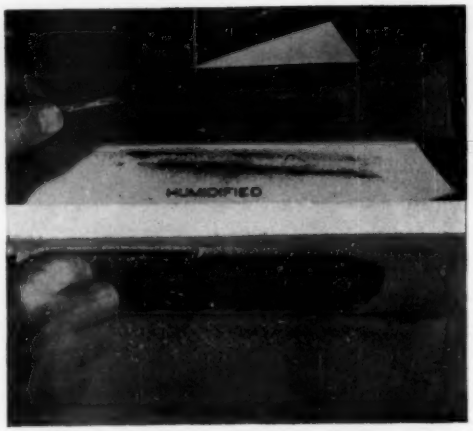

FIG. 9 EFFECT OF HUMIDIFICATION ON AMOUNT AND APPEARANCE OF DEPOSITS COLLECTED IN 1 HR ON SHIELDED PROBES IN SUPERHEATER

Effect of Degree of Humidification Upon Rate of Deposition on Superheater, Economizer, and Air-Heater Surfaces. As previously mentioned, the amount of humidification used was arbitrarily set, for the tests on No. 7, as being nearly the maximum that would occur in naturally humid summer weather. Obviously, it was desirable to determine whether the amount so chosen was optimum, not only for maintaining clean superheater surfaces but also for the economizer and air-preheater surfaces. The probes designed for the superheaters were suitable for use in the economizer because there the gas stream passes over the outside of the tubes also. For the air preheaters, the probes were not too well suited, for there the gases pass through the long cylindrical tubes. Justification for the use of the shield was not established for the economizer and air-preheater probes for, according to generally accepted theory, only sulphuric acid was supposed to condense from sulphur trioxide and water in those regions. For the sake of consistency, however, the same probes as were used in the superheater were used, both shielded and unshielded, in the economizer and air preheater. The probes were in position 60, 75, and 90 min for the superheater, economizer, and preheater, respectively. All the tests were made at a rating of 350,000 lb of steam per hr.

The weights of deposit collected on both the shielded and the unshielded probes are shown in Fig. 12. In both cases the "dry runs," represented by the values shown on the left side of the figure, were made under whatever humidity condition prevailed at the time of test. Progressing to the right in the figure, the total humidities were, in order: 4000, 7460 (which is the arbitrarily chosen humidity for a steaming rate of 350,000 lb per hr), and 12,000 lb of water per hr.

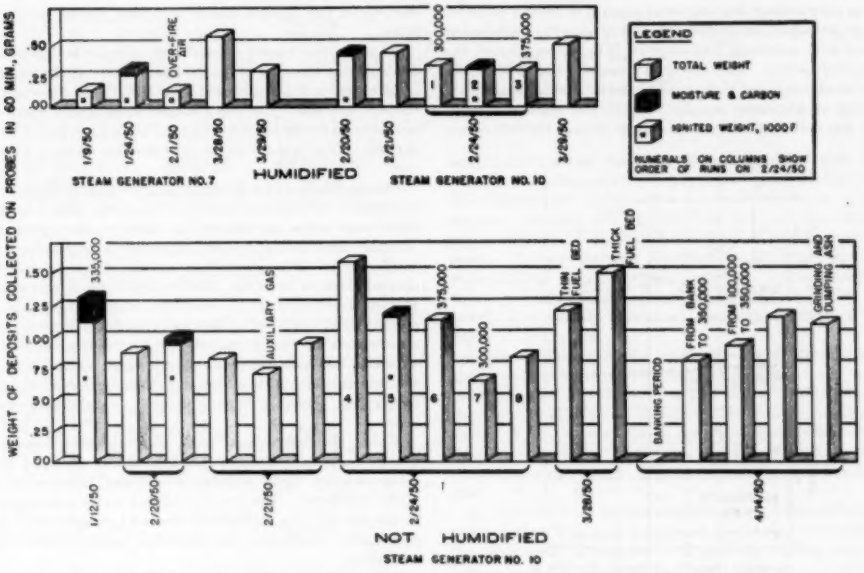

FIG. 10 EFFECT OF HUMIDIFICATION ON RATE OF DEPOSITION ON SHIELDED PROBES IN SUPERHEATER
(Steaming rate 350,000 lb per hr unless otherwise noted.)

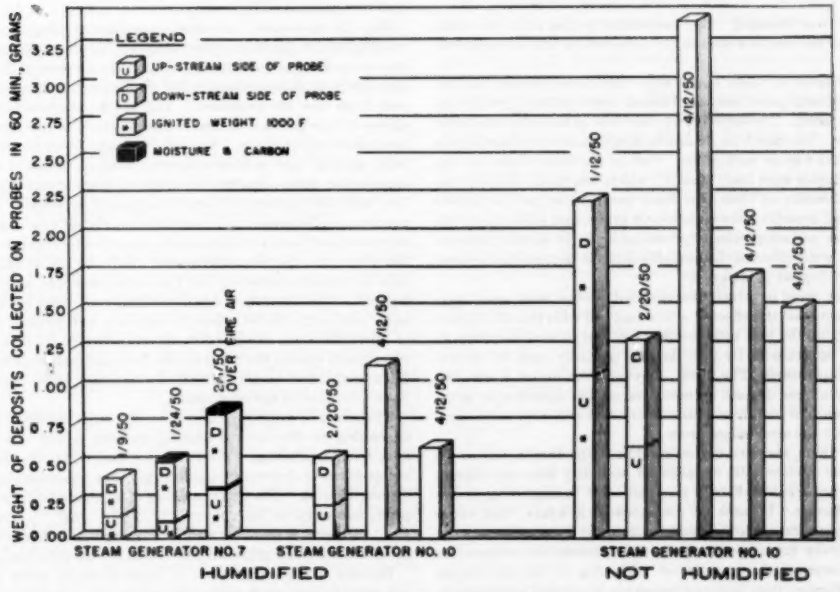

FIG. 11 EFFECT OF HUMIDIFICATION ON RATE OF DEPOSITION ON UNSHIELDED PROBES IN SUPERHEATER
(Steaming rate 350,000 lb per hr.)

It is at once evident that the total amount of deposit collected in the air preheater and economizer, as well as in the superheater, decreased with increasing humidity for both the unshielded and the shielded probes. The effect on quantity was greatest for the superheater samples, both shielded and unshielded, and for the unshielded air-preheater samples. Nearly the same amount of deposit was collected on the economizer probes whether or not

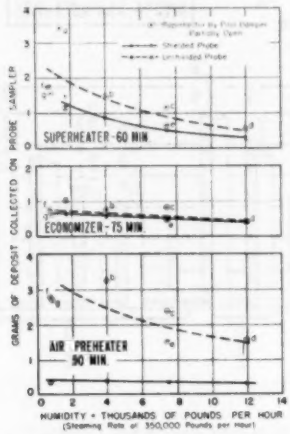
SUPERHEATER-60 MIN
ECONOMIZER-75 MIN
AIR PREHEATER
90 MIN
GRAMS OF DEPOSIT COLLECTED ON PROBE SAMPLER
HUMIDITY - THOUSANDS OF POUNDS PER HOUR
(Steaming Rate of 350,000 Pounds per Hour)

FIG. 12 EFFECT OF DEGREE OF HUMIDIFICATION ON RATE OF DEPOSITION ON PROBES IN SUPERHEATER, ECONOMIZER, AND AIR PREHEATER
(Order of runs for unshielded samples shown by letters.)

the probe was shielded. The unshielded probes collected much more than the shielded ones in the superheater and air preheater as shown.

In the series of tests made with unshielded probes the unknown variable previously mentioned crept in to a greater extent than usual. The experiments were run in the order shown by the letters. For run A an unusually large amount of deposit even for dry runs was on each probe. Part of the economizer and air-heater samples were lost. Run C, which was made with the arbitrary humidity of 7460 lb of water per hr, also gave an abnormally large deposit on the superheater probe, and probably on the economizer and air-preheater probes as well. In spite of these irregularities the effect of the humidification in decreasing the total volume of deposit is apparent.

The dry runs in which the shielded probes were used were made to contrast the effect of a thin fuel bed with that of a heavy bed. During the test with the thin fuel bed, it was necessary to keep the superheater by-pass damper partially open to control steam temperature. The result, shown by the circled X's in Fig. 12, was that less deposit accumulated on the superheater probe with a thin fuel bed than with a heavy fuel bed, and more accumulated on the economizer probe.

Taken alone, the variation in weight of deposit collected on the economizer probes with variation of humidity does not explain fully the remarkable effect of humidification in improving economizer behavior. It must be remembered, however, that under normal operation without humidification, the waterwall and front bank of boiler tubes become fouled and increase the temperature of gases entering the superheater. Opening of the superheater by-pass damper then becomes necessary to control superheated-steam temperature. As described in the previous paragraph, the opening of the damper causes increased fouling of the economizer.

An effect that cannot be shown graphically is that of humidification upon the color of the deposit collected in the superheater, economizer, and air preheater, particularly in the cases of the shielded samples. The color ranged from nearly white for low humidity to nearly black for high. The composition of the probe samples offers further clue to the beneficial effect of humidification.

Composition of Probe Samples. In selecting a procedure for the analysis of the probe samples, as well as for their collection, an effort was made to differentiate between the materials that volatilize from the fuel bed and those that are carried to the tubes mechanically. Because analyses of superheater deposits had indicated them to be of the alkali-matrix type, it was desired especially to differentiate between the sodium and potassium compounds that volatilized as halides or oxides and those that were constituents of earthy materials. For such a differentiation, solubility behavior seemed to offer a rough means of separating the former, which by the time they were deposited on the superheater had probably been converted to sulphates, from the latter.

Water, the first solvent tried, was discarded because it extracted only approximately one half of the sulphates from the probe samples. Acid solutions were found, however, to extract all the sulphates. Ten per cent boiling acetic acid was selected as the solvent. In this solvent the solid samples were digested repeatedly. Solutions and insoluble residues were analyzed separately.

At the time the probe samples were being collected, samples of the coal being burned were also taken. A typical analysis of the coal is given in Table 3. The coal samples were ashed at a low temperature, 850 F for at least 24 hr, and the ash was analyzed the same way as the probe samples. The total chloride in the coal was determined separately.

Fig. 13 shows the principal constituents, with respect to weights, of the shielded-probe samples. At once apparent is the enormous effect of humidification upon the amount of SiO_2 in the deposits from the superheater and economizer, and to a lesser extent from the air preheater. The actual composition of the silicon compound that is reported as SiO_2 is of course unavailable from chemical analyses. Analyses of many other deposits from both shielded and unshielded-probe samples obtained from the superheater region confirm the marked effect of the humidification upon the amount of silicon compound deposited. Humidification also decreases the amount of nearly all other noncarbonaceous constituents collected in the superheater region but not to the extent that the SiO_2 is decreased. Only the one complete set of data is available presently for the economizer and air-preheater regions. The amounts of Al_2O_3 and Fe_2O_3 collected in the economizer and air preheater appear to be nearly independent of degree of humidification, except when the superheater by-pass damper was opened during the run with the thin fuel bed, causing part of the material that would normally be deposited in the superheater to be deposited in the economizer.

The effect of humidification upon the total amount of carbon depositing on the several heating surfaces is still obscure, the data being conflicting. Presently it appears that the amount is independent of degree of humidification but dependent upon conditions of firing. The total amounts of soluble materials that deposit, measured as Na^+, K^+, Ca^{++}, Fe^{+++}, Al^{+++}, SO_4^{--}, and PO_4^{---}, seem to diminish with increasing humidification for the economizer and air preheater, as well as for the superheater.

Because of the large effect of humidification upon the SiO_2 concentration of the deposits, the percentage compositions of the other constituents gives no indication of whether they are being

TABLE 3 TYPICAL ANALYSIS OF COAL BURNED

Proximate analysis, per cent		Ultimate analysis, per cent		Heating value, Btu per lb		Ash-fusion temperature, deg F		Swelling index
Moisture.....	5.2	C	78.6	Moisture free.....	13890	Initial def.	2580	5.25
Volatile matter..	31.3	H_2	4.9	Leaving breaker...	13160	Softening..	2660	
Fixed carbon....	55.1	N_2	1.5	Moisture and ash-free.	15230	Fluid	2800	
Ash.....	8.4	O_2	5.1					
		S	1.0					
		Ash	8.9					

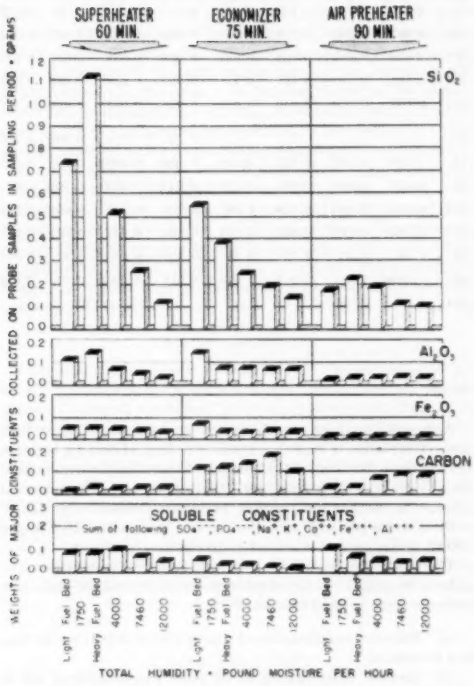

FIG. 13 EFFECT OF DEGREE OF HUMIDIFICATION ON LARGEST CONSTITUENTS OF SHIELDED-PROBE SAMPLES FROM SUPERHEATER, ECONOMIZER, AND AIR-PREHEATER REGIONS

volatilized selectively from the fuel bed. In an effort to establish this point, the ratios of all constituents to the total alumina have been determined for both the ash and the probe samples. Alumina was selected as the base, not because there is no chance of its being volatilized selectively, but because it is next to SiO_2 in proportion and probably is representative of earthy materials in the ash. These ratios, by equivalents, are given in Table 4, where the insoluble constituents are listed arbitrarily as oxides, and the soluble constituents as ions. Inasmuch as the equivalent weights are used in computing the ratios to total Al_2O_3, or total Al^{+++}, the ratios for soluble and insoluble materials are directly comparable.

The ratios of SiO_2 to Al_2O_3 for the coal ashes were slightly less than 2 as shown. The ratios for the samples taken from the superheater probes, when running without humidification, ranged between 4.8 and 8.0, in the cases of the shielded probes and the downstream side of the unshielded ones. For the corresponding samples when humidification was used, the ratios ranged from 2.6 to 4.7. The limited data on economizer and air-preheater samples show similar behavior. Thus it is evident that marked selective volatilization of silica takes place from the fuel bed, and that this selective volatilization is reduced markedly by humidification. Selective volatilization was not, however, eliminated completely by the degree of humidification used in these experiments. Further, the same degree of humidification does not always produce equally beneficial results. Some presently unknown variable affects not only the amount of the deposit collected, as previously mentioned, but also the ratio of SiO_2 to Al_2O_3.

Deposits collected on the upstream side of unshielded probes appear to be mixtures of materials that condense and of mechanically borne ash. Apparently a part of the condensed material that initially deposits upon superheater probes is eroded by the stream of ash, for the back of the probe usually held more material than the front. In the case of the unshielded air-preheater probes, however, most of the deposit is collected on the upstream side.

As further shown in Table 4, the ratios of the insoluble Fe_2O_3 to total Al_2O_3 were nearly the same in all the probe samples as in the ash samples. Insoluble CaO seems to be selectively volatilized to a small degree; that degree seems to be unaffected by humidification. The ratio of insoluble Na_2O to Al_2O_3 in the probe samples is only slightly higher than that in the ash, except for the shielded air-preheater samples where the increase is more apparent. Insoluble K_2O seems definitely to be selectively volatilized, with respect to Al_2O_3, and the degree of that selective volatilization seems to be reduced by humidification. The ratio of insoluble phosphate to alumina is appreciably higher in the probe samples than in the ash samples. The same was true for the soluble phosphates, thus confirming British experience that phosphorous compounds are volatilized selectively. Whether humidification affects the selective volatilization of the phosphorus compounds cannot be proved from the available data.

The ratios of both the soluble sodium and soluble potassium compounds to alumina are much greater for all the probe samples than for the ash samples, as would be expected if those compounds are selectively volatilized as claimed in the literature. Whether humidification affects the degree of their selective volatilization is still obscure, the data being conflicting. The ratio of sulphate to alumina is likewise much greater for the probe samples than for the ash. Again the data to show the effect of humidification upon this ratio are conflicting.

Chlorides present in the original coal are driven off as the coal is ashed even at 850 F, as indicated by the difference between the total Cl^- and the soluble Cl^- shown in the table under "coal ashes." Fragmentary data show that for some of the deposits, however, the ratio of Cl^- to Al_2O_3 was nearly the same as in the original coal.

Before leaving Table 4, it seems well to point out the high ratios of soluble calcium and of sulphate to alumina for the shielded-probe samples from the air preheater, particularly when no humidification was used. The low ratios for soluble sodium, potassium, and sulphate in the economizer deposits, as compared with the corresponding ratios for the superheater deposits are also noteworthy. Apparently, the fouling of the economizer when humidity is low was caused almost entirely by selective volatilization and condensation of the silicon compound. Humidi-

TABLE 4 RATIOS, BY EQUIVALENTS, OF CONSTITUENTS OF ASH AND PROBE SAMPLES, TO TOTAL Al_2O_3

Constituents	Coal ashes Range of results on six samples	Extensive survey, March 28 and 29, 1950 — Superheater H S	Extensive survey, March 28 and 29, 1950 — Superheater N S	Extensive survey, March 28 and 29, 1950 — Economizer H S	Extensive survey, March 28 and 29, 1950 — Economizer N S	Extensive survey, March 28 and 29, 1950 — Air preheater H S	Extensive survey, March 28 and 29, 1950 — Air preheater N S	Superheater surveys, January 24 to April 12, 1950 (numerals indicate number of runs analyzed) — 3 H S	3 N S	2 H D	2 N D	2 H U	2 N U	Air preheater April 12, 1950 — N D	N U
Insoluble						Range or Average									
SiO_2	1.7 to 1.9	3.6 to 4.7	6.9 to 8.0	2.2 to 2.8	4.1 to 5.7	2.8 to 2.9	7.4 to 7.9	2.6 to 2.8	4.8 to 5.9	2.5 to 2.7	5.7 to 6.0	2.3 to 2.5	2.7 to 3.1	3.7	2.8
Fe_2O_3	0.14 to 0.30	0.39	0.20	0.26	0.25	0.23	0.17	0.35	0.33	0.25	0.37	0.38	0.40	0.39	0.40
CaO	0.015 to 0.020	0.047	0.030	0.067	0.052	0.065	0.084	0.037	0.056	0.040	0.046	0.050	0.030	0.036	0.015
Na_2O	0.011 to 0.020	0.025	0.037	0.015	0.020	0.060	0.060	0.024	0.044	0.031	0.036	0.027	0.034	0.035	0.024
K_2O	0.029 to 0.045	0.085	0.20	0.065	0.080	0.070	0.10	0.057	0.13	0.062	0.11	0.060	0.066	0.072	0.064
P_2O_5	0.004 to 0.005	0.090	0.015	0.016	0.015	0.023	0.015	0.032	0.020	0.040	0.013	0.034	0.035	0.018	0.013
Soluble															
Al^{+++}	0.08 to 0.12	0.085	0.10	0.065	0.065	0.15	0.21	..	..	..	..	..	..	0.070	0.040
Fe^{+++}	0.003 to 0.007	0.032	0.027	0.036	0.033	0.090	0.13	0.016	0.023	0.017	0.018	0.010	0.0050	0.048	0.027
Ca^{++}	0.012 to 0.025	0.016	0.013	0.0090	0.013	0.15	0.20	0.015	0.020	0.012	0.026	0.021	0.017	0.022	0.012
Na^{+}	0.002 to 0.003	0.075	0.040	0.0045	0.015	0.026	0.043	0.058	0.090	0.058	0.087	0.038	0.046	0.031	0.018
K^{+}	0.0020 to 0.0026	0.12	0.040	0.015	0.023	0.031	0.057	0.037	0.076	0.040	0.064	0.020	0.011	0.031	0.014
SO_4^{--}	0.023 to 0.039	0.21	0.11	0.035	0.072	0.23	0.80	0.10	0.18	0.12	0.23	0.083	0.050	0.17	0.075
PO_4^{---}	0.0013 to 0.0028	0.020	0.015	0.0050	0.0070	0.019	0.024	0.0090	0.012	0.015	0.013	0.018	0.0030	0.019	0.010
Cl^{-}	0.0005 to 0.0015	..	0.0035	0.010	0.017	..	0.023	0.0025	0.0060	..	..	..	..	..	..
Total* Cl^{-}	0.018 to 0.024														

Key: Humidified. N Not humidified. S Shielded probes
D Downstream side of unshielded probes
U Upstream side of unshielded probes
* Total chloride in coal sample from which ash was obtained

fication nearly eliminated this phenomenon and hence nearly eliminated the fouling of the economizer. Humidification reduced selective condensation of silica in the superheater as well as in the economizer and also appeared to have reduced general volatilization of all constituents of the ash. Humidification seems not, however, to have reduced the selective volatilization of sodium and potassium compounds, which may account for the less phenomenal effect of humidification in the superheater regions as compared with that in the economizer.

A few probe samples taken from the superheater region have been subjected to x-ray-diffraction analyses primarily for the purpose of determining the nature of the silicon-containing material present in samples representing unhumidified conditions. Apparently that material is amorphous. The only crystalline materials present in appreciable concentrations that were definitely identified were hematite, sodium sulphate, and potassium sulphate, the latter from calcined samples representing both humidified and unhumidified conditions.

Summary and Speculation

Addition of moisture to the combustion air used in the 910 F, 865-psig stoker-fired steam generators at Delray, to bring the total humidity of the combustion air to approximately 16.4 lb per 1000 lb of dry air, markedly reduced the rate of fouling in the superheater, economizer, and air preheater. The amount of fouling in the economizer was practically negligible. To the present, data for only one long-time humidification test are available. From those limited data it seems probable that, through use of humidification, the average steam-generator efficiency is improved sufficiently to compensate thermally for the water used, leaving a distinct gain through better availability and lower maintenance. The gain in efficiency is believed to come from greater heat transfer caused by

(*a*) Less thickness of heat-insulating deposits.

(*b*) Better radiation absorption by a dark-colored surface than by a light-colored surface.

Although long-time tests have not yet been made, short-time probe tests indicate that the extent of fouling of heating surfaces is an inverse function of the amount of water in the combustion air, at least up to 25 lb water per 1000 lb of dry air. The optimum amount to use has not yet been evaluated economically. Presently it seems probable that the amount is near the 16.4 lb per 1000 lb of dry air that was used in the one long-time test.

The mechanism by which moisture, added to combustion air, reduces deposition on superheater, economizer, and air-preheater surfaces seems to be at least twofold:

(*a*) Selective volatilization of silicon compounds from the fuel bed is reduced.

(*b*) General volatilization of all other constituents of ash is also reduced.

The silicon compounds that deposit on the heating surfaces are the materials of high reflectivity that probably cause the poor radiation absorption previously mentioned. These white materials are apparently amorphous silica. Selective volatilization of sodium and potassium compounds from the fuel bed, as claimed by previous investigators, seems confirmed. Whether humidification reduces the selective volatilization has not been proved; the amounts of these materials that collect on tube surfaces are, nevertheless, reduced presumably through reduction of general volatilization.

It is recognized that use of the probe-tester shield to prevent impingement of solid particles does not insure that all materials which collect on the shielded probes actually volatilize from the fuel bed and condense on the probe. Nevertheless, the uniformity of the thickness, appearance, and composition of the deposits suggest strongly that the iron and aluminum compounds, and the silica that is normally associated with them, reach the probes by the same mechanism as brings the sodium and potassium compounds. There seems to be a distinct possibility that the vapor pressure of the iron and aluminum silicates, although exceedingly low, is still high enough at fuel-bed temperature to provide trans-

port for those materials to the tube. Possibly, however, these materials are carried by flames as described by Corey (10) for sodium and potassium compounds.

The phenomena that take place between the time the materials first deposit and the time they form hard layers have not yet been investigated. Part of the deposits collected on the upstream side of the unshielded superheater probes invariably stuck tenaciously, even though the maximum surface temperature of the probe probably did not exceed 1125 F. Little, if any, sticking occurred with the shielded probes where the upstream surface, protected from the radiation by the shield, remained closer to the 950 F to 1000 temperature of the thermocouple within the wall of the probe. In the superheater of the steam generators in question, the sticking phenomena seem to be related to the sintering behavior described in the literature. The sticking behavior of the economizer deposits may be related to an observation that the fluffy silica deposits, upon being moistened with acids and ignited to 500 F, become hard masses.

Presently it has not been proved whether the endothermic reaction mentioned in the theory actually takes place. Attempts to measure fuel-bed temperatures with and without humidification of combustion air thus far have been unfruitful. Much more investigation will be required before the phenomena involved are thoroughly understood.

Acknowledgments

The authors are pleased to acknowledge the co-operation of many colleagues in the undertaking described. It would be impractical to list all who helped, particularly those who aided in the clarification of the complications that obscured the fireside-deposit problem at Delray up to 1949. Concerning the fireside-deposit problem itself, the early suggestion, previously mentioned, that humidification might affect deposition was made by Glenn Coley, Metallurgist, Sales Department. Boyd Griffin, Technical Engineer, Delray Plant, and his staff conducted the efficiency tests and assisted in obtaining the probe samples. Most of the large number of analyses involved in the probe tests were carried out by A. G. Fleiger and Miss Gray Campbell. The x-ray diffraction data were obtained by C. M. Schwartz of Battelle Memorial Institute.

Bibliography

1 "Minimized Fireside Deposits," anon, *Mechanical Engineering*, vol. 72, 1950, p. 334.

2 "Device for Eliminating Smoke in Boiler Furnaces," by C. P. Johnson, U. S. Patent 1565463, December 15, 1925.

3 "Fireside Slag and Soot Prevention Experiment," anon, *Marine Engineering and Shipping Review*, vol. 54, May, 1949, p. 63.

4 "High-Pressure Extension of Detroit Edison's Delray Plant, Part 2, Coal Handling System, Combustion Equipment, and Steam-Generating Plant," by M. W. Benjamin, *Power Plant Engineering*, vol. 43, May, 1939, pp. 317–331.

5 "High-Pressure Extension of Detroit Edison's Delray Plant, Part 5, First Ten Months of Operation," by M. W. Benjamin, *Power Plant Engineering*, vol. 43, November, 1939, pp. 696–709.

6 "External Corrosion of Superheater Elements at Delray Station," by W. T. Reid, Private Correspondence, May 31, 1945.

7 Discussion of (8), by Paul Murphy, Jr., *Power*, vol. 94, 1950, p. 93.

8 "Some Aspects as to the Cause and Prevention of Slag Deposits on the Heating Surfaces of Modern High-Pressure Boilers," by E. F. Walsh, Mimeograph, ASME paper No. 49—S-19, 1949 Spring Meeting; résumé in *Power*, vol. 94, 1950, p. 91.

9 "Deposits on the External Heating Surface of Boiler Systems—an Account of the Work of the Boiler Availability Committee," by H. E. Crossley, Fuel Economy Conference of the World Power Conference, The Hague, Holland, 1947, Conference Proof, Section C2, Paper No. 3, pp. 1–13. (9a) "Deposits on the External Heating Surfaces of Watertube Boilers," by H. E. Crossley, The Institution of Chemical Engineers, Proof copy of a paper read at Burlington House, London, England, December 14, 1948. (9b) "Interim Report on External Deposits and Corrosion in Boiler Plant," The Boiler Availability Committee, London, England, Bulletin MC/153.

10 "External Corrosion of Furnace-Wall Tubes. I. History and Occurrence," by W. T. Reid, R. C. Corey, and B. J. Cross, Trans. ASME, vol. 67, 1945, pp. 279–288. (10a) II. "Significance of Sulphate Deposits and Sulphur Trioxide in Corrosion Mechanism," by R. C. Corey, B. J. Cross, and W. T. Reid, ibid., vol. 67, 1945, pp. 288–302. (10b) "Further Data on Sulphate Deposits, and the Significance of Iron Sulphide Deposits," by R. C. Corey, H. A. Grabowski, and B. J. Cross, ibid., vol. 71, 1949, pp. 951–963.

11 "Untersuchungen über die Ursachen der Ansatzbildung bei der Vergasung und Verfeuerung von Steinkohlen," by W. Lange, *Glückauf*, July 27, 1940, pp. 410–413.

12 "Chemische Einflüsse bei der Verschmutzung und Verschlackung von Kesselanlagen und Gaserzeugern," by Rudolph Lessni, *Feuerungstechnik*, vol. 28, July 15, 1940, pp. 145–149.

13 "The Influence of Silica Smokes on the Dewpoint of Combustion Gases Containing Sulphur Oxides," by G. Whittingham, *Journal of the Society of Chemical Industry*, vol. 67, 1948, pp. 411–414.

14 "Methods of Cleaning Modern Stoker-Fired Boiler Plant," The Boiler Availability Committee, London, England, Bulletin No. MC/131, p. 14.

15 "Über die Ansatzbildung an den rauchgas-berührten Heizflachen," by K. Prantner, *Die Wärme*, vol. 62, April 15, 1939, pp 254–257.

16 "Beseitigung von Ansatzbildungen auf der Rauchgasseite von Dampfkesseln," by E. Schumann, *Die Wärme*, vol. 62, December 9, 1939, pp. 745–749.

17 "Methods of Cleaning Boilers and Researches of Boiler Plant Manufacturers," Paper No. 3, by W. G. Marskell, Seven Papers on Boiler Availability, The Boiler Availability Committee, London, England, Bulletin MC/160, p. 29.

18 "Researches at the British Coal Utilisation Association," Paper No. 5, by G. Whittingham, ibid., p. 41.

19 "Causes of Flue Gas Deposits and Corrosion in Modern Boiler Plants," by W. F. Harlow, *Journal and Proceedings*, The Institution of Mechanical Engineers, vol. 160, December, 1949, pp. 359–368; discussion, pp. 369–374; communications, pp. 374–379.

"Causes of High Dewpoint Temperature in Boiler Flue Gases," by W. F. Harlow, Proceedings of The Institution of Mechanical Engineers, vol. 151, 1944, pp. 293–298.

20 "The Catalytic Oxidation of Sulphur Dioxide on Metal Surfaces," by G. Tolley, Part I, *Journal of the Society of Chemical Industry*, vol. 67, 1948, pp. 369–373. Part II, "The Reaction of Sulphur Dioxide and Oxygen at a Mild Steel Surface," vol. 67, 1948, pp. 401–404.

Discussion

J. S. Bennett.[6] As a representative of the manufacturer of the stokers included in this report, it was the writer's good fortune to have an opportunity to discuss this subject with the authors prior to the writing of their paper. The writer went to Delray as a skeptic and came away convinced that they had something. The authors had investigated every conceivable blowhole in their theory and, as far as was humanly possible, had eliminated those factors which might have caused the improvement other than humidification. It is gratifying that the experience of the public utility in Pittsburgh has confirmed the Detroit results.

One factor influencing fireside deposits is interruptions to coal flow. Feed to the stoker itself can be insured by the installation of coal-hopper agitators which are available with any first-class multiple-retort underfeed stoker. A great deal of attention should be given to the flow of coal from the bunker to the stoker hopper.

Because of the increase in ash content and general deterioration in coal quality, it is likely that most stoker-fired boilers that have capacities on the order of 300,000 lb per hr and larger will be spreader-fired. Following the authors' theory, that portion of the total coal on the grate of a spreader stoker is burned with a large excess of air which should reduce the tendency toward fireside deposits on boiler tubes. Again, the authors mention that a reduc-

[6] Vice-President, American Engineering Company, Philadelphia, Pa. Mem. ASME.

tion in the time that the ash is exposed to the heat of the furnace should reduce fireside deposits. In the case of the spreader stoker, the ash is in the furnace a shorter time than with the underfeed stoker. Our experience with spreader-stoker-firing of large boilers to date confirms the fact that fireside deposits are less serious than with any other types of firing. It should be remembered, however, that multiple-retort stoker-firing of boilers of the sizes of 200,000 lb per hr and down involves much less serious conditions, and boiler fouling is rarely a problem.

The authors have made no comment on the effect of humidification on stoker maintenance. Comments along this line would be of interest.

R. C. Corey.[7] Although the authors are careful to state that further work is necessary to establish definitely whether or not humidification is beneficial in reducing the volatilization of deposit-forming constituents from the fuel bed, the preliminary results and correlations which they report point strongly in the affirmative. Considering the difficulties of securing data from an operating boiler, where the variables cannot be controlled with bench-scale precision, the authors have obtained a great deal of significant data that will be of use to other workers in this field.

Their probe technique for collecting samples of deposits is unique, and it is hoped that this phase of the investigation will be extended to probe the furnace atmosphere at a few elevations between the fuel bed and the furnace outlet. In this manner it may be possible to establish if gas temperature affects the nature of the deposits, for example, if sulphates are formed close to the fuel bed. Of course the surface temperature of the probe should be kept as near as possible to that of the furnace tubes.

The authors suggest that alkali-matrix-type deposits are more prone to form in stoker-fired boilers than in pulverized-coal-fired boilers. The writer is inclined to believe that greater volatilization of certain inorganic constituents occurs with pulverized-coal firing, but deposition takes place largely on the furnace-wall tubes, where usually it is unnoticed unless external corrosion becomes active.

The theory that the moisture takes part in a steam-carbon reaction, lowering the mean bed temperature and thereby reducing volatilization of certain constituents, has merit. This might be easily studied on a laboratory scale.

It is suggested that the authors indicate in Table 2, item e, whether the air weight represents dry or moist air. Furthermore, since the fuel alone supplied about 1705 lb per hr of water, part of which probably decomposed during underfeed action, this quantity should also be included in Table 2.

Assuming the saturated steam added to the bed (7470 lb per hr) is heated approximately to 2000 F, the heat absorbed from the bed is roughly one third the amount that would be absorbed if the amount of carbon shown in Table 2 reacted completely with steam. However, since the percentage steam decomposition probably is closer to 50 per cent, the endothermic heat and sensible heat absorbed by the water vapor probably are about the same magnitude. It is suggested therefore, that the enthalpy increase of the saturated steam may have about the same effect in reducing the fuel-bed temperature as the endothermic reactions.

It is conceivable that for the same amount of heat removed from the fuel bed, the temperature-distribution pattern may be different when the water-gas reaction takes place than when only steam is being superheated in the fuel bed. This can only be determined satisfactorily from vertical temperature traverses in the fuel bed; a most difficult procedure in an operating boiler, as the authors suggest.

[7] Supervising Engineer, Combustion Research Section, Coal Branch, U. S. Bureau of Mines, Pittsburgh, Pa. Mem. ASME.

Although the boiler has been described previously, the reader might appreciate an additional figure showing the side elevation and the approximate location of the sampling points.

Do the authors have an explanation for the fact that the deposit found on the probe was darker in color when the air was humidified?

J. H. DeVisser.[8] The authors and The Detroit Edison Company are to be complimented on making available the results of the outstanding work reported in this paper. It is hoped that additional information will be made available to the Society as more experience is gained in this new method of stoker operation.

The writer has been identified in a small way for over 40 years with the outstanding underfeed-stoker developments accomplished by The Detroit Edison Company in their several stoker-fired plants. The use of humidification is another one of these developments. In the past the use of large underfeed stokers with metered air control and later restricted tuyères has resulted in an economical fuel-burning arrangement. By eliminating frequent boiler outages because of tube-fouling, additional operating savings will result. It will be interesting to know what reduction in iron replacement cost will be realized when such information is available.

Also, it would be of interest to have the authors comment on the change in firing characteristics and the elimination of large clinkers with certain grades of fuel.

R. B. Donworth.[9] Many readers who have excessive slagging and limited outputs from boilers fired by underfeed stokers, no doubt will endeavor to humidify the forced-draft air. The paper itself presents sufficient data to show that under certain conditions it gives great promise of keeping boilers clean and of reducing both furnace and stoker maintenance costs.

There is, however, a serious problem in this connection, namely, that of make-up. The maximum rate of steam use for such humidification appears to be on the order of $1\frac{1}{2}$ per cent of the boiler output, which will probably more than double the make-up requirement. The obvious answer, if make-up capacity is limited, is to humidify by direct evaporation of water by the forced-draft air, but this is not as easy as it sounds. It will be found that the evaporation of the quantity of water required in extreme cold weather, will reduce the forced-draft air temperature by approximately 75 F. Since the required absolute humidity of 115 grains per pound of dry air represents 100 per cent relative humidity at 71 F, it will be necessary either to preheat the air to at least 146 F before humidifying, or to add the equivalent heat during the period of adding moisture. It will also be found that it is very difficult to obtain complete and effective evaporation in this manner, and it may prove necessary to add moisture in excess and remove the surplus in a separator, as is done in some types of air washer. Even if steam is used for humidification, it will be necessary that the air be at all times above 71 F, and attention must also be given to the temperature of the air-duct metal on which moisture may condense.

One method of heating the forced-draft air is to recirculate some boiler-outlet gas. It will be necessary to overcome the difference in draft by mechanical means; and, since steam is to be added anyway, it is logical to introduce the steam for humidification through an injector which also boosts the pressure by several inches of water. In one station where this arrangement is now being installed on a 325,000-lb per hr boiler, two 20-in. round ducts will carry gas at 700 F from the economizer inlet to the

[8] Vice-President and Treasurer, The Coon-DeVisser Company, Detroit, Mich. Mem. ASME.

[9] Betterment Engineer, Power Stations Department, Duquesne Light Company, Pittsburgh, Pa. Mem. ASME.

forced-draft-fan inlets, the maximum expected gas recirculation being about 8 per cent of the air flow.

WILHELM GUMZ.[10] This paper is an excellent contribution to the art of burning solid fuels, and the authors and The Detroit Edison Company deserve full credit for this fine piece of large-scale investigation. In a sense, the results confirm the views expressed by W. Lange[11] and R. Lessnig,[12] who explain the increase in silicon oxide in the deposits by silicon-sulphide (mono and bi-sulphide) formation which vaporize at relatively low temperatures, but can condense on the surfaces of the tubes. The boiling point of SiS is only 1724 F. Lange also recommends either large amounts of excess air—it would be preferable to say a complete mixing of excess oxygen and the vaporized constituents by a perfectly operating overfire-air system—or the addition of moisture. The other possibility of volatilization of silicon, silicon-monoxide formation,[13,14] can be counteracted by the same measures, so that differences in opinion concerning these theories or reaction mechanisms are of little consequence for the power-station man.

In the light of the reaction mechanism of silicon transport from the fuel bed to the superheater tubes, it seems to be more appropriate to speak of an oxidation or hydrolization of the silicon compounds rather than a "reduction of their volatilization." This oxidation takes place in the interstices of the fuel bed, but continues in the furnace space above the fuel bed. In so far as it takes place in the fuel bed and the silicon is retained in the fuel bed, it would be a reduction of the volatilization, but the very fine particles of SiO_2 formed from the vapor-phase sulphides are most likely at least partly carried out of the fuel bed, as well as part of the sulphides which are oxidized in the gas space above the fuel bed. The effect of overfire air on the reduction of slagging tends to confirm such an explanation. More light could be thrown on this problem if the authors added to the information of Table 4 the analyses of the residues and the fly ash to complete the picture of the material balances of the mineral matter.

As additional measures for the improvement of operating conditions, the following are suggested:

1 Addition of limestone to the coal to bind silicon into silicates and to reduce the amount of silicon sulphide formed.

2 The use of overfire air for thorough mixing of the gases leaving the fuel bed for complete reaction not only of the combustible gases but also of the oxygen and water vapor with the silicon compounds.

The first measure was found successful by J. Bronn[15] in gas-producer operation; the second has shown marked decreases in deposit formation.[16] If overfire air with adequate air pressures to achieve full penetration and perfect mixing has had good results even without additional moisture, the combination of both these measures, overfire air and humidification of the combustion air, can be expected to achieve even better results. It could be hoped that this combination would permit a reduction in the amount of moisture added and thus a reduction in the loss of heat of evaporation; even higher boiler efficiencies would then result. This paper provides an excellent foothold for further economic studies.

[10] Consultant, Battelle Memorial Institute, Columbus, Ohio.
[11] Authors' Bibliography (11).
[12] Authors' Bibliography (12).
[13] Authors' Bibliography (9) and (13).
[14] "Siliziummonoxyd," by E. Zintl, et al., *Zeitschrift anorg. und Allgem. Chemie*, vol. 249, 1940, pp. 1–7.
[15] "Verringerung und Verhalten des im Generatorgas enthaltenen Schwefels im Siemens-Martin-Ofen," by J. Bronn, *Stahl und Eisen*, vol. 46, 1926, pp. 78–81.
[16] "Abhilfe gegen das Verschlacken von Dampfkesseln," by Karl Cleve, *Archiv. Waermewirtsch*, vol. 22, 1941, pp. 185–189.

Regarding the authors' remark that the endothermic reaction of the water vapor with carbon has not been proved, it can be said that it is unlikely that even the most refined methods applicable to such a full-scale experiment could detect the small lowering in temperature of the carbon surface to be expected from the use of air saturated at 58 to 70 F, as compared to the use of air with its natural moisture content. The writer has published[17] a curve which shows the calculated reduction in reaction temperatures of carbon by air saturated at various temperatures. The reduction in temperature by saturation at 70 F, as compared to saturation at 32 F, is only in the order of 180 F, and between the humidified air as compared to air with the natural moisture content a fraction thereof. Yet the obvious difference of a slagging-ash producer which uses dry air and a "dry-bottom" conventional gas producer which uses air saturated at 120 F is a perfect proof of the effect that moisture can have on the behavior of ash in a fuel bed.

W. F. HARLOW.[18] The paper shows conclusively that a remarkable reduction in the flue-gas deposits has been achieved, not only in the superheater, as intended, but also in the economizer and air heater.

Quite apart from the improvement in thermal efficiency which may accrue from this, after taking into account the expenditure of steam for humidification, the increased availability of the generating units from 53 days to something over 133 days is a noteworthy result.

It is quite clear that the fuel characteristics played no part in this improvement, since the fuel remained unchanged and was, in fact, of a nature considered from general experience in England to be the least likely to produce the troubles from which the unit suffered. This proves that fuel quality is not the dominant factor in this controversial and widespread problem, as so often thought.

Less evident is the mechanism by which this improvement has been brought about and a fuller understanding of the reasons for the results must be obtained to make the best use of the information in other circumstances. In the absence of more detailed information than is given in the paper, this matter is somewhat speculative.

It seems that the theory which prompted the experiments, namely, the reduction of the superheater deposits by suppressing the vaporization of the alkali salts which form one of their constituents, is not altogether borne out: (*a*) Because no diminution in fuel-bed temperature was detectable and, (*b*) because the deposits in the economizer and air heater which do not depend on the presence of alkali sulphates have practically disappeared. This indicates, quite clearly, that the sulphur trioxide in the flue gases, which is known to play such an important part in the production of all deposits, of which it invariably forms a major constituent, has definitely been suppressed. For a complete explanation of the results, therefore, a reason for this must be sought. In the writer's view, this lowering of sulphur trioxide is the fundamental reason for the improvement.

It is an undisputable fact that sulphur trioxide will occur when flue gases pass over heated iron surfaces, and no permanent means have yet been found to avoid this formation, although it will vary with the temperature and surface conditions and, according to Tolley,[19] with the moisture content of the gases. The following explanations for the reduction of the sulphur trioxide appear possible:

[17] "Gas Producers and Blast Furnaces," by Wilhelm Gumz; John Wiley & Sons, Inc., New York, N. Y., 1950, fig. 7, p. 26.
[18] Director and Chief Engineer, General Engineering Division, International Combustion, Ltd., London, England.
[19] Authors' Bibliography (20).

1 The removal of the corrosion products on the superheater tube by the washing.

2 The subsequent application of alkali to these tubes.

3 A reduction of the catalytic effect, due to the increased moisture content of the flue gas.

4 A lowering of the surface temperature of the superheater tubes.

Both items 1 and 2 are stated in the paper to have been comparatively unsuccessful although these have given reported improvements elsewhere. The writer has found the effectiveness of these methods depends to a great extent on the mode of application and accessibility of the superheater. Fig. 14, herewith, shows the difference in deposit formation on sandblasted tube sections with and without spraying with soda solution, the sections being exposed to similar flue gases when heated to the same gradation of temperature as described in the writer's recent paper.[30]

The third possibility that the increased moisture in the flue gases has suppressed the catalytic action, does not appear feasible since their total moisture with the humidified air would not be greatly in excess of those from oil-fired plants, which contain a much higher proportion of moisture of combustion due to the greater hydrogen content of the fuel.

Therefore it appears that there has been some considerable lowering of the surface temperature of the superheater tubes, and this easily might have been brought about by the improvement in

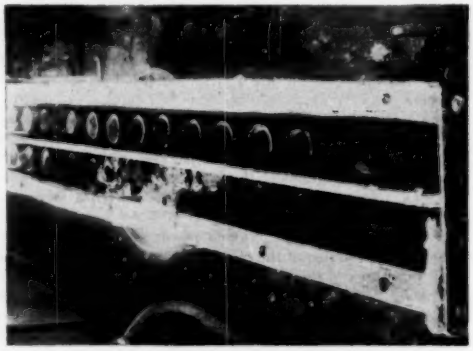

FIG. 14 EFFECT ON FLUE-GAS-DEPOSIT FORMATION OF SPRAYING CLEAN TUBE SURFACES WITH SODA SOLUTION, AFTER EXPOSURE FOR 556 HR WITH 3 PER CENT SULPHUR COAL

the combustion process, resulting from the humidification. In England the wetting of coal on chain-grate stokers to the maximum extent which can be carried, has been general practice for many years and, owing to the increased porosity of the fuel bed, this invariably leads to more prompt and complete combustion. It seems possible that a similar effect may be obtainable with retort stokers by humidifying the air, leading to an important reduction in the flame length of the burning gases from the fuel bed, with a consequent lowering of the temperature in the superheater zone. A measurement of the tube temperatures on further humidified boiler tests would establish whether this is, in fact, the reason for the improvement. From the remarkable reduction in flue-gas temperatures which have been recorded, it will be surprising if a considerable drop in tube temperature has not been achieved.

[30] Authors' Bibliography (19).

There is, of course, a certain lowering of the theoretical flame temperature, due to the greater heat capacity of the combustion products leaving the fuel bed as a result of the added water, but this appears too small to account for any important reduction in the tube temperatures.

The writer cannot subscribe to the theory that the deposits depend on the fuel-bed temperature, since no parallel explanation is possible for pulverized-fuel and oil-fired plants where similar deposits form. According to his experience, in one notable plant where the deposits were corrected, partly by operational methods, the furnace and fuel-bed temperature was actually increased, but owing to shortening of the flame, the temperature of the superheater tubes was substantially decreased.

It is difficult to believe that the vaporization of the alkalies or silica is so susceptible to the relatively small changes of fuel-bed temperature which could be expected, as to have any appreciable effect. In any case an increase in endothermic reaction within the bed (which always proceeds to some extent when this exceeds 4 in.) would result in increased heat liberation and temperature above the bed where the vaporization of the harmful material could equally well take place.

J. A. KEETH.[31] The authors of this paper have presented a valuable contribution on the subject of "fireside deposits," this being a problem that almost all operators of coal-fired stations face to some degree. Although great progress has been made during the past 10 years in reducing the amount of tube deposits, it has been accomplished largely through the use of larger heat-absorbing furnaces with lower accompanying gas temperatures, and through the use of wider spaced screen and superheater tubes. The use of washed coal has also been a factor in reducing deposits in many installations. Almost all companies, however, are operating, to some extent, boilers installed a number of years back, where these structural improvements cannot now be effected, and any solution which will relieve the slagging condition in these older boilers will prove extremely valuable.

The company with which the writer is connected has faced this slagging problem for many years, particularly in connection with forced-draft chain-grate-stoker installations. It has been the practice here to add moisture to the coal before feeding it to the chain grates, this being done largely to improve the condition of the fuel bed. The addition of this moisture has resulted in a total moisture of about 16.4 lb per 1000 lb of dry gas, which is similar to the figure referred to in the paper. Severe slag conditions continue to exist, even with the addition of this moisture. These conditions were worse than is experienced today with a lower-moisture coal. The answer, however, probably lies in the fact that the coal which resulted in the most severe conditions of slagging was a low-Btu unwashed coal containing a high percentage of impurities. The washed coal of higher Btu value which is being used today, containing a much lower quantity of moisture per thousand pounds of dry gas, is resulting in far less slag or fireside deposits than the previous coal. Therefore it is difficult to draw any conclusions as to the effect of the moisture added to the fuel bed.

Our company has done considerable experimenting with the injection of high-velocity steam over forced-draft stokers, largely for the purpose of increasing turbulence and reducing the tendency to create smoke. The same effect has been produced by the use of high-velocity air jets. No difference was noted during these tests on the accumulation of fireside deposits on the upper tube banks. Admittedly, however, one might expect a different effect from the admission of overfire moisture than that obtained

[31] Manager of Production, Kansas City Power & Light Company, Kansas City, Mo. Fellow ASME.

in the authors' experiments where the moisture was admitted with the combustion air below the fuel bed.

The results reported in the paper are quite conclusive, and it is hoped that they and other experimenters will carry the work further, possibly extending the field of application to pulverized-coal-fired installations. Undoubtedly, the success reported in the authors' paper will lead to other operators carrying the work further with the hope and belief that a thorough understanding of the process will be forthcoming, and that the benefits received in The Detroit Edison plant can be extended to all other installations suffering from the difficulty of heavy fireside deposits.

P. R. Loughin.[22] The authors have made no mention of the latest development in a parallel investigation to solve the same problem that has been carried on in England. The operators of the Battersea Station in London of the British Electricity Authority, in collaboration with the writer's company, have been endeavoring for many years to reduce boiler and superheater fouling on their large units fired with multiple-retort underfeed stokers. The authors have mentioned some of their earlier work. The latest development was the application of recirculating flue gas by returning 10 per cent of the flue gas from the induced-draft fan and introducing this with the combustion air through the fuel bed. The object was to reduce the temperature in the fuel bed and therefore decrease the volatilization of troublesome constituents in the ash. Operation with this gas recirculation has shown very definite improvement. Maximum permissible boiler ratings have been increased, and they can now operate 4500 hr between outages for cleaning with no hand-lancing, compared to original periods of 600 to 800 hr with extensive hand-lancing. It is reported that maximum fuel-bed temperatures were reduced about 150 F by use of 10 per cent flue-gas recirculation.

Considerable of the writer's work with humidification has involved adding moisture to obtain 16.4 lb per 1000 lb of dry air. During the dry seasons without humidification the operation was with a water content of about one sixth of this amount, or 2.7 lb per 1000 lb of dry air. Based on the assumption that all the water vapor undergoes the endothermic reaction with carbon, an attempt to calculate a theoretical adiabatic temperature for these two conditions indicates the effect of humidification is to reduce this temperature about 160 F.

A similar calculation for 10 per cent gas recirculation with the moisture in the flue gas also reacting with the carbon indicates a temperature reduction in the order of 300 F.

It is hoped that the results of the gas-recirculation trials will be reported soon in the English technical literature. If this is done as well and as thoroughly as the authors' paper on humidification, we may be able to appraise the comparative results and the economics of these methods.

E. M. Parrish.[23] Our appraisal of the work reported in this excellent paper can best be given by a brief review of our own experience in the control of fireside deposits which work, incidentally, was started as a direct result of information given us by the authors.

The formation of fireside deposits on stoker-fired steam generators in the several stations of our company has been a major problem. The steam generators in the James H. Reed Station have been the most serious offenders, and for brevity this discussion will be limited to these units.

Six stoker-fired steam generators are installed in the Reed Station. Nos. 1, 3, and 5 were installed in 1930, with a steaming capacity of 325,000 lb per hr. Nos. 2 and 4 were installed in 1937, with a capacity of 375,000 lb per hr; No. 6 was installed in 1940, with a capacity of 400,000 lb per hr. In many respects these units are similar to the steam generators in the Delray Station. Each steam generator is of the four-drum Stirling design equipped with waterwall furnaces, superheaters, and economizers. Nos. 2, 4, and 6 units are also equipped with tubular air heaters. The stokers are Westinghouse underfeed stokers with undulating sections and clinker grinders.

Reed Station has been operated as a base-load station, and the steam generators are being operated at practically their maximum capacity on a continuous basis. For the last 8 years it has been necessary to remove these steam generators from service on week ends for 2-day periods at 6-week intervals for stoker maintenance and heating-surface cleaning. Approximately 150 man-days were required per outage, one half of which was at overtime rates. An average of 500 to 700 stoker castings were used at each outage to maintain the stoker. During the life of the steam generators several changes were made, both in operating and maintenance practices and in the equipment, to alleviate the condition.

Loss in steam-generating capacity due to fouling of heating surface at times amounted to more than 10 per cent of the maximum clean-condition capacity. Loss in economy was 2 per cent or more.

Work at Delray on humidification of combustion air to reduce fireside deposits came to our attention in early May, 1950. We were impressed with the results of their work to the extent that we started humidification of combustion air on No. 1 steam generator at Reed on May 31, and on No. 4 steam generator on June 5, both on an experimental basis. These steam generators have operated since with air containing moisture equivalent to saturation at 71 F at atmospheric pressure or about 115 grams total moisture per lb of combustion air. Saturated steam from the boiler is used for humidification.

In order to provide a source of steam quickly for the humidification of combustion air, we have taken steam directly from the drum of the steam generator involved. Some improvement can be effected by use of extracted steam or vapor from an evaporator properly placed on the station heat-balance arrangement. Where steam generators are equipped with air heaters, humidification can be accomplished by introduction of water in the preheated air by atomizing nozzles.

Steam-generator heating surfaces were cleaned to bare metal before humidification of combustion air by washing with water at 160 to 180 F containing 0.1 per cent of soda ash with a wetting agent added.

When No. 1 steam generator was returned to service after cleaning, the net reduction in gas temperature at the economizer outlet at maximum load was 120 F. After 5 months of operation with humidified combustion air, the gas temperature increased by about 40 F so that at present we still retain $^3/_4$ of the improvement we had after water-washing the heating surfaces. On No. 4 steam generator the net reduction in gas temperature at the air-heater outlet at maximum load was 80 F. At the end of 5 months this improvement is 70 F. The sustained maximum capacity of these units is definitely higher since we are operating with humidified air.

No cleaning has been done on either steam generator since humidification of combustion air was started. The steam generators are now being removed from service for 2 days in 12 weeks for stoker maintenance. Stoker iron used is about the same as was previously required on 6-week outage schedules. Labor requirements are approximately 60 man-days per outage every 12 weeks, compared to the former 150 man-days every 6 weeks, a reduction of 60 per cent.

On the basis of the promising results obtained at Delray and on our own early experience, we have continued to equip additional

[22] Chief Staff Engineer, Babcock & Wilcox Company, New York, N.Y. Mem. ASME.

[23] Duquesne Light Company, Pittsburgh, Pa.

steam generators for humidification of combustion air. At present the six steam generators at Reed are operating with humidified combustion air. Seventeen underfeed-stoker-fired steam generators in Brunot Island Station, ranging in capacity from 40,000 to 50,000 lb of steam per hr, are being so equipped. One 120,000-lb per hr stoker-fired steam generator at the Colfax Station is now operating with humidified combustion air for test purposes.

To summarize tentatively the improvement due to humidification of combustion air on the basis of our experience to date, the gain in the dry-gas heat loss due to lower stack-gas temperature is greater than the cost of steam for humidification. The steam-generator capacities are being maintained at practically clean-boiler conditions. Steam-generator outage time for stoker maintenance has been reduced by 50 per cent; stoker-iron replacements have been reduced by 50 per cent. Labor for heating-surface-cleaning probably will be reduced by 85 per cent.

In order to evaluate fully the advantage of humidification of combustion air on stoker-fired steam generators, we believe a full year's experience will be necessary to determine its year-round effectiveness and to establish completely heating-surface cleaning schedules and stoker-maintenance schedules.

Possibly results of our experience to date have stirred our enthusiasm too greatly, but even if the final benefits prove to be appreciably less than those presently indicated, we, as well as other companies who are confronted with the problem, will be indebted to the authors of this paper and their associates for their pioneering work.

F. SHAKESHAFT.[34] The authors state that the deposits occurring in the superheater region of the Delray boilers appear to be of the alkali-matrix type, and we feel that the inclusion of detailed analyses of these deposits would have been of interest and of value. From the results of the probe tests given in Table 4 of the paper, it would appear that the proportion of acid-soluble material is much lower than is normally encountered in alkali-matrix deposits.

The authors refer to the desirability of minimizing the volatilization of alkalies, silica, etc., from fuel beds either by fuel selection as advised by Crossley, or by operating with fuel-bed temperatures as low as circumstances permit. In the former connection they will be interested to hear that recent long-term trials on a stoker-fired boiler have shown the advantages to be gained from coal selection.[35] The length of run at M.C.R. before it was necessary to shut down because of superheater fouling varied from 500 hr with a coal containing 1 per cent of chlorine, to over 8000 hr with a coal containing less than 0.1 per cent of chlorine.

The work of The Boiler Availability Committee has established beyond doubt that the deposit-forming constituents are released during the second stage of the combustion of fuel beds on a traveling grate, when the bed consists of a mass of burning coke. Deposits grow more rapidly when fires are long and ragged and "blowholes" or craters in the bed are particularly bad, as hot spots rapidly develop.

The broad aspects of the effect of water, added either to the fuel as such or to the air stream, has been the subject of much research work by the committee. The conditioning of fuels, by water or steam, is a well-known practice and is known to improve the combustion of fuels probably by creating a more open and permeable bed structure. It is important to realize, however, that on traveling-grate stokers the water present in or added to the fuel, as well as the water produced from the hydrogen in the coal is generally evolved during the ignition stage corresponding to the combustion of the volatile matter, and the burning-out of the residual coke takes place under relatively "dry" conditions. It is not surprising, therefore, that the latter process, including reactions in and above the fuel bed, may be susceptible to the amount of water vapor in the air supply.

A consideration of these and other factors suggested that recirculation of flue gases with the air supply might have beneficial effects on deposits and corrosion. It was thought that not only would the fuel-bed temperature be lowered by endothermic reactions, thereby minimizing the release of volatile ash constituents, but that the possible reduction in furnace and boiler-outlet temperatures would reduce the deposition of solid matter without greatly affecting the heat absorption in the superheater region. Experiments with gas recirculation have been carried out in Great Britain on two retort-stoker-fired boilers with spectacular results.[35]

Previously these boilers had suffered from phosphatic deposits in the superheater to such an extent that it was not possible to run more than 600 hr. The introduction of auxiliary pulverized-fuel-firing, 10 per cent of the fuel burned, above the bed, and the use of the methods of cleaning advocated by The Boiler Availability Committee led to some improvement, runs of 1200–1400 hr being obtained with water-lancing. With gas recirculation (approximately 10 per cent) the period of operation extended to 4500 hr, and practically no water-lancing was employed.

Although the use of gas recirculation has more than quadrupled the length of a run, the character of the deposits[35] has not changed overmuch. It is evident that phosphorus compounds are still being volatilized from the fuel bed but that the rate of deposition is decreased, probably due to the operation of such factors as changes in gas velocity and temperature. Fundamental work on the effects of gas recirculation is proceeding, but it would appear that gas recirculation has much more to commend it than steam injection. It is a more economical proposition and has the added advantage that endothermic reactions between the fuel bed and CO_2 are superimposed on those with steam.

Although the analytical results obtained from relatively short-term probe investigations and quoted in the paper show that the quantity of silica volatilized, and by inference the fuel-bed temperature, is reduced, the extent to which the bed temperature is lowered is difficult to determine in practice. Recent experiments into the effect of steam additions to the primary air fed to a stationary bed of coal and carried out on a combustion pot of the type used by Nicholls,[36] Marskell,[37] and others, suggest that with 1.6 per cent of added steam, the reduction in fuel-bed temperature is likely to be of the order of 60–80 F (Table 5 of this discussion).

TABLE 5 EFFECT OF ADDED STEAM ON MAXIMUM FUEL-BED TEMPERATURE OBTAINED DURING COMBUSTION OF A FREE-BURNING, HIGH-VOLATILE COAL

Steam (per cent of primary air by volume)	Maximum fuel-bed temperature, deg F
0	3056
5	2810
10	2810
15	2642
20	2390

There is no apparent reason why the economizer deposits, referred to in the paper, are lessened by the introduction of steam to the air unless they peel off from the tubes as soon as they have formed a thin skin. This could be expected in the circumstances.

So far our comments have been confined to the effect of the modification on fuel-bed reactions, but the processes obtaining

[34] Generation Design Engineer, Chief Engineer's Department, British Electricity Authority, London, England.

[35] Various communications from members of The Boiler Availability Committee not yet published.

[35] U. S. Bureau of Mines Bulletin No. 378, 1934.

[37] "Mode of Combustion of Coal on a Chain Grate Stoker," by W. G. Marskell, et al., *Fuel*, vol. 25, 1946, pp. 4–12, 50–58, 78–85, 109–112, and 159–162.

above the fuel bed and on heating surfaces may be modified to an even greater extent. The well-known benefits which can accrue from water injection into oil-fired furnaces, with a view to the suppression of fouling troubles, do, in fact, indicate that the reactions in which the water plays a part are not essentially confined to a fuel bed.[28]

The behavior of SO_3 in the boiler system, known to be of major importance not only in relation to air-heater corrosion and blockage but also to high-temperature deposits, has not received much attention in the paper. The authors refer to the question of secondary or "delayed" combustion and it is now known that this can lead to the production of SO_3 in at least two ways. Whittingham[29] has shown in laboratory experiments that a high degree of oxidation of SO_2 occurs during the combustion of relatively dry CO and that this can be greatly reduced in the presence of moisture. The work of Harlow on the catalytic oxidation of SO_2 on heating surfaces, particularly when the latter are overheated by flame impurities, is well known, and the work of Tolley referred to in the paper shows that water vapor has an inhibiting effect.

The phenomena associated with the condensation of sulphuric acid on surfaces, the temperature of which is below the acid dew point of the gases, have received much attention from the committee. It is known that the degree of corrosion obtaining is dependent on the strength of condensed acid,[28,29] and this is a function of water-vapor content and surface temperature. It might be expected that an increase in water-vapor content would lead to the condensation of a more dilute and corrosive film of acid, but recent work has shown that steam additions of the order used in the present work would only slightly affect the acid concentration. It would be valuable to know whether any tests have been made or are contemplated on the dew-point characteristics of the flue gases with or without humidification.

J. W. Shaw.[30] It is hoped that this comprehensive paper will provoke further research on the burning of coal, because it is a general rule that the more efficiently coal is burned, the less air pollution results.

A review of this paper reveals no reference to the physical characteristics of the fuel bed. When the burning rate on multiple-retort stokers exceeds 40 lb of coal burned per sq ft of grate area per hr, the increased static pressure necessary to furnish sufficient combustion air causes blowholes in the fuel bed. This condition results in higher quantities of fly ash in the combustion gases. The authors state that there is secondary combustion in the steam generators at the Delray plant. Is it not then possible that the heat from this secondary combustion causes the fly ash to be plastic when it reaches the superheaters and thus build up when impinging on these tubes?

Is it not possible that the addition of the water to the combustion air could cause the fuel bed to be more porous so that there is a decrease in the blowholes and the resultant fly ash?

There is also no mention of the clinker formation. Does not the addition of the water in the combustion air with its endothermic reaction result in less dense clinker formation with the resultant more uniform fuel bed?

If the fireside deposits were caused exclusively by the volatilization of the metals in the mineral matter of the coal, why is this problem not more serious in pulverized plants where the ash is much finer and is carried through the hot combustion chambers of the steam generator?

The investigations and observations resulting in this paper were obviously very carefully done. The writer believes, however, that further study is necessary before specific conclusions are reached regarding volatilization and condensation.

R. A. Sherman.[31] The use of steam to control slag formation and clinkering in the fuel beds of gas producers has been established practice for many years and, since the first note on the use of steam at the Delray Station for the control of fireside deposits was published,[32] a number of fuel engineers have told the writer that they had used steam under the grate of boilers many years ago. Nevertheless, the writer has never heard anyone propose the use of steam for the control of the deposition of ash and slag on boiler tubes, despite the apparently increasing severity of the difficulties which result from increased rates of operation.

Consequently, the engineers of the Detroit Edison Company deserve great credit for their conception of this solution to the problem and for the thorough and careful research they have done to obtain conclusive evidence on the effect of the use of steam.

Some years ago, in a study of refractories-service conditions in boiler furnaces,[33] the writer found evidences of a considerable degree of segregation of different constituents of coal ash both in generators fired with stokers and pulverized coal, with the result that the composition of the ash or slag deposited on the tubes and of the clinker differed from that of the original ash of the coal. One of the striking findings in that work was that the content of the alkalies in the initial deposit on the boiler tubes was greater than in the coal ash. In this connection, he reviewed the published data to look for any evidence of the transport of silica, but none was found. A possible explanation is that the rates of burning used in the writer's investigations were much below those used at the Delray Station and at most modern stations today.

A further possibility is that the transport of silica is affected by the characteristics of the ash. If this is true, then the use of steam might be less effective in the control of deposits with other coals. To establish this, not only should experimental trials be made with coals whose ash differs in composition, but also an attempt should be made to obtain a complete understanding of the method by which silica is transported from the bed. The volatilization of silica has been observed by many people, and the authors cite a number of references which present various explanations of the mechanism of transfer.

The authors make no reference to the theory that the mechanism of transport of silica is through the formation in reducing sections of the fuel bed of a sulphide of silicon which has a much higher vapor pressure than silica. The sulphide is oxidized to silica in the oxidizing atmosphere above the fuel bed. This explanation was proposed by Lange[34] and has been discussed by Zinsen.[35]

An interesting question that has been raised in the minds of a number who have discussed this work is that of just how and where the introduction of steam to a fuel bed decreases the temperature attained. A simple explanation, of course, and the

[28] "Third Symposium on Combustion Flame and Explosion Processes," by G. Whittingham, Williams and Wilkins Company, Baltimore, Md., 1949, p. 448.

[29] "The Corrosion of Heating Surfaces in Boiler Plants: Further Studies in Deposit Formation," by J. R. Rylands and J. R. Jenkinson, Proceedings of The Institution of Mechanical Engineers, vol. 158, 1948, pp. 405–414.

[30] Chief Smoke Inspector, Department of Buildings and Safety Engineering, City of Detroit, Detroit, Mich.

[31] Assistant Director, Battelle Memorial Institute, Columbus, Ohio. Fellow ASME.

[32] "*Mechanical Engineering*," vol. 72, April, 1950, p. 334.

[33] "A Study of Refractories Service Conditions in Boiler Furnaces," by R. A. Sherman, U. S. Bureau of Mines Bulletin No. 334, 1931.

[34] Authors' Bibliography (11).

[35] "Results of New Research on the Causes of Ash Deposits on Boiler Heating Surfaces," by A. Zinsen, TR *Zeitschrift des Vereines deutscher Ingenieure*, vol. 88, 1944, pp. 171–177.

one always offered, is that the heat absorbed by the endothermic reaction of water with carbon to form carbon monoxide and hydrogen lowers the temperature. However, the work of Haslam and others,[25] the only work found in which the reaction was followed by sampling gases from the fuel bed, shows that no hydrogen is found until all of the oxygen of the air has been consumed. The endothermic reaction would thus seem to take place above the oxidizing zone of maximum temperature and the cooling in that zone, where it is most needed, would appear to be only by dilution.

The possibility exists, of course, that the steam does react at the surface of the carbon and absorbs heat, but the hydrogen and carbon monoxide are oxidized immediately as they pass into the space between the pieces of fuel. This is similar to today's conception of the reaction between oxygen and carbon as being first to carbon monoxide, which burns immediately as it leaves the surface to carbon dioxide, with the result that little or no carbon monoxide is found until all of the free oxygen is consumed.

Inasmuch as the absorption and reliberation of the heat occur so rapidly and so closely in the same zone and under such excellent conditions for transfer of heat, it is somewhat difficult to understand how the maximum temperature in the oxidizing zone is greatly affected. The measurement of the temperatures in the fuel bed with and without humidification is a difficult experimental procedure in a full-scale operating stoker. However, the degree of reduction in temperature, the level at which it occurs, and the mechanism of the reactions are facts which would throw much light on this entire subject.

Such investigations would best be carried out in laboratory apparatus of 1 to 2 ft diam, such as used by Kreisinger and others. The behavior of ash in the bed, its carry-over, volatilization, and deposition on surfaces above the bed could also be studied in such a laboratory apparatus. The optimum degree of humidification for various types of ash and rates of burning could be established.

The authors have given so much to the literature in this paper that perhaps one should not ask for more, but an interesting addition to the data would be the comparative heat balances with and without humidification. They have clearly established the gain in efficiency through improved heat absorption of the cleaner surfaces, as shown by the reduction in flue-gas temperature. There was, however, a loss in the superheating of the steam in the furnace as well as that in generating the steam. The magnitude of these opposing gains and losses would add to the paper.

The loss of good make-up water exhausted up the stack is not inconsiderable. Would it not be possible to use atomized water under the grate, or preferably, to generate the steam by waste heat?

A final comment on this excellent paper is that the writer doubts that the lighter color of the deposits could affect the heat absorption by radiation. It is well known that the absorption of heat in the infrared range of the spectrum by white paint is as great as by green, brown, red, or black paint. Only by a truly reflecting surface such as bright metal can the absorption of radiation be reduced. The over-all reduction of the gas temperature by dilution by steam would reduce the absorption by radiation, although this would be partly offset by the increased radiation from the gas because of its higher content of steam which radiates in the infrared.

Authors' Closure

The authors appreciate the attention given their paper by the several discussers and thank each for his thoughtful comments. The following closure is directed principally toward those comments that invite additional information or discussion.

Mr. Bennett and Mr. DeVisser have requested, in their discussion, some comment about the effect of humidification on stoker operation and maintenance.

Humidification has improved stoker operation and enabled the firemen to maintain a more even and controllable fuel bed. There has been a noticeable reduction of large mass clinkers since the introduction of humidification.

Improved fuel-bed conditions have reduced stoker burned-iron and maintenance manpower requirements by at least 35 per cent.

Mr. Corey suggests the use of the sampling probes at a few elevations between the fuel bed and the furnace outlet. Up to the present, only two such tests have been made, one on the water walls of a pulverized-fuel-fired, and the other in front of the boiler tubes of a stoker-fired steam generator at the company's Marysville power plant. In both cases the temperature of the furnace at the point of sampling was too high to permit the probe temperature to be controlled as well as is desirable. The probe will have to be redesigned to provide it with better cooling before a careful investigation can be made in the hotter regions of the furnace.

As intimated in the paper, the thought that alkali-matrix-type deposits are more prone to form in stoker-fired than in pulverized-fuel-fired steam generators came entirely from study of the literature. The limited number of probe tests thus far made on a pulverized-fuel-fired steam generator were made with unshielded probes. The rate of total deposition on the furnace-wall tubes was much greater than on the superheater tubes, but how much of that deposition can be ascribed to volatilization and how much to mechanical impingement is presently unknown.

Answering Mr. Corey, item (*e*) of Table 2 refers to dry air. Concerning his comment that the amount of water in the fuel should be added to the quantities shown in the table, the authors have considered that the water in the fuel probably escapes by evaporation instead of entering into any of the fuel-bed reactions. Dr. Gumz's Table 18, subsequently mentioned, appears to support this view.

Mr. Corey's suggestion that the enthalpy increase of saturated steam may have the same effect in reducing fuel-bed temperature as the endothermic reaction adds another thought to the complex picture. The authors have not investigated this possibility.

Fig. 15, herewith, shows an elevation of the steam generators in question including the probe-sampling points as Mr. Corey requested. Concerning Mr. Corey's last query as to why the deposits were darker in color when the air was humidified, the authors point out that the analyses, shown in Fig. 13 of the paper, demonstrate the remarkable reduction in the SiO_2 content of the deposits, caused by humidification. This SiO_2, amorphous in so far as Dr. Schwartz's x-ray diffraction data could discern, is a white material that caused the total deposit to appear less dark in the case of the samples collected while no humidification was being used. Carbonaceous material tends to cause all the deposits as collected to be darker than the tan to gray they would be if all traces of carbon were burned.

Mr. R. B. Donworth points out a very important problem in cases where make-up capacity is limited. Humidification of combustion air will require approximately $1^1/_2$ per cent of the boiler output during the winter months if steam is used. At Delray the capacity of the evaporators is inadequate to provide sufficient make-up. A solution for the problem is being sought in the development and use of nozzles that will permit introducing raw water into the preheated, 320 F air. To date, one such nozzle, capable of vaporizing 1500 lb of water with 500 lb of steam, has been developed.

[25] "Reactions in the Fuel Bed of a Gas Producer," by R. T. Haslam, F. E. Entwistle, and W. E. Gladding, *Industrial and Engineering Chemistry*, vol. 17, 1925, pp. 586–588.

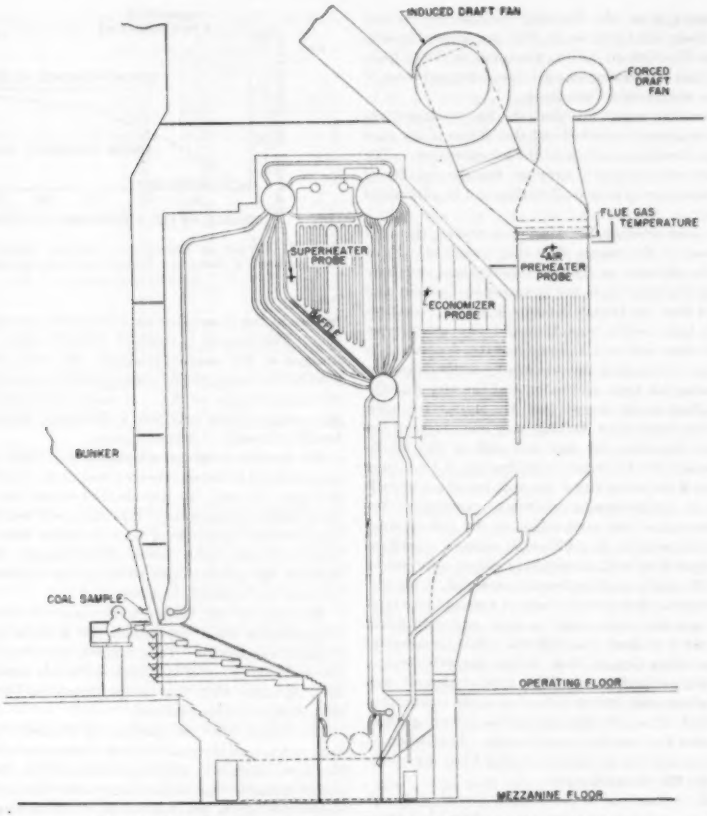

FIG. 15 SIDE ELEVATION OF STEAM GENERATOR SHOWING PROBE POINTS

Mr. Donworth's proposal for using a steam injector to recirculate gas from the economizer sounds interesting and may provide a satisfactory method for humdifying the combustion air of steam generators that are not equipped with air preheaters. Unless some means for heating the air is provided, the steam condenses as a fog. In one installation where steam was introduced directly into unpreheated air forming a fog, humidification was less effective than has been described in the paper. Whether or not the lessened effectiveness was related to the mode of introduction is, however, presently unknown.

The authors agree with Dr. Gumz that "reduction of volatilization" may be too simple a term to describe the reduction in the transport of silicon compounds from the fuel bed to the heating surfaces. They believe with him that oxidation and hydrolysis probably either changed the silicon compounds in the fuel to other silicon compounds that were less volatile or caused the volatile compounds to be converted to dusts that would not be collected on the shielded probes. They further agree that it would be desirable to have analyses of fly-ash and cinder residues to complete the picture of material balances. Samples of the fly ash were collected in the superheater pass at the time a few of the probe samples were collected, but these unfortunately, were too contaminated by the materials comprising the apparatus used for collection to justify completing the analyses. Apparently, use or not of humidification caused much less difference in amount or composition of dust collected than it did in the amount or composition of the probe samples. Possibly, information on the composition of the fly ash, as it leaves the air preheater, and of the cinder may be available at a later date. Obtaining a cinder sample that is representative of the ash being formed at a given time, however, presents problems.

Use of limestone to bind the silicon compounds might be a solution if transport of the silicon compounds were the only phenomena occurring. Murphy (7) previously has told of actual experience with lime in which it made the over-all conditions worse. Whether compounds of calcium volatilized or whether the addition of the lime increased volatilization of sodium and potassium compounds is presently unknown because only visual results were used in the evaluation of the experiment.

Use of overfire air, as stated in the paper, did not reduce fireside-deposit troubles at Delray. The overfire air system used, however, did not employ high-pressure jets, which may be the reason that negative results were obtained whereas others have reported that use of overfire air is beneficial.

Before commenting upon Mr. Harlow's remarks the authors wish to express their indebtedness to him for supplementing, during his visit to The Detroit Edison Company in June, 1949, published information concerning his own researches and those of The British Boiler-Availability Committee.

Mr. Harlow correctly points out that the fuel remained unchanged in the experiments described and that it was of the kind least likely to cause trouble according to British experience. The authors would not want to imply, however, that the quality of the fuel is of no consequence or that all fouling can be eliminated by humidification.

The authors wonder whether Mr. Harlow is chiding them for shooting down more of the enemy than they aimed at. From the analyses of the deposits on Delray superheaters and from descriptions of deposits as given in the literature by Crossley and others, it appeared that the Delray deposits fitted the classification alkali-matrix type better than they did any other type. Consequently, the aim was at alkali-matrix-type deposits. In spite of poor success in removing the deposits by methods recommended for removing this type, and in spite of the fact that the inner layer of an alkali-matrix deposit that Mr. Harlow had with him was thicker and whiter than the blue-gray inner layer of the Delray superheater deposits, the aim was still at the alkali-matrix type. The aim was to reduce volatilization, if Dr. Gumz will permit the use of the term, either through reduction of fuel-bed temperature or by promoting hydrolysis reactions. Apparently, humidification of the combustion air did reduce volatilization of alkali compounds; in addition, it reduced volatilization of other compounds as well, particularly silicon compounds. After analyses of the probe samples became available, it became evident that the deposits that initially formed were not purely of the alkali-matrix type but were mixed in some way with silica. Apparently there were at least two different kinds of deposits: (*a*) An amorphous silica deposit that fouled the superheater, economizer, and the air preheater. That type of deposit was nearly completely eliminated by humidification of the combustion air. (*b*) A deposit of other volatilized materials including alkali sulphates, that fouled the superheater primarily. Deposition of the latter type of material was apparently reduced but not eliminated completely by the humidification.

The authors wish to point out to Mr. Harlow that they do not intend to infer that no detectable diminution of fuel-bed temperature took place upon humidification of the combustion air, but simply that the method used to measure the temperature gave inconclusive results. The method was to direct a cooled optical pyrometer into a crevice in the fuel bed from close range. The temperature of a given crevice and its contour changed so rapidly that the method was not reliable for the purpose.

Mr. Harlow may be right in his claim that formation of SO_3 is suppressed by humidification of the combustion air, but the following evidence tends to refute that point of view. In an effort to determine whether volatilization of alkali compounds or formation of SO_3 was the dominant factor in the Delray problem, an experiment was carried out as follows during the winter of 1950: Films of sodium hydroxide or of sodium carbonate were placed over the surface of the probes. These probes, shielded, were introduced into the superheater for 1 hr in the usual manner. The amounts of soluble sodium and potassium compounds found on the probe are plotted against the determined amounts of sulphate in Fig. 16 of this closure. The total amount of sodium and potassium compounds, there shown, include the amount of the original sodium compounds that adhered to the probe plus the amount of soluble sodium and potassium compounds that deposited within the hour. Within 1 hr, as there shown, much of the sodium alkali was converted to sulphate, the portion depending upon the thickness of the alkali layer. There was little difference in rate of sulphate formation with and without humidification. The amount of sulphate formed seems, therefore, to be a function of the amount of alkali; that is to say, the alkali will soon be converted nearly quantitatively to sulphate regardless of the concentration of SO_3. It seems probable that reduction in SO_3 concentration was not a dominant factor in causing the beneficial results of humidification.

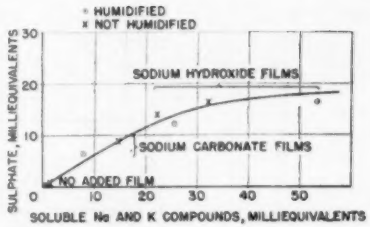

FIG. 16 EFFECT OF AMOUNT OF SOLUBLE SODIUM AND POTASSIUM COMPOUNDS ON SHIELDED PROBES IN SUPERHEATER ON AMOUNT OF SULPHATE FORMED IN 1 HR

Mr. Harlow is right in presuming that tube temperatures have been reduced in the superheater zone as the result of using humidified air. In fact, the superheated-steam temperature is lower than design temperature. The apparent reason is that greater than normal quantities of heat are being absorbed in the water wall and front boiler tubes. Experimental changes are being made at the present time to bring the superheated-steam temperature up to design temperature.

Referring to Mr. Harlow's reluctance to believe that fuel-bed temperatures affect deposition, the authors have no desire to promote any theory. They suggest, however, that in comparing the probable extent of volatilization of ash constituents in stoker-fired furnaces with that of pulverized-fuel-fired furnaces, the time element be remembered.

Mr. Keeth raised the question of whether water added to the coal, as has been the practice with chain-grate stokers,[27] behaves in the same manner as moisture added to the combustion air. It seems probable that most of the water that is added to the coal evaporates and is thus lost before it can undergo reaction in the fuel bed. On the basis of that reasoning, the authors did not adjust the humidity of the combustion air for changes in moisture concentration of the coal. As previously stated, use of wet coal at Delray appeared to increase fouling troubles by causing interruption of the coal feed.

To the present, experiments with humidification in pulverized-fuel plants have been limited to one steam generator. Under the conditions there tried, humidification did not reduce fouling.

In response to Mr. Loughin's inquiry concerning whether the authors were aware of the gas-recirculation experiment at Battersea, the authors wish to state that Mr. Harlow described a part of that experiment. It is the authors' understanding that Mr. Harlow ascribed the remarkable results to the recirculation of silica dusts that minimized the formation of SO_3. The work was not mentioned because it has not yet been published. The authors join with Mr. Loughin in hoping that those experiments will soon be described in available literature.

The authors are pleased to have Mr. Parrish report successful use of the humidification method. His experiences indicate that the beneficial effect is not limited to one plant or one coal.

In response to Mr. Shakeshaft's interest in the composition of the Delray boiler deposits, the authors are pleased to submit

[27] "Water Makes It Burn Better," by R. H. Kuss, *Power*, vol. 81, November, 1937, pp. 674–675.

TABLE 6. COMPOSITION OF DEPOSITS TAKEN FROM DELRAY STEAM GENERATOR NO. 10, FEBRUARY 13, 1950

	—Percentage composition based— upon weight of material dried at 105 C (3 hr)			
Sampled designation	1	2	3	4
Acetic acid, soluble	11.85	34.25	5.47	16.68
SO_3	6.74	23.87	3.30	10.97
PO_4	0.12	0.12	0.15	0.16
Na	0.59	3.76	0.32	0.82
K	0.88	6.10	0.35	1.70
Ca	0.34	0.86	0.66	0.34
Fe	0.70	1.36	0.03	1.03
Al	0.65	0.54	0.12	0.90
Calculated sum of soluble ions	10.02	36.61	5.13	15.92
Acetic acid, insoluble	88.15	65.75	94.53	83.32
SiO_2	53.71	45.50	54.45	56.37
$Al_2O_3 + TiO_2$	17.93	0.56	18.35	13.25
Fe_2O_3	6.75	9.13	9.75	5.06
Na_2O	0.46	0.32	1.48	0.47
K_2O	1.81	2.20	4.43	1.94
CaO	1.64	0.42	1.77	1.30
P_2O_5	0.90	2.76	2.66	1.37
Calculated sum of insoluble radicals	83.20	60.89	92.89	79.76
Calculated total (soluble + insoluble)	93.22	97.50	98.02	95.68

Conditions: Deposits taken when the steam generator had been shut down for cleaning at the end of 40 days of normal operation. At the beginning of the period the heating surfaces had been subjected to a routine cleaning consisting of blowing, scraping, and alkaline-water washing.
Identification of samples:

1 Back bank of boiler tubes, fluffy gray deposit, pH 3 to 4.
2 Superheater, inner layer next to metal, gray with blue to green tinge, pH 3 to 4.
3 Superheater, reddish outer layers, pH 4.
4 Economizer, cross section of deposit, striated in different shades of gray, pH 2 to 3.

Table 6 with this closure. The samples were taken from No. 10 steam generator when it was shut down for cleaning prior to the installation of the humidification system. Perhaps the authors did not make it clear that their classification of the deposits as of the alkali-matrix type was a tentative classification based upon information available from the literature before the experimental part of the investigation began. The inner deposit on the superheaters was high in alkali sulphates although not quite so high as the analysis given by Crossley.[28] Presently it is believed that the deposits were not purely of the alkali-matrix type but a mixture of that and silica, combined in some way to make them much more resistant to aqueous cleaning methods than alkali-matrix type alone.

The authors are pleased to acknowledge that they found the data and theories published by The British Boiler Availability Committee of much value in the study of the phenomena taking place at Delray. They were unaware, however, that the committee was studying the effect of water in its recirculation experiments. Use of recirculation was considered for Delray but not tried partially because of space and induced-draft-fan limitations. It would be interesting to compare the effect of recirculation with that of humidification under conditions such that the same concentration of water would be in the combustion air and the same concentration of oxygen in the flue gas. To provide the same concentration of water as was used at Delray, over 30 per cent of the flue gases would have to be recirculated during approximately half of the year. Information concerning the part played by water, carbon dioxide, and silica dusts in recirculated flue gases would be most welcome.

Concerning the reason the economizer deposits are reduced through the use of humidification, the authors believe that the mechanism is similar to that in the superheater. The primary fouling process is believed to be either sublimation or a phenomenon closely associated with it. As judged by observation of the shielded probes, a nearly uniform and surprisingly adherent film is first formed. Much of that film is an apparently amorphous silica. On the upstream side of the superheater, a part of that film is continuously abraded off. In the economizer, the rate of deposition seems to be less but so also seems to be the rate of abrasion. Thus the sedimentary deposit builds up, layer upon layer. Humidification markedly reduces the rate of deposition of silica. Further, because the water walls are kept cleaner with humidification than without, the superheater by-pass damper is kept closed with the result that the economizer is not subjected to gases coming directly from the furnace. The effect of opening the by-pass damper on rate of deposition in the economizer has been discussed in connection with Fig. 13 of the paper.

Only two tests have thus far been made on the dew point of the stack gases without and with humidification. The values obtained were 128 F and 150 F, respectively, when the steam generator was operating under conditions for which the theoretical dew points were 111 F and 115 F, respectively. The authors do not believe the data are adequate for use in determining the effect of humidification on sulphur-trioxide concentration.

Mr. Shaw states that the increase of underfire pressure when operating multiple-retort stokers in excess of 40 lb of coal per hr per sq ft of grate surface tends to cause blowholes in the fuel bed. The authors agree that this is true, but point out that humidification has, however, improved fuel-bed conditions by reducing large mass clinkers, thus enabling the operators to maintain a more even and controllable fuel bed. Improved fuel-bed conditions have reduced stoker maintenance and burned-iron costs.

Although secondary combustion still occurs at times in the Delray steam generators, troubles from secondary combustion had been overcome before this investigation was started.

The length of time that the fuel is in the high-temperature zone probably explains why stoker-fired plants have more difficulty with volitalization than do pulverized-fuel-fired plants.

Mr. Sherman has an interesting comment that use of steam may be less effective than is described in the paper if steam is used with different fuels, or in steam generators where the burning rate per unit area is less than obtains for the steam generators in question. Tests on a 740-F, 350-psig steam generator at the Marysville plant, which under normal full load operates at approximately 40 lb of coal per sq ft per hr, but which is not equipped with air preheaters, gives qualitative support to his view. The work has not progressed sufficiently to warrant description at this time.

The authors were aware of the theory of Lange that the mechanism of transport of silica is through silicon sulphide. They have data from Delray, intended for later publication, showing that neither silicon sulphide nor any other sulphide reached the probes in the superheater region during operation either without or with humidification. These data do not eliminate the possibility, however, that the compound initially volatilized may be the sulphide.

The authors do not dispute the claim made by Mr. Sherman and Dr. Gumz that the extent of the water-gas reaction would be negligible until all of the oxygen has been consumed. This contention had also been called to their attention by their colleague, Dr. Andrew Gemant. The steam generators in question operate with approximately 20 per cent excess air. It seems likely, however, that an appreciable fraction of the combustion air by-passes the fuel bed through the ash pit and that another portion passes through large cracks in the fuel bed. It is at least possible, therefore, that in the mass of glowing coal there is no excess oxygen. Of course, this is only speculation. The authors recognize the merit of attacking some phases of the problem by means of a laboratory furnace as Mr. Sherman suggests, and of employing mathematical treatment as has Dr. Gumz.[29] Because conditions vary so much from furnace to furnace and time to time, the su-

[28] "Research Work at the Fuel Research Station on Boiler Deposits," by H. E. Crossley, reprinted from *Fuel and the Future*, vol. 1. His Majesty's Stationery Office, 1948, 4 p. print, Table 1.

[29] See reference (17) of Dr. Gumz's discussion, Fig. 17, and Table 18.

TABLE 7 SUMMARY OF HEAT-LOSS TEST DATA ON NO. 7 HIGH-PRESSURE STEAM GENERATOR

			Losses																	
					Moisture			Incomplete combustion						Absorbed by auxiliary						
Test no.	Evaporation rate, 10^3 lb/hr	Heat output, 10^6 Btu/hr	Unburned solid carbon, per cent	Dry flue gas, per cent	Coal, per cent	H_2 in coal, per cent	Air, per cent	CO, per cent	H_2, per cent	$CH_4 + C_2H_6$, per cent	Radiation and convection, per cent	Total, per cent	Efficiency, per cent	Induced-draft fan, per cent	Forced-draft fan, per cent	Stoker, per cent	Total, per cent	Efficiency adjusted for auxiliary power, per cent	Saturated steam for humidification, per cent	Efficiency adjusted for humidification, per cent
After 129 Days of Operation With Humidified Combustion Air																				
Test A																				
7A	204.1	218.2	1.97	4.67	0.39	3.25	0.04	...	...	...	0.52	10.84	89.16	0.56	0.28	0.03	0.87	88.29	2.01	86.28
5A	241.4	257.0	1.58	5.27	0.54	4.34	0.05	...	...	...	0.44	12.22	87.78	0.75	0.33	0.03	1.11	86.67	1.94	84.73
1A	251.2	267.8	2.33	5.65	0.47	4.57	0.05	...	...	...	0.43	13.50	86.50	0.85	0.37	0.03	1.25	85.25	1.81	83.44
2A	305.8	328.4	2.97	5.35	0.46	4.54	0.05	...	...	...	0.35	13.72	86.28	0.98	0.40	0.03	1.41	84.87	1.71	83.16
6A	350.8	379.5	4.44	5.20	0.50	4.60	0.05	...	...	...	0.32	15.11	84.89	1.30	0.47	0.03	1.80	83.09	1.64	81.45
3A	353.5	383.4	3.50	5.45	0.57	4.24	0.05	...	...	...	0.31	14.12	85.88	1.35	0.50	0.03	1.88	84.00	1.77	82.23
4A	381.5	414.0	3.82	5.51	0.53	4.11	0.05	...	...	...	0.29	14.31	85.69	1.48	0.53	0.03	2.04	83.65	1.73	81.92
133 Days With Humidification Followed by 24 Days Without Humidified Combustion Air																				
Test B																				
7B	209.0	220.8	1.08	6.99	0.40	4.39	0.11	0.22	..	...	0.37	13.56	86.44	0.83	0.26	0.03	1.12	85.32	0	85.32
6B	233.8	247.4	0.53	7.68	0.42	3.99	0.10	0.66	....	0.89	0.34	14.61	85.39	1.11	0.26	0.02	1.39	84.00	0	84.00
5B	250.4	268.3	0.59	7.43	0.39	4.17	0.09	0.42	...	...	0.29	13.38	86.62	1.31	0.32	0.03	1.66	84.96	0	84.96
3B	250.4	269.6	0.94	7.58	0.43	3.86	0.07	0.26	0.36	....	0.28	13.78	86.22	1.18	0.32	0.02	1.52	84.70	0	84.70
4B	275.0	296.4	1.56	7.65	0.44	4.13	0.09	0.17	....	....	0.27	14.30	85.70	1.50	0.35	0.02	1.87	83.83	0	83.83
1B	299.4	327.2	1.40	7.26	0.52	3.93	0.09	...	....	....	0.25	13.45	86.55	1.53	0.40	0.02	1.95	84.60	0	84.60
2B	307.0	334.4	1.86	7.44	0.42	3.85	0.09	0.40	....	....	0.27	14.33	85.67	1.69	0.40	0.02	2.11	83.56	0	83.56
Clean Boiler With Humidified Combustion Air																				
Test C																				
7C	202.0	220.8	0.76	4.84	0.51	3.90	0.06	...	....	...	0.37	10.44	89.56	0.53	0.25	0.03	0.80	88.76	1.76	87.00
8C	213.7	232.6	0.71	4.49	0.46	3.78	0.05	...	....	...	0.32	9.81	90.19	0.47	0.24	0.02	0.73	89.46	1.67	87.79
1C	248.0	262.4	1.98	4.58	0.43	3.69	0.10	0.28	....	...	0.29	11.65	88.35	0.59	0.32	0.02	0.93	87.42	1.02	86.40
5C	255.5	273.7	1.37	4.84	0.50	4.11	0.13	0.04	....	...	0.27	11.26	88.74	0.63	0.35	0.02	1.00	87.74	0.53	87.21
2C	308.5	331.2	2.66	4.51	0.41	3.90	0.11	...	....	...	0.23	11.82	88.18	0.74	0.41	0.03	1.18	87.00	0.67	86.33
3C	346.9	375.4	3.11	4.90	0.46	3.98	0.12	0.04	....	...	0.22	12.83	87.17	0.99	0.49	0.02	1.50	85.67	0.65	85.02
6C	350.7	379.1	2.68	4.77	0.51	3.49	0.11	...	....	...	0.20	11.75	88.25	0.95	0.51	0.03	1.49	86.76	0.57	86.19
4C	384.1	419.6	3.34	4.80	0.45	3.72	0.12	...	....	...	0.20	12.63	87.37	1.13	0.58	0.03	1.74	85.63	0.48	85.15

thors believe that much of value may also be learned by pursuing somewhat further, along lines described in the paper, the study

TABLE 8 INFRARED DIFFUSE PERCENTAGE REFLECTING POWERS OF DRY PIGMENTS[40]

Wave length, microns	Dark pigments		Light pigments		
	Co_3O_4	CuO	Al_2O_3	$PbCO_3$	$MgCO_3$
0.60	3	..	84	88	85
0.95	4	24	88	93	89
4.4	14	15	21	29	11
8.8	13	..	20	10	4
24.0	6	4	6	7	9

of the phenomena occurring in the large furnaces of steam generators.

Concerning comparative heat balances with and without humidification, the authors recognize that if the heating surfaces are equally clean in both cases, any water or steam used for humidification causes a loss of heat. By minimizing fouling, humidification reduces, however, the heat loss caused by dirty surfaces. A fair heat-balance test would be to run an initial test on two nearly identical steam generators immediately after heating surfaces are well cleaned. One steam generator would then be run with, and the other without humidification until the one running without became fouled to the extent that it would not carry normal full load. Heat-loss tests would be run at intervals during the period and the heat balances computed. Presently no such data are available. The only data available are those from which Fig. 7 of the paper was made. These are summarized in Table 7 of this closure. The possibilities of using atomized water under the grate and of using waste heat either to generate steam or to heat the water for atomization have both been under consideration. The use of water sprays in the preheated-air ducts and plenum chamber has been under trial for over a year. Experiences with these and other engineering features of the humidification method may constitute another report.

Mr. Sherman rightfully points out that the color of deposits is not usually considered to affect heat absorption by infrared radiation. This generalization is not strictly true, however, for the entire infrared band. Reference to Table 362 of the Smithsonian Physical Tables[40] shows a strong dependence upon color in the near infrared region below approximately 5 microns. A few values are reproduced in Table 8.

Just what wave lengths are involved in the absorption of radiant energy at the water walls and boiler tubes is a subject of conjecture. Probably 2000 K is a conservative estimate. For 2000 K, the maximum radiation intensity is at approximately 1.5 microns. At that wave length the percentage reflection is probably quite significant judging from the data cited. Even in the superheater region, where the gas temperature is approximately 1500 K, there is probably considerable reflection from a white body. Further support of the authors' belief that the white silica deposits cause reflection losses has been given by Bennett and Haynes,[41] who have shown that dark paints reach a higher temperature and bake much faster than light ones when baked with lamps having maximum energy output of approximately 1.1 microns.

[40] Smithsonian Physical Tables, Third Reprint of Seventh Revised Edition, Smithsonian Institution, 1927, p. 299.

[41] "Paint Baking With Near Infrared," by H. J. Bennett and Howard Haynes, *Chemical and Metallurgical Engineering*, vol. 47, 1940, p. 106.

Developments in Spreader-Firing Wet Wood

By A. S. WEIGEL,[1] NEW YORK, N. Y.

The spreader, with its ability to burn a wide range of coals, has been one of the most widely accepted stokers for many years. In recent years it has been increasing in popularity by demonstrating a natural ability to burn cellulose fuels. The same inherent characteristics which give the spreader fuel flexibility when burning coal, are proving to be equally effective in broadening its application to include among other cellulose fuels wet wood. Wet wood as a fuel is usually considered to be those refuse fuels which are by-product in the manufacture of lumber, pulp and paper, and naval stores.[2] They take the form of hogged wood and bark, "spent" chips, and other wood wastes which fall within the size range and moisture content suitable for spreader firing.

ALTHOUGH the principles of spreader firing certainly would have been applied in time to the problems of burning wet wood, it was the increased value of this fuel and the resulting demand to meet higher furnace efficiencies that supplied the impetus for these recent developments. In meeting this demand the spreader has demonstrated a number of other positive advantages that might have been foretold by the nature of this type of firing. These advantages are low maintenance and operating costs, ability to control accurately the fuel-air ratio which allows the application of automatic controls, rapid response to load demands, high heat-release rates, and practically continuous boiler availability.

Principles of Spreader Firing Applied to Wet Wood

In spreader firing the fuel is fed at a measured rate to distributors. The distributors are generally of the mechanical type, and consist of revolving drums to which blades are fixed for spreading the fuel evenly over the grate surface. The fuel particles in their travel from the distributor blades to the fuel bed, pass through a rising column of hot gases, and the green fuel lands on an actively burning fire. It is this basic principle of this type of firing that has proved most effective in burning wet wood. The flash-drying action obtained by exposing a maximum surface of the wet wood to the furnace gases dries the wood so that the smallest particles burn in suspension. The larger particles are surface-dried and either start burning in suspension, or immediately upon landing on the grate. Ignition of the incoming fuel is from the actively burning fire on the grate, and, since the particles that land on the fuel bed are evenly distributed over the grate surface, the maximum surface of these particles is exposed to the fire, and their oxidation is rapid.

Experience indicates that for best operation this fuel should be hogged or sized so that approximately 95 per cent will pass through 2-in. square-mesh screen. Of the remaining percentage, there can be occasional maximum oversize pieces up to 12 in. long and 1 in. thick, that will pass a 4-in. bar screen. An excess of these oversize pieces will cause material-handling problems in the feeders, chutes, and distributors, and blanketing of the fuel bed. The maximum moisture content should not exceed 60 per cent as fired; any additional drying within commercial limits will of course, improve operating results.

Experiments at a northwestern lumber mill have demonstrated that best operating results are generally obtained with a thin active fire. The optimum fuel depth is about 2½ in., which is required to keep the grates completely covered. This fuel depth is maintained over a gradually thickening layer of ash between dumping periods on a dumping-grate stoker, and from the rear to the front on a front ash-disposal continuous-discharge type. The air passes freely through the thin, even fuel bed, and the unagitated ash bed insulates the heat of the fire from the grate surface so that grate maintenance is extremely low, and grate temperatures ordinarily run from 50 to 100 F above forced-draft temperatures. Ash disposal to a pit is automatic on the continuous-discharge type and is easily handled on the dumping-grate type, since no clinkers will form in the relatively cool porous ash bed. This results in a reduction in labor costs for fire cleaning. With the dumping-grate stoker, the grate sections in front of each distributor are cleaned one at a time. By increasing the burning rate on the active sections, the boiler is able to meet load demands with little if any drop in steam pressure during cleaning periods.

Air for combustion is supplied at relatively low pressure under the grates, and either air or steam at higher pressure is directed through the furnace walls over the fire to create furnace turbulence. This insures a good mixture of furnace gases plus supplying additional combustion air if required. The low-pressure air passing through the grates and fuel bed is well distributed over the whole grate area since the resistance to air flow through the low air-space grates and level fire is about equal at all sections of the grate. This even flow of air through the fuel bed minimizes furnace stratification by assuring a good mixture of air and fuel at the grate line. The overfire air or turbulence through the furnace walls is supplied at high pressure to provide sufficient penetration for mixing the furnace gases. This mixing of the rich and lean gases reduces flame travel, smoke, and the carry-over of small partially burned particles from the furnace, and decreases slagging of furnace walls and boiler surfaces.

All air to the furnace, except for a small percentage of leakage, is under control since there are no openings through which large quantities of uncontrollable air may enter. The quantity of fuel fed is measured and can be varied to meet instantaneous load demand so the fuel-air ratio can be regulated closely and excess air held to a desired quantity of 20 to 25 per cent. The ability to regulate fuel and air quantities accurately prevents fluctuating excess air which is common in previous popular methods of burning wet wood. This reduces periodic high furnace velocities and results in a lower percentage of char carry-over from the furnace. It has the further advantage of decreasing refractory spalling by preventing rapid furnace-temperature changes and so reduces furnace maintenance. With these principles of fuel feed and air control, automatic regulation can be applied easily and the desired fuel-air proportions maintained over a load range of approximately 3 to 1. The combination of the thin responsive fire and automatic control gives this type of firing an ability to follow

---

[1] Manager, Stoker Engineering, Combustion Engineering—Superheater, Inc.

[2] Naval stores are resin, pitch, and their derivatives; this name comes from the time when these products were used mainly by naval vessels.

Contributed by the Fuels and Power Divisions and presented at the Spring Meeting, Atlanta, Ga., April 2–5, 1951, of The American Society of Mechanical Engineers.

Note: Statements and opinions advanced in papers are to be understood as individual expressions of their authors and not those of the Society. Manuscript received at ASME Headquarters on April 26, 1951.

load demands practically instantaneously and maintain a close control of steam pressure.

The return to the furnace of the partially burned char particles that are collected in hoppers under the boiler is economically justified and advisable if the wood is not sand-bearing, that is, if there is less than 1 per cent of sand in the ash. This material is generally returned to the furnace through the rear wall using high-pressure air or steam as a conveying medium. Its purpose is to reduce carbon loss and do away with the material-handling costs otherwise involved in its disposal. It is questionable, however, whether it is advisable to return the material that is caught in the hoppers under dust collectors. With this procedure the dust concentration in the furnace gases may increase with a high-efficiency collector to the extent that erosion of metal surfaces and increased slagging will cause more trouble than can be justified by increased efficiency or decreased handling costs.

Since ignition with spreader-firing is from the bottom up, that is, the incoming fuel lands on an established fire, there is no need to depend on radiation from hot refractory surfaces to establish or maintain ignition. Water-cooled furnace walls have proved to have no adverse effects on operation. For that reason the water-cooled furnace makes the preferred arrangement with the decreased maintenance costs inherent with this furnace type. Although the water-cooled furnace is the preferred type, refractory furnaces have given satisfactory service and can be used where necessary, such as the application of a spreader stoker to an existing boiler. The relatively even furnace temperature obtained by the absence of stratification and fluctuating excess air helps to keep maintenance of refractory surfaces to a minimum.

The principles of spreader firing lead to increased unit availability. This is particularly true for new installations where advantage is taken of waterwall furnace construction to minimize boiler outage for deslagging the furnace or repairing refractory surfaces. These new units are designed for continuous availability except for scheduled outages during boiler inspection and cleaning. It is, however, also true for spreader applications to existing boilers with refractory furnaces, since there is no need for periodic shutdowns to clean the furnaces and secondary combustion chambers.

Problems Met in These Developments

Most of the problems that have been encountered in developing the spreader stoker for burning wet wood have been in allied equipment rather than in the stoker proper. The most important problem has been the material-handling and feeding equipment for delivering the fuel to the distributors continuously at a rate that can be varied to meet load demands. For best operating results, this fuel should reach the distributors without undue size segregation and at an even feeding rate, since excessive slugging or erratic feed can cause blanketing of the fuel bed. To assure continuity of fuel supply, live bottom-bin-type feeders are used to iron out the surges in the material-handling equipment. These feeders have been of the multiple or single screw and chain type, the rate of feed depending on the speed of the screws or chains. With adjusted arrangements these feeders have operated satisfactorily. At the present time, however, the development of a hogged fuel feeder specifically designed to meet the requirements of the spreader stoker is definitely needed.

Applications of Spreader Firing for Wet Wood

The installation shown in Fig. 1 demonstrates the application of a dumping-grate spreader stoker to an existing boiler at a northwestern lumber mill. The boiler was previously equipped with a Dutch-oven cell-type furnace. Existing design limitations in furnace volume dictated the installation of the stoker in the Dutch oven rather than in the water-cooled combustion chamber. This 17 ft 6 in. wide × 9 ft 2 in. long stoker was proportioned to burn sufficient hogged fuel and mill waste to produce 70,000 lb of steam per hr. The fuel is refuse wood from sawmills, a planing mill, a pulpwood room, a plywood plant, and hydraulic barkers. It is mostly Douglas fir, hemlock, and cedar, varies widely, in sizing and has a moisture content up to 60 per cent. This fuel is fed from the chain-type feeder at the bottom of the storage bin through chutes that carry it to the distributors which spread it over the grate surface. The forced draft through the grates is supplemented by steam-air jets through the bridge wall. Additional steam jets are located through the rear wall of the combustion chamber which have been entirely satisfactory in burning out the char that carries over the bridge wall.

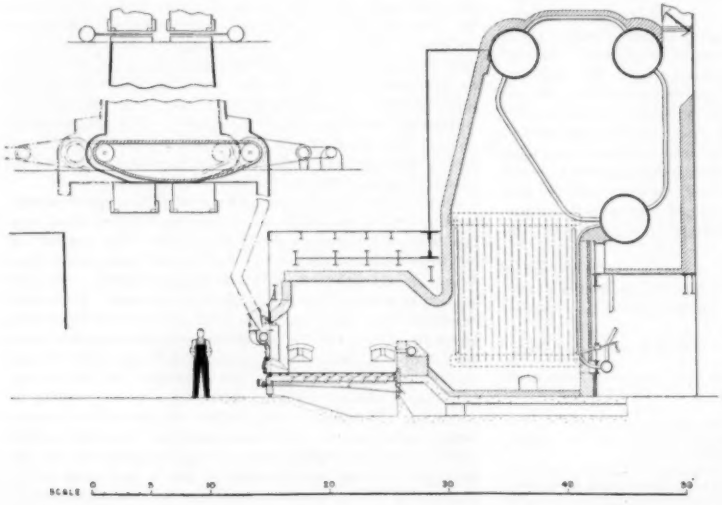

Fig. 1 Application of a Dumping-Grate Spreader to an Existing Boiler

Since the installation of this stoker, the boiler has carried an average of over 75,000 lb of steam per hr for 24-hr periods, and 90,000 lb per hr for extended peak loads, while a companion boiler of duplicate design still using cone firing has a maximum capacity of 65,000 to 70,000 lb of steam per hr. An interesting series of tests were run to compare the char and cinder carry-over on these two boilers with the different firing methods. These tests indicate that the

carry-over from the stoker-fired boiler is considerably less because of lower furnace velocities. The over-all successful operation of the stoker-fired boiler has been demonstrated clearly by comparing capacity, efficiency, maintenance costs, operating-labor costs, availability, and ability to follow load demands with the companion boiler burning the same fuel in the cell-type furnace. In every respect the results obtained from the spreader stoker were definitely superior to those with the older type of firing.

The two-drum bent-tube boiler shown in Fig. 2 illustrates a modern, medium-size, well-balanced design of boiler, superheater, water-cooled furnace, and dump-grate stoker for burning wet wood. This unit is designed to produce 70,000 lb of steam per hr at 165 psi and 425 F. To do this it will burn 20,600 lb per hr of 40 per cent moisture hogged wood, and mill waste. The

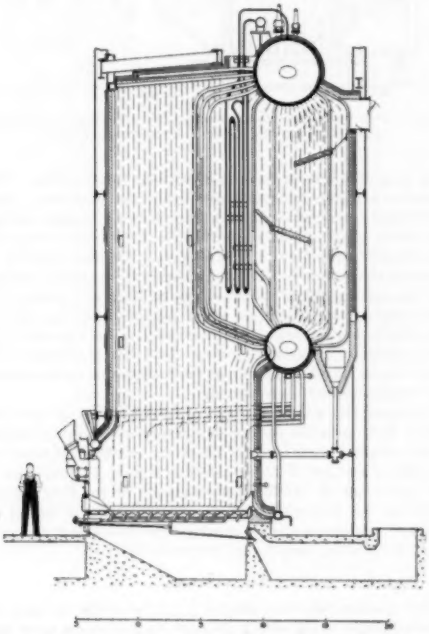

FIG. 2 MODERN DESIGN OF MEDIUM-SIZE BOILER WITH DUMPING-GRATE SPREADER

stoker is 13 ft 6 in. wide × 11 ft 2 in. long and has three distributors mounted on the stoker front.

The overfire steam-air jets and the cinder-recovery arrangement through the rear furnace wall have been combined in one system. Normally, about 5 to 10 per cent of total air will be required to obtain the turbulence desired with this type of design. Less than 1 per cent of the total air is needed for returning the cinder and char collected under the boiler hoppers. The remainder then is used for furnace turbulence.

This particular boiler has been put in service recently and has not yet run long enough to obtain operating results.

Fig. 3 shows a boiler installed in a southern paper mill arranged to burn a combination of natural gas through the burners in the front wall and hogged bark on the continuous-discharge-type spreader stoker. The stoker is 16 ft wide × 13 ft 3 in. long and has four distributor units. The ash is discharged automatically at the front of the traveling-grate-stoker body. This unit has a designed maximum continuous rating of 150,000 lb of steam per hr on gas, or on a combination of gas and bark, and a maximum continuous rating of 90,000 lb per hr on bark alone, using 45 per cent moisture hogged bark. Actually, it has carried 115,000 lb of steam per hr on bark.

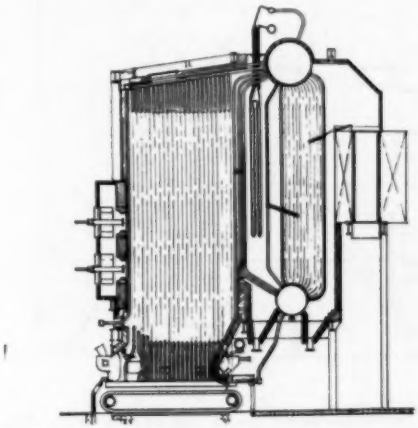

FIG. 3 CONTINUOUS-DISCHARGE STOKER-FIRED BOILER ARRANGED FOR BURNING WET WOOD AND NATURAL GAS

Furnace turbulence is obtained with high-pressure air through nozzles in the rear wall. This air is delivered by a high-pressure blower at 30 in. static. The nozzles are on 7-in. centers to get the effect of a blanket of air sweeping the gases from the rear of the furnace to the front. Overfire-air nozzles spaced on too-wide centers have a tendency to bore holes through the furnace gases at the rear of the stoker and permit a large part of the gas stream to pass between the nozzles with little turbulent effect.

The primary advantage of the continuous-discharge stoker over the dumping grate is, of course, its ability to discharge ash continuously and automatically with no interruption whatsoever to operation during fire cleaning. The higher cost of the continuous-discharge machine can be better justified on the larger more efficient units, but the choice of the stoker type does not depend upon size alone. Local plant conditions, such as the percentage of ash in the wood, are important determining factors. With less than 1 per cent ash, the fires may need cleaning only several times a week on a dump-grate stoker, but when the ash is more than 4 per cent, a continuous-discharge stoker may be justified, even in the medium sizes, to reduce labor costs.

The boiler installation, illustrated in Fig. 4, shows an interesting application of a new design for a large unit to burn wet wood in combination with another solid fuel, pulverized coal. This furnace has been arranged to prevent the coal ash from falling on and interfering with the stoker fuel bed. The boiler has a maximum design capacity of 200,000 lb of steam per hr on coal, or a combination of wood and coal, and 175,000 lb of steam on wood alone. It has, however, carried loads of over 200,000 lb of steam per hr with completely smokeless operation on wood only. When operating at 175,000 lb of steam per hr on hogged fuel and mill waste of 50 per cent moisture, this stoker burns 63,000 lb of wood per hr. The stoker is 25 ft wide × 16 ft long, and the fuel is spread on the grate by five distributors.

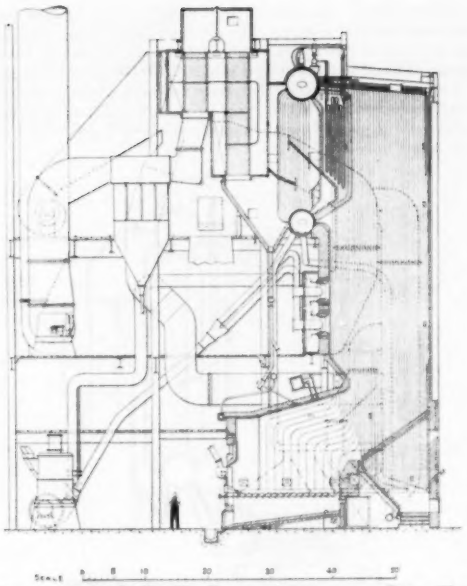

FIG. 4 200,000-LB-PER-HR BOILER ARRANGED TO BURN WET WOOD AND PULVERIZED COAL

Air under forced draft is delivered to the stoker at 370 F. Overfire turbulence in the stoker furnace is obtained by steam-air jets using preheated air through the bridge wall and through the furnace roof. An additional set of steam-air jets is located in the rear wall just above the ash-removal doors. These jets are for burning out the char that carries over the bridge wall and settles out in this ash-removal section of the furnace.

The char and cinder collected in the hoppers under the boiler are returned through the roof of the stoker furnace for reburning using steam-air jets for carrying this material. Originally, the material collected in the hoppers under the dust collector was also returned to the stoker furnace, but this has been discontinued because of operating difficulties experienced. The material from the dust collector is now discharged to a sluice, not shown in the illustration, and discarded.

The design, illustrated in Fig. 5, shows a continuous-discharge-stoker installation with several new features. This boiler is installed in a southern naval-stores plant and burns "spent" wood chips, having an average moisture content of 35 to 40 per cent. These chips are a by-product refuse fuel from which practically all resin and pitch have been removed so that they lack some of the flashy burning characteristics of the other wet-wood fuels described.

The water-cooled furnace for this two-drum bent-tube boiler is unusually high and the three distributor units are set high above the grate surface. There are burners in the front wall for oil as an auxiliary fuel. The tubular air heater supplies air through a forced-draft fan to a series of overfire-air nozzles in

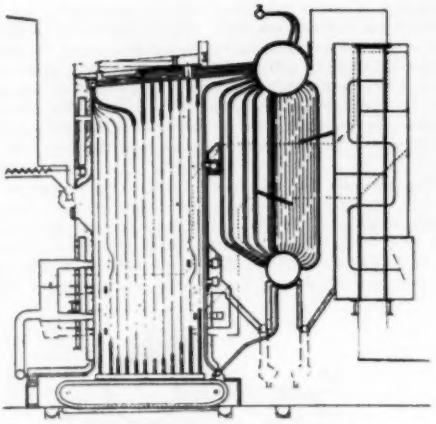

FIG. 5 CONTINUOUS-DISCHARGE STOKER WITH HIGH-SET DISTRIBUTOR UNITS AND TANGENTIAL OVERFIRE AIR JETS

four tangential belts arranged for alternate flow direction. This provides a highly turbulent zone below the distributor units. Additional controlled air at room temperature is brought through the stoker grate by induced draft. The fuel is fed by screws in the live-bottom bin to the distributors. The fine particles on entering the furnace burn in suspension, and the larger particles fall through the highly turbulent zone on their way to the grate. The increased travel of these larger particles from the high set distributors in conjunction with the action of the high turbulent zone affords a greater flash-drying effect than is obtained with the lower set distributors, so that the fuel landing on the grate is well conditioned for rapid burning.

Although this was an experimental application, its operating results have exceeded performance predictions in every respect. It now carries a normal load of 120,000 to 140,000 lb of steam per hr with an average of 20 per cent excess air. This amounts to the high figure of 14,000 lb of steam per hr per ft of furnace width for this 10-ft-wide furnace. Another boiler of similar design has been put in service recently, and preliminary operation predicts the same high-quality performance.

CONCLUSIONS

The spreader has demonstrated a natural ability to burn wet wood of proper sizing with a moisture content of not more than 60 per cent. The spreader principles applied to burning wet wood have resulted in the following: High furnace efficiencies; low grate and furnace maintenance; low operating-labor costs; accurate control of fuel-air ratio; easy application of automatic controls; rapid response to load demands; high steam release per foot of furnace width; high boiler availability.

The stokers can be of either the continuous-discharge or dumping-grate type and can be applied to existing boilers as well as to new installations. The wet wood can be burned in conjunction with gas, oil, or coal. The distributor units can be set the conventional height above the grate or well up in a high furnace for high heat- and steam-release rates.

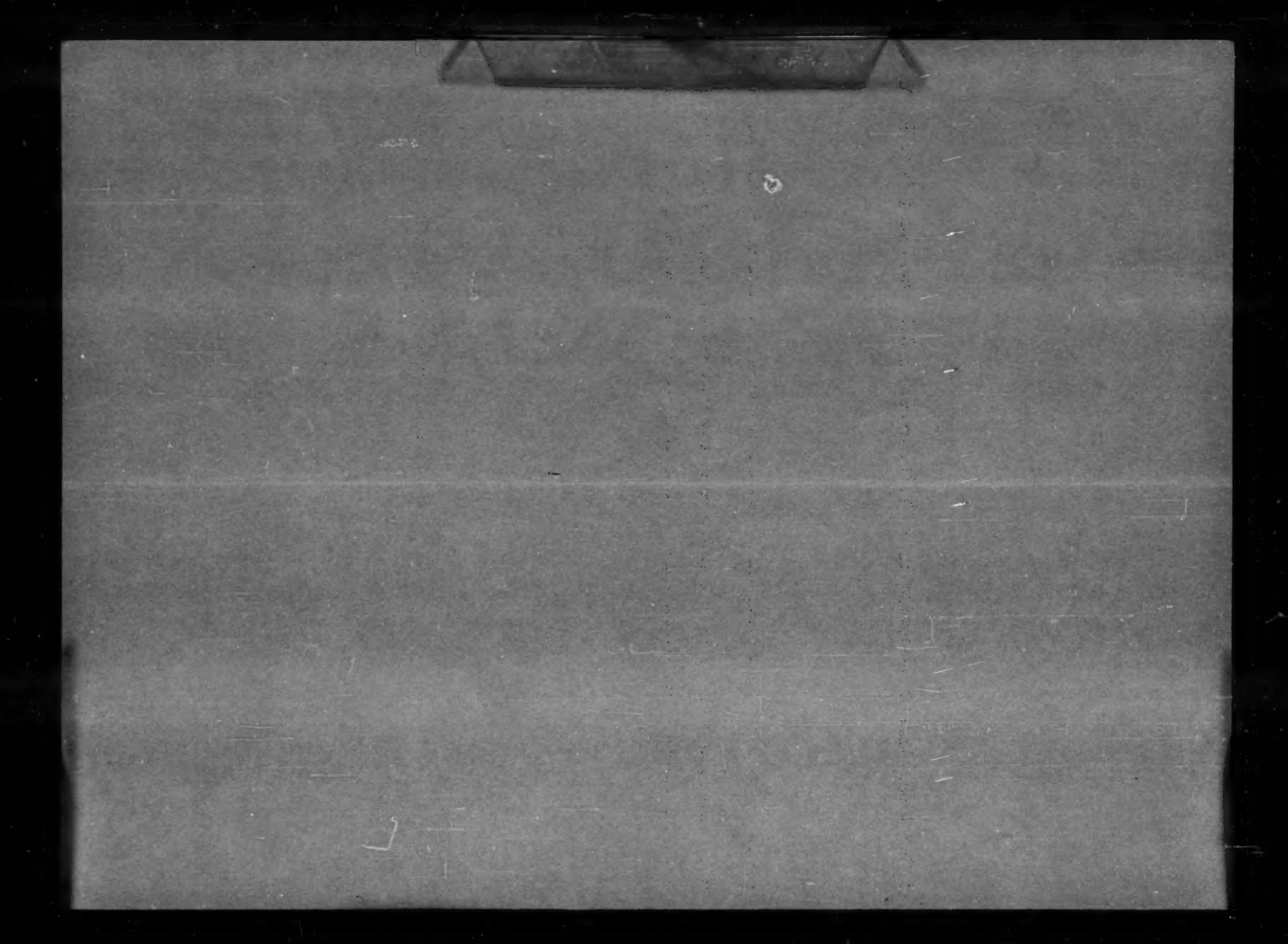

AN ASME PAPER

Its Preparation, Submission and Publication, and Presentation

To a large degree the papers prepared and presented under the ASME sponsorship are evidence by which its professional standing and leadership are judged. It follows, therefore, that to qualify for ASME sponsorship, a paper must not only present suitable subject matter, but it must be well written and conform to recognized standards of good English and literary style.

The pamphlet on "AN ASME PAPER" is designed to aid authors in meeting these requirements and to acquaint them with rules of the Society relating to the preparation and submission of manuscripts and accompanying illustrations. It also includes suggestions for the presentation of papers before Society meetings.

CONTENTS

PREPARATION OF A PAPER—

General Information—Style, Preferred Spelling, Length Limitation, Approvals and Clearances.

Contents of the Paper—Title, Author's Name, Abstract, Body of Paper, Appendixes, Acknowledgments, Bibliographies, Tables, Captions, Photographs, Other Illustrations.

Writing the Paper—Outline, Tabulations, Tables, Graphs, Charts for Computation, Drawings, Mathematics, Accuracy, Headings and Numbering, Lantern Slides, Motion Pictures, Typing, Number of Copies.

SUBMISSION AND PUBLICATION OF A PAPER—

Intention to Submit Paper Required in Advance, Meeting Dates, Due Dates for Manuscript, Discussers, Review and Acceptance, Proofs, Advance Copies and Reprints, Discussion and Closure, Publication by Others.

PRESENTATION OF A PAPER—

Time Limit, Addressing Your Audience, Public Address Systems, Use of Slides.

REFERENCES—

References on Writing and Speaking, Engineering Standards.

Price 35¢. No discount allowed. *A remittance must accompany all orders for $2.00 or less. U. S. Postage Stamps are acceptable.*

THE AMERICAN SOCIETY OF MECHANICAL ENGINEERS
29 West 39th Street, New York 18, N. Y.